FINAL REPORT

Characterization of Off-Road Diesel Emissions of Criteria Pollutants

SERDP Project WP-1336

OCTOBER 2008

John G. Watson
Hans Moosmuller
Hampden D. Kuhns
Judith C. Chow
Oliver Chang
Nicholas Nussbaum
Claudio Mazzoleni
Dongzi Zhu
Peter W. Barber
Desert Research Institute

J. Wayne Miller
David R. Cocker
CE-CERT

Michael R. Kemme
US Army Engineering Research and Development Center

Strategic Environmental Research and Development Program

Report Documentation Page

Form Approved
OMB No. 0704-0188

1. REPORT DATE	2. REPORT TYPE	3. DATES COVERED
OCT 2008	**N/A**	**-**

4. TITLE AND SUBTITLE	5a. CONTRACT NUMBER
Sustainability Assessment of a Military Installation: Design for a System of Reporting	5b. GRANT NUMBER
	5c. PROGRAM ELEMENT NUMBER
6. AUTHOR(S)	5d. PROJECT NUMBER
	5e. TASK NUMBER
	5f. WORK UNIT NUMBER
7. PERFORMING ORGANIZATION NAME(S) AND ADDRESS(ES) **Desert Research Institute**	8. PERFORMING ORGANIZATION REPORT NUMBER
9. SPONSORING/MONITORING AGENCY NAME(S) AND ADDRESS(ES)	10. SPONSOR/MONITOR'S ACRONYM(S)
	11. SPONSOR/MONITOR'S REPORT NUMBER(S)

12. DISTRIBUTION/AVAILABILITY STATEMENT
Approved for public release, distribution unlimited

13. SUPPLEMENTARY NOTES
The original document contains color images.

14. ABSTRACT

15. SUBJECT TERMS

16. SECURITY CLASSIFICATION OF:			17. LIMITATION OF ABSTRACT	18. NUMBER OF PAGES	19a. NAME OF RESPONSIBLE PERSON
a. REPORT	b. ABSTRACT	c. THIS PAGE			
unclassified	**unclassified**	**unclassified**	**UU**	**210**	

EXECUTIVE SUMMARY

The main goal of this project was to identify and fill knowledge gaps concerning emissions and activities of non-road military diesel engines. This required the development of new measurement methods that quantify a larger number of chemical compounds and particle sizes for fuels and operating cycles that are not well represented by engine certification tests.

Specific project objectives are: 1) Develop, test, and apply new methods for quantifying non-road emissions that more efficiently and realistically represent actual operations than engine dynamometer certification tests do; 2) develop source-, activity-, and fuel-specific emission rate estimates for representative Department of Defense (DoD) mobile and stationary diesel equipment, most of which is not used on public roadways. Emitted pollutants include carbon monoxide (CO), oxides of nitrogen (NO_x), volatile organic compounds (VOC), particulate matter (PM), sulfur dioxide, (SO_2), and ammonia (NH_3). Chemical source profiles for total PM and VOC are also quantified; and 3) integrate results into emissions modeling databases and software.

A comprehensive literature review found that several different test methods were found to be applied to diesel emission tests including: 1) laboratory engine or chassis dynamometer tests; 2) in-plume measurements from mobile laboratories and roadside monitors, 3) on-board exhaust measurements by portable emission monitoring systems, and 4) cross-plume measurements by remote sensors. Real-world tests have been made with in-plume and crossplume systems, and these emission rates often differ substantially from those of certification tests due to the greater range of engine age and maintenance, a wide variety of operating conditions, and fuels that often differ from those specified for certification. Portable emissions monitoring systems have not yet achieved the reliability and accuracy needed for useful emission factors. Tests using thermal denuders showed that $PM_{2.5}$ and UP emission factors vary with temperature, with more condensable material found at ambient temperatures than at the higher temperatures found in exhaust pipes. $PM_{2.5}$ source profiles are important for speciated emission inventories and source apportionment, but few of these are available for: 1) typical ambient temperatures that allow for condensation and initial chemical transformation, 2) non-road engines, applications and fuels; and 3) in a form that allows for easy access and use. EPA's SPECIATE software allows for archiving of profiles acquired in this study for use by a broader applications community. The NONROAD emission model lacks real-world representations for many nonroad diesel emission factors. Measurements from tests such as those carried out in this report can be added to the NONROAD model. Although more than 1600 publications related to diesel emissions and fuels were identified, with 650 of them since the project commencement in 2003, knowledge about non-road emissions is minimal. Most tests have used certification methods that do not adequately reflect real-world emissions.

Engine and fuel use data are well defined on an annual basis for the Army, but not for the other services. The US Marine Corps also has good overall records, but does not have the spatially and temporal detail of the Army data base that would allow emissions to be easily estimated for individual military bases. Fuel use data is available for the Air Force and Navy, but the relatively small amount used for non-road diesel engines cannot be separated from the total fuel use, which is dominated by aircraft and ships. M1 tanks used 16% of all fuel for CY2001-2003. These tanks use turbines rather than CI engines. For the CI engines, the HMMWV (GM6.2L engine) use 18% of the total, the HEMTT (Detroit Diesel 8V92TA engine) used 11% of the total, 5-ton trucks (Cummins NHC250 and 6CTA8 engines) used 12% of the total, the

LAV/APCs (Detroit Diesel 6V53T engine) used 7% of the total, and the FMTV (Caterpillar 3116-ATAAC engine) used 4% of the total. Together these engines and units accounted for more than 75% of the Army and Marine Corps fuel use. There was some, but not major, difference in year-to-year fuel consumption amounts. Operating cycles for military engines are not well understood. New engines with electronic control modules (ECMs) acquire some of the operating information needed to determine these, but these ECMs are not on most of the older military equipment. Using ECM data as these new engines penetrate the military fleet offers a higher potential to better characterize their operating characteristics.

Commercially-available Portable Emission Monitoring Systems (PEMS) for gas exhaust measurements were evaluated and found insufficient to meet the project goals. The commercial gas PEMS show promise for NO_x and CO_2 emissions, but their current detection limits are too imprecise for quantifying VOC, CO, and PM emissions from diesel engines. PEMS have the advantage of being less costly to procure than other methods and being located on engines without causing interference with the routine operations.

A large part of the project was dedicated to developing and evaluating the UCR Mobile Emissions Laboratory (MEL) and the DRI In-Plume Emissions Test Stand (IPETS), the DRI Vehicle Emissions Remote Sensing System (VERSS) and the DRI on-board PM monitor. The MEL is the most well established technology, replicating the sampling, dilution system, and measurement devices that are usually confined to an emission testing laboratory. It offer the advantage of mobility, but its large size make it difficult to position in a location to record realworld source emissions. For real-world mobile source emissions, the MEL is only applicable to sampling the exhaust of the tractor that is towing it. The MEL, however, is the only instrument that can provide a bridge between certification tests expressed in g/bhp-hr and the g/kgfuel fuelbased emission factors that are more useful for air quality planning inventories. The IPETS is intermediate between the MEL and the PEMS, offering a movable platform that can be used in field situations, but is still too large and requires too much power to be mounted on the engine. IPETS is oriented toward real-world emissions, allowing exhaust samples to dilute and cool to ambient conditions prior to measurement. Simultaneous CO_2 measurements allow emissions concentrations in the plume to be related to the fuel consumption, resulting in a fuel-based emission factor. The current IPETS design has multiple measurements for CO2 and PM mass concentrations. Particle number measurements in different size fractions allow the important UP fraction to be determined. The Fourier Transform Infrared (FTIR) spectrometer is capable of quantify non-criteria pollutants such as NH_3 along with the normal certification pollutants. As with the MEL, the IPETS challenge is being able to extract a portion of the plume for analysis. While this is relatively straightforward for stationary sources such as generators where a probe can be located in the plume, it is more difficult for mobile sources. The VERSS remote sensing system is applicable to mobile sources following a set path. However, many non-road sources don’t follow such paths.

VERSS is a cutting edge technology that takes advantage of recent advances in lasers, radiation detection, and high speed data acquisition. VERSS feasibility was proven in this project, but it was not deemed practical for taking many measurements. A major limitation is the lack of commercial replacement parts, as several components were produced specifically for the system. Although many advances were made in the technology as part of the project, time and

budget limitations did not permit the development and implementation of the system as envisioned at the project onset.

Comparison tests among the different methods on the same emissions showed promising results, typically within ±30% for fuel-based emissions factors, but sometimes as high as a factor of two or more. PM was the most difficult observable to measure, owing to its many different measurement methods and the fact that its semi-volatile components are susceptible to temperature differences as the plume ages and cools.

Practical real-world emissions tests were carried out in four phases: 1) MEL tests of stationary diesel generators at UCR; 2) MEL chassis dynamometer tests mobile sources at UCR; 3) IPETS tests of stationary diesel generators at Camp Pendleton; and 4) IPETS, VERSS, and onboard PM tests of mobile sources at 29-Palms Marine Base. These tests demonstrated the feasibility of making measurements under field conditions, but not necessarily the practicality. On-base testing was difficult to arrange, owing to high demand from 2004-2007 for training and equipment. High staff turnover at the bases required multiple applications to be submitted for testing. Tests were costly and cumbersome for the VERSS, which seems more suited to on-road than to non-road applications. The IPETS functioned well for stationary diesel generators, but it missed many of the elevated exhaust plumes from the large military mobile sources. The portable PM prototype, however, functioned well, and with further miniaturization, packaging, and combination with PEMS having lower detection limits could be adapted into a viable system for testing many engines without major interference to base operations. The MEL was too large and cumbersome for use on the bases, so engines were brought from cooperating bases for testing.

Large differences were found in emissions between different engines and operating modes. In general, real-world emissions were lower than those reported for certification of the same or similar engines. Cold starts for generators had the highest emissions, much higher than those found during the prescribed certification test cycles. Ultrafine particles emission factors for non-road diesels were estimated for the first time and were found to be $(1.05 \pm 1.09) \times 10^{15}$ #/kgfuel for ten MTVR 7-ton truck, $(2.35 \pm 1.12) \times 10^{16}$ #/kgfuel for two LVS, and $(6.3 \pm 1.9) \times 10^{15}$ #/kgfuel for a single HDV. More than 95% of the measured particles were in the ultrafine particle mode.

The project resulted in a substantial increase in the number of $PM_{2.5}$ source profiles with organic speciation, and 25 of these valid individual profiles and composite profiles are being submitted to EPA's SPECIATE source profile software. On average, organic carbon (OC) accounted for 26 – 66% of $PM_{2.5}$, with 30 – 52% of OC found in the IMPROVE OC1 fraction. Elevated n-alkane abundances (4.6 ± 4.1%) were found for the MTVR, with lower abundances of ~0.4% in the LVS and AAV emissions. Branched n-alkane abundances were less than 0.04% for the diesel generators, and ranged from 0.5 ± 0.59% (MTVR) to 0.1 ± 0.008% (AAV) for the mobile source emissions. Polycyclic aromatic hydrocarbon (PAH) abundances were in the range of 0.03 to 0.08%. Trace element abundances were low, but they were ~3 – 10 times higher in mobile source $PM_{2.5}$ than in $PM_{2.5}$ from the diesel generators. Elevated potassium (K; 0.13 ± 0.28%), Ca (0.17 ± 0.11%), and Fe (0.32 ± 0.4%) abundances were found for the MTVR. Elevated Ca (0.5 ± 0.2%) was also reported for LVS. $PM_{2.5}$ $SO_4^=$ was comparable to the generators, in the range of 0.3 – 1.1%.

Though emission factors derived from the study were limited, they still make a substantial addition to the available information on emissions from non-road diesel engines, especially those used for military applications. Electronic data files were created that can be pasted into EPA's NONROAD emissions model that can be used to better estimate base emissions than would be available using the default emission factors.

Although this project made progress in developing and evaluating non-road measurement technologies, the number of tests is still small relative to the number needed to represent real-world emission distributions. Although the MEL, IPETS, and VERSS were shown to be feasible for military engine emissions quantification, they interfere too much with normal military operations to be practical. Smaller, portable units that acquire continuous measurements and can be mounted on mobile diesel sources are needed to acquire these larger data bases. Although these were not available for this project, technology is advancing rapidly and such instruments should be pursued in future non-road measurement studies.

Acknowledgements

The investigators are indebted to the personnel at Camp Pendleton and 29-Palms training centers for their cooperation in providing access to the base, engines to be tested, and personnel to participate in the testing program. This service was rendered in spite of many demands on personnel and equipment. The test program could not have gone forward without this cooperation.

The financial support of the Strategic Environmental Research and Development Program is gratefully acknowledged.

Table of Contents

List of Tables

List of Figures

1. INTRODUCTION

1.1 Background

Compression ignition (CI) diesel engines are in widespread use for non-road applications. Non-road refers to vehicle and engine use beyond normal operation on public, paved roads. Typical non-road mobile sources include construction equipment, aggregate haulers, farm implements, locomotives, and marine vessels. Typical non-road stationary diesel engine uses include back-up generators (BUGs), pumps, and materials and cargo handling equipment. The U.S. military uses CI diesel vehicles and engines for all of these purposes and others related to base maintenance and troop training. Most non-road applications are exempt from highway fuel taxes, on-road fuel formulation requirements, and after-engine exhaust treatment, although regulations have been promulgated (U.S.EPA, 2003a) to bring non-road diesel emissions into harmony with on-road diesel requirements (U.S.EPA, 2001).

Non-road diesel emission rates and inventories are extrapolated from limited tests on similar engines by simulating on-road driving conditions and fuels. Test methods and cycles are intended to certify emissions from different engine designs on a common basis. Certification test methods emphasize accuracy and precision at emission concentrations near the certification limits, which are much higher than the levels emitted by many modern engines. Certification tests do not represent real-world emissions for on-road, let alone non-road engine use. Better information is needed to estimate emissions from stationary and mobile non-road diesel engines used on military bases.

1.2 Project Goals and Objectives

The goal of this project is to identify and fill knowledge gaps concerning emission testing methods, emission factors and rates, and activities that create emissions for non-road military diesel engines. This requires the development of new measurement methods that quantify a larger number of chemical compounds and particle sizes, at concentration levels much less than the certification requirements, and for fuels and operating cycles that are not well represented by engine certification tests.

Specific project objectives are:

- Develop, test, and apply new methods for quantifying non-road emissions that more efficiently and realistically represent actual operations than engine dynamometer certification tests.
- Develop source-, activity-, and fuel-specific emission rate estimates for representative Department of Defense (DoD) mobile and stationary diesel equipment, most of which is not used on public roadways. Emitted pollutants include carbon monoxide (CO), oxides of nitrogen (NO_X), volatile organic compounds (VOC), particulate matter (PM, including $PM_{2.5}$ [particles < 2.5 μm aerodynamic diameter], and ultrafine particles [UP, particles less than 0.1 μm aerodynamic diameter]), sulfur dioxide, (SO_2), and ammonia (NH_3). Chemical source profiles for $PM_{2.5}$ are also quantified.
- Determine how non-road emissions can be integrated with emissions modeling databases and software that estimate total diesel emissions.

1.3 Report Overview

Section 2 identifies and surveys publications and reports relevant to the objectives to provide guidance and a context for the experimental work. Section 3 summarizes available information on military diesel engines, fuels, and operating conditions that might serve as a basis for estimating total emissions. Data availability and limitations are identified. Section 4 describes and evaluates emission testing methods developed as part of this project. These include a mobile emissions laboratory that simulates certification methods, a cross-plume remote sensing system, an in-plume extraction system, and on-board emission monitors. Section 5 describes the tests performed on stationary and mobile sources by the different test methods and summarizes the emission factors achieved. Section 6 describes PM emission source profiles. Section 7 describes how emission factors and profiles can be integrated into EPA emission models and data bases. Section 8 summarizes study results, identifies their limitations, and describes remaining knowledge gaps. Bibliographic references are provided in Section 9.

2. LITERATURE REVIEW

Periodic literature searches were conducted since the beginning of the project in 2003 to keep abreast of related developments in diesel engine development, fuels (including biodiesel), emission standards and tests, non-regulated pollutant emissions, VOC and PM chemical composition, and diesel exhaust health effects. Nearly 1600 citations were compiled in a reference data base, with abstracts where possible, with more than a third (650) published since 2003.

A number of reviews on various diesel topics have been published (Amann and Siegla, 1982; Burtscher, 2005; Cernansky, 1983; Chow, 2001a; Chow, 2001b; Chow, 2002; Clean Air Scientific Advisory Committee, 2000; Demirbas, 2007; Eichlseder and Wimmer, 2003; Fino, 2007; Gillies and Gertler, 2000; Green and Armstrong, 2003; Hansen et al., 2005; Kittelson, 1998; Kittelson, 1999; Lee et al., 1998; Li et al., 2003a; Lloyd and Cackette, 2001; Ma and Hanna, 1999; Maricq, 2007; Mauderly, 2001; McCormick, 2007; NRC (National Research Council), 1982; Prucz et al., 2001; Ramadhas et al., 2004; Ribeiro et al., 2007; Sawyer et al., 1998; Schexnayder and David, 2002; Somers and Kittredge, 1971; St.Denis and Lindner, 2005; U.S.EPA, 2000; U.S.Mine Safety and Health Administration, 2001; Vouitsis et al., 2003; Wan and az-Sanchez, 2007; Wichmann, 2007; Zheng et al., 2004) but these are specific to the topics treated, and many of them need to be updated. The following sections summarize findings from this literature with emphasis on more recent publications that are relevant to current and future diesel emissions, fuels, and operating cycles used by the U.S. military.

2.1 Diesel Engines and Uses

Diesel engines use CI, rather than the spark-ignition (SI) of gasoline-fueled engines, to ignite the fuel. In the diesel cycle, a lean air-fuel mixture (i.e., stoichiometrically more air than fuel) is compressed to a much higher pressure than in SI engines to achieve auto-ignition. The lean mixture results in more complete combustion and reduced emissions of VOCs and CO, while NO_x emissions increase due to the high combustion temperature. Diesel engines also emit large amounts of primary PM, mostly during transient operating conditions such as high load (acceleration) and cold start. PM emission rates and particle size are influenced by the fuel sulfur content that also causes diesel SO_2 emissions. Some of the SO_2 and NO_x transform into $PM_{2.5}$ that is regulated by National Ambient Air Quality Standards (NAAQS) (Bachmann, 2007; Chow et al., 2007c; U.S.EPA, 2006) and the regional haze rule (Chow et al., 2002; U.S.EPA, 1999a; Watson, 2002). VOC and NO_x emissions are precursors to ozone (O_3) that is also regulated by NAAQS (U.S.EPA, 1997; U.S.EPA, 2007a).

Diesel engines are used in a variety of non-road applications, both mobile and stationary (Chow, 2001a; Lloyd and Cackette, 2001). Small engines (<37 kW and 37 to 75 kW) generally with direct injection are used in refrigeration units, portable generators, skid loaders, forklifts, water pumps, and turf mowers. Medium engines (75 to 130 kW) are used in backhoes, rubber-tired loaders, semi-portable generators, and air compressors. Large engines (130 to 450 kW) are used in large haul trucks, earthmoving equipment, tracked vehicles such as bulldozers, semi-portable and fixed generators, and cranes. Very large engines (>450 kW) are used in mining trucks, generators, marine vessels, locomotives, and certain construction equipment.

Military engines may differ from civilian engines owing to their optimization for durability, power, and tolerance of sub-optimal fuels (Durbin et al., 2007a; Kelly et al., 2003;

Markle and Brown, 1996). Jet fuel (typically JP-8), a distillate similar to diesel fuel, is used at times in many of these engines to facilitate fuel transport and storage during remote operations and combat (Rakopoulos et al., 2004). JP-8 has a sulfur content as high as 3000 ppmw, compared to commercial on-road fuels that were required to have <500 ppmw sulfur before 2006 and <15 ppmw sulfur after 2006 (U.S.EPA, 2001). Low-sulfur fuel is needed to permit the application of after-engine treatment devices that further reduce diesel PM and NO_x emissions. Diesel fuel is similar to kerosene and is also used to power turbines used in the M-1 Abrams tank, in jet aircraft engines, and in large power generators. It is also used in military heaters (Cheng et al., 2001) and for other direct combustion needs. This study limits itself to CI applications.

2.2 Diesel Emission Standards

Emission standards and engine certification methods are defined by the Code of Federal Regulations (40 CFR, Parts 86 and 89). Table 2-1 summarizes recent and current U.S. standards applicable to on-road engines for criteria pollutants. Engines are certified against these standards using the engine dynamometer and test cycles specified in the CFR. This certification is a necessary part of pollution control, as it puts all engine designs and control devices on an equivalent standard and allows an objective comparison among them and with respect to the standards. Certification emissions are not the same as real-world emissions because: 1) they represent relatively new engines in a design operating under ideal conditions; 2) they are tested in laboratories on engine dynamometers rather than in the vehicle or on the platform in which they are used; 3) fuels are fresh an carefully tested against specifications; and 4) set operating cycles are used that cannot match the range of real-world operating conditions. For air quality planning, especially that which creates emission inventories for modeling the formation and sources of $PM_{2.5}$ and O_3, real-world emissions are preferable.

Table 2-1. U.S. emission standards for on-road diesel engines.

		2000 Standard (g/bhp –hr)	2004 Standard (g/bhp –hr)	2007 Standard (g/bhp –hr)	Phase-In by Model Year*			
					2007	2008	2009	2010
Diesel Fleet	NO_x	4.0	N/A	0.20	25%	50%	75%	100%
	NMHC	1.3	N/A	0.14				
	NMHC + NO_x	N/A	2.4	N/A				
	CO	15.5	15.5	15.5	100%	100%	100%	100%
	PM	0.10	0.10	0.01	100%	100%	100%	100%

* Percentages represent percent of sales. NO_x=Oxides of Nitrogen, sum of nitric oxide (NO) and nitrogen dioxide (NO_2) expressed as NO_2, CO=Carbon Monoxide, NMHC=Non-Methane Hydrocarbons, PM=Particulate Matter.

Heavy duty engine certification testing provides emissions in mass per unit work done or (grams per brake horsepower-hour [g/bhp-hr] or grams per brake kilowatt hour [g/bkW-hr]. For emission inventories, emission factors are required in units of mass per distance traveled (e.g., grams per kilometer [g/km] or grams per mile [g/mi]) for relation to vehicle activity, in terms of vehicle kilometers traveled (VKT) or vehicle miles traveled (VMT). This distance based

emission factor, E, (Machiele, 1989) is related to g/bhp-hr using brake-specific fuel consumption (BSFC in lb fuel/BHP-hr), fuel density (ρ in lb/gal), and fuel economy (FE in miles/gal) by:

$$E(g/mile)=(g/BHP\text{-}hr) \times (\rho/[BSFC \times FE]) \quad (2\text{-}1)$$

VKT and VMT are not usually relevant to non-road applications. Stationary units don't move, and even mobile sources spend much time idling or in abrupt starts and stops. Fuel-based emission factors (g/kg fuel) are often used in these cases as the amount of fuel used for an activity is easier to estimate than the VMT or VKT. Using the carbon mass balance technique described by Moosmüller et al. (2003) and Fraser et al. (1998), fuel-based emission factors (EFs) can be calculated as:

(2-2)

$$EF_P = CMF_{fuel} \frac{C_P}{C_{CO_2}\left(\frac{M_C}{M_{CO_2}}\right) + C_{CO}\left(\frac{M_C}{M_{CO}}\right)}$$

where EF_P is the emission factor of pollutant P in g pollutant per g fuel. CMF_{fuel} is the carbon mass fraction of the fuel, typically 85% to 88% for gasoline and diesel. C_i is the mass concentration of species i in grams per cubic meter, and M_i is the molecular (or atomic) weight of species i in grams per mole.

2.3 Non-Road Diesel Emissions

Non-road emissions have been unregulated until recently (U.S.EPA, 2003a), even though non-road emissions from mobile and stationary diesel engines are an important part of the U.S. inventory. Figure 2-1 shows that non-road engine exhaust contributed ~5% and on-road engine exhaust constituted ~3% of total U.S. $PM_{2.5}$ emissions in CY2000. When on-road and non-road emissions are combined, diesel exhaust contributed ~5% of $PM_{2.5}$ from all sources, while gasoline engines constituted ~3%. Although anthropogenic fugitive dust (e.g., road dust, construction, agriculture) is estimated to be the source of nearly one-half the $PM_{2.5}$, this fraction is probably overestimated by a factor of four or more owing to rapid impaction and deposition near the point of origin (Countess et al., 2001; Watson et al., 2000).

Non-road engines constituted the third largest SO_2 category for national CY2000 emissions, after power stations and other industrial combustion. Diesel engine SO_2 emissions constituted 35% and marine vessels contributed 59% of the 1.3 Tg/yr from non-road sources. On-road vehicle emissions contributed less than 25% of non-road SO_2 emissions with 40% from diesels and the rest from gasoline engines. CY2000 total NO_x emissions were 54% from on-road and non-road engines, with non-road accounting for 39% of this fraction. Non-road NO_x emissions have grown more than any other category with 3.3 Tg/yr from diesel exhaust (including railroads and non-military aircraft). Construction equipment (1.1 Tg/yr diesel), farming implements (0.8 Tg/yr diesel), and ships (0.9 Tg/yr residual oil) were the largest non-road NO_x emitters. The remaining 0.45 Tg/yr was mostly from gasoline engines, constituting less than 10% of non-road emissions. Of the on-road fraction, 41% was from diesel engines with the remainder from gasoline engines. Military emissions are not explicitly identified by U.S. EPA.

There is a growing literature on non-road diesel emissions, especially in the last few years (Chung et al., 2008; Duc and Wattanavichien, 2007; Durbin et al., 2007a; Huang et al., 2007; Kean et al., 2000; Kelly et al., 2003; Lindgren and Hansson, 2004; Liu et al., 2005; Pandiaraj et al., 2002; Poola and Sekar, 2003; Rogers et al., 2003; Ryu and Oh, 2004; Saiyasitpanich et al., 2005; Samaras and Zierock, 1995; Sattler, 2002; Sawant et al., 2007a; Shah et al., 2006a; Yanowitz, 2003), but the number of tests is small compared to on-road emission estimates. In addition to these criteria pollutants, diesel exhaust contains several compounds that are believed to be toxic (Bunn et al., 2004; Mauderly and Chow, 2008; Riedl and az-Sanchez, 2005; Wichmann, 2007), and diesel PM by itself is listed as a toxic air contaminant in California (California Air Resources Board, 1998).

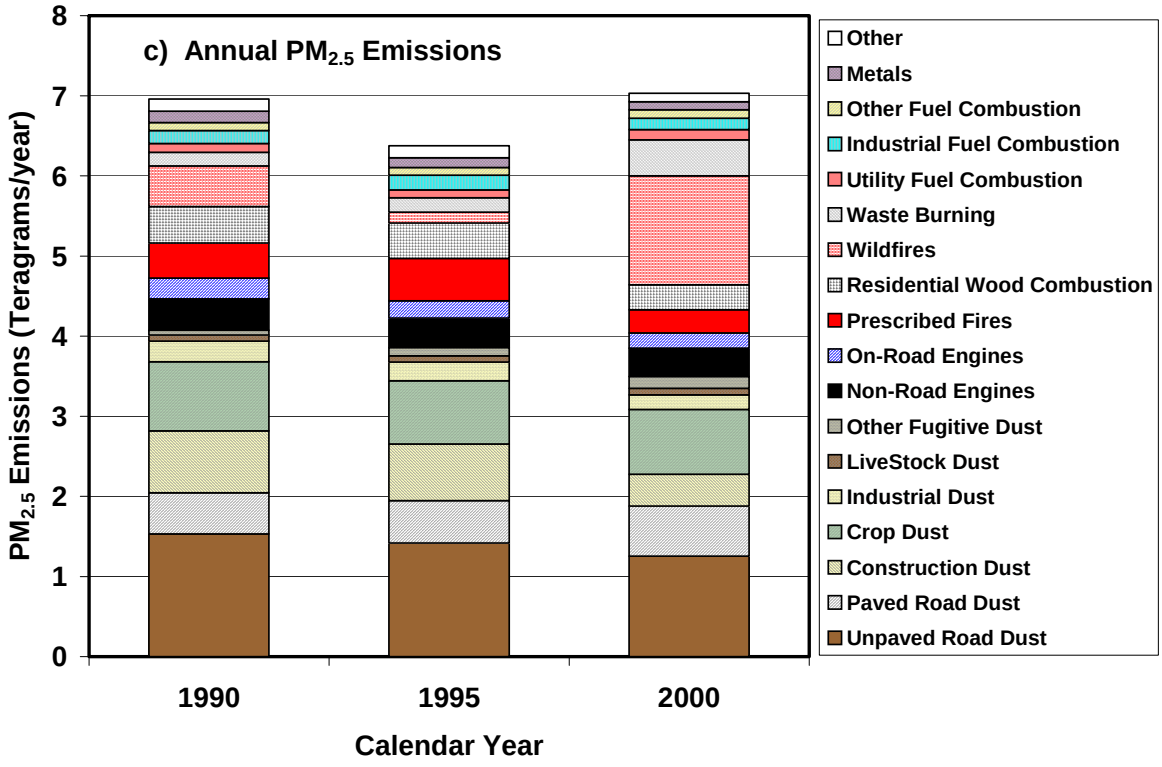

Figure 2-1. U.S. emissions of $PM_{2.5}$ for major source categories from the National Emissions Trends inventory (U.S.EPA, 2003b).

2.4 Diesel Fuels

Diesel fuels have been changing as a result of air quality regulations and a desire for secure and renewable energy. The military has shown interest in alternatives to JP-8, not only to reduce workplace exposure and reduce emissions, but also to move toward on-site fuel manufacturing from local materials to assure supply and reduce transportation costs. Much recent effort has been expended on biodiesel and the potential benefits from its use (Agarwal, 2007; Agarwal and Agarwal, 2007; Bagley et al., 1998; Bari et al., 2002; Bilcan et al., 2003; Biluck, 2007; Buchholz et al., 2004; Bunger et al., 1998; Bünger et al., 2000; Canakci, 2007; Canakci and Van Gerpen, 2003; Carraretto et al., 2004; Cetinkaya and Karaosmanoglu, 2005; Chandraju and Prathima, 2004; Chauhan et al., 2007; Chen and Wu, 2002; Choi and Oh, 2006;

Chung et al., 2008; Corporan et al., 2005; Correa and Arbilla, 2006; Correa and Arbilla, 2008; Demirbas, 2002a; Demirbas, 2002b; Demirbas, 2007; Dewulf et al., 2005; Dorado et al., 2002; Dorado et al., 2003; Duffield, 2007; Duran et al., 2003; Duran et al., 2004; Duran et al., 2006; Durbin et al., 2000; Durbin et al., 2007a; Durbin and Norbeck, 2002; Dwivedi et al., 2006; Fernando and Hanna, 2004; Fontaras et al., 2007; Forson et al., 2004; Frank et al., 2007; Giannelos et al., 2002; Graboski and McCormick, 1998; Hamelinck and Faaij, 2006; Hansen et al., 2005; Hill et al., 2006; Hribernik and Kegl, 2007; Johnston and Holloway, 2007; Jung et al., 2006; Kalam and Masjuki, 2002; Kalam and Masjuki, 2004; Kameda et al., 2007; Kaul et al., 2007; Kegl, 2007; Keskin et al., 2007; Khan et al., 2007; Kowalewicz, 2005; Kowalewicz, 2007; Krahl et al., 2002; Kumar, 2007; Labeckas and Slavinskas, 2006; Landis et al., 2007; Lapuerta et al., 2003; Lapuerta et al., 2007; Lebedevas et al., 2006; Lebedevas et al., 2007; Lee et al., 2004; Lima et al., 2004; Lin and Lin, 2006; Lin and Lin, 2007; Lin et al., 2006b; Lin et al., 2006a; Lin et al., 2008b; Lin et al., 2008a; Ma and Hanna, 1999; Mazzoleni et al., 2007a; McCormick et al., 2001; McCormick, 2007; Megahed et al., 2004; Munoz et al., 2004; Murillo et al., 2007; Nwafor, 2003; Nwafor, 2004a; Nwafor, 2004b; Oguz et al., 2007; Pang et al., 2006; Peiro et al., 2008; Peng et al., 2006; Peng et al., 2008; Pereira et al., 2007; Pradeep and Sharma, 2007; Pramanik, 2003; Prueksakorn and Gheewala, 2008; Puhan et al., 2005; Puhan and Nagarajan, 2007; Raadnui and Meenak, 2003; Raheman and Phadatare, 2004; Rakopoulos et al., 2007; Ramadhas et al., 2004; Reddy et al., 2008; Rejesus et al., 2004; Ren et al., 2007; Reyes and Sepulveda, 2006; Ribeiro et al., 2007; Ropkins et al., 2007; Ryu and Oh, 2004; Sahoo et al., 2007; Sastre et al., 2003; Savvidis et al., 2006; Semenov, 2003; Sendzikiene et al., 2006; Shi et al., 2006; Silva et al., 2007; Singh et al., 2007; Sivaprakasam and Saravanan, 2007; Sonntag et al., 2008; Stauffer and Byron, 2007; Swanson et al., 2007; Tan et al., 2004; Tat et al., 2007a; Tat et al., 2007b; Tsolakis et al., 2003; Tsolakis and Megaritis, 2004; Turrio-Baldassarri et al., 2004; U.S.EPA, 2002; Ulusoy et al., 2004; Uma et al., 2004; Usta, 2005; Vivek and Gupta, 2004; Wang et al., 2000b; Wynne et al., 2004; Yang et al., 2007b; Yang et al., 2007a; Ying and Zhou, 2007; Yuan et al., 2007; Zabetta et al., 2006; Zhang et al., 2006; Zou and Atkinson, 2003).

Engine dynamometer tests show that CO, VOC, and PM emissions can be slightly lower with some biodiesel fuels than with petroleum diesel fuel. NO_x emissions tend to be equivalent or slightly higher with biodiesel than with petroleum diesel. U.S. EPA (2002) summarized several engine dynamometer emissions studies investigating the effects of biodiesel on exhaust emissions. Emissions from heavy-duty diesel engines running on 100% biodiesel had ~50% lower emissions of CO and PM, ~65% lower emission of HC, and ~10% higher emissions of NO_x when compared with petroleum diesel. These estimates were based on tests conducted on 43 heavy duty engines varying in model year from 1980 to 2001. Emission changes in using a blend of petroleum diesel and biodiesel may be approximated by multiplying the emission changes from 100% biodiesel by the fraction of biodiesel in the blend.

Canakci and Van Gerpe (2003) found that emissions decreased with the mixing fraction of biodiesel with petroleum diesel, consistent with other chassis dynamometer tests (Wang et al., 2000b; Zou and Atkinson, 2003). In contrast, Durbin et al. (2000) and Durbin and Norbeck (2002) found a variable increase in PM emissions after the vehicles were refueled with biodiesel. On most fuel comparison dynamometer studies, the fuel handling system on the engine is bypassed and the fuel supply is delivered directly to the carburetor or fuel injectors. This procedure has the advantage that there is negligible carry-over influence associated with switching from one fuel to another. However it also has the disadvantage of not accurately

simulating the effects of adding the new fuel to the test vehicles fuel tank as would be done under typical usage.

In conjunction with this study, Mazzoleni et al. (2007b) conducted a real-world test of diesel school buses that switched from petroleum diesel to biodiesel. PM emissions increased, up to a factor of 1.8, after the switch from petroleum diesel to a 20% biodiesel blend. The fuel used during this campaign was provided by a local distributor and was independently analyzed at the end of the on-road experiment. The analysis found high concentrations of free glycerin and reduced flash points in the B100 parent fuel, indicating improper separation of the biodiesel product during production. This study underlined the importance of setting and attaining fuel standards at the point of delivery, as well as the need for more real-world emission testing.

2.5 Diesel Emission Testing Methods

Emission factors depend as much on the test method as they do on the actual emissions. Available methods are: 1) engine and chassis dynamometers with simulated use cycles; 2) in-plume measurements made by mobile or stationary instruments; 3) on-board monitors that extract samples directly from the exhaust pipe; and 4) cross-plume remote sensing. Each of these methods has advantages and disadvantages, and a more accurate estimate of diesel emissions will only come when results from all of these methods are systematically studied and integrated. The analytical sections of the CFR specify details of sampling and analysis for certifying diesel engines with respect to the standards in Table 2-1. For example, the CFR specifies that sample lines must be heated to 190°C and that nitrogen oxides (NO_x) must be measured using a chemiluminescence analyzer. The CFR also provides details on quality control and quality assurance for each method. Many of these requirements cannot be reproduced in real-world monitoring. As noted earlier, the certification tests emphasize accuracy and precision for levels near the emissions standards. Instruments are calibrated and compared at these levels, and detection limits may not be sensitive enough to detect the low levels from properly operating modern engines.

2.5.1 Engine and Chassis Dynamometer Testing

Engine emission certification tests are performed with an engine dynamometer on which the engine is mounted and its energy output is absorbed by a water brake. Diesel engines are usually tested at various speeds and loads in steady-state modes. Cold start and transient emissions are not included. Steady state resistances are defined for certification of non-road, marine and locomotive engines. A few large chassis dynamometers are available in which the vehicle wheels are rotated on a roller with varying degrees of resistance that can represent a driving cycle (including hard accelerations and decelerations). These are used to evaluate emissions from trucks and buses.

Engine and chassis dynamometer tests direct all of the exhaust to a full-scale dilution chamber and employ the use of a constant volume system (CVS), laboratory-grade emissions measurement instrumentation, an environment control system, and associated data acquisition and control systems. Different dilution ratios have yielded different particle size distributions because small particles form and combine with each other depending on their concentrations and mixing characteristics (Abdul-Khalek et al., 2000; Brown et al., 2000; Desantes et al., 2004; Duran et al., 2002; Lipsky and Robinson, 2006; Lyyranen et al., 2004; Maricq et al., 2003; Ning et al., 2004; Ronkko et al., 2006; Wong et al., 2003). Temperatures in the dilution chamber are

>50 °C, which also mitigates condensation of semi-volatile compounds into the PM phase at ambient temperatures (15 to 20 °C).

Several types of resistance can be applied to the roller in a chassis dynamometer to follow a number of test cycles (www.dieselnet.com/standards/cycles). The Federal Test Procedure (FTP) heavy-duty transient cycle for heavy-duty on-road engines (40 CFR, Part 86.1333) includes transient (acceleration and deceleration) as well as steady state components to better represent on-road conditions. The transient test accounts for the variety of heavy-duty trucks and buses driven in American cities, including traffic in and around the cities on roads and expressways. The FTP includes "motoring" segments and requires an electric dynamometer capable of both absorbing and supplying energy. The test consists of four phases simulating light urban traffic with few stops, crowded urban traffic with frequent stops and starts, freeway traffic and a repeat of the first phase. The average FTP load factor is about 25% of the maximum power at a given speed. The Urban Dynamometer Driving Schedule (UDDS, CFR 40, 86, App.I) simulates urban driving, having a 1060 second duration, an equivalent 8.9 km driving distance, an average speed of 30.4 km/hr, and a maximum speed of 93.3 km/hr, with accelerations and decelerations.

The EPA 13-mode steady-state cycle is included in supplemental tests when certifying engines for on-road vehicles. The Central Business District (CBD) cycle (Society of Automotive Engineers Recommended Practice SAE J 1376, 1993) is used for transit buses. Europe and Japan use only steady-state modes for certifying their on-road vehicles. The AVL 8-Mode test is a steady-state engine test procedure meant to correlate with the exhaust emission results over the US FTP heavy-duty engine transient cycle. The test involves 8 steady state modes. The composite value is calculated by applying weighing factors on the modal results.

The Not To Exceed Cycle (NTE) certifies that emissions are controlled over the full range of speed and load combinations commonly experienced in use. NTE testing does not involve a specific driving cycle of any specific length (mileage or time), but it includes driving of any type that could occur within the bounds of a defined control area, such as steady-state and transient operating under varying ambient conditions. Emissions are averaged over a minimum time of thirty seconds and then compared to the applicable NTE emission limits. NTE cycles are used to determine compliance with the Table 2-1 emission limits.

Certification cycles for non-road sources are multi-mode, steady state and depend on the application. Backup generators are certified using the five-mode ISO-8178 D2 cycle. In this cycle, the generator is run at a rated speed of 1800 RPM and five power levels: 100%, 75%, 50%, 25% and 10%. Emission factors are measured at each level and a single emission factor is determined by applying the weighting factors provided in the CFR.

Manufacturers usually select the engine and the testing laboratory when applying for certification of a new engine design. Certification tests using laboratory and chassis dynamometers are intended only to determine compliance with standards, and are not intended represent real-world emissions encountered in practice (Sawyer et al., 2000) . Unfortunately, the certification measurements are often the only ones available for constructing emission inventories.

2.5.2 Roadside and Mobile Laboratory In-Plume Measurements

Mobile laboratories can sample exhaust emissions under real-world operating conditions by extracting a portion or all of the exhaust into an analysis system while the vehicle is operating (Beckerman et al., 2008; Bukowiechi et al., 2002; Bukowiecki et al., 2003; Canagaratna et al., 2004; Cocker et al., 2004a; Durbin et al., 2007b; Durbin et al., 2008; Giechaskiel et al., 2005; Herndon et al., 2004; Herndon et al., 2005a; Herndon et al., 2005c; Isakov et al., 2007; Jiang et al., 2005; Johnson et al., 2005; Kittelson et al., 2004b; Kittelson et al., 2006a; Kittelson et al., 2006c; Maciejczyk et al., 2004; Morawska et al., 2007; Pirjola et al., 2004; Pirjola et al., 2006; Pollack et al., 1998; Sawant et al., 2007b; Schneider et al., 2005; Shah et al., 2004; Shen et al., 2002; Shorter et al., 2005; Tang and Wang, 2006; Velasco et al., 2007; Vogt et al., 2003a; Vogt et al., 2003b; Weijers et al., 2004; Westerdahl et al., 2005; Xu et al., 2007; Yao et al., 2006; Yao et al., 2007a; Yli-Tuomi et al., 2005; Zavala et al., 2006).

Using a mobile laboratory, Brown et al. (2000) showed the importance of load and grade on increasing NO_x emissions. Johnson et al.(2005) applied their mobile laboratory as a chase vehicle on interstate highways in the Minneapolis metropolitan area. Using the difference between relative volumes of heavy duty diesel and light duty gasoline vehicles on weekdays and weekends, they estimated contributions from each type of emitter. UP emissions were $1.34\pm0.2 \times 10^{16}$ particles/kg of fuel for diesel exhaust and $7.1\pm1.6 \times 10^{15}$ particles/kg for gasoline engines. Heavy duty diesel engines produced much higher absolute emissions owing to their higher fuel consumption per distance traveled. This work represented on-road summer conditions, and it is believed that gasoline emissions of ultra fine particles might be higher for cold start and colder ambient conditions.

As part of this study, Shah et al. (2005) applied the University of California, Riverside (UCR) mobile laboratory to quantify emission rates of polycyclic aromatic hydrocarbon (PAH) and n-alkane compounds from on-road emissions of nine heavy-duty diesels following the California Air Resources Board's (ARB) Four Phase Cycle. Large differences emission rates occurred over the different phases of the cycle. Creep phase fleet average emission rates of PAHs and n-alkanes were an order of magnitude higher than those for the Cruise phase. PAH and n-alkane source profiles remained relatively constant for the different modes of operation. Variability of source profiles within the vehicle fleet exceeded the variability due to different operating modes.

2.5.3 On-Board Measurements

On-board measurements are carried by the test engine throughout its real-world operating cycle. Because space and power are limited on a typical vehicle or generator, on-board instrumentation must be portable, small, and low in power consumption. This imposes severe limitations on the accuracy and precision of the measurements. There has been some recent developments of on-board portable emission measurement systems (PEMS) (Boughedaoui et al., 2008; Chen et al., 2007; Collins et al., 2007; Durbin et al., 2007b; Frey et al., 2003; Frey et al., 2008; Gardetto et al., 2005; Gautam et al., 2001; Gouriou et al., 2004; Joumard et al., 2003; Krishnamurthy et al., 2007; Lenaers, 1996; Lenaers et al., 2003; Lenaers and DeVlieger, 1997; Nakamura et al., 2003; Unal et al., 2004; Vlieger, 1997; Yao et al., 2007b; Zhang and Frey, 2008), but reliable commercial systems are only recently becoming available.

Ramamurthy (1998) noted that while on-board instruments are useful for measuring in-use emission factors, the majority of the on-board systems only measure concentration levels of

the exhaust constituents and/or report the results in time-specific (g/s) and/or distance-specific (g/km) mass units through knowledge of the exhaust flow. Ramamurthy noted the difficulty of converting between these units and the brake- specific mass units (g/bkW-hr) in which the certification standards are stated and that are reported from engine dynamometer certification testing.

As part of this study, Durbin et al. (2007b) compared four commercial PEMS with a mobile laboratory Federal Reference Method (FRM) for exhaust from a back-up generator over steady-state loads and a diesel truck on transient and steady-state chassis dynamometer cycles. The best performing PEMS was within 12% of the FRM for NO. For the generator testing, several PEMS agreed with FRM measurements to within 5% for CO_2. For the chassis dynamometer testing, the best PEMS agreement was within 5% for CO_2, but the others showed larger discrepancies. PM measurements for the generator testing were 20% lower than those of the FRM for the best performing PEMS.

2.5.4 Cross-Plume Measurements

Cross plume measurements consist of remote sensing instruments that measure transmission and scattering in the infrared (IR), visible (VIS), and ultraviolet (UV) portions of the spectrum across an exhaust plume. These can be related to chemical and physical properties in the exhaust that differ from those in the atmosphere (Barber et al., 2004; Baum et al., 2000; Baum et al., 2001; Bishop et al., 1989; Bishop et al., 1994; Bishop et al., 1996; Bishop et al., 2000; Bishop and Stedman, 1990; Bishop and Stedman, 1996; Bradley et al., 2000; Burgard et al., 2006; Ekstrom et al., 2004; Guenther et al., 1995; Jack et al., 1996; Jack et al., 1997; Jiménez et al., 1999; Jimenez, 1999; Jiménez et al., 2000a; Jiménez et al., 2000b; Johnson et al., 1998; Knapp, 1994; Ko and Cho, 2006; Kuhns et al., 2002; Kuhns et al., 2004; Mazzoleni et al., 2004b; Mazzoleni et al., 2004a; Moosmüller et al., 2003; Moosmüller and Keislar, 2003; Morris et al., 1999; Nelson et al., 1998; Pokharel et al., 2002; Popp et al., 1999; Ross et al., 1998; Schoepflin and Dailey, 2003; Singer et al., 1998; Stephens and Cadle, 1991; Walsh et al., 1996; Walsh, 1996; Wang et al., 2000a; Watson et al., 2007; Zahniser et al., 1996; Zhang et al., 1994; Zhang et al., 1995; Zhang et al., 1996).

Cross-plume systems measure the mass column content of several pollutants and consequently obtain fuel-based emission factors by normalizing the measurements of individual pollutants to the total carbon content of the column measurement. With this method emission factors can be obtained without a priori knowledge of the changing plume dilution as the exhaust plume enters the ambient atmosphere.

Gaseous cross-plume sensors use IR absorption for CO_2, CO, and some VOCs. UV absorption is used for NO. Cross-plume sensors can measure gaseous emission factors for large numbers of individual vehicles (>1,000 per hour), albeit under a limited variety of operating conditions largely determined by monitoring location. These measurements have a high temporal resolution (~10 ms) resulting in 20 to 50 measurements before, during, and after vehicle passage through the measurement path. Since the carbon mass fraction of automotive fuel is known, the ratio of the two mass column contents can be used to calculate the mass emission of the pollutant of interest per mass of fuel consumed, yielding a fuel-based emission factor, as described above. Remote sensing studies have shown that comparatively few vehicles cause a majority of the emissions, that is, gaseous emission factors do not follow a symmetric

frequency distribution (Zhang et al., 1994). This emphasizes the importance of measuring emissions from many engines to obtain meaningful emission distributions.

For exhaust VOCs, the situation is more complex because VOC is not a single component, but consists of hundreds of individual compounds. In fresh exhaust, these are typically non-oxygenated hydrocarbons (HC), which are unusually quantified as non-methane hydrocarbons (NMHC) because methane (CH_4) is not considered to be a major cause of O_3 formation and it is usually a small component of engine VOC emissions. Concern about engine CH_4 emissions is changing, however, as methane is a potent greenhouse gas and is more abundant in exhaust from natural gas fueled engines. A cross-plume monitor measures absorption spectra for individual species that have distinctive IR absorption patterns and that are highly abundant in engine exhaust. Cross-plume PM measurements have quantified the opacity of exhaust plumes, which assumes they contain a large quantity of black carbon that efficiently absorbs IR radiation (3.9 μm) (Morris et al., 1998; Morris et al., 1999). However, as engines and fuels have improved, the black carbon content of diesel engine exhaust has decreased, even though non light-absorbing PM emissions are still important, as discussed below. A Lidar-based system that measures backscattered light (Barber et al., 2004; Moosmüller et al., 2003; Moosmüller and Keislar, 2003) was further developed as part of this project and is described in Section 4.

2.6 PM Emissions

PM emissions are among the most difficult to quantify from diesel exhaust, although these are the most noticed owing to their effects on visibility (Chow et al., 2002; Watson, 2002) and demonstrated adverse health effects (Chow et al., 2006b; Mauderly and Chow, 2008; Pope, III and Dockery, 2006). Given the results of recent health effects studies, it is likely that diesel emission standards will be revised in the future to take into account their size distributions and chemical composition.

2.6.1 Particle Size Distributions and Composition

Much of the quantification difficulty relates to the volatile nature of the ultrafine particles in the diesel exhaust. Ultrafine particles (UP) are loosely defined as those with diameters in the range of ~1 nm to 100 nm (nanometers). UP are bigger than air molecules (~0.3 nm), but they are smaller than the upper limits regulated by ambient air quality standards (Biswas and Wu, 2005; Chow et al., 2005b).

Figure 2-2 shows a conceptual framework of how diesel particulate is formed. Primary emissions include precursor gases (e.g., SO_2, SO_3, H_2SO_4, H_2O, low-volatile organic species, and semivolatile organic species) as well as soot particles (Schneider et al., 2005). The soot particles are fractal-like agglomerates of approximately solid spheres with diameters of ~20 nm. Primary UP diesel morphology differs from that of other fossil fuel combustion emissions, as shown in Figure 2-3. These particles form in oxygen-poor regions within the engine cylinder. As the exhaust is diluted and cooled after being removed from the cylinder, a competition between nucleation of the low-volatile species and condensation on the surface of the existing particles occurs. The non-spherical soot particles have been observed to undergo compaction when low- and semivolatile species condense on their surfaces (Saathoff et al., 2003). This moves the particle size into the accumulation mode with soot particles as cores and various species as condensates.

After dilution and cooling, nucleation particles with diameters in the range of 10-50 nm may form, especially when the primary soot particles are low in number. This nucleation is caused by the same sulfuric acid/water mechanisms observed in the atmosphere. Nucleation of organic vapors with low vapor pressures might derive from the recondensation of lubricating oil that passes through the engine (Brandenberger et al., 2005; Gomez-Rico et al., 2003; Spencer et al., 2006; Tritthart et al., 1992; Vaaraslahti et al., 2005), as shown by the dotted line in Figure 2-2. The sulfuric acid/sulfate fraction in total mass emissions may depend on the fuel sulfur content (Arnold et al., 2006; Liu et al., 2007; McDonald et al., 2004d; Ristovski et al., 2006; Saiyasitpanich et al., 2005), while the organic carbon fraction, consisting mainly of unburned fuel and lube oil, is influenced by engine operating conditions and is highest for engines operating at light loads when exhaust temperatures are low and soot formation is at its minimum. Figure 2-4, derived from tests in this project, shows an example size distribution shifts toward larger particles with load for a diesel generator. While the number size distribution changes substantially, the mass distribution remains similar owing to the dominance of mass emissions by the particles >100 nm.

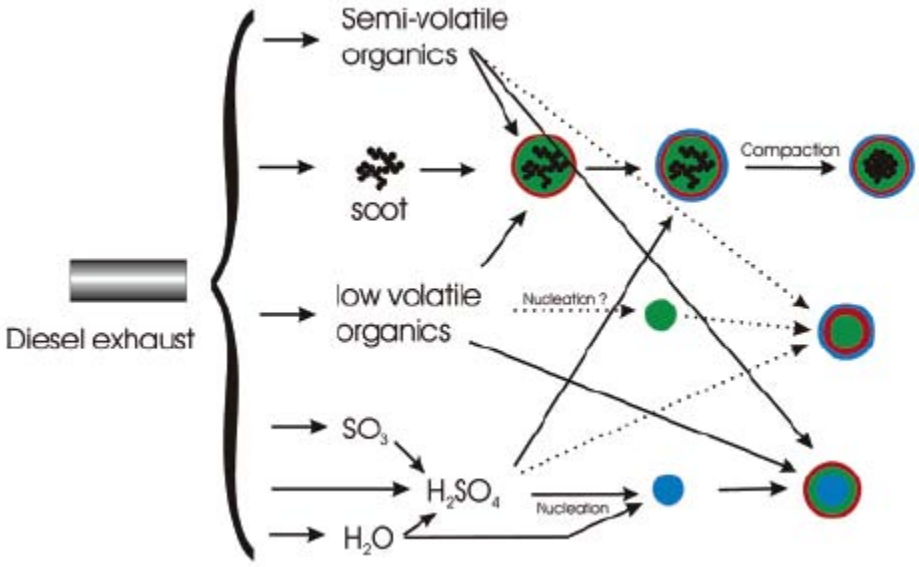

Figure 2-2. UP formation processes in diesel exhaust (Schneider et al., 2005).

Shi and Harrison (1999) determined that binary nucleation of sulfuric acid/water with condensation of organic vapors provided a qualitative rationale for their observations, but calculated nucleation rates were too low, indicating an alternative mechanism involving NH_3 as has been observed in atmospheric studies (Coffman and Hegg, 1995). Yu (2006) postulated that chemions might enhance nucleation in diesel exhaust.

Many new engines incorporate, and older engines are being fitted with, filters and traps that remove the primary soot from the exhaust stream (Cauda et al., 2006; Fino, 2007; Kittelson et al., 2006b; Schaefer-Sindlinger et al., 2007; Shah et al., 2007; Tang et al., 2007; Zabetta et al., 2006), usually at temperatures (>250 °C) that are well above ambient levels. Volatile material, such as unburned fuel and volatilized lubrication oil, passes the trap in the gas phase. Figure 2-5 shows that without the trap, most particles are in the 30 to 300 nm size range. When the particle trap is added to the same engines, the accumulation mode particles are nearly two orders of magnitude lower, but the number in the UP mode increases. Owing to the lack of available

surface on the larger particles, more of the semi-volatile organic compounds remain in the vapor phase, supersaturation is achieved resulting in nucleation. This occurs with high and low sulfur fuels, indicating that sulfuric acid nuclei may not always be necessary for UP formation. Most of the newly formed nucleation particles do not have a solid core and can be evaporated or dissolved.

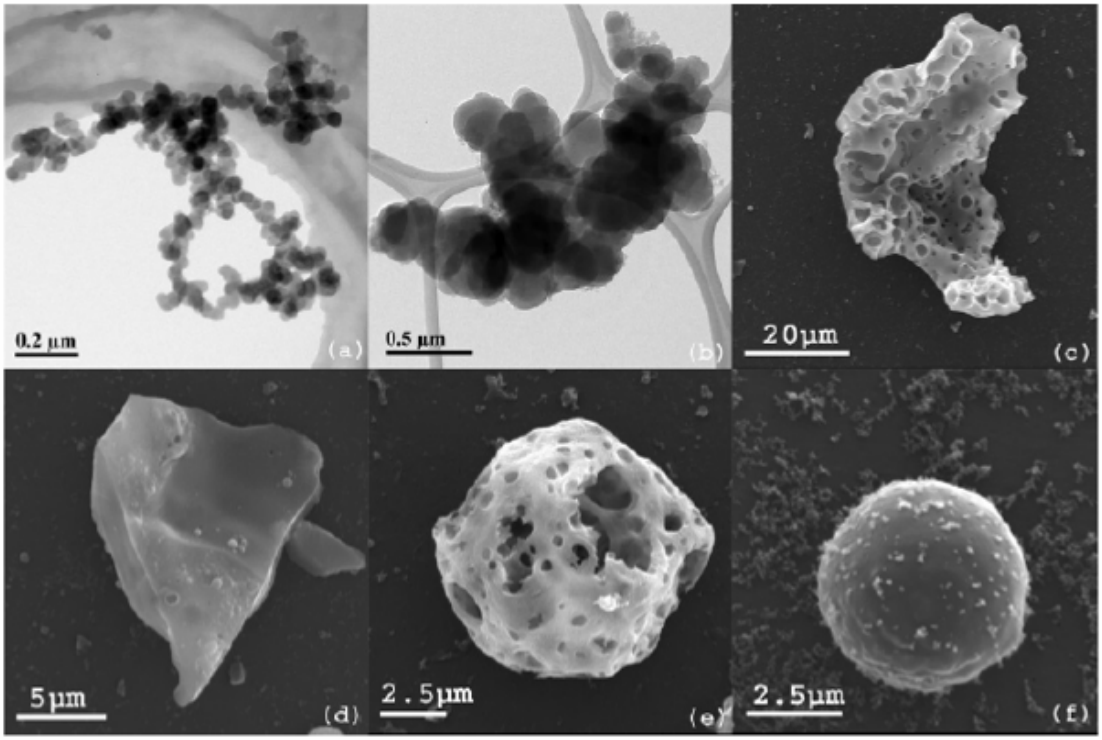

Figure 2-3. Scanning electron micrographs (from upper left) of: a) UP diesel engine emissions, b) coal combustion emissions, c) porous coal char, d) solid coal char, e) residual oil char, and f) high temperature combustion residual oil cenosphere (Chen et al., 2005). Note the differences in shape owing to the different combustion conditions for similar fuels.

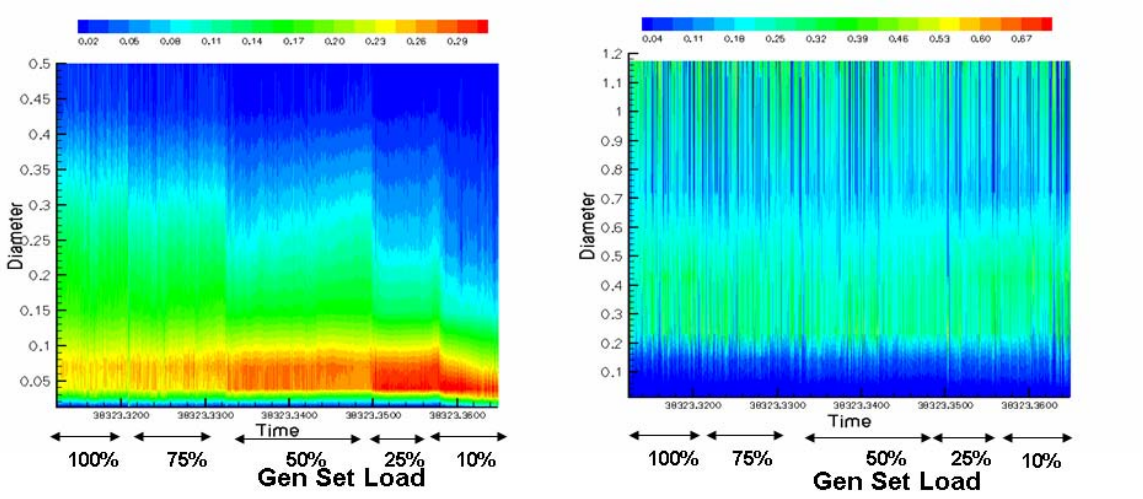

Figure 2-4. Normalized number distribution in exhaust for a 30 kW Camp Pendleton diesel generator (Gen Set) cooled and diluted to ambient conditions (left panel) and normalized mass distribution (right panel) for the same engine as a function of load. Note that the number distribution increases in size for increasing load while the mass distribution remains the same. Data were acquired in this project.

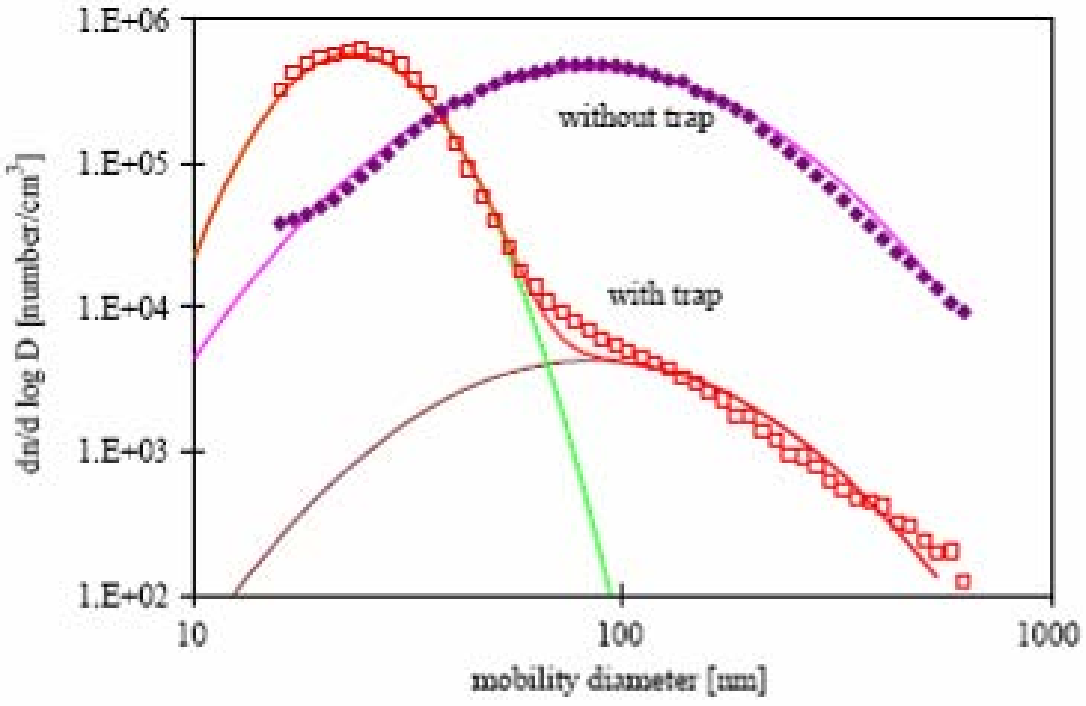

Figure 2-5. Size distributions from a diesel engine with (open squares) and without (filled diamonds) a particle trap. The removal of the large surface area provided by diesel soot implies that sulfuric acid and organic vapors can reach supersaturation levels that, upon cooling, nucleate into ultrafine particles (Burtscher, 2005).

Nucleation can be enhanced by oxidation due to catalytic systems that regenerate the particle traps. Oxidation of SO_2 to SO_3, in combination with water, may lead to the formation of sulfuric acid droplets. Although the occurrence of nucleation and the fuel sulfur content are correlated, the sulfur content of these particles is only a few percent or lower (Sakurai et al., 2003b; Sakurai et al., 2003a; Tobias et al., 2001). Their organic composition is similar to that of the lube oil with a small fraction similar to that of the fuel. This is consistent with the first step in nucleation particle formation as the nucleation of sulfuric acid and water, followed by particle growth by condensation of organic species.

Low temperature volatilization may be an identifying characteristic of lubricating oil, as shown in Figure 2-6. Most of these particles disappear when the temperature rises above 250 °C while most of them remain below 120 °C. This suggests that the OC2 fraction (organic carbon leaving a sample at 250°C in an inert atmosphere) of the IMPROVE carbon analysis method (Chow et al., 1993; Chow et al., 2001; Chow et al., 2004b; Chow et al., 2005a; Chow et al., 2007b; Watson et al., 1994) may be good indicator of the presence or absence of these particles in ambient samples, and this method is being applied to filters acquired from the in-plume sampler for diesel emissions.

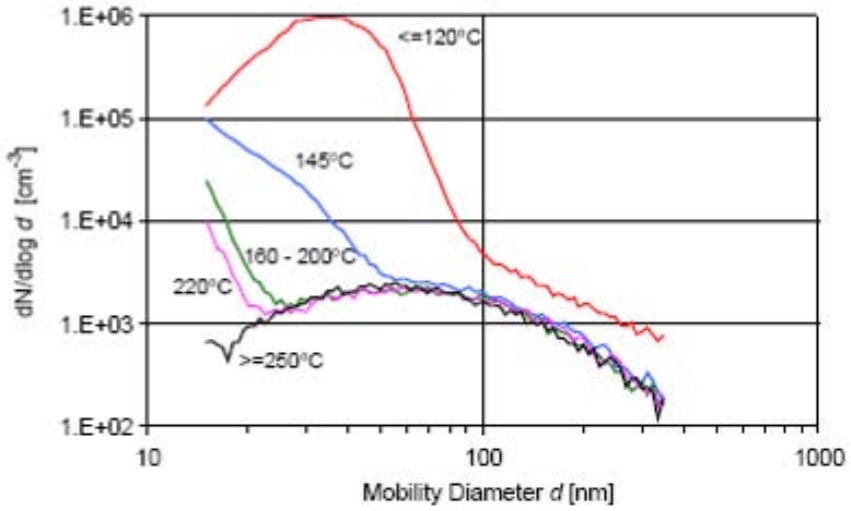

Figure 2-6. Volatility of ultrafine particles in diesel emissions with a particle trap (Burtscher, 2005). Most of these particles evaporate at temperatures <250 °C.

The UP formation process is similar in principle, but different in detail, for gasolinefueled spark ignition engines. Kayes and Hochgreb (1999a; 1999b; 1999c) postulate that liquid fuel, in droplet form or sometimes coating the cylinder, is ignited followed by locally fuel-rich diffusion burning. PM formation depends on the amount of in-cylinder liquid fuel and the probability that fuel and oxygen ignite in a diffusion flame. Particles are formed by heterogeneous-phase combustion and homogeneous gas-phase combustion, in particular under rich conditions. Once particles nucleate, they can growth or shrink, depending on available

surface areas and vapor pressures. VOC can be adsorbed on soot surfaces or can react with them.

2.6.2 Implications for PM Testing Methods

The dynamic nature of the diesel exhaust size distribution presents several problems for estimating emission rates for these particles. For certification testing, exhaust is diluted with clean air to obtain temperatures ~50 °C. For chemical source profile testing, the exhaust is brought into a dilution and aging chamber (Chang et al., 2004; Chang et al., 2005; England et al., 2007a; England et al., 2007b) that brings the temperature down to ambient (typically 15 °C to 25 °C) and allows a residence time of 10 to 90 seconds.

The following mechanisms are taking place during the cooling and aging period:

- Nucleation: When the atmosphere is supersaturated with a gas, spontaneous nucleation of small particles with ~1 nm diameter occurs. This dominates mostly in clean environments, as condensation onto existing particles is favored in more polluted environments.
- Condensation and evaporation: When the ambient vapor pressure is higher than the saturation vapor pressure, condensation occurs and particles are formed or grow to larger sizes. Saturation pressures are larger over very small particles (>5 to 10 nm) than they are over larger particles owing to their curvature (Kelvin effect), so condensation is favored on larger particles and evaporation is favored on smaller particles. Evaporation occurs with increasing temperature and with dilution of the gaseous precursors below the saturation vapor pressure. Owing to the Kelvin effect, small particles may evaporate with their vapors condensing on larger particles, thereby leading to growth.
- Coagulation: Particles collide and combine with each other when concentrations are high, thereby decreasing their number and increasing their size.
- Deposition: Particles diffuse and adhere to surfaces that they encounter.

For this reason, Zhang et al. (2005) propose the concept of "distance-based emission factors." These consider several regions:

1. At the tailpipe, where the particles are most concentrated and are at the temperature of exhaust gases.
2. In the exhaust plume, after the hot exhaust has been moderately diluted with background air and temperatures have been cooled to ambient air.
3. At the "roadside," with roadside being somewhere between the curb and ~100 m downwind of the roadway.
4. "Grid level," referring to the average over a square of ~1,000 m on a side. This would be similar to effective emissions experienced in a neighborhood that is not adjacent to a heavily traveled roadway.

Figure 2-7 shows an example of how particle number emission factors might change with distance from the point of emissions and how these might vary by season. For both highways, the I-405 which is dominated by gasoline-powered vehicles, and the I-710 which is dominated by diesel powered vehicles, there is a large difference between the roadside and grid level

emissions for the summer situation. This is probably due to higher temperatures and more photochemical activity that hastens the aerosol evolution process. The wintertime comparison (lower four panels) does not show as much variation, owing to the lower temperatures and photochemical activity. In any case, this example demonstrates that substantial variability is to be expected among the four different scales described above.

Burtscher (2005) reviewed the challenges of developing more realistic PM diesel exhaust certification methods PM. Owing to the high UP vapor pressures, their number, size, and composition distributions change rapidly with temperature and dilution. Diesel UP consists of solid soot particles with mean diameters of ~80 nm, and volatile material with diameters ~30 µm. Older engines emit more soot particles that have large surface areas for adsorption of volatile material and, therefore, lower particle numbers and larger diameters. Gas to particle nucleation becomes important after soot-removal traps that reduce the larger surface area for adsorption. Burtscher (2005) recommends that diesel exhaust size distributions be measured using a device with resolution sufficient to distinguish between different size modes. Dilution ratios need to be explicitly reported with the results. Time resolution of the measurement should be able to detect changes during transients (on the order of a few seconds).

2.7 Source Profiles

Source profiles are important for source apportionment modeling and for creating speciated emissions inventories used for photochemical dispersion models (Russell, 2008; Watson et al., 2008). Source profiles consist of the mass fractions of measured VOCs, elements, ions, carbon fractions, organic compounds, isotopic abundances, and morphological properties in emissions from different sources. Source profiles can consist of individual measurements, but they are most useful as averages from emission tests of several emitters within a same source category along with the standard deviation of the average that expresses their uncertainty. Weighted averages of sub-categories (e.g., diesel engines of a given type operating with different fuels and operating conditions) are calculated to represent different emission mixtures.

Most engine emission profiles are normalized to $PM_{2.5}$ mass emissions for compatibility with ambient samples. $PM_{2.5}$ source profiles from engine certification tests are not useful because the temperature in these tests (~50°C) does not allow for the condensation of organic vapors that occurs when exhaust cools to ambient levels (~20 °C). Engine certification tests often miss high emitting vehicles and cold starts that have higher emission rates than other parts of the operating cycle and very different source profiles (Watson et al., 2002).

VOC source profiles are expressed in ratios of $\mu g/m^3$ (which assumes all of the compounds can be identified) or parts per billion carbon (ppbC). They are normalized to a total VOC measurement (which is not always available), to the sum of measured compounds, or to the sum of the most commonly measured compounds. Watson et al. (2001) recommend VOC normalization to the sum of the commonly measured 56 compounds obtained by the Photochemical Air Monitoring Station (PAMS) (U.S.EPA, 2008a)

Diesel engine exhaust contains high EC and OC abundances (Watson et al., 1994), but on-road EC abundances have been decreasing with time as more modern engine designs and fuels penetrate the fleet (Lloyd and Cackette, 2001). Non-road engines are often of older design and may use high sulfur fuels, so the EC abundances are still substantial.

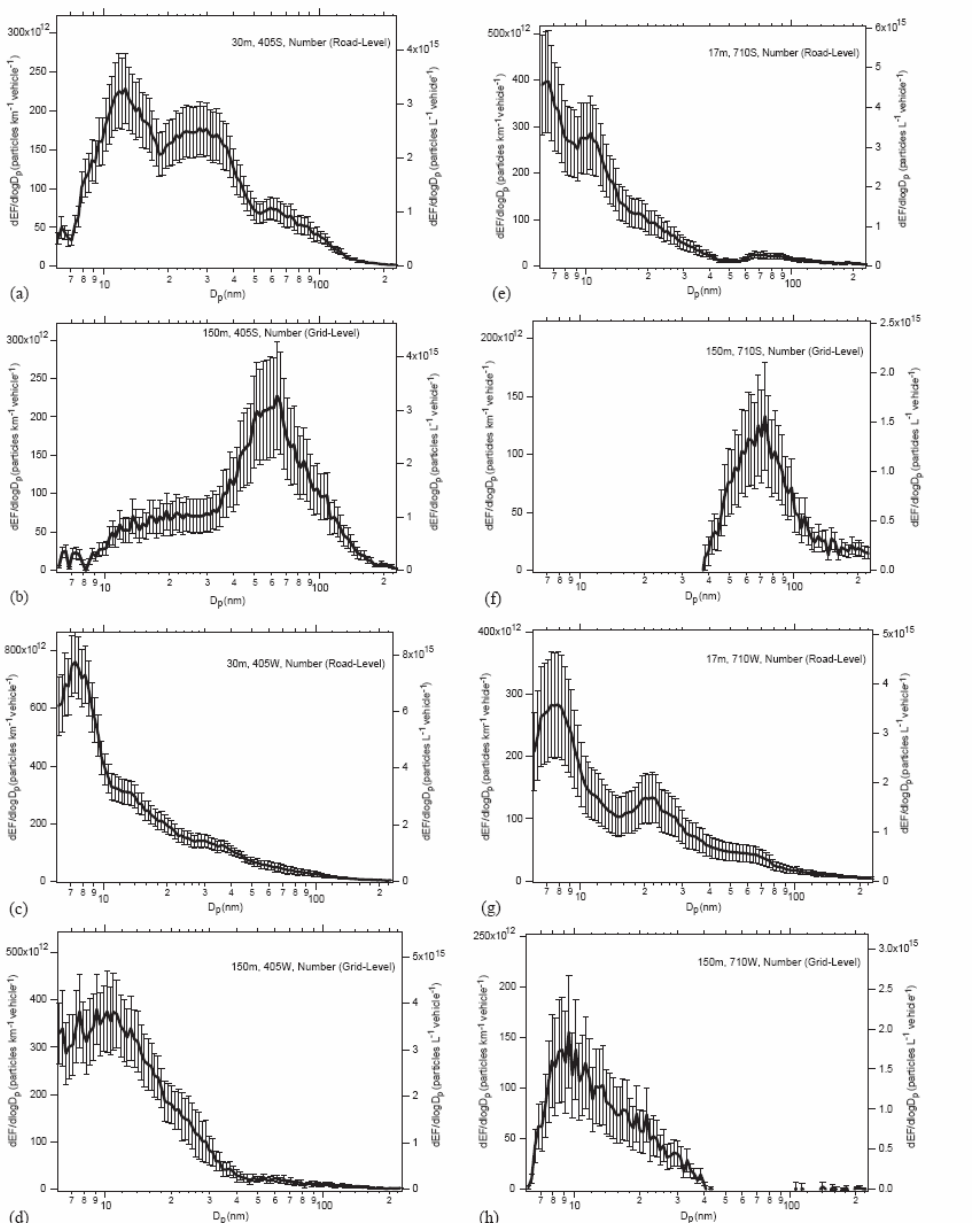

Figure 2-7. Distance-based particle number emission factors (with uncertainty bars) downwind of the I-405 and I-710 freeways in southern California (Zhang et al., 2005) for summer (top and winter (bottom). I-710 has more diesel trucks. Right axis is in terms of km traveled and left axis is in terms of particle number per liter of fuel consumed. Note the large difference in emission rate between the roadside and grid level distances**.**

OC and EC are insufficient to distinguish diesel exhaust contributions from other carbon-containing sources such as biomass burning (wildfires, prescribed burns, and residential combustion), cooking, biogenics (pollens, spores, fungi), humic-like material (fugitive dust), and secondary organic aerosol (formed from the oxidation of VOCs). More specific organic compounds are being measured along with ions, elements, and carbon fractions to better distinguish diesel exhaust contributions from those of other carbon-containing sources (Behymer and Hites, 1984; Brandenberger et al., 2005; Caravaggio et al., 2007; Chow et al., 2007d;

Fernandes and Brooks, 2003; Fraser and Lakshmanan, 2003; Fujita et al., 1998; Fujita et al., 2007a; Fujita et al., 2007b; Haefliger et al., 2000; Hildemann et al., 1991; Jakober et al., 2007; Khalili et al., 1995; Khillare et al., 2005; Kleeman et al., 2008; Lara and Feng, 2006; Lin et al., 2007b; Lough et al., 2007; Lowenthal et al., 1994; McDonald et al., 2004b; McDonald et al., 2004c; Miguel et al., 1998; Phuleria et al., 2007; Riddle et al., 2007; Riddle et al., 2008; Rogge et al., 1993; Saitoh et al., 2003; Schauer et al., 1999; Schuetzle et al., 1981; Schuetzle and Perez, 1983; Siegl et al., 1999; Strommen and Kamens, 1997; Tong et al., 1984; Tong and Karasek, 1984; Westerholm and Li, 1994; Westerholm et al., 1991; Zheng et al., 2002; Zielinska et al., 2008).

Diesel exhaust is rich in and polycyclic aromatic hydrocarbons (PAH). Hopanes are often present in the condensed lubrication oil. This contrasts with hardwood burning which is rich in guaiacols and syringols, but low in sterols such as steroid-m and cholesterol. Just the opposite is true for the meat cooking, where cholesterol is among the most abundant species. Syringols are more abundant in hard woods, such as oak or walnut, and they are depleted in softwoods such as pine, thereby allowing even greater differentiation to be achieved in source apportionment. Simoneit (1999) cites several examples of odd and even numbered carbon molecules in the n-alkane series as indicating the presence or absence of OC from manmade sources in the presence of ubiquitous contributions from natural sources.

Biogenic material, such as plant waxes or secondary organic aerosols from vegetative VOC emissions, tend to have more molecules with odd-numbers of carbon atoms, whereas carbon from combustion processes has nearly equal quantities of even and odd carbon-numbered molecules. A Carbon Preference Index (CPI), the ratio of odd to even n-alkane masses, is used to estimate the relative abundances of odd and even compounds to separate natural from manmade contributions.

Solvent extraction methods have been used to determine organic compounds (Mazurek et al., 1987), but this method requires large samples (often composites of many samples) and are costly. Solvent-extraction is costly and cumbersome for real-world diesel exhaust profiles. Thermal desorption methods (Chow et al., 2007e; Ho et al., 2008; Labban et al., 2006) have been perfected) that evaporate OC directly from a small sample, only a fraction of the normal 47 mm diameter circular filters that are acquired in speciation networks. Compounds in the desorbed materials are separated by a gas chromatograph and detected with a mass spectrometer. There are clear differences between the patterns from different sources, as seen in Figure 2-8. As more source samples are analyzed by these methods, it will become clearer which patterns (spikes and humps in Figure 2-8) are similar within a source type, but different between types. This method holds great potential for source apportionment, even in the absence of associating each pattern with a specific chemical component.

SPECIATE (Chow et al., 2004a; U.S.EPA, 2007b) is the EPA's repository of VOC and PM source profiles for a wide variety of sources. SPECIATE was recently updated and now has the capacity to incorporate new source profiles as they are submitted. $PM_{2.5}$ profiles derived from this study are to be integrated into the SPECIATE software.

2.8 Emission Models

Emission models integrate activity, emission factor, and control effectiveness information so that overall emissions can be determined. Vehicle exhaust emission models follow the form of:

$$Q_{jkn}=R_{jkn}K_{jkn}A_{jkn}(1-P_{jkn})$$

where

Q_{jkn}=Emissions rate from source type j corresponding to time period k and area n (µg/sec)

R_{jkn}=Rate of emissions (emissions factor) for a specific size fraction per unity of activity for source type *j* corresponding to time period *k* and location of sub-type *n (µg/unit of activity).*

A_{jkn}=Activity that causes dust emissions for source type *j* over corresponding to time period *k* for source sub-type *n (unit of activity/sec)*

P_{jkn}=Fractional reduction due to emissions controls applied to source j over time period *k* and location of sub-type *n (unitless)*

Each of the components of Q_{jkn} is empirically derived from a limited number of tests. These tests are intended to represent the entire population of emission factors, activity levels, size distributions, and emissions reduction effectiveness. Averaging periods are typically for a year or season and averaging areas are typically the sizes of counties or states. Each of these components of fugitive dust emission rate contains uncertainties when applied to a specific situation.

Emission models developed to implement this framework include the EPA's MOBILE6 model (Cook et al., 2007; Harley et al., 2001; Miller et al., 2003; U.S.EPA, 2008b; Yao et al., 2005) for on-road vehicles and its NONROAD model (U.S.EPA, 2005) for non-road emissions. California uses its EMFAC (EMission FACtor) (California Air Resources Board, 2007) model for on-road emissions estimates. MOBILE6.1 produces PM_{10} emission factors, replacing the earlier PART5 (Lamoree and Turner, 1999; Mishra and Padmanabhamutry, 2003; U.S.EPA, 1995)

The emphasis in all of these emission models has been on NO_x and VOC emission factors, mostly related to excessive O_3 concentrations. PM_{10}, $PM_{2.5}$, and UP emissions have been treated in a rudimentary fashion. PART5 used a single emission factor for each model year, regardless of the vehicle type, and weighted the overall emission factor by the estimated vehicle miles traveled by each model year. MOBILE6.2 added emission estimates of the air toxic pollutants benzene, methyl tertiary butyl ether (MTBE), 1,3-butadiene, formaldehyde, acetaldehyde, and acrolein.

EMFAC uses the same methodology as MOBIL6, but it is tailored to California's on-road emissions standards, vehicle mixes, and planning needs. EMFAC estimates VOC, CO, NO_x, SO_2, CO, lead (Pb), and PM emission factors in grams/mile for 1965 and newer on-road vehicles powered by gasoline, diesel, and electricity for calendar years 1970 to 2040. Emissions are reported for ten broad on-road vehicle classes defined by usage and weight. Results can be

obtained for each vehicle class by calendar year, by month, and over a 24-hour period for each district, basin, county and sub-county in California.

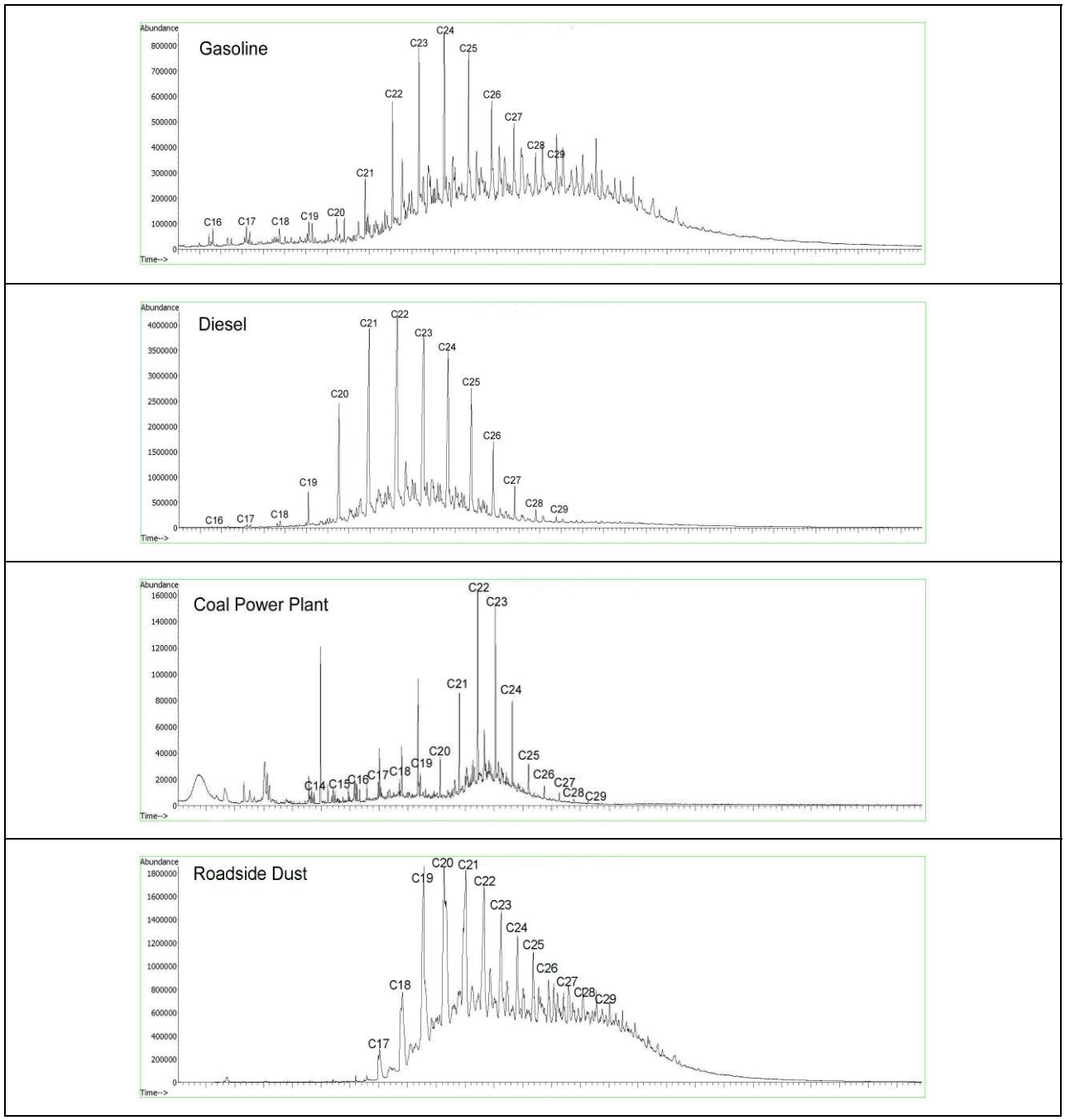

Figure 2-8. Thermal desorption gas chromatographic mass spectra for ion 57, representative of alkanes. The C labels indicate the number of carbon atoms in each peak. Similar spectra are produced for a large number of ions. Note differences in the peak structure as well as in the size and shape of the hump under the peak for different source types (Watson and Chow, 2007)..

NONROAD is the framework most amenable for adaptation to the emission factors measured in this study. It includes model estimates emissions for the following categories of vehicles and equipment: 1) recreational vehicles, such as all-terrain vehicles and off-road motorcycles; 2) logging equipment, such as chain saws; 3) agricultural equipment, such as tractors; 4) construction equipment, such as graders and back hoes; 5) industrial equipment, such as fork lifts and sweepers; 6) residential and commercial lawn and garden equipment, such as leaf and snow blowers; and 7) recreational marine vessels, such as power boats. It does not estimate emissions for commercial marine, locomotive, aircraft, or military non-road equipment. NONROAD includes more than 80 basic and 260 specific types of non-road equipment and further stratifies equipment types by horsepower rating. Fuel types include gasoline, diesel, compressed natural gas, and liquefied petroleum gas. Pollutants include VOC, NO_x, CO, CO_2, SO_x, and PM. NONROAD can be used for geographical areas encompassing the entire country, or down to the state, county, and sub-county level. It can estimate current year emissions as well as project future year emissions and backcast past year emissions for calendar years 1970 through 2050. NONROAD does not include emissions predictions for commercial marine, locomotive, aircraft, or military non-road equipment.

2.9 Summary of Literature Review

Several different test methods were found to be applied to diesel emission tests including: 1) laboratory engine or chassis dynamometer tests; 2) in-plume measurements from mobile laboratories and roadside monitors, 3) on-board exhaust measurements by portable emission monitoring systems, and 4) cross-plume measurements by remote sensors. .

Real-world tests have been made with in-plume and cross-plume systems, and these emission rates often differ substantially from those of certification tests due to the greater range of engine age and maintenance, a wide variety of operating conditions, and fuels that often differ from those specified for certification. Portable emissions monitoring systems have not yet achieved the reliability and accuracy needed for useful emission factors.

Tests using thermal denuders show that $PM_{2.5}$ and UP emission factors vary with temperature, with more condensable material found at ambient temperatures than at the higher temperatures found in exhaust pipes.

$PM_{2.5}$ source profiles are important for speciated emission inventories and source apportionment, but few of these area available for: 1) typical ambient temperatures that allow for condensation and initial chemical transformation, 2) non-road engines, applications and fuels; and 3) in a form that allows for easy access and use. EPA's SPECIATE software allow for archival of profiles acquired in this study for use by a broader applications community.

The NONROAD emission model lacks real-world representations for many non-road diesel emission factors. Measurements from tests such as those carried out in this report can be added to the NONROAD model.

3. MILITARY ENGINES, FUEL USE, AND ACTIVITY LEVELS

The different military services use a wide range of engines and fuels under a variety of operating conditions. These greatly affect the emission estimates from these sources. Military data bases were identified and studied to better understand where activity data might be obtained for emission inventories and to determine which fuels and engines are in use (Kemme et al., 2004)

3.1 Military Data Sources

Available information was insufficient to determine non-road diesel information for the Navy and Air Force, but information was available for the U.S. Army and Marine Corps (USMC). A data base of non-road diesel equipment for these services was developed in Microsoft Access with information about fuels, equipment, engines, inventories, usage, and fuel consumption (Kemme et al., 2004). The database includes an interface that allows users to view data in onscreen forms or analyze data using built in reports.

Fuel information was obtained from fuel surveys completed between 1998 and 2003 and performed first by TRW Petroleum Technologies and later by Northrop Grumman Mission Systems. These surveys contain chemical and physical information for military fuels, on-road and off-road diesel fuels, and winter and summer grade gasoline. Table 3-1 summarizes military fuel specifications.

Non-road diesel powered equipment includes combat, tactical, and ground support equipment such as: 1) wheeled vehicles, 2) tracked vehicles, 3) generator sets, 4) power plants, 5) construction equipment, and 6) material handling equipment. An engine used at a single location, such as a diesel power plant, is categorized as a stationary source, while the remaining source types are classified as mobile or area sources. Stationary source emissions are certified by different test methods than mobile sources, thereby resulting in different emission factors for the same engines, fuels, and operating conditions (Chow and Watson, 2008). Only mobile source emissions are considered in this study. Wheeled vehicles, tracked vehicles, and generators make up most of the equipment found in the database. Figures 3-1 to 3-3 show examples of military wheeled vehicles, tracked vehicles, and field generator sets.

The FED LOG Interactive Database, updated to August 2003, was accessed for equipment characteristics, cross-referencing the table of authorized material control numbers (TAMCN) to the national stock numbers for USMC equipment. Technical manuals that describe engine maintenance and operation were also consulted for detailed equipment data such as weight and fuel consumption. Engine displacement and horsepower data were collected for each engine with a unique manufacturer and model number. In some cases, a specific engine's power output varies with the type of equipment it is powering, and power ratings were averaged to assign a single value to each engine.

Equipment activity and inventory information for the Army are compiled in the Operating and Support Management Information System (OSMIS). The Navy and Air Force use the Visibility and Management of Operating and Support Costs (VAMOSC) system that contain information on ships, aircraft, missiles, torpedoes, ship systems, and aircraft subsystems, but VAMOSC does not provide information on diesel powered support equipment.

Table 3-1. Characteristics for JP-8 and Jet A military fuels (averaged analyses results of 30 samples from 6 different suppliers throughout the U.S.)

Year	2001			2002		
Number of fuels	7			28		
Fuel Type	JP-8			Jet A		
Test	Min	Avg.	Max	Min	Avg.	Max
Gravity, °API	37.3	43.1	46	39.6	42.2	46.7
Distillation Temperature:						
10% recovered, °F	333	355	388	341	369	386
50% recovered, °F	375	396	417	368	413	431
90% recovered, °F	455	465	474	410	473	510
Freezing point, °F	-81	-65	-54	-74	-52	-41
Viscosity, kinematic, -4 °F, cSt	3.71	4.59	6.5	3.11	5.28	6.85
Analine point, °F	134.1	-	134.1	129.7	139.7	154
Analine-gravity product No. °F	5,941	-	5,941	5,136	5,904	6,405
Acidity, KOH, mg/g	0.001	0.002	0.003	0.001	0.012	0.03
Sulfur:						
Total, wt.%	0.004	0.033	0.08	0	0.05	0.205
Mercaptan, wt.%	0	0	0.001	0	0.001	0.002
Naphthalenes, vol.%	0.54	1.17	1.6	0.19	1.78	2.7
Aromatic content, vol.%	15	19.8	22.1	12.1	18.6	24.8
Olefin content, vol.%	0.7	1.3	2.6	0	1.5	3.8
Smoke point, mm	19	20.9	25	18	22.3	26
Gum, mg/100ml:						
Existent, at 450 °F	0	0.3	1	0	0.7	6.4
Heat of combustion, net, BTU/lb	18,565		18,565	18,616	18,477	18,605
Thermal stability:						
Pressure drop, mm Hg	0	0.9	3	0	1.2	14
Water separometer index, No.	94	97	98	90	96	99

3.2 Database Design and Contents

Kemme et al. (2004) provide a detailed description of the data base and its contents, as summarized in Figure 3-4. Multiple tables are used with relationships indicated by the lines connecting the tables. For example, the Engines table is linked to the Equipment table using the fields “Engine_Manufacturer” and “Model_Number.” The “1” symbol in the diagram indicates the table that contains a single record that is related to many records in the other table of the relationship. For all the relationships in the database, referential integrity was enforced and the cascade update feature was activated. Enforcing referential integrity ensures that data remains consistent within the database.

Figure 3-1. Examples of military wheeled vehicles. Top left: a heavy equipment transporter (HET). Top right: a heavy expanded mobility tactical truck (HEMTT). Bottom left: a high mobility multi-purpose wheeled vehicle (HMMWV). Bottom right: interim armored vehicle (IAV), Stryker.

Figure 3-2. Examples of military tracked vehicles. Top left: Bradley fighting vehicle. Top right: M9 combat earthmover. Bottom left: M88 Hercules recovery vehicle. Bottom right: M113 armored personnel carrier (APC).

Figure 3-3. Examples of military field generators. Top left: 3 kW mobile electric power (MEP), tactical quiet generator (MEP-TQG). Top right: 30 kW trailer mounted power unit (PU); Bottom left: 200 kW MEP- TQG. Bottom right: 200 kW MEP-TQG.

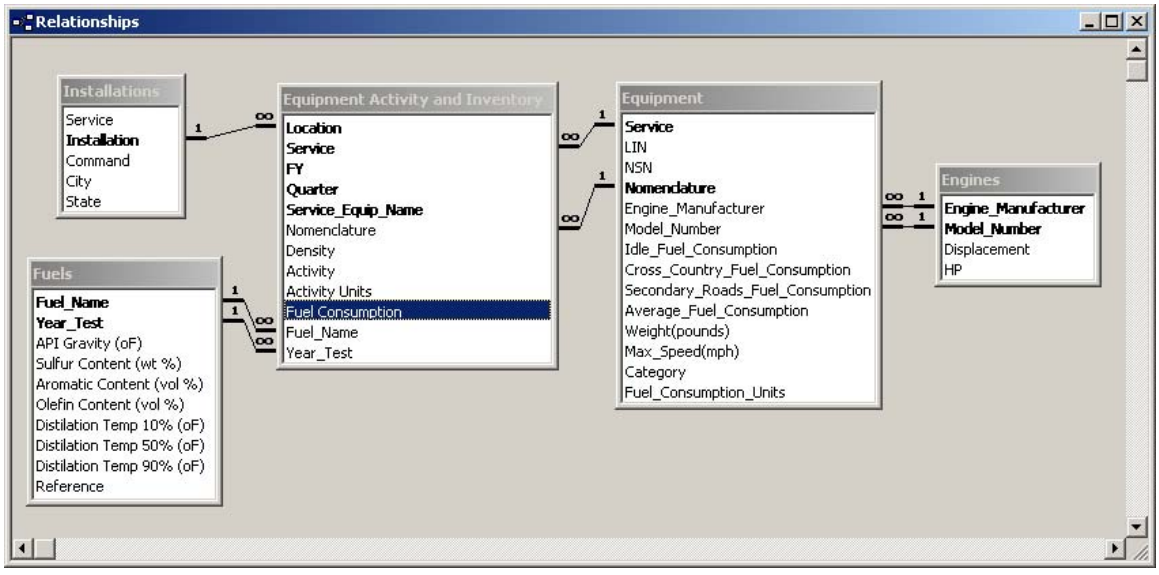

Figure 3-4. Activity data base structure.

3.3 Data Base Summaries

Table 3-2 summarizes fuel use by engine type for the top twenty consumers. A typical user of this fuel is shown in the "Representative Equipment" column. The top five ranked engines account for over 50% of the fuel usage, the top ten almost 75%, and the top 20 almost

89%. Humvees (HMMWVs), tanks (M1A1, M1A2); trucks (HEMTT, 5 ton), family of medium tactical vehicles (FMTV, 10 ton), amphibious assault vehicles (AAV), logistics vehicle systems (LVS), and Bradley fighting vehicles (M2A2, M3A2) used almost 80% of the fuel. Three generators and a forklift are included in Table 3-2, but fuel use is only from the USMC for these units because OSMIS does not report activity correctly for equipment that has usage measured in hours.

Table 3-2. Top 20 Army and USMC off-road diesel engine fuel consumption for FY2001 through FY2003.

Manufacturer	Model	Typical Equipment	No. of units	Fuel Usage (gallons)	% of Total	Cumulative Fraction
GENERAL MOTORS	6.2L	HMMWV	99,398	44,906,900	17.5%	17.5%
ALLIED SIGNAL	AGT 1500	M1A1, M1A2	4,673	40,630,794	15.8%	33.3%
DETROIT DIESEL	8V92TA	HEMTT	13,694	29,108,653	11.3%	44.6%
CUMMINS	NHC 250	5 ton truck	25,985	20,375,687	7.9%	52.5%
DETROIT DIESEL	6V53T	LAV, APC	5,395	18,513,284	7.2%	59.7%
CUMMINS ENGINE	6CTA8.3	5 ton truck	13,866	12,007,328	4.7%	64.4%
CATERPILLAR	3116 ATAAC	FMTV	12,944	10,041,649	3.9%	68.3%
CUMMINS	VT400	AAV	1,147	9,449,304	3.7%	72.0%
DETROIT DIESEL	8V-92	MK48 LVS	1,308	8,379,559	3.3%	75.2%
CUMMINS	NTC 400	10 ton truck tractor	4,103	6,020,515	2.3%	77.6%
CUMMINS	VTA-903T	M2A2, M3A2	3,528	5,628,003	2.2%	79.8%
JOHN DEERE	6466 6.8L	Tractor, Loader	513	5,501,174	2.1%	81.9%
CATERPILLAR	3126B	Stryker, FMTV	3,018	4,840,063	1.9%	83.8%
ALLIS CHALMERS	3500	60 kW generator	1,023	4,504,264	1.8%	85.6%
CONTINENTAL	LDS465-1	M35A2, 2.5 ton truck	11,227	3,851,595	1.5%	87.1%
CONTINENTAL	AVDS1790-2DR	M88A1 recovery vehicle	1,799	3,196,994	1.2%	88.3%
HERCULES	D298ERX37	30 kW generator	1,089	2,928,512	1.1%	89.4%
CONTINENTAL	LD465-1	M35A2 2.5 ton truck	7,798	2,388,461	0.9%	90.4%
ONAN DIV	DN4M1	10 kW generator	2,977	2,209,545	0.9%	91.2%
JOHN DEERE	6059T	Truck forklift	2,291	2,093,352	0.8%	92.0%

Since the activity information in the database includes FY2001 through FY2003, the data might reflect changes in equipment usage that occurred within DoD over that time period. To illustrate that change, the Engine Fuel Consumption report was run for both the Army and USMC FY2003, as shown in Table 3-3. Ranking of the top six engines remained the same as in that in Table 3-2, and the total fuel consumption for these six engines accounted for almost the same fraction of the total. The Caterpillar 3126B engine showed the largest increase in fuel consumption due to increased deployment and use of the Stryker vehicle between FY2001 and

FY2003. Engines used in generators also increased over this period. Decreased fuel use is evident for the Cummins Engine VT 400 which powers the USMC AAV, the Cummins Engine NTC 400 which powers Army 10 ton trucks, and the John Deere 6466 6.8L which powers a USMC tractor/loader. These changes over a three-year period indicate that the data base can and should be periodically updated.

Table 3-4 shows the top ten engines ranked by their fuel consumptions in FY2003 for the Army and Table 3-5 shows the same information for the Marine Corps. A similarity between the services is that the top ten engines account for a large percentage of the overall fuel usage with overall percentages of 92.9% and 84.5% for the Army and USMC respectively. The M1 tank, powered by the Allied Signal AGT 1500 turbine engine, accounts for the 2nd highest fraction of fuel usage for both services. One difference between the services is the larger amount of overall fuel usage by the Army. The tables also indicate a larger reliance on trucks for the Army with the engines that power trucks accounting for 42.8% of overall fuel consumption in Table 3-4 and 20.8% in Table 3-5.

Table 3-3. Top 20 Army and USMC off-road diesel engine fuel consumptions for FY2003.

Manufacturer	Model	Typical Equipment	No. of units	Fuel Usage	% of Total	Cumulative Fraction
GENERAL MOTORS	6.2L	HMMWV	94,928	14,743,248	17.3%	17.3%
ALLIED SIGNAL	AGT 1500	M1A1, M1A2	4,973	14,129,437	16.5%	33.8%
DETROIT DIESEL	8V92TA	HEMTT	12,693	10,223,560	12.0%	45.8%
CUMMINS	NHC 250	5 ton truck	23,525	7,112,306	8.3%	54.1%
DETROIT DIESEL	6V53T	LAV, APC	5,451	4,812,455	5.6%	59.7%
CUMMINS	6CTA8.3	5 ton truck	12,142	4,409,017	5.2%	64.9%
CATERPILLAR	3126B	Stryker, FMTV	5,017	3,822,348	4.5%	69.3%
CATERPILLAR	3116 ATAAC	FMTV	11,952	3,536,020	4.1%	73.5%
CUMMINS	VTA-903T	M2A2, M3A2	3,493	2,566,129	3.0%	76.5%
ALLIS CHALMERS	3500	60 kW generator	1,215	2,554,053	3.0%	79.5%
DETROIT DIESEL	8V-92	MK48 LVS	1,298	2,175,720	2.5%	82.0%
CUMMINS	VT400	AAV	1,161	2,167,047	2.5%	84.6%
CUMMINS	NTC 400	10 ton tractor	3,820	1,893,010	2.2%	86.8%
HERCULES	D298ERX37	30 kW generator	1,439	1,127,779	1.3%	88.1%
CONTINENTAL	LDS465-1	M35A2, 2.5 ton truck	10,036	1,018,161	1.2%	89.3%
ONAN DIV	DN4M1	10 kW generator	3,864	1,004,081	1.2%	90.5%
CONTINENTAL	AVDS1790-2DR	M88A1 recovery vehicle	1,889	899,277	1.1%	91.5%
GENERAL MOTORS	6.5L	Heavy HMMWV	5,701	823,044	1.0%	92.5%
JOHN DEERE	6059T	Truck forklift	2,453	660,040	0.8%	93.2%
DETROIT DIESEL	DDEC II	20 ton truck	1,375	618,550	0.7%	94.0%

Table 3-4. Top 10 Army off-road diesel engine fuel consumptions for FY2003.

Manufacturer	Model	Typical Equipment	No. of units	Fuel Usage (gallons)	% of Total	Cumulative Fraction
GENERAL MOTORS	6.2L	HMMWV	82,877	13,004,748	21.4%	21.4%
ALLIED SIGNAL	AGT 1500	M1A1, M1A2	4,570	11,023,169	18.1%	39.5%
DETROIT DIESEL	8V92TA	HEMTT	12,693	10,223,560	16.8%	56.4%
CUMMINS	NHC 250	5 ton truck	17,521	4,939,199	8.1%	64.5%
CUMMINS	6CTA8.3	5 ton truck	12,142	4,409,017	7.3%	71.7%
CATERPILLAR	3126B	Stryker, FMTV	5,017	3,822,348	6.3%	78.0%
CATERPILLAR	3116 ATAAC	FMTV	11,952	3,536,020	5.8%	83.8%
CUMMINS	VTA-903T	M2A2, M3A2	3,493	2,566,129	4.2%	88.1%
CUMMINS	NTC 400	10 ton tractor	3,820	1,893,010	3.1%	91.2%
CONTINENTAL	LDS465-1	M35A2, 2.5 ton truck	10,036	1,018,161	1.7%	92.9%

Table 3-5. Top 10 USMC off-road diesel engine fuel consumptions for FY2003.

Manufacturer	Model	Typical Equipment	No. of units	Fuel Usage (gallons)	% of Total	Cumulative Fraction
DETROIT DIESEL	6V53T	LAV	679	4,153,055	16.8%	16.8%
ALLIED SIGNAL	AGT 1500	M1A1, M1A2	403	3,106,268	12.6%	29.4%
ALLIS CHALMERS	3500	60 kW generator	609	2,553,774	10.4%	39.8%
DETROIT DIESEL	8V-92	5 ton truck, MK48 LVS	1,298	2,175,720	8.8%	48.6%
CUMMINS ENGINE	NHC 250	5 ton truck, M923A1	6,004	2,173,107	8.8%	57.4%
CUMMINS ENGINE	VT400	AAV	1,161	2,167,047	8.8%	66.2%
GENERAL MOTORS	6.2L	HMMWV	12,051	1,738,500	7.0%	73.2%
HERCULES	D298ERX37	30 kW generator	1,010	1,127,608	4.6%	77.8%
ONAN DIV	DN4M1	10 kW Generator	1,343	1,004,037	4.1%	81.9%
JOHN DEERE	6059T	Truck forklift, 60 kW generator	613	659,871	2.7%	84.5%

Although engines in the most frequently used categories were sought out for the tests described in subsequent chapters were sought for testing, these were not always available owing to operational and equipment availability constraints at the test sites.

3.4 Non-Road Vehicle Activity Measurements

Non-road military engine activities that might affect emissions are unknown. They probably do not correspond to the test cycles used for engine certification. Methods to measure

these activities for relation to emission factors are under development, but they are not yet ready for practical application. Modern on-road diesels have electronic control modules (ECMs) that register information summarized in Table 3-6. ECMs require a data logger for long-term measurements, as their memory capacity is limited. The primary purpose for acquiring these data are to electronically optimize engine operation, with a secondary purpose being to diagnose problems. Their use for emissions activity levels is a secondary consideration. Non-road engines, especially older ones, do not have ECMs, and many military engines fall into this category.

Table 3-6. Parameters monitored by ECMs on modern, on-road diesel engines by manufacturer.

Parameter	Caterpillar	Cummins	Detroit Diesel
Vehicle #	√	√	√
Date	√	√	√
Manufacturer	√	√	√
Engine Model	√	√	√
VIN	√	√	√
Engine Serial Number	√	√	√
ECM Serial Number	√	√	√
Advertised Power	√	√	√
Governed Speed	√	√	√
Peak Torque	√	√	√
RPM at Peak Torque	√	√	√
Total Time	√	√	√
Total Distance	√	√	√
Total Fuel Used	√	√	√
Total Fuel Economy	√	√	√
Total Idle Fuel	√	√	√
Total Idle Time	√	√	√
% Time at Idle	√	√	√
Total PTO Fuel	√	√	√
Total PTO Time	√	√	√
% Time at PTO	√	√	√
Total Cruise Time			√
% Time at Cruise			√
Total Brake Time			√
Avg Load Factor	√		
Brake actuations/1000 miles		√	

As part of this project, data from 270 on-road in-use heavy-duty diesel vehicles was compiled when they entered an independent repair shop for maintenance work and the utility of these data was explored for determining vehicle fleet characteristics and activity analysis (Huai et al., 2006). Figure 3-5 compares operating cycles for long-haul and short-haul trucks. The

long-haul spends most of the time at high speed while the short-haul spends most of the time at idle and low speeds. Total emissions will be substantially different for the different operating modes, but the certification emission rates will be the same.

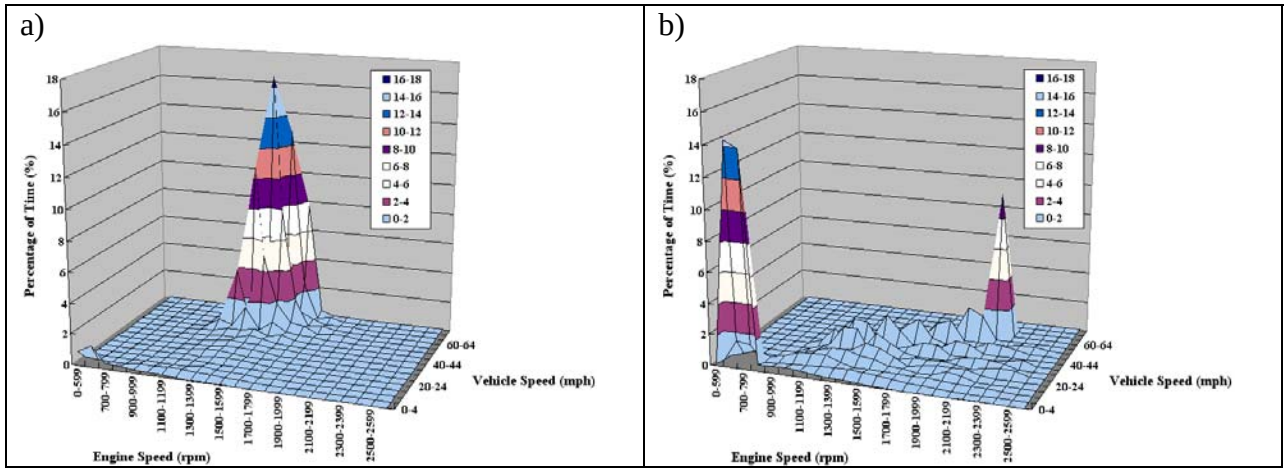

Figure 3-5. Histograms of RPM and Speed for: a) a long-haul truck; and b) a short-haul/intra-city truck

Although not currently practical for most military engines, there may be more potential to take advantage of newer engines equipped with ECMs as they penetrate the military engine fleet.

3.5 Summary of Engine, Fuel Use and Activity Findings

Engine and fuel use data are well defined on an annual basis for the Army, but not for the other services. The US Marine Corps also has good overall records, but does not have the spatially and temporal detail of the Army data base that would allow emissions to be easily estimated for individual military bases. Fuel use data is available for the Air Force and Navy, but the relatively small amount used for non-road diesel engines cannot be separated from the total fuel use, which is dominated by aircraft and ships.

M1 tanks used 16% of all fuel for CY2001-2003. These tanks use turbines rather than CI engines. For the CI engines, the HMMWV (GM6.2L engine) use 18% of the total, the HEMTT (Detroit Diesel 8V92TA engine) used 11% of the total, 5-ton trucks (Cummins NHC250 and 6CTA8 engines) used 12% of the total, the LAV/APCs (Detroit Diesel 6V53T engine) used 7% of the total, and the FMTV (Caterpillar 3116-ATAAC engine) used 4% of the total. Together these engines and units accounted for more than 75% of the Army and Marine Corps fuel use. There was some, but not major, difference in year-to-year fuel consumption amounts.

Operating cycles for military engines are not well understood. New engines with electronic control modules acquire some of the operating information needed to determine these, but these ECMs are not on most of the older military equipment. Using ECM data as these new engines penetrate the military fleet offers a higher potential to better characterize their operating characteristics.

4. DEVELOPMENT OF TEST METHODS AND PROCEDURES

Advances were made on each of the emissions measurement methods developed for this project: 1) Mobile Emissions Laboratory (MEL), 2) on-board Portable Emissions Monitoring Systems (PEMS) for gases, 3) In-Plume Emissions Testing Systems (IPETS), 4) cross-plume Vehicle Remote Sensor Systems (VERSS), 5) on-board PM monitor. Comparisons among the emissions rates derived from several of these were undertaken and evaluated.

4.1 Mobile Emissions Laboratory (MEL) System

The University of California at Riverside (UCR) MEL (Cocker et al., 2004a; Cocker et al., 2004b; Durbin et al., 2007b; Durbin et al., 2007a; Durbin et al., 2008; Sawant et al., 2007b; Shah et al., 2004; Shah et al., 2005; Shah et al., 2006b; Shah et al., 2006a) is illustrated in Figure 4-1 with monitoring equipment detailed in Table 4-1.

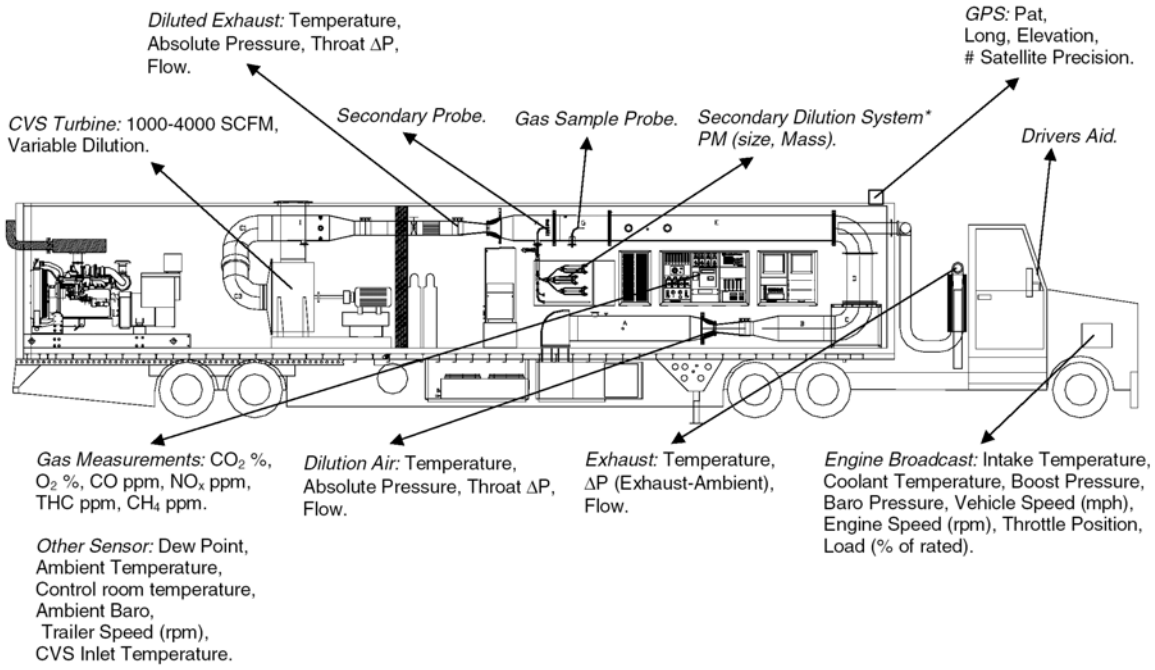

Figure 4-1. The UCR Mobile Emissions Laboratory (MEL).

The MEL samples the full output from a diesel engine as input into a primary dilution tunnel. The primary dilution system is configured as a full-flow constant volume sampling (CVS) system with a smooth approach orifice (SAO) venturi and dynamic flow controller. The SAO venturi has no moving parts and repeatable accuracy at high throughput with low-pressure drop. The SAO with dynamic flow control eliminates the need for a heat exchanger, as is required for dilution tunnels with a positive displacement pump or a critical flow orifice. Tunnel flow rate is adjustable from 1000 to 4000 scfm with accuracy of 0.5% of full scale. It is capable of total exhaust capture for engines up to 600kW.

Gas analyzers are mounted on shock absorbing benches and continuously record concentrations of the gases in Table 4-1 at one second intervals. 200-L Tedlar bags collect tunnel and dilution air samples over a complete test cycle. Eight bags are suspended in the MEL allowing four test cycles to be performed for a single run. Filling of the bags is automated with Lab View 7.0 software (National Instruments, Austin, TX).

Table 4-1. MEL instrumentation and observables measured.

Instrument/Method	Observable	Sample Duration	Lower Quantifiable Limit
Pierburg NDIR	CO_2, CO	1 s	50 - 500 ppm
California Analytical Instruments/ Flame Ionization Detection	THC, CH_4	1 s	10 - 30 ppm
California Analytical Instruments/ Chemiluminescence	NO, NO_2	1 s	10 ppm
Various/Filter*	$PM_{2.5}$ Mass and Chemical Composition	0.25 - 2 hrs	Various
Tedlar Bag/GC-FID	VOC's ($C_2 - C_{12}$)	0.25 - 2 hrs	10 ppbC
DNPH Cartridges/Shimadzu HPLC/UV	Aldehydes and Ketones	0.25 - 2 hrs	0.02 µg/mL

*****Includes Teflon and quartz media for mass, metals, ions, elemental/organic carbon and PAHs by GC/MS on extracts from filters.

MEL emission estimates were compared with those measured by the ARB during 2002 on a Freightliner tractor equipped with a 475 hp, MY2000 Caterpillar C-15 diesel engine. The truck was operated on ARB's heavy-duty chassis dynamometer following the transient Urban Dynamometer Driving Schedule (UDDS), a 40 mph steady state, and a 55 mph steady state.

MEL emission estimates were slightly higher than the ARB estimates for the UDDS (10.1% for HC, 13.0% for CO, 8.9% for NOx, and 5.2% for CO_2. MEL emissions for the 40 mph test were 7.4% higher for HC, 12.3% higher for CO, 4.0% higher for NOx, and 4.9% higher for CO_2. For the 55 mph test, the MEL yielded 16.4% higher HC, 3.7 higher CO, 4.0% NO_x, and 5.5% higher CO_2 emissions.

A second comparison was performed using the same, but adding PM filter measurements with the MEL filter face temperature adjusted to 27 °C (81°F) to match the ARB's PM collection system. A retest in the MEL with the filter face temperature set to 47 °C (117°F) recovered ~11% less PM mass than the MEL test at 27 °C, consistent with the literature findings in Section 2 that lower temperatures allow more condensation of volatile material. MEL emissions measurements were higher than those of ARB by 11.8% for HC, 18.4% for CO, 8.0% for NO_x, 2.7% for CO, and 0.1% for PM at the 27 °C temperature. Such differences are common among different test methods, and even among duplicate tests of the same engines, fuels, and cycles operating on the same test stand.

A more comprehensive comparison was executed during 2006 using the Southwest Research Institute's (SwRI) testing facilities. Emissions were generated from a modern diesel engine on the Not to Exceed (NTE) test cycle (Krishnamurthy and Gautam, 2006) that intends to better simulate real-world on road driving activities, and on the Ramped Modal Cycle (RML) (Jackson et al., 2005). Tables 4-2 and 4-3 compare results from replicate tests among the laboratories and test cycles. For the NTE emissions cycle, the MEL was 2.1% higher than the SwRI measurement for NO_x and 2.7% higher than the SwRI rate for CO_2 emissions. For the RMC, the MEL was 3.8% higher than the SwRI measurement for NO_x and 2.3% higher for CO_2.

The deviations were much larger for other pollutants, mostly because the emissions were low for this modern engine under both driving cycles. PM emissions, for example, were not detected by these certification methods.

Table 4-2. Comparison of MEL and SwRI emissions for the Not to Exceed (NTE) cycle.

Test Day	Test Date	Test Laboratory	Transient Emissions[a], g/hp-hr							Work hp-hr
			THC	CH_4	NMHC	CO	NO_x	PM	CO_2	
1	6/29/2006	SwRI	0.003	0.000	0.004	0.057	1.98	0.000	541.1	84.6
1	6/29/2006	MEL	0.001	0.002	-0.001	0.043	2.03		557.8	
		Day 1 comparison	-288%	119.7%	546.0%	-31.7%	2.4%		3.0%	
2	6/30/2006	SwRI	0.003	0.002	0.002	0.056	2.02	0.000	542.3	
2	6/30/2006	MEL	0.001	0.002	0.000	0.041	2.04		552.3	
		Day 2 comparison	-148.3%	8.2%	556.3%	-38.2%	1.0%		1.8%	
3	7/5/2006	SwRI	0.004	-0.001	0.005	0.053	2.00	0.000	540.4	
3	7/5/2006	MEL-3	0.001	0.002	-0.001	0.042	2.06		557.1	
		Day 3 comparison	-159.4%	152.1%	960.2%	-26.2%	2.9%		3.0%	
Standard			0.14	0.14	0.14	15.5	2.2			
NTE	SwRI	Mean	0.004	0.000	0.004	0.056	2.001		541.3	
		Stdev	0.001	0.004	0.004	0.002	0.020		1.1	
	MEL	Mean	0.001	0.002	-0.001	0.042	2.044		555.7	
		Stdev	0.000	0.000	0.000	0.001	0.014		2.9	
		%point	-65.1%	2336.2%	-117.4%	-24.2%	2.1%		2.7%	
		%standard	-1.6%	1.3%	-2.9%	-0.1%	1.9%		n/a	

[a]THC=Total Hydrocarbons, CH_4=Methane, NMHC=Non-Methane Hydrocarbons, CO=Carbon dioxide, NO_x=Oxides of Nitrogen, PM=Particulate Matter, CO_2=Carbon Dioxide.

These comparisons illustrate one of the major limitations of certification methods as a way to quantify real-world emissions. The test methods are designed for accuracy near the upper limits set by the emission standards. As long as the emissions are well below that limit, accuracy and precision are not deemed to be important because the engine passes the certification test. For air quality planning purposes, however, even low emission rates are important as they may add up to a large source over the many engines that are in operation.

Table 4-3. Comparison of MEL and SwRI emissions for the Ramped Modal Cycle (RMC).

Test Day	Test Date	Test Number	Transient Emissions[a], g/hp-hr							Work hp-hr
			THC	CH_4	NMHC	CO	NO_x	PM	CO_2	
1	6/29/2006	SwRI	0.004	0.001	0.003	0.055	1.80	0.000	499.8	164.0
1	6/29/2006	MEL	0.000	0.001	-0.002	0.050	1.88		511.1	164.1
		Day 1 comparison	-109%	23%	-160%	-9.5%	4.6%		2.3%	
2	6/30/2006	SwRI	0.002	0.000	0.002	0.053	1.84	0.000	500.8	164.0
2	6/30/2006	MEL	0.001	0.002	-0.001	0.042	1.90		508.5	164.0
		Day 2 comparison	-72%	1586%	-161%	-21%	3.6%		1.5%	
3	7/5/2006	SwRI	0.002	0.002	0.000	0.052	1.85	0.000	499.0	163.9
3	7/5/2006	MEL	0.000	0.001	-0.001	0.043	1.91		514.4	164.3
		Day 3 comparison	-84%	-35%	-314%	-17%	3.2%		3.1%	
Standard			0.14	0.14	0.14	15.5	2.2			
RMC	SwRI	Mean	0.003	0.001	0.002	0.053	1.827		499.9	
		Stdev	0.001	0.001	0.001	0.002	0.024		0.9	
	MEL	Mean	0.000	0.002	-0.001	0.045	1.897		511.3	
		Stdev	0.000	0.001	0.001	0.004	0.015		2.7	
			-92.6%	42.9%	-171.9%	-16%	3.8%		2.3%	

[a]THC=Total Hydrocarbons, CH_4=Methane, NMHC=Non-Methane Hydrocarbons, CO=Carbon dioxide, NO_x=Oxides of Nitrogen, PM=Particulate Matter, CO_2=Carbon Dioxide.

4.2 Portable Emissions Monitoring Systems (PEMS)

Small, battery-powered sensors that could be located on vehicles or engine housings to analyze a portion of the exhaust stream after it cools to ambient temperatures would be ideal for characterizing non-road diesel emissions. The engines could be used in their normal manner, with little cooperation needed from the operator. By moving PEMS among different units, a large emissions data base could be acquired for many different engines, fuels, and modes of operation. As noted in Section 2, PEMS have not yet reached the level of compactness, power efficiency, reliability, precision, and accuracy needed for their use on a routine basis. PEMS development was tracked throughout the duration of this project, and several systems were obtained and evaluate. Unfortunately, none of these proved useful for the emissions tests to be described later.

The following PEMS were operated alongside the MEL for evaluation purposes:

- Clean Air Technologies, Inc.'s (CATI, test.cleanairt.com) Montana system that measures NO_x, HC, CO and CO_2 gases and infers PM mass emissions from laser light scattering.
- Engine, Fuels and Emissions Engineering's (www.efee.com) RAVEM system which measures NO_x, HC, CO and CO_2) and quantifies PM by integrated filter sampling.
- Horiba's (www.ats.horiba.com/obs2000.html) OBS-2000 series system that measures THC, CO, NO_x, and CO_2.
- Sensors, Inc.'s (www.sensors-inc.com) Semtech D system that measures NO, NO_2, THC, CO and CO_2.

The PEMS and the MEL simultaneously sampled the diluted exhaust generated by a CAT 3406C diesel backup generator operating at 5%, 25%, 65%, and 100% of full power. Figure 4-2 compares differences of each PEMS with respect to the MEL operating in its Federal Reference Method (FRM) mode.

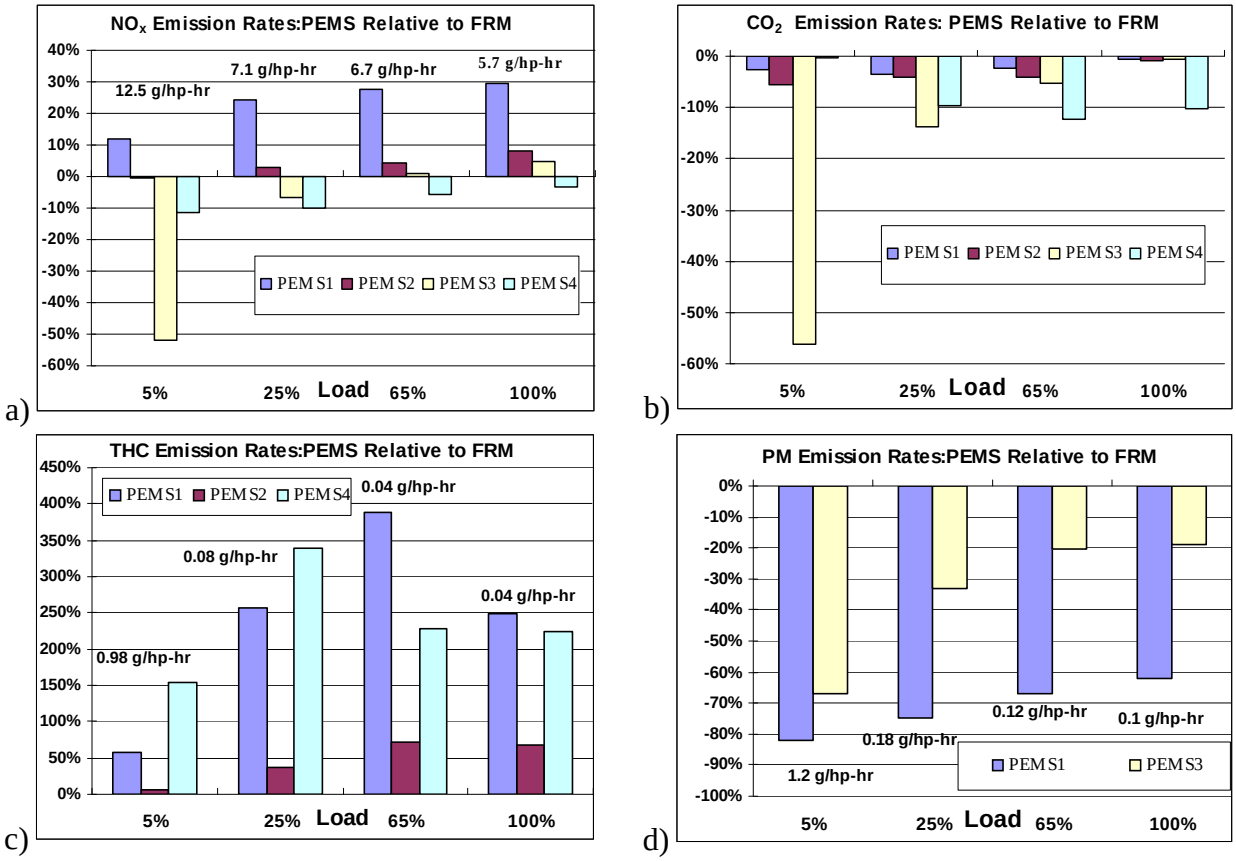

Figure 4-2. Over (positive) or under (negative) estimation (y-axis) of different PEMS relative to the MEL FRM emission rate for a) NO_x, b) CO_2, c) THC (total hydrocarbons), and d) PM. MEL FRM emission rates are listed above each set of data. PEMS are labeled PEMS1, PEMS2, PEMS3, and PEMS4 owing to non-disclosure agreements with the manufacturers made prior to the test.

The agreement for CO_2 was good for PEMS1, 2, and 4, with PEMS4 having the highest overall difference, about 10%. The agreement of PEMS3 was good at the highest engine load and flow rates, but the difference was about 50% at the lowest engine load. The PEMS3 manufacturer found a failed component that caused the errors at the low flow rates.

NO_x values agreed within ~10% for PEMS2 and 4. PEMS3 showed good agreement at high loads, with larger differences at the lowest load. For PEMS3, the NO_x/CO_2 ratios, which minimize the effects of flow rate inaccuracies, were within 10% of those measured by the MEL FRM for all engine loads. PEMS1 values were 12% to 30% higher. Some of the differences in NO_x emissions for the PEMS1 are related to the omitted humidity correction (~10%) and a bias of about the same magnitude observed with the calibration gases, since the flow rates agree with those of the MEL FRM.

PEMS THC values were much higher than those quantified by the MEL FRM. As in the MEL/SwRI comparisons, THC values were much lower than the emission limits. Since PEMS1, 2 and 4 had accurate flow measurements, the source of the difference must be in the measured concentration. These instruments (including the MEL) are designed for certification rather than real-world emission purposes, deviations are expected at these low emission rates. The PEMS2 vendor noted that THC concentrations were outside the range of the instrument design.

PEM1 and 3 PM emissions were 20% to 80% lower than those determined by the MEL, but the differences were smaller at higher engine loads. Actual PM emissions were again much lower than the certification limits. This again illustrates the difficulty in obtaining accurate PM emission measurements by all of the instruments.

PEMS were also evaluated on ARB's heavy duty chassis dynamometer with emissions from a 1993 Kenworth T600 truck equipped with a 2003, 475 hp Caterpillar C-15 ACERT engine certified to 2.5 g/bhp-hr NO_x + NMHC and 0.1 g/bhp-hr PM standards. Test cycles included: 1) a three-mode steady-state NTE; 2) a stepped NTE; 3) The UDDS; and 4) a 50-mph steady state cruise mode from the ARB 5-mode test cycle.

Within each engine speed, three loads were tested, nominally 40%, 70%, and 100%. Two full tests were conducted at each engine speed. A second NTE cycle was designed with a "stepped" pattern, intended to simulate NTE-type vehicle/engine operation in a predictable and controlled manner (i.e., gentle accelerations between modes and steady-state operation at each load point). This test cycle was designed to clearly delineate entry into, operation within, and exit, from the NTE-defined zone of engine operation. For the NTE stepped cycle, two sets of three runs were performed. The UDDS and 50-mph cruise cycle were intended to represent real-emissions. Seven runs were conducted for both the UDDS and 50-mph cruise cycles.

Emissions from the NTE steady state and stepped cycles were integrated over the entire cycle period for a particular speed (for the NTE steady state cycle) and over all steps (for the NTE stepped cycle). Figure 4-3 compares CO_2 and NO_x emissions among the different measurement systems.

PEMS measured slightly higher CO_2 emissions than the MEL FRM for each of the different cycles. PEMS2 CO_2 emissions were within 5% of the FRM for most of the tests, with no statistically significant differences for the NTE 1290 rpm, 1500 rpm and 1770 rpm steady state cycles. PEMS3 CO_2 emissions differences ranged from 9 to 14% higher for the different cycles. PEMS4 CO_2 emissions were 11 to 26% higher than those measured by the MEL FRM.

When a CO_2 audit standard was submitted to PEMS4 it read ~17% higher than the specified audit value.

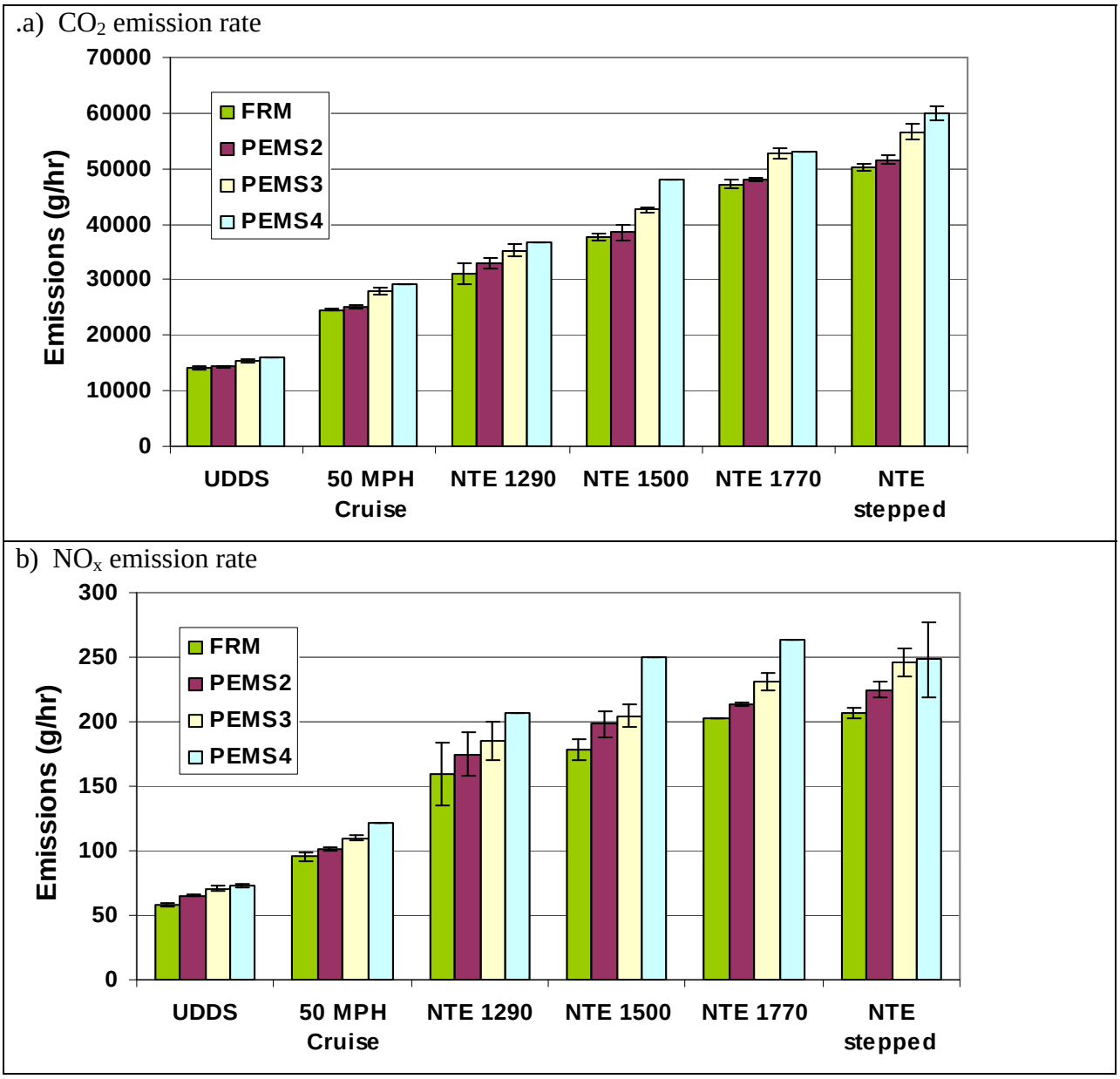

Figure 4-3. Mass emissions rates (g/hr) for a) CO_2 and b) NO_x measured by PEMS and the MEL FRM. Error bars are 95% confidence limits calculated when multiple test results were available.

PEMS NO_x readings were higher than those measured by the MEL FRM. PEMS2 yielded results 5 to 12% higher than the FRM for the different cycles. PEMS3 NO_x emissions were 14 to 21% higher than the FRM, and PEMS4 showed the largest differences ranging from 19 to 40% above the MEL FRM values.

Normalizing NO_x to CO_2, which is done for fuel-based emission factors, shows lower fractional differences with respect to the MEL FRM, ranging from 3 to 10%. PEMS3 showed the

greatest improvement, with the normalized NO_x emissions agreeing within 5% for most cycles. This normalization shows another benefit of fuel-based emissions factors. Biases introduced by differences in measuring volumetric flows, corrections to equivalent temperatures and pressures, differing moisture contents, and different dilution ratios among the instruments cancel out because they affect CO_2 and NO_x concentrations in the same way for a given measurement device.

A final PEMS comparison with the MEL was conducted under real-world driving conditions to better understand how these instruments might behave in the field. The MEL sampled exhaust from its tractor powered by a 475 hp Caterpillar C-15 ACERT modern engine and a diesel particulate filter. Driving routes were: 1) round trip between Riverside to San Diego, CA, and 2) round trip between Riverside and Bishop, CA. These routes include many NTE-type events in hot, cold and moist weather with elevations ranging from sea level to 8,000 ft above mean sea level. Six test runs were conducted with PEMS and the MEL and three "audit" runs were made with the MEL by itself. PEMS were positioned inside and outside the tractor cab for different tests.

Different events that could represent portions of the NTE cycle were identified and CO_2 and NO_x emissions were averaged over these events. CO_2 emissions were estimated in terms of total grams emitted during the event (gCO_2). Brake specific NO_x emissions were calculated by three different methods: 1) based on speed and torque, 2) based on brake specific fuel consumption, and 3) based on mass fuel flow (a fuel specific method). Figure 4-4 illustrates the events and the NO_x emission factor deviations of the PEMS from the MEL for the six test runs. Each of the three methods is equally valid for converting emissions to values comparable with the brake-specific emission standards, but they give substantially different deviations from the FRM certification value. Deviations were greatest for Method 1 with an average deviation of +11%±6% relative to the MEL. Deviations for Methods 2 and 3 were +4%±7%. These differences are related to positive bias of CO_2 levels. The humidity correlation factor was 1-1.5% higher than that for the MEL, which contributed in part to the bias.

PEM and MEL FRM CO_2 emissions for matching NTE events are compared in Figure 4-5. PEM CO_2 emissions were consistently biased higher than the MEL measurements, with a average deviation of +5%±2%. PEM vs. MEL NO_x emission factors in Figure 4-5 are not as well correlated as those for CO_2. PEM NO_x values are consistently higher than those of the MEL with $R^2 = 0.749$.

4.3 In-Plume Emissions Testing System (IPETS)

The schematic for the IPETS system is shown in Figure 4-6. The base components are an FTIR Spectrometer (Illuminator series, Midac, Costa Mesa, CA) and two LI-840 CO_2/H_2O Gas Analyzers (Licor Biosciences, Lincoln, NE) for gaseous analysis. An Electrical Low Pressure Impactor (ELPI, Dekati, Finland), two DustTraks™ (Model 8520, TSI, Shoreline, MN) and 2 GRIMM optical aerosol particle counters (Model 1.108, Grimm Aerosol, Ainring, Germany) are used for the measurement of PM size distribution and mass concentrations, and a filter sampler for PM chemical and gravimetric analysis. Instrument properties are summarized in Table 4-4.

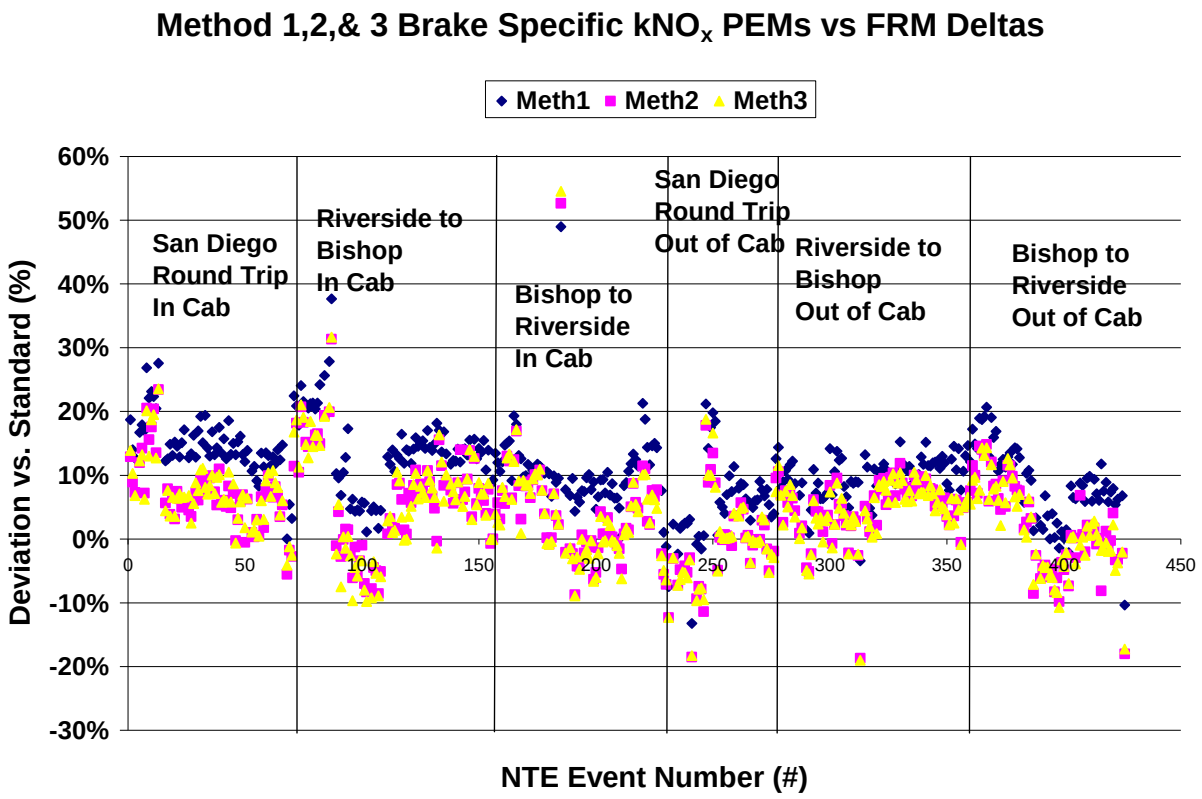

Figure 4-4. Fractional differences between PEM and MEL FRM emission rates (in brake-specific power units of g/bkW-hr) for NTE-like events in on-road test runs. Meth1 is based on speed and torque, Meth2 is based on brake specific fuel consumption, and Meth3 is based on mass fuel flow (a fuel specific method).

Sample air is drawn into the IPETS through 2-cm ID conductive tubing (TSI, Shoreline, MN) at approximately 220 L/min. The tubing length depends on the source type and field access and the sample air generally reaches the instrument in less than 2 seconds. The inlet of the system is flexible and can be positioned to reach elevated sources such as high-stacks of heavy-duty diesels, or it can be placed on the road surface, protected by rubberized cable protectors, for on-road sources. For easy transport and setup in the field, these components are mounted on three handcarts and can be operated from within a cargo van, or can be set up by themselves at the sampling location.

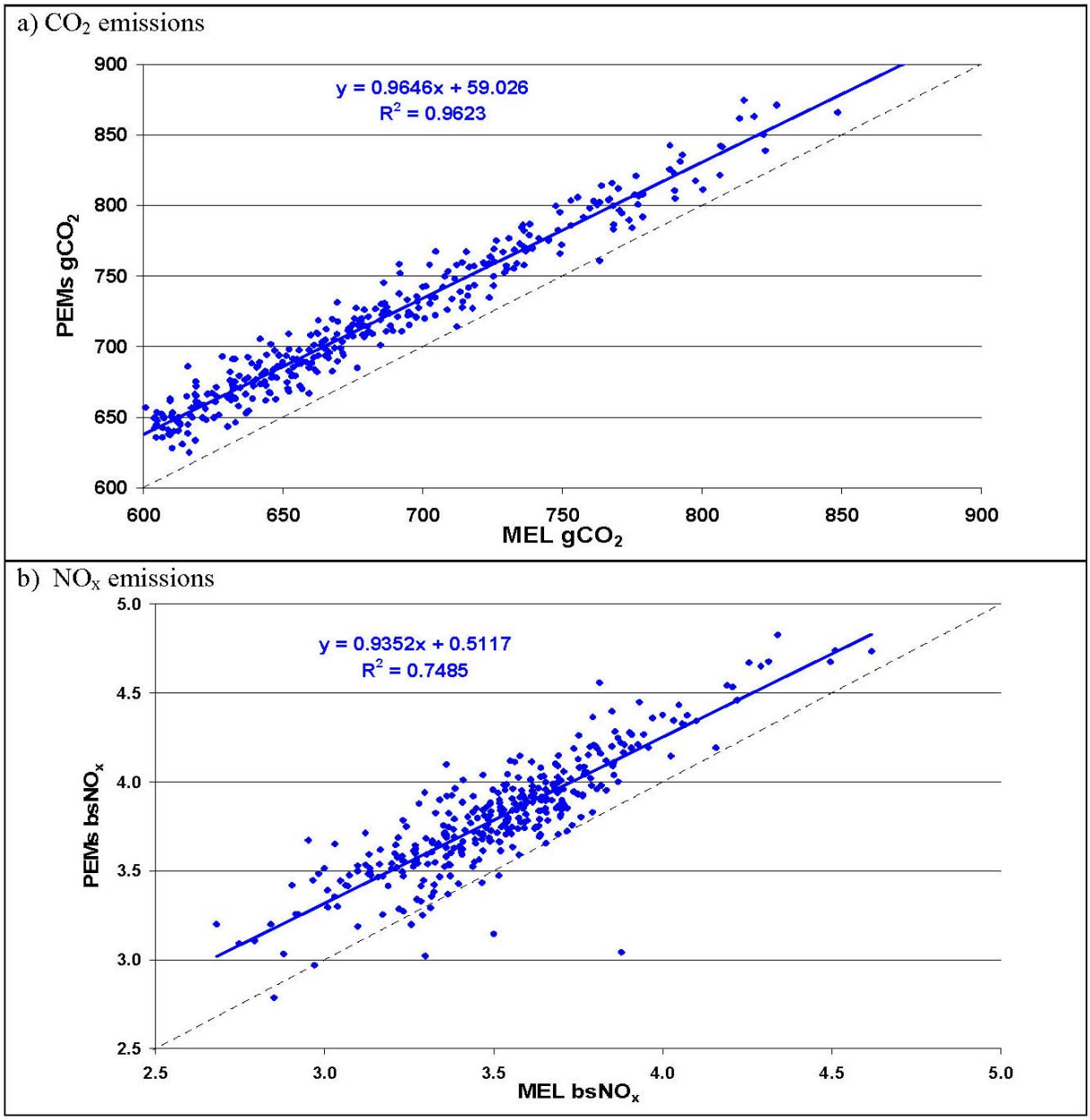

Figure 4-5. Comparison between PEMS and the MEL FRM for a) CO_2 (grams emitted per events) and b) brake-specific NO_x ($bsNO_x$) mass emissions (g/bkW-hr). Emissions were averaged over the events illustrated in Figure 4-4.

Using the carbon mass balance technique (Moosmüller et al., 2003), the emission ratios (ER) and fuel-based emission factors (EFs) can be calculated as:

$$ER_p = \frac{C_p}{Cco_2\left[\frac{Mc}{Mco_2}\right] + Cco\left[\frac{Mc}{Mco}\right]} \qquad (4\text{-}1)$$

And

$$EF_P = CMF_{fuel}\frac{C_P}{C_{CO_2}\left(\frac{M_C}{M_{CO_2}}\right) + C_{CO}\left(\frac{M_C}{M_{CO}}\right)} \qquad \text{Eq. 4-2}$$

where ERp is the emission ratio of pollutant P to total carbon, EF_P is the emission factor of pollutant P in g pollutant per g fuel. CMF_{fuel} is the carbon mass fraction of the fuel, typically 85% to 88% for gasoline and diesel, and 45% to 50% for wood fuel. C_i is the mass concentration of species in grams per cubic meter, and M_i is the molecular (or atomic) weight of species i in grams per mole.

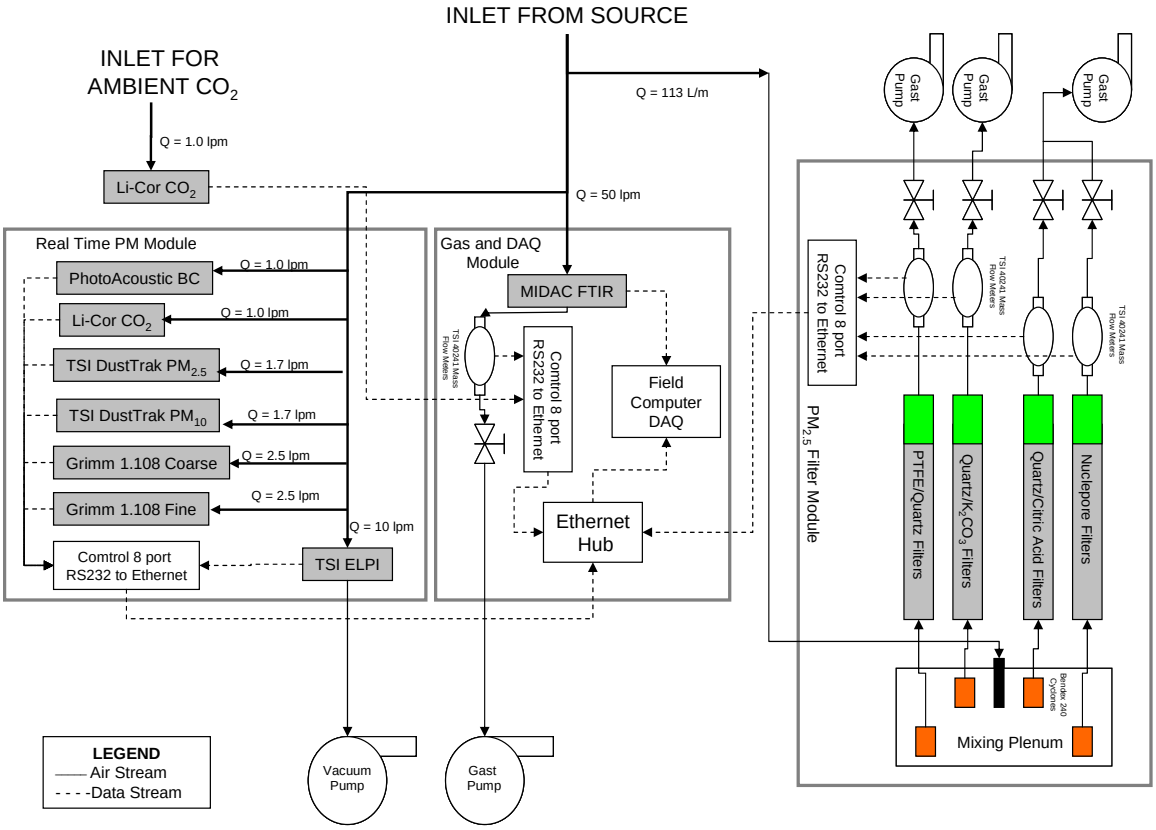

Figure 4-6. IPETS schematic diagram showing the sampling train for continuous and filter monitors.

Table 4-4. IPETS instrumentation.

Instrument	Measurement	Method	Response Time(s)
Midac I-Series FTIR	Molecular gas species concentration	Dispersive IR	1.5
Dekati Electronic Low Pressure Impactor (10 L/min)	Aerodynamic number size distribution of particles	Current dissipation arising from deposition of charged particles to impactor substrates	5
TSI DustTrak	Particle mass	780 nm laser light scattering of particle stream at 90 degrees	1
Nuclepore filter sampler	Mass and chemical composition of particles and gases	Collection and analysis of exposed filters	>1000
TSI 4043 Mass Flow Meters	Mass flow through filter	Hot wire anemometer	<1
GRIMM aerosol spectrometer	Particle size distribution	Light scattering	6
Li-Cor 840 CO_2/H_2O gas spectrometer	CO_2 (parts per million) and H_2O (parts per thousand)	NDIR (non-disperse infrared)	1

Extractive FTIR spectroscopy has been previously used to characterize combustion emissions (Arrigone and Hilton, 2005; Cantu et al., 1998; Goode et al., 1999; Gu et al., 1998; Li et al., 2003b; Lin et al., 2007a; Reyes et al., 2006; Wright et al., 1998). More than 15 chemical species, including CO_2, CO, and NH_3 have been measured above biomass fires, and CO_2, CO, and N_2O from vehicular exhaust downwind of a freeway onramp. However, other species of interest, particularly NO and NO_2 have proven difficult to measure due to interference from water vapor. By using only spectral analysis regions where NO and NO_2 have absorption peaks and water vapor does not, the interference due to water vapor can be minimized.

The IPETS FTIR measures IR absorption spectra at 1.5 second intervals with a spectral resolution of 0.5 cm^{-1} (i.e., wave numbers) between 1100 and 6500 cm^{-1}. The gas cell consists of a 10-m length optical path, folded within a two liter analytical volume. Sample air flow through the cell is set at 60 L/min resulting, resulting in the ~1.5 second residence time. Internally mounted pressure and temperature sensors account for changes in sample density. The FTIR spectrometer is based upon a Michelson interferometer with a mercury-cadmium-tellurium (MCT) liquid nitrogen-cooled detector. Calibration spectra were prepared for CO_2, CO, NH_3, NO, H_2O, C_4H_{10}, C_6H_{14}, C_2H_4, NO_2, and SO_2 using U.S. EPA (Environmental Protection Agency) certified gases diluted with ultra-pure nitrogen using an Environics 2020 computerized-

gas-dilution-system (Environics, Tolland, CT). Spectral regions used for the measurement of individual gas concentrations, detection limits and calibration concentration ranges are specified in Table 4-5. Prior to taking diesel exhaust measurements, the cell is purged with ultra-pure nitrogen to reduce measurement interferences from background air. Detection limits were calculated as twice the standard error of a zero measurement, which is the instrument response to a nitrogen purged cell. FTIR spectrometer spectral analysis regions, calibration ranges, and detection limits.

Table 4-5. FTIR spectrometer spectral analysis regions, calibration ranges, and detection limits

Species	Reference Region (cm^{-1})		Detection Limit (ppm)	Calibration Range (ppm)	
	Lower υ_1	Lower υ_2			
CO_2	723.0	750.0	17	100	4730
CO	2133.5	2142.0	0.05	1.0	1005
NH_3	955.5	976.0	0.01	1.0	110
NO	1873.0 1880.5 1898.5 1926.0 1934.5	1878.5 1884.0 1901.5 1932.0 1940.0	0.13	0.2	20
H_2O	1200.0	1300.0	27	5.0	5294
C_4H_{10}	3041.5	2825.5	0.05	1.0	100
C_6H_{14}	3030.0	2818.0	0.04	0.2	200
C_2H_4	958.0	936.5	0.08	0.5	20
NO_2	1584.0 1597.5 1604.0 1610.5	1588.5 1600.0 1606.0 1614.0	0.11	0.2	20
SO_2	1112.5 1123.5 1138.5 1153.5 1166.5 1176.5 1188.0 1200.0 1227.0	1120.5 1134.0 1148.0 1164.0 1172.5 1185.0 1197.0 1209.0 1236.0	0.14	1.0	100

Figure 4-7 shows a FTIR absorption spectrum of a typical gasoline vehicle exhaust sample, as well as calibration spectra of water vapor at 5,000 ppm and NO at 50 ppm, concentrations typical of our dilute sampling conditions. Spectral regions at 1873.0 to 1876.5 cm^{-1} and 1898.5 to 1901.5 cm^{-1} show peaks in NO absorbance, but not in water absorbance, i.e., interference from water vapor is reduced in these two regions for NO. The same approach was used to choose additional regions in the NO spectra and in the spectra of other species. For the same sample spectrum, a similar spectrum of NO_2 is shown in Figure 4-8 with the spectral regions, 1584.0 to 1588.5 cm^{-1} and 1597.5 to 1600.0 cm^{-1}, chosen for NO_2 analysis.

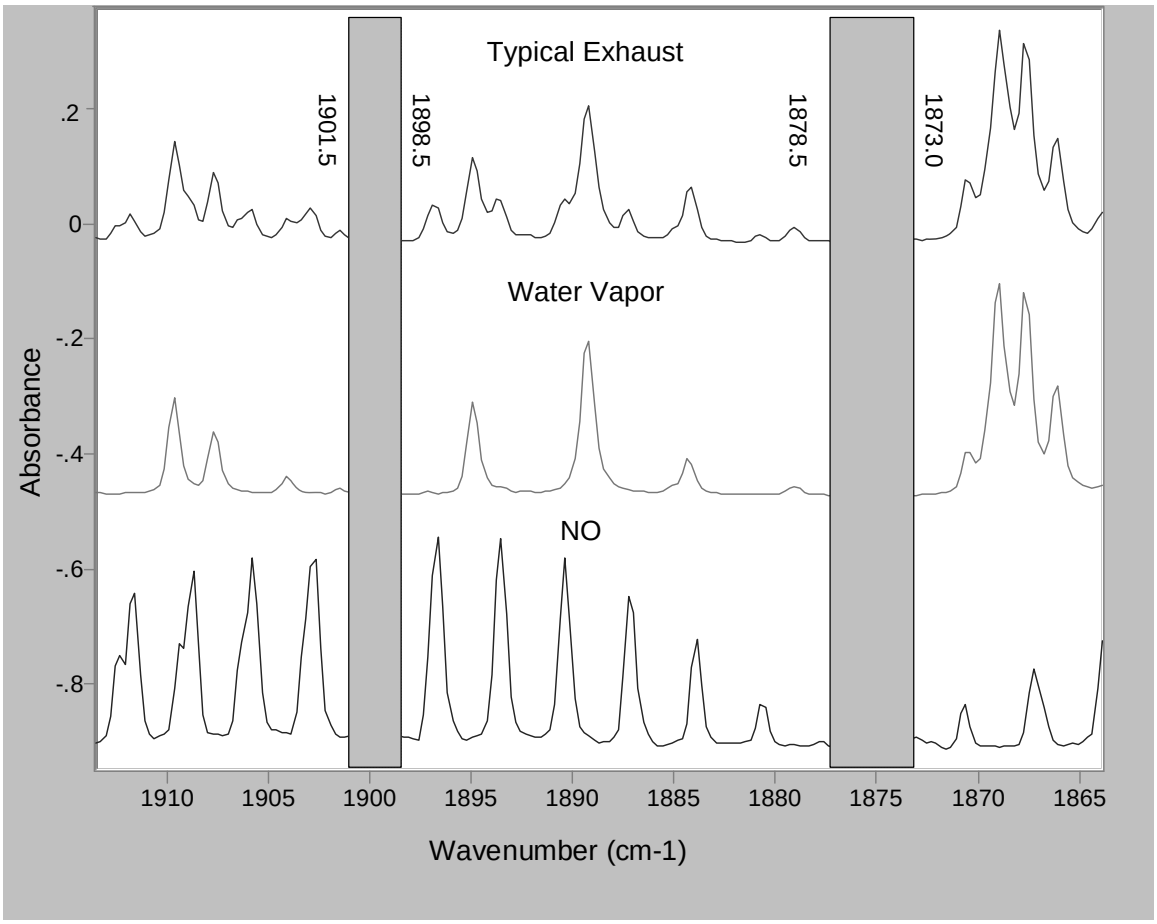

Figure 4-7. Region of FTIR absorption spectra for NO analysis.

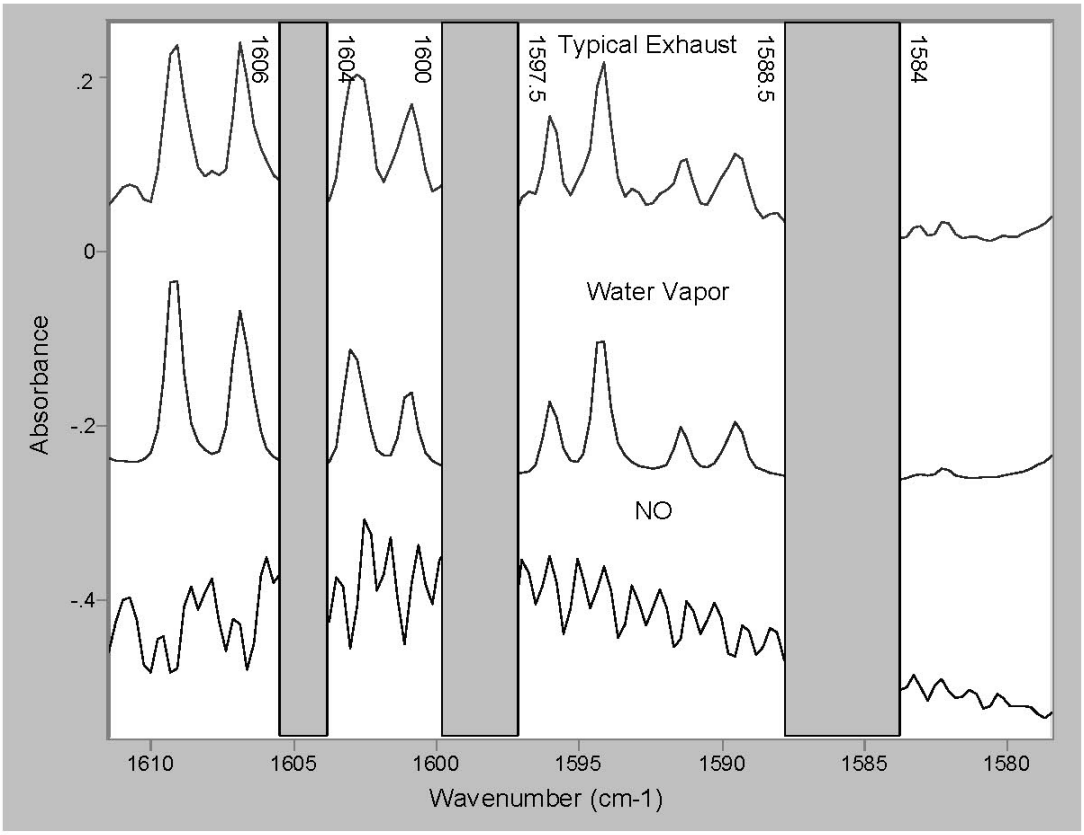

Figure 4-8. Region of FTIR absorption spectra for NO_2 analysis.

The LI-840 CO_2/H_2O Gas Analyzer applies non-dispersive infrared (NDIR) absorption using a single-path, dual-wavelength (2347 and 3853 cm^{-1} wavenumbers) infrared detection. The LI-840 samples at 1 L/min at 1 second intervals. An in-line filter before the sampling inlet reduces contamination of the cell by particles. The LI-840 CO2/H2O Gas Analyzer is used as a redundant measurement of CO_2, in addition to the FTIR.

The ELPI has been used for fast response size distribution measurements in many prior studies (Arnold et al., 2006; Gouriou et al., 2004; Held et al., 2007; Herndon et al., 2005b; Holmen and Qu, 2004; Ji and Harrison, 1999; Keskinen et al., 2003; Khalek, 2000; Kinsey et al., 2006; Lehmann et al., 2004; Lemmetty et al., 2005; Mamakos et al., 2006; Maricq et al., 1999; Maricq et al., 2006; Marjamäki et al., 2000; Marjamäki et al., 2005; Mohr et al., 2005; Pagels et al., 2005; Pattas et al., 1998; Peters et al., 1993; Ristimaki et al., 2007; Shi et al., 1999b; Shi et al., 1999a; Tsukamoto et al., 2000; Vaaraslahti et al., 2005; Vaaraslahti et al., 2006; van Gulijk et al., 2000; van Gulijk et al., 2001; van Gulijk et al., 2003b; van Gulijk et al., 2003a; van Gulijk et al., 2004; Virtanen et al., 2001; Virtanen et al., 2004; Witze et al., 2004; Yi et al., 2006; Zervas et al., 2005; Zervas and Dorlhene, 2006)

The ELPI samples air at 10 L/min with a sampling period of 1 second. Sample air is drawn through a unipolar corona charger, which imparts a positive charge to the aerosol. Particles are separated into 12 different size ranges in a cascade impactor based on their aerodynamic diameter. The 50% cutpoint of each impactor stage depends on the choices of impaction substrate and the use of the filter stage. An oiled sintered impaction substrate and the

filter stage were used for engine exhaust tests, resulting in 12 different aerodynamic cutpoints: 0.024, 0.03, 0.056, 0.1, 0.22, 0.32, 0.59, 0.91, 1.5, 2.5, 3.8, and 6.4 μm. The sintered oil impaction substrate reduces bounce of larger particles to lower stages and extends the loading capacity of the impaction substrates (van Gulijk et al., 2003b). The filter stage extends the lower size limit of UP from 30 nm to 7 nm. The substrates are electrically isolated with Teflon supports and the accumulating charge on each of the substrates is measured by an array of electrometers. The measured current on each of the stages is proportional to the number of particles deposited on the stage (Pagels et al., 2005).

The DustTrak^{tm} measures the near perpendicular scattering of a laser diode beam by particles at a wavelength of 780 nm. PM_{10} and $PM_{2.5}$ aerodynamic size cut inlets are installed upstream of its analytical chamber to limit the size of measured aerosol particles. The DustTrak^{tm} has a flow rate of 1.7 L/min and is factory calibrated to the respirable fraction of standard ISO 12103-1 A1 test dust (previously called "Arizona test dust"). The DustTrak has been used in several aerosol studies (Chan et al., 2005; Chow et al., 2006a; Chung et al., 2001; Etyemezian et al., 2005; Gertler et al., 2006; Gillies et al., 2005; Gillies et al., 2007; He et al., 2007; He et al., 2004; He et al., 2005; Heal et al., 2000; Jamriska et al., 2004; Kingham et al., 2006; Kinsey et al., 2006; Levy et al., 2003; McDonald et al., 2004a; Moosmüller et al., 2001a; O'Shaughnessy and Slagley, 2002; Salcedo et al., 2006) Moosmüller et al., (2001) found that the DustTrak^{tm} provides reasonable (within a factor of 2) measurements of aerosol mass for diesel exhaust particles.

The GRIMM 1.1.108 optical aerosol particle counter (Gerhart and Rettenmoser, 2006; Peters et al., 2006; Teikari et al., 2003) measures scattering from individual particles rather than from the entire distribution as is done by the DustTrak. The intensity of the scattered light is related to the particle size by light scattering theory assuming spherical particles and a unit density. With the entire size distribution a more accurate measure of particle mass can be estimated. Sampling period of the GRIMM 1.108 is 6 seconds for a full scan of particles (16 bins) from ~0.3 μm to 20 μm.

For PM chemical speciation and gravimetric measurements, sample air is drawn through a plenum with a parallel array of Bendix 240 cyclones (Chan and Lippmann, 1977) that to remove particles larger than 2.5 and 10 μm at the flowrate of 113 and 45 L/min, respectively. After passing through the cyclone, the flow is split equally into 2 filter packs. This results in a flowrate of 23 L/min for each PM_{10} filter sampler and 57 L/min for each $PM_{2.5}$ filter sampler. Sample air passes through filter packs containing either Teflon filters for the measurement of PM mass by gravimetry and elements (Na to U) by x-ray fluorescence (XRF), or quartz-fiber filters for water-soluble cations and anions by ion chromatography IC), organic and elemental carbon by thermal optical reflectance (TOR), and organic marker compounds by thermal desorption gas chromatographic mass spectrometry (Chow et al., 2007e; Hays and Lavrich, 2007; Ho et al., 2008; Ho and Yu, 2004).

A citric acid impregnated cellulous-fiber filter is placed behind the quartz fiber filter to adsorb NH_3 as a gas and a potassium carbonate impregnated cellulous fiber filter is placed behind the Teflon membrane filter to adsorb SO_2 gas. A Nuclepore polycarbonate filter collects particles on a flat surface that can be examined by scanning electron microscopic (SEM) analysis. Flow through each filter is accurately (± 2%) monitored with a digital mass flow meter (TSI 4000 series, TSI, Shoreview, MN). When the filter sampler is not needed, a bypass flow with the same flowrate as the filter sampling system is used to maintain a constant total flowrate

through the cyclones. Sampling and analysis details are provided elsewhere (Chow et al., 1993; Chow, 1995; Chow et al., 2007e; Chow et al., 2007a; Chow and Watson, 1999; Watson et al., 1999)

Data from all instruments are logged in real time through a serial port to a laptop Ethernet server mounted on one of the handcarts. The FTIR Spectrometer communicates with the laptop through its A/D PCMCIA card.

The ELPI and LI-840 CO_2/H_2O Gas Analyzer use software provided by the manufacturer to log data. The TSI flowmeters and TSI DustTrak^{tm} use a custom data acquisition program written in Labview (National Instruments, Inc. Austin, TX). The FTIR spectrometer uses the software package Autoquant Pro v1.0.104 to both log IR spectra and quantify gas concentrations. The data acquisition system assigns a common time stamp to all measurements to ensure that data are synchronized at 1 Hz frequency. The use of real time displays increases data recovery in the field because the operator can monitor the status of each instrument from a single location.

IPETS measurements were compared with MEL measurements in a December 2004 test at UCR (Nussbaum et al., 2008). Emissions were generated by a Kamatzu SA6D125E-2 engine with power output rated at 303 KW and 11 L displacement mounted in a 250KW (actual electrical output) DEWYO Model # DF-3300K power generator. This model year 2000 engine had logged 316 service hours prior to this comparison study. The MEL test cycle consisted of a 5-mode test at 100%, 75%, 50%, 25%, and 10% of gull engine load. Emission factors were measured over a two day period, with replicate measurements made for JP-8 and ultra low sulfur diesel (ULSD) fuels. Emission factors were determined from five minute measurements for each mode. Each test fuel was directly fed to the engine from the fuel drum. After fuel switches, the engine was operated for 30-60 minutes at 100% load with the new test fuel to assure complete removal of the previous test fuel from the engine and fuel line.

Figure 4-9 shows that CO EFs from IPETS and the MEL were highly correlated (r^2 = 0.93, p = .000019) with a linear regression slope close to unity (slope =0.98 ± .09 and intercept = 0.22 ± .56). IPETS and MEL NO and NO_2 comparisons in Figures 4-10 and 4-11 were highly correlated but the slope and intercept differ from unity at d NO_2, with a slope of 1.34 ± .35 and 1.42 ± .11, respectively. The cause of this difference unclear, as IPETS recalibration after sampling showed agreement with NO and NO_2 standards within 5% over the calibration range.

The GRIMM particle size was not operational during this comparison. PM derived from the IPETS ELPI, filter, and DustTrak measurements are compared with the MEL measurements with the ELPI example shown in Figure 4-12. The slope of all three particle measurement methods was close to unity (0.96 ± .21, 1.01 ± .19 and 1.01 ± .19 for ELPI, filters and DustTrak), but there was a significant offset as seen in the intercept (0.39 ± .11, 0.32 ± .11 and 0.45 ± .18). Some of this discrepancy between IPETS and MEL PM emission factors may be due to temperature differences, as noted in earlier comparisons. MEL samples PM onto Teflon filters from a secondary dilution tunnel kept at a fixed temperature of 47C. The elevated temperature in the MEL sampling system may cause losses of semi-volatile species. In contrast, IPETS measurements are made at ambient temperatures, varying between 10 and 22C and therefore volatile compounds may condense onto particles or the filter media, thereby adding mass. This difference in sampling temperature implies that IPETS PM measurements include some semi-volatile particle mass that is volatilized at the higher MEL sampling temperatures.

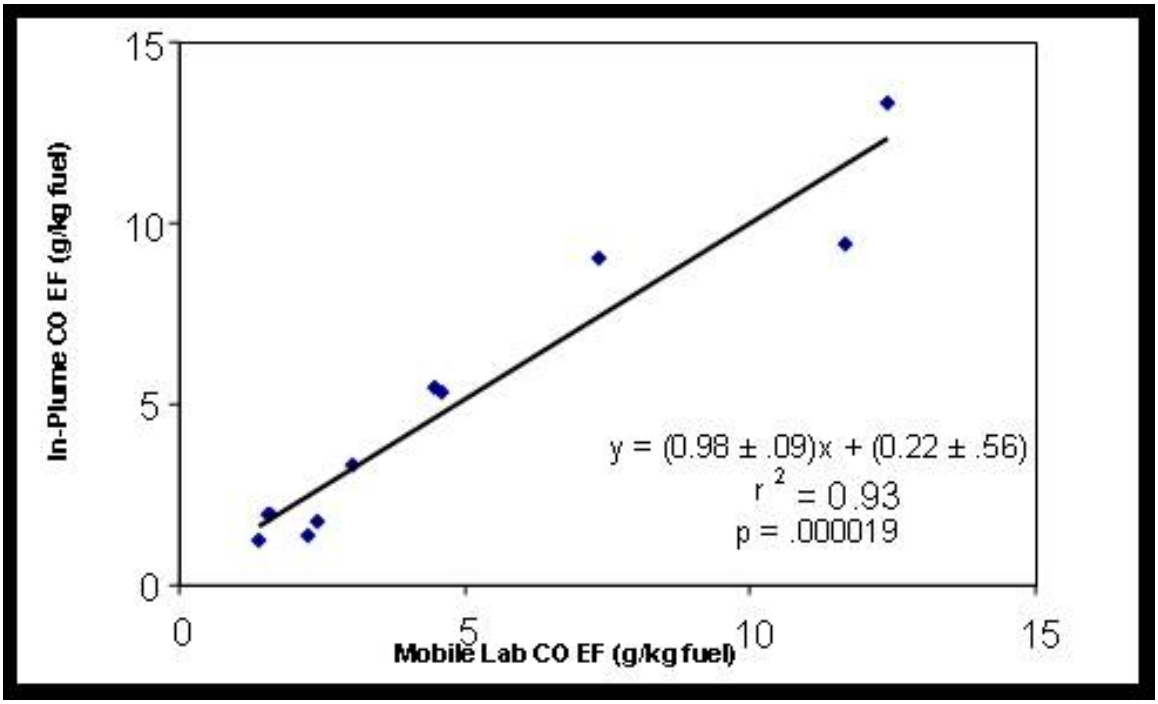

Figure 4-9. Comparison of CO emission factors from the IPETS with the MEL for the same engine exhaust.

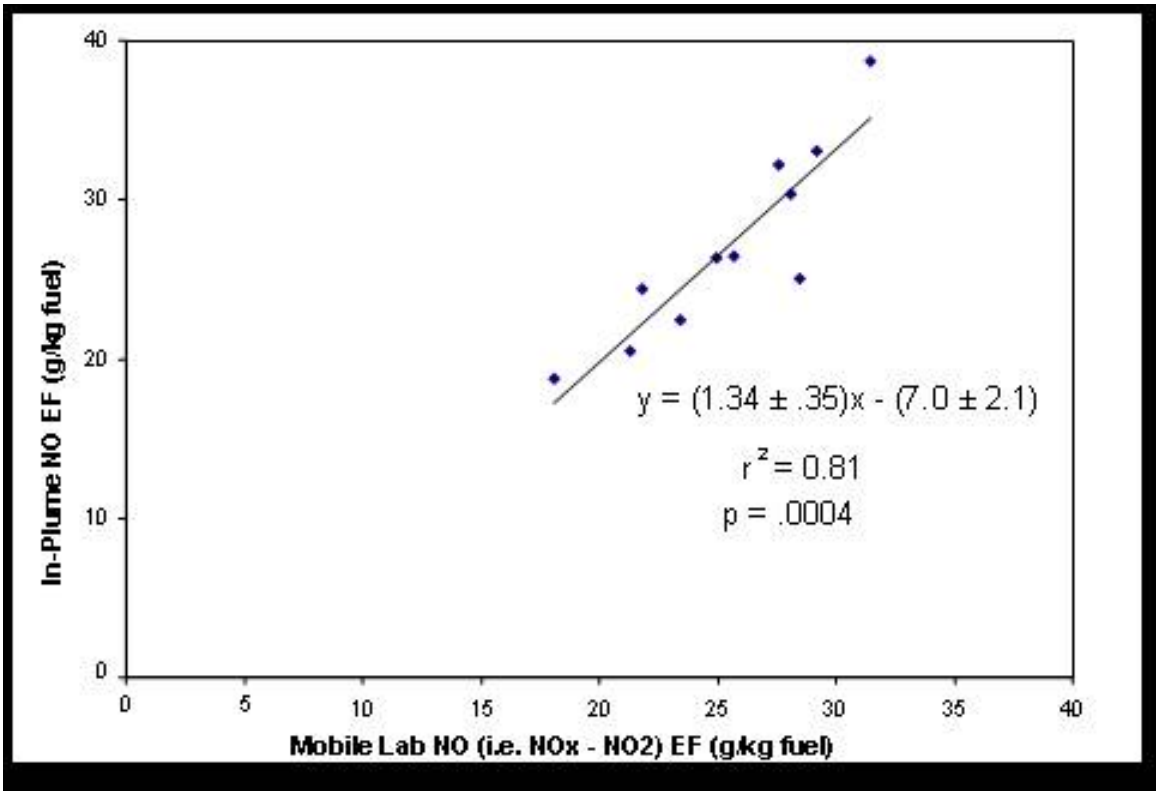

Figure 4-10. Comparison of NO emission factors from the IPETS with the MEL for the same engine exhaust.

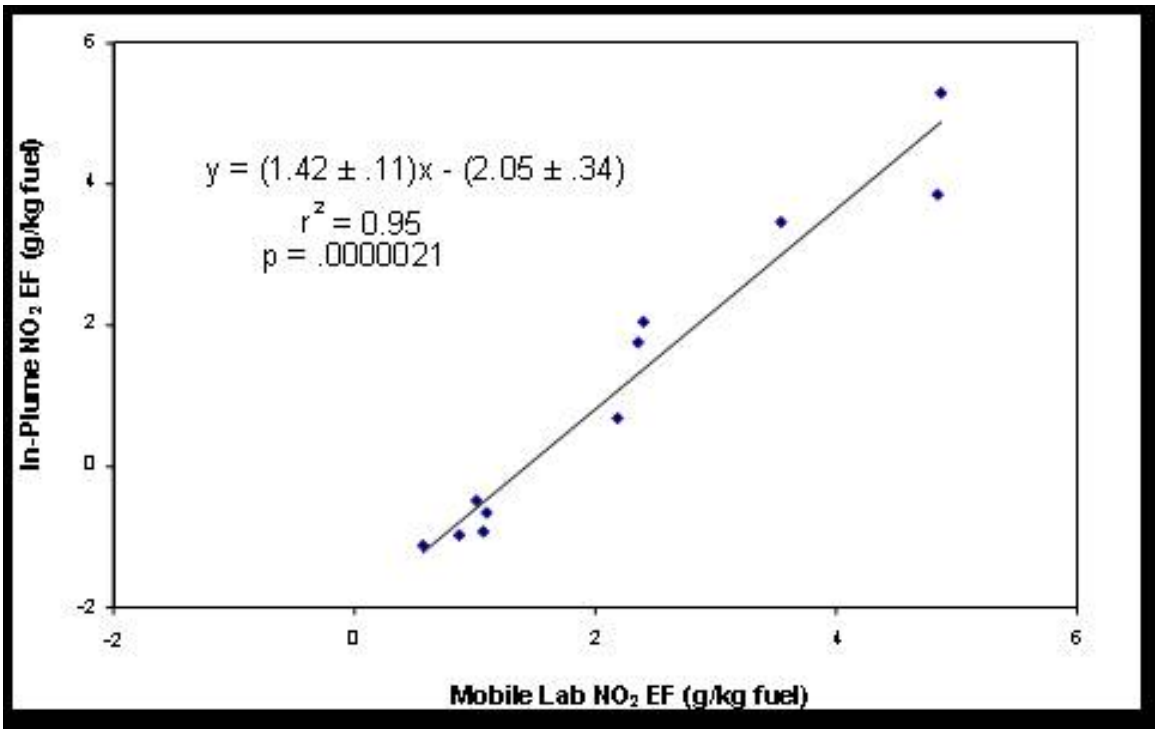

Figure 4-11. Comparison of NO_2 emission factors from the IPETS with the MEL for the same engine exhaust.

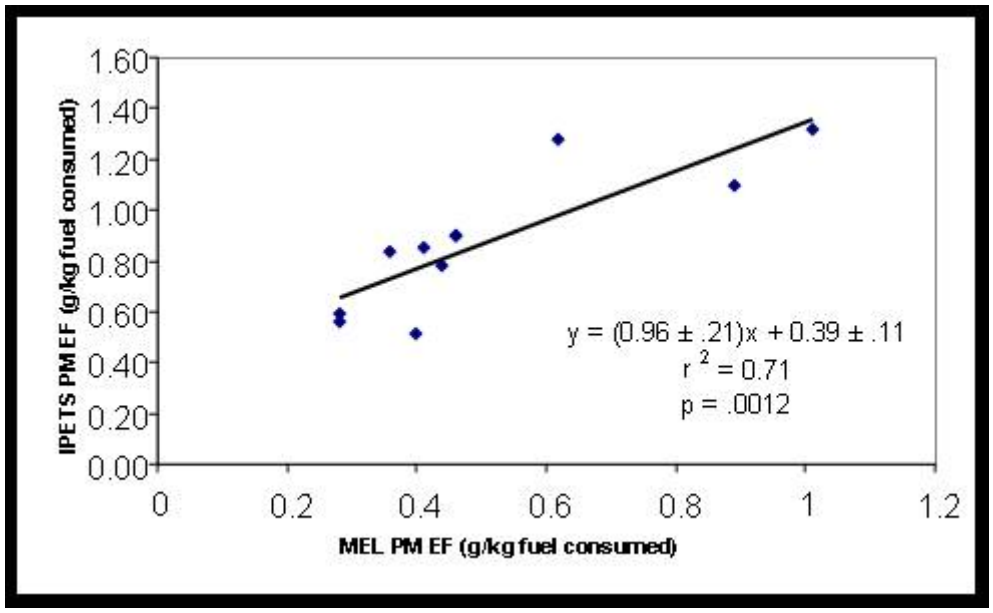

Figure 4-12. Comparison of ELPI PM with MEL PM emissions for the same engine exhaust.

4.4 Cross-Plume Vehicle Remote Sensing System (VERSS)

The VERSS consists of an IR cross-plume sensor for the measurement of gaseous emissions and a UV system (Moosmüller et al., 2003) for PM measurements. The PM system uses both back scatter and transmittance signals to measure the PM mass column content behind a passing vehicle. Ratioing the PM mass column content with the carbon mass column content,

simultaneously measured with IR absorption, yields the fuel-based PM mass emission factor. The transmissometer directly yields PM extinction coefficients without calibration, while the Lidar backscatter measurement is calibrated through laboratory measurements of gases with well-known backscatter coefficients. The PM mass column content is calculated from these extinction and backscatter coefficients with the help of mass backscatter and extinction efficiencies obtained from theoretical calculations (Barber et al., 2004).

This system has been applied in several on-road measurement programs to evaluate and perfect its operation (Kuhns et al., 2004; Mazzoleni et al., 2004a; Mazzoleni et al., 2004b; Mazzoleni et al., 2004c). Figure 4-13 shows a typical VERSS setup for on-road applications.

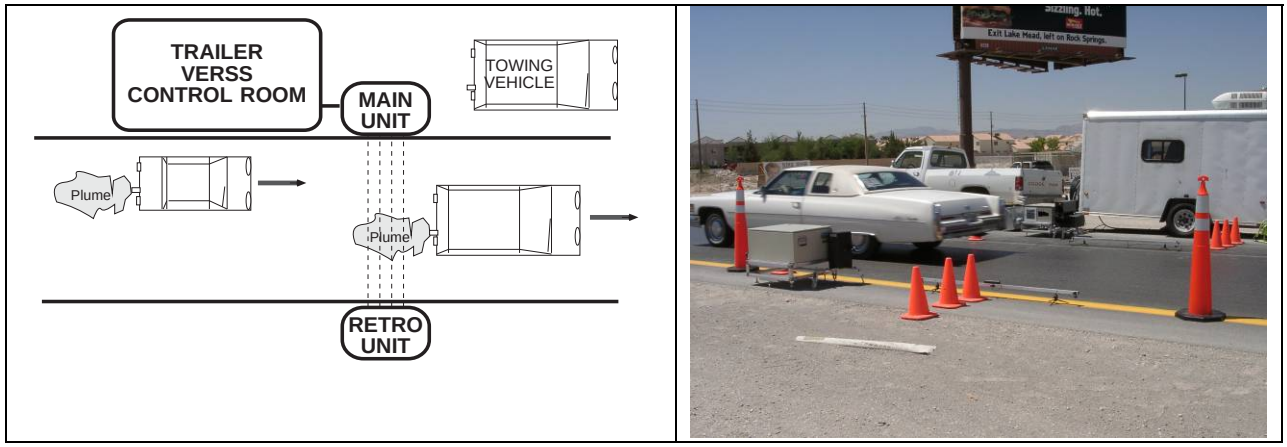

Figure 4-13. Schematic diagram and photograph of the DRI VERSS setup.

The "main unit" containing transmitter and receiver and the "retro unit" containing mirror for the retro-reflection of optical beams back to the main unit are shown in Figures 4-14 and 4-15. Only the main unit contains active components that require electrical power and connections to the data acquisition and instrument control units and computer located in the VERSS control room/trailer. Further development of the cross-plume system for this project included a second generation Lidar system, software for reducing Lidar data, an independent gaseous IR measurement, and modifications for non-road exhaust measurements.

To reduce signal noise, increase detection limit and increase data recovery the PM VERSS was redesigned as part of this project and an improved Lidar and transmissometer unit was built and tested. New software and algorithms for data analysis were also developed to more efficiently handle the large data sets acquired by the VERSS. This effort improved the Lidar signal-to-noise ration by one order of magnitude and the PM emission factor detection limit by a factor of four. This is in addition to having a simpler, easier to operate PM VERSS with greatly improved data analysis and visualization capabilities. The second-generation system improvements are summarized in Table 4-6.

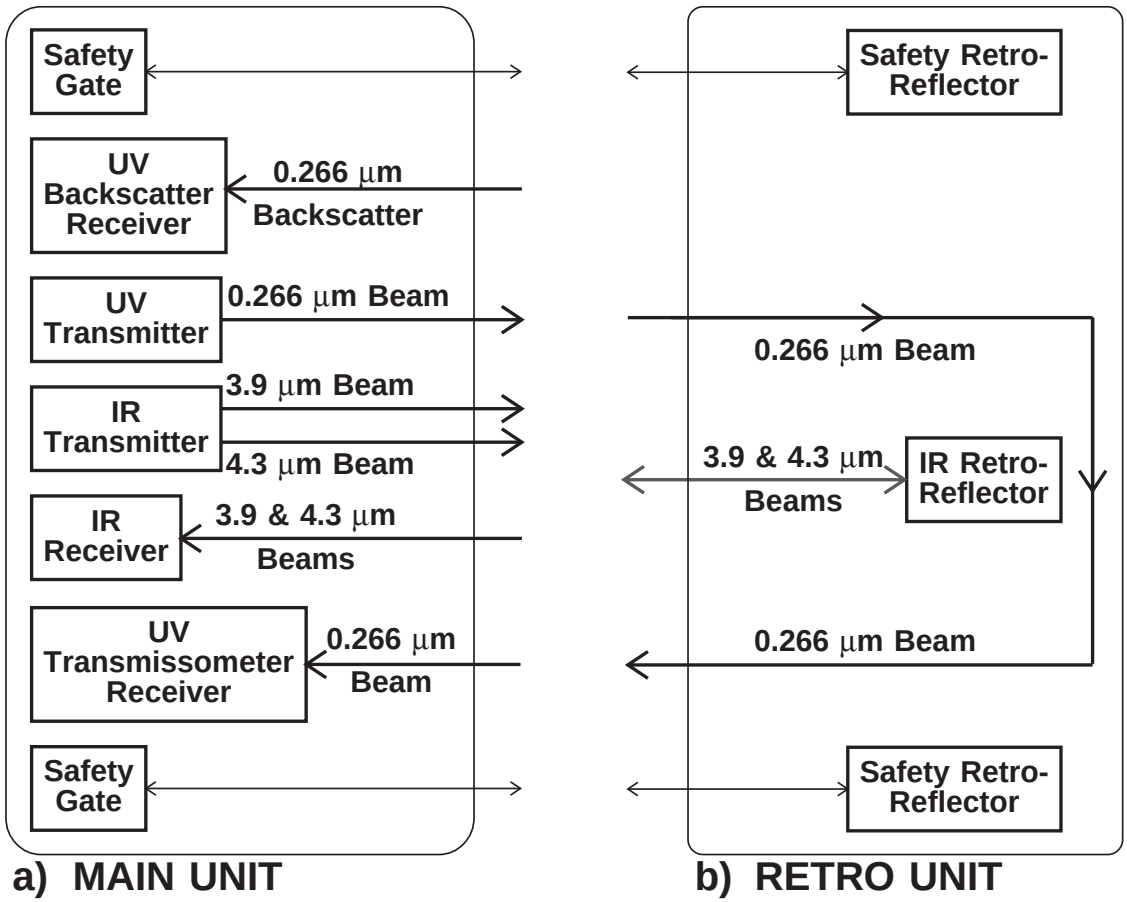

Figure 4-14. Schematic diagram of Lidar cross-plume remote sensor.

Figure 4-15. Photographs of main and retro units.

Table 4-6. Improvements in the SERDP second generation PM VERSS.

VERSS	1st Generation	2nd Generation
Transmitter: - Laser Model - Pulse Energy - Pulse Repetition Frequency	 NanoUV-266 0.19 μJ 6.9kHz	 PNU-001025-040 10μJ 1kHz
Receiver Lidar: - Telescope Type - Diameter - Sensor Type - Sensor Quantum Efficiency	 Refractor: Fused Silica Lens 5cm Hamamatsu PMT ~ 14% @ 266 nm	 Reflector: HR UV Coated 15cm Solar-blind Hamamatsu PMT ~ 28% @ 266 nm
Receiver Transmissometer: - Collection	 No collimation element	 7.5cm Fused Silica Lens
Data Analysis Tool: -Dense Plume Algorithm - Plume PM Concentration Visualization - PMT nonlinearity Correction - PM Emission Factors Calculation	 No No No Linear Regression Method only	 Implemented Implemented Implemented Both linear regression and ratio methods
- Signal-to-Noise Ratio (Clean Air) - PM Detection Limit (Freeway Operation Mode)	2.8 ~ 0.25 g_{PM}/kg_{Fuel}	26 $\leq$ 0.06 g_{PM}/kg_{Fuel}

PM mass column content is measured with a 266 nm backscattering Lidar (light detection and ranging) system. This system has been greatly improved by employing a more powerful (pulse power increased by 50) Nd:YAG laser (Uniphase PowerChip NanoLaser PNU-001025-040), operating at a reduced (by a factor of 7) pulse repetition rate to increase the duty factor of the data acquisition system to unity. Unfortunately, JDS-Uniphase/Nanolase has since discontinued producing this laser, and it was not possible to acquire a similar laser as replacement or for use in additional systems. Without a replacement laser, field operations are risky, as a laser failure means the instrument will not function. No suitable laser fulfilling our requirements was found to be commercially available.

After discussions with several laser manufacturers, Laser Path Technologies attempted to develop a replacement laser with near identical mechanical, electrical, and optical specifications as the original JDS-Uniphase/Nanolase UV laser. Laser Path Technologies was not able to build this laser in compliance with the mandatory specifications.

However, during 2006 the JDS-Uniphase/Nanolase Powerchip laser product line was sold to Teem Photonics with the intent of renewing the product line. However, Teem Photonics decided not to sell the 266-nm laser needed for the VERSS. To solve this problem, Laser Path Technologies purchased a 532 nm powerchip laser from Teem Photonics and added a frequencydoubling unit yielding the 266 nm IR wavelength. This laser served as the replacement for the mobile source field emission tests described in Section 5, but it has not been fully evaluated for equivalence to the original JDS-Uniphase/Nanolase laser. The VERSS is a cutting-edge technology that eventually holds promise for remote sensing of exhaust measurements from mobile engines and other sources. However, its practical use will require some evolution of the available components for other purposes to assure a reliable supply of spare parts.

The new Lidar receiver features an increased collection area (by a factor of about nine) and a new and improved detection system. The use of a solar blind, high quantum efficiency photomultiplier tube (PMT) (Hamamatsu R7400U-06) in combination with a bandpass filter (Corion G10-265-F) eliminates the need for additional spectral filters. This 2nd generation detection system is greatly simplified and increases the signal power due to higher collection area, higher quantum efficiency, and reduced signal losses in spectral filters. The improved and simplified schematic and photo of the Lidar main unit are shown in Figure 4-16.

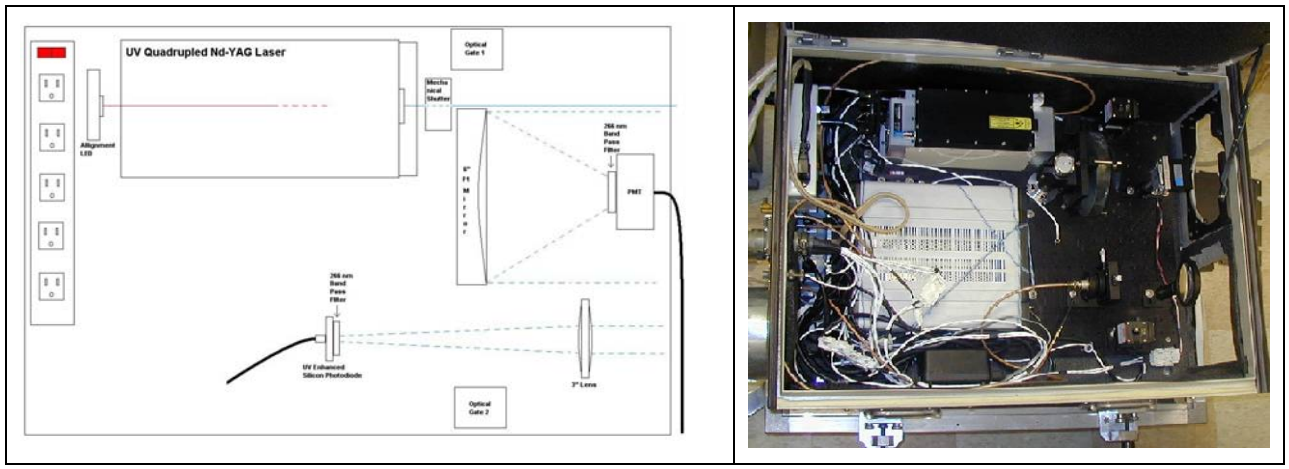

Figure 4-16. Improved and simplified UV Lidar and transmissometer main unit (schematic and photo).

The 1st generation transmissometer measured optical extinction in dense plumes with the laser beam directly terminated by a large area photodiode operated in photovoltaic mode (UDT Sensor, Inc. UV-100). This configuration created artifacts when the laser beam moved slightly on the photodiode due to vehicle induced turbulence in the beam path. In the 2nd generation instrument this artifact was reduced by focusing the returning beam with a 2" diameter UV fused silica lens, thereby making the signal largely independent of turbulence.

Laboratory calibration of the 1st generation Lidar was performed by enclosing the measurement area with a large (3.5" diameter), rigid tube filled with filtered air and CO_2 to obtain two calibration values. Due to its large size, this tube was difficult to handle and introduced some erratic signal from laser light scattering at its perimeter. It was also difficult to completely displace ambient air with the calibration gas. The second generation Lidar system replaces the rigid tube with a larger (22" diameter) tube constructed of thin plastic foil, which can be easily inflated with filtered air or calibration gases such as CO_2 (Figure 4-17).

As a result of these improvements, the clean air (smallest signal) signal-to-noise ratio of the 2nd generation Lidar (S/N = 26) was improved by nearly an order of magnitude compared to that of the 1st generation Lidar (S/N = 2.8). These improvements were evident in field experiments where the detection limit for a single vehicle PM emission factor was reduced from 0.25 g_{PM}/kg_{Fuel} for the 1st generation system to less than 0.06 g_{PM}/kg_{Fuel} for the 2nd generation system.

Figure 4-17. Second generation calibration setup.

In addition, a faster PCI signal sampling board was integrated in the PM VERSS data acquisition system. This board can acquire up to 1,300 waveforms per second (more than the laser pulse repetition frequency, resulting in maximum duty factor of one) while the maximum acquisition rate of the prior data acquisition system, based on a digital HP oscilloscope, was 200 waveforms per second. This increased performance in data acquisition speed allows for the calculation of vehicle PM EF using averages over larger data sets, which has resulted in an increased signal to noise ratio by approximately an amount of 2.2, equal to the square root of the ratio between the new laser pulse repetition frequency (1KHz) and the previous data acquisition rate (0.2 KHz) thereby further lowering the PM EF detection limit.

VERSS data analysis software was enhanced to make emission factor calculations more efficient. The new code includes visualization and display tools, which permit an immediate interpretation of the data by the user and allow a much easier identification of problems in Lidar datasets, as shown in Figure 4-18.

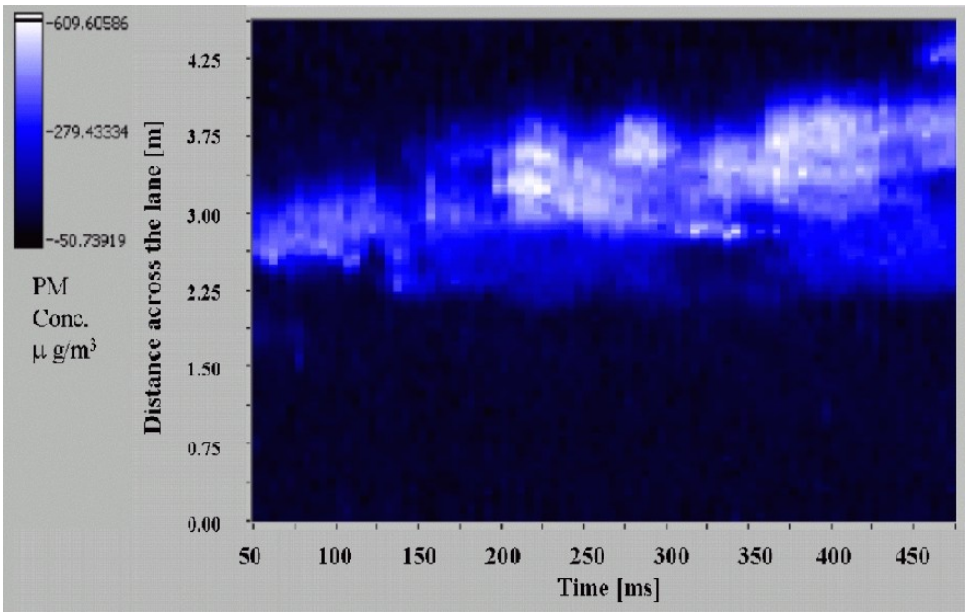

Figure 4-18. PM concentration (colors intensity) vs. range across the lane (y axis) and vs. time elapsed after the vehicle passage through the sensor (x axis).

The 2nd generation software corrects for the non-linearity of the photomultiplier tube, which is especially important for very large signals from diesel engine emissions. The correction is obtained by using the improved calibration system discussed above and by using neutral density optical filters of known transmission as additional calibration points together with a measure of the photomultiplier saturation point by using a hard target. Software includes a Lidar inversion algorithm for dense plumes. It calculates PM emission factors as: 1) the slope of a linear regression between the temporal evolution of the exhaust PM column content vs. the correspondent temporal evolution of the exhaust CO_2 column content, and 2) the ratio of the temporal average of the exhaust PM column content over the temporal average of the exhaust CO_2 column content. These results can be compared and differences can be interpreted and used to understand which approach is most appropriate for a specific experiment. The ratio approach is probably more suitable for stationary sources with emissions that change slowly with time, while the linear regression approach is probably better for emissions that pass rapidly through the analysis path.

The VERSS measures gas emission factors using a commercial unit (ESP RSD 3000) with proprietary hardware and software. This presents problems integrating the mechanical, optical, electrical, and software components of this commercial gaseous system with the UV PM sensor. An attempt was made to develop a customized IR system for the cross-plume sensing of CO_2, CO, and HC as part of this project. This system was successfully operated in the laboratory and is available for use with the UV PM sensor. However, within the time and budgetary constraints of the project, it was not possible to outfit and integrate this core sensor with the multitude of ancillary measurements included in the commercial RSD 3000 infrared sensor. The ancillary measurements needed for successful operation include the coordinated triggering of the various sensors, the measurement vehicle speed and acceleration, and the acquisition of the vehicle image including its identification markings.

The IR system is based on a miniature broadband blackbody IR emitter (Cal Source S1037-5M2) operating at a temperature of 1170 K. This emitter is enclosed in a TO-5 semiconductor can with internal parabolic reflector to provide near collimated and uniform IR output. The blackbody IR emitter is heated to its operating temperature of 1170 K with 2.1 W of electrical power. The emitted IR radiation is time and wavelength modulated with a wavelength-selective chopper (filter wheel) rotating at 50 Hz (i.e., 3000 rpm). The chopper wheel includes twenty 0.5" diameter wavelength selective filters. There are five sequences of four filters each, with each sequence consisting of one filter at a wavelength of 4.3 μm for the measurement of CO_2, one filter at 4.6 μm for the measurement of CO, one filter at 3.3 μm for the measurement of HC, and one reference filter (Ref) at 3.9 μm to normalize for wavelength independent IR extinction (Figure 4-19).

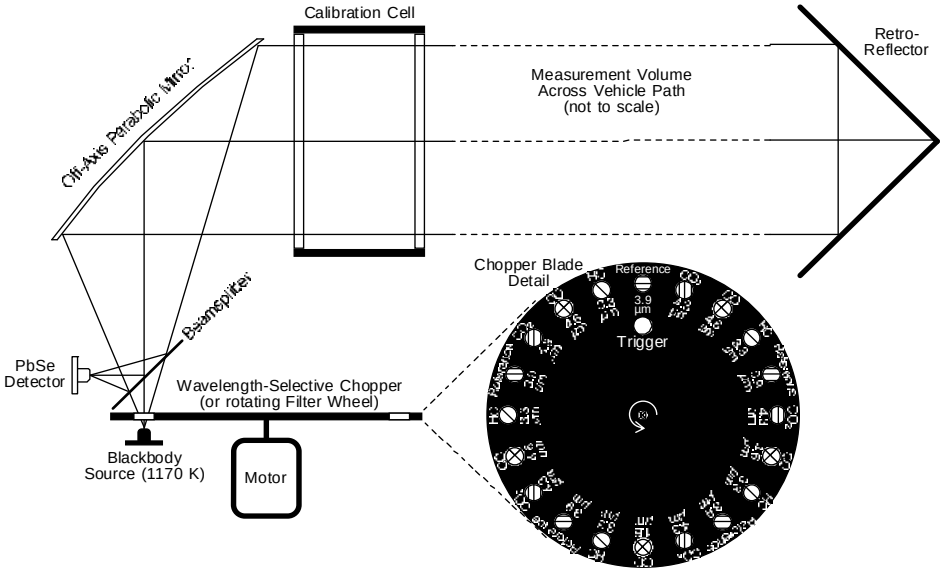

Figure 4-19. Diagram of the IR cross-plume sensor with chopper wheel for signal modulation.

As the chopper wheel rotates at 50 Hz, five transmissions of the wavelength sequence CO_2, CO, HC, and Ref occur per revolution, allowing repetitive measurements of gaseous concentrations at 250 Hz. The wavelength-modulated IR radiation is transmitted through a beam splitter, further collimated with a 2" diameter, off-axis, parabolic mirror and transmitted through an internal calibration cell followed by transmission through the measurement volume extending across the vehicle path. On the opposite side of the vehicle path, the IR radiation is reflected back towards the transmitter with a 2.5" diameter corner cube used as retro-reflector. The retro-reflected light is focused by the off-axis, parabolic mirror onto a Peltier-cooled, lead-selenide (PbSe) detector (Cal Sensors BXT1-28T). This detector produces a voltage signal proportional to the incident IR power that is shown in Figure 4-20 for one filter sequence.

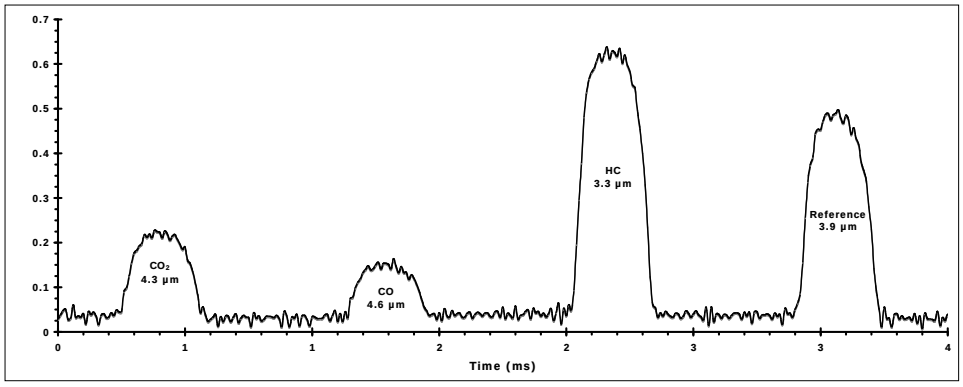

Figure 4-20. Detector signal for one filter sequence.

Extinction and absorption processes can be described by Beer's law if the absorption coefficient α is constant within the time, wavelength, and area that the measurement integrates over. In our case, we integrate over relatively large wavelength intervals. While, the extinction due to particles stays fairly constant over these intervals, those of gases may not. Therefore, gaseous extinction coefficients are not necessarily proportional to gaseous concentrations and absorption path lengths. Nevertheless, the change of optical power due to extinction can still be written to look like Beer's law

$$P_i = P_{0\_i} \exp\left[-\alpha_{p\_i} x\right] \exp\left[-\alpha_{g\_i} x\right], \tag{4-3a}$$

where P_i is the optical power measured by the detector after the measurement path, P_{0_i} the generally unknown optical power before the measurement path, α_{p_i} and α_{g_i} the particle and gaseous extinction coefficient (dimension of inverse distance) over the wavelength range i averaged over the absorption path length x.

For the reference channel, gaseous absorption is negligible simplifying the equation to

$$P_{ref} = P_{0\_ref} \exp\left[-\alpha_{p\_ref} x\right], \tag{4-3b}$$

where the subscript *ref* indicates the wavelength band of the reference channel.

To measure the concentration of a gas i, the ratio of eq. 1a and 1b may be written as

$$\frac{P_{ref}}{P_i} = \frac{P_{0\_ref}}{P_{0\_i}} \frac{\exp\left[-\alpha_{p\_ref} x\right]}{\exp\left[-\alpha_{p\_i} x\right]} \exp\left[\alpha_{g\_i} x\right]. \tag{4-4a}$$

The ratio P_{0_ref}/P_{0_i} is constant but unknown and can be replaced by a constant k.

$$k = \frac{P_{0\_ref}}{P_{0\_i}} \tag{4-4b}$$

Under the assumption that the particulate extinction α_p is wavelength independent, and eq. 4-4a simplifies to

$$\frac{P_{ref}}{P_i} = k \exp\left[\alpha_{g\_i} x\right]. \tag{4-4c}$$

The gaseous absorption coefficient α_{g_i} can be replaced with the product of absorption mass efficiency E_{g_i} and mass concentration c_{g_i} as

$$\alpha_{g\_i} = E_{g\_i} c_{g\_i}. \tag{4-4d}$$

If Beer's law doesn't apply, the absorption mass efficiency E_{g_i} is not a constant but a function of the concentration depth $c_{g\_i} x$. In any case the ratio P_{ref}/P_i can be written as

$$\frac{P_{ref}}{P_i} = k \exp\left[E_{g\_i} c_{g\_i} x\right]. \tag{4-4e}$$

Taking the natural logarithm of this equation, the concentration c_{g_i} of gas i can be obtained as

$$c_{g\_i} = \frac{1}{E_{g\_i} x} \ln\left[\frac{1}{k}\frac{P_{ref}}{P_i}\right]. \tag{4-4f}$$

To obtain the concentration c_{g_i} of gas i from a measurement of P_{ref}/P_i and eq. 4f, knowledge of the constants x and k and of the function (or constant) E_{g_i} is required. The absorption path length x can be directly measured and the other unknowns can be obtained through calibration of the instrument as described below.

Taking the natural logarithm of eq. 4-4e yields

$$\ln\left[\frac{P_{ref}}{P_i}\right] = \ln[k] + E_{g\_i} c_{g\_i} x, \tag{4-5}$$

which makes it possible to calibrate the measurement. For this calibration, the gaseous concentration depth, that is the product of concentration c_{g_i} of gas i and of the absorption path length x, is varied by introducing different concentrations of gas i into the calibration cell. If Beer's law applies (i.e., $E_{g\_i} = const$), $\ln[P_{ref}/P_i]$ is a linear function of $c_{g\_i} x$ with a zero offset of $\ln[k]$ and a slope of E_{g_i}. In this case (i.e., $E_{g\_i} = const$), the previously unknown constants can be determined by linear regression. In the more common case that the gaseous absorption is inhomogeneous over the broadband wavelength range used for the measurement, Beer's law does not apply, and the function E_{g_i} must be determined by fitting an empirical function to the experimental data. Once the constants and potentially the function E_{g_i} have been determined through the calibration process, the average gas concentrations over the absorption path can be calculated from the measurements of P_{ref}/P_i using eq. 4-4f.

VERSS measurements were compared with those from IPETS on school bus emissions operating on regular diesel and a B-20 biodiesel mixture as part of this project (Mazzoleni et al., 2007a). For CO, Figure 4-21 shows a slope of 0.86 with a correlation of 0.75. Elimination of a few outliers improves these statistics. Average CO EFs measured by the two systems on this dataset are: CO EF = 60 ± 8 g_{CO}/kg_{Fuel} from the VERSS, and CO EF = 69 ± 7 g_{CO}/kg_{Fuel} from the IPETs, which represents a good agreement. Figure 4-22 shows a similar comparison for NO, for which the slope is 1.0 and the correlation coefficient is 0.68. Again, a few outliers dominate the statistics. Average NO was 17±1 g_{CO}/kg_{Fuel} for the in-plume system and 18±1 g_{CO}/kg_{Fuel} for the in-plume system. As with CO, average emissions are nearly the same.

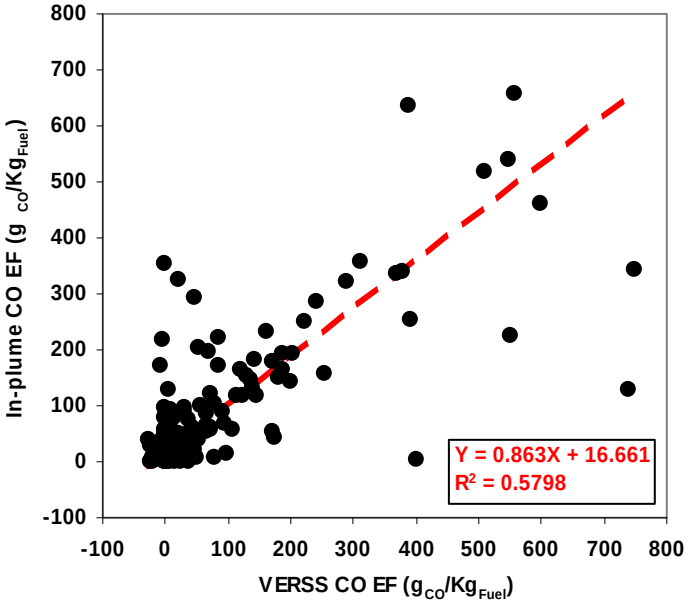

Figure 4-21. Comparison of in-plume and cross-plume Vehicle Exhaust Remote Sensing System (VERSS) emission factors (EF) for CO.

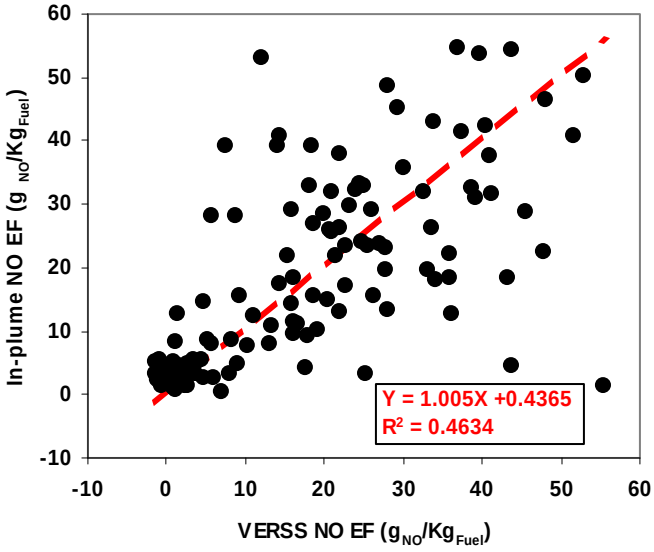

Figure 4-22. In-plume vs. cross-plume VERSS NO EFs for individual vehicles.

Individual vehicles measured by the IPETS are identified by a sharp peak in the CO_2 signal. However, it is not always possible to match without ambiguity vehicles measured by the VERSS with vehicles measured by the PETS. Random noise mostly cancels out in the average calculation, which results in the good agreement between the averages.

In-plume EFs were calculated by normalizing PM concentrations integrated over ELPI stages to the CO_2 concentration measured by the FTIR or Li-Cor in the IPETS. Due to different time lags and time responses of these different instruments, it is difficult to match individual PM and gas concentration peaks corresponding to individual vehicles. This is especially challenging and error prone in heavy traffic conditions such as those found during the Boise experiment. Time averaging reduces biases between the two measurements. Half-hour averages of in-plume PM background subtracted concentrations were calculated and normalized to in-plume CO_2. Inplume measurements were averaged over the same time periods. In-plume and cross-plume PM EFs are compared in Figure 4-23. Due to different validity rates between the two instruments and throughout the day, the two instruments did not record data for exactly the same vehicle. Nevertheless, the EFs track each other during most of the day. This is true regardless of the composition of traffic passing both sensors.

Figure 4-24 compares VERSS and IPETS emission factors for half-hour averages, with a linear regression slope of 0.71 and a correlation coefficient of 0.69. The average PM EFs measured by the two systems were 0.78±0.09 g_{PM}/kg_{Fuel} for the cross-plume and 0.80±0.006 g_{PM}/kg_{Fuel} for the in-plume system. Again, the average agreement is good with no apparent bias.

4.5 On-Board PM Measurement System

As explained in Section 4.2, the commercial PEMS were inadequate for all but NO_x and CO_2 measurements. Only two of them made rudimentary attempts to quantify PM emissions. The PM on-board system developed for this project consists of the following components: 1) a power generator supplying all instruments and subsystems with electric power, 2) a data acquisition system recording measurement data and operating parameter, 3) a global positioning system (GPS) recording vehicle location, speed and acceleration, 4) a Compact Exhaust Sampling and Dilution (CESD) system that samples raw exhaust from the vehicle tailpipe, dilutes the raw exhaust and provides a sampling manifold for other instruments, and 5) emissions measurement instruments.

The emissions measurement instruments include: 1) a TSI DustTrak (DT) for the measurement of light scattering from PM to be used as surrogate for a PM mass measurement, 2) a DRI Photoacoustic Analyzer for the measurement of black carbon (BC) concentrations, 3) Filter Sampling (FS) system (parallel Teflon and quartz filters) for integrated determination of mass, elements, ions, and carbon fractions; and 4) a LiCor (LI-840) CO_2/H_2O Gas Analyzer for the measurement of CO_2 emissions allowing the determination of fuel-based emission factors for all other measured quantities.

These components were integrated into a portable, robust onboard measurement system shown in Figure 4-25 for the real time measurement of PM and BC mass emission factors and time-integrated measurement of these quantities with filter techniques for the calibration and validation of the real time instruments and data.

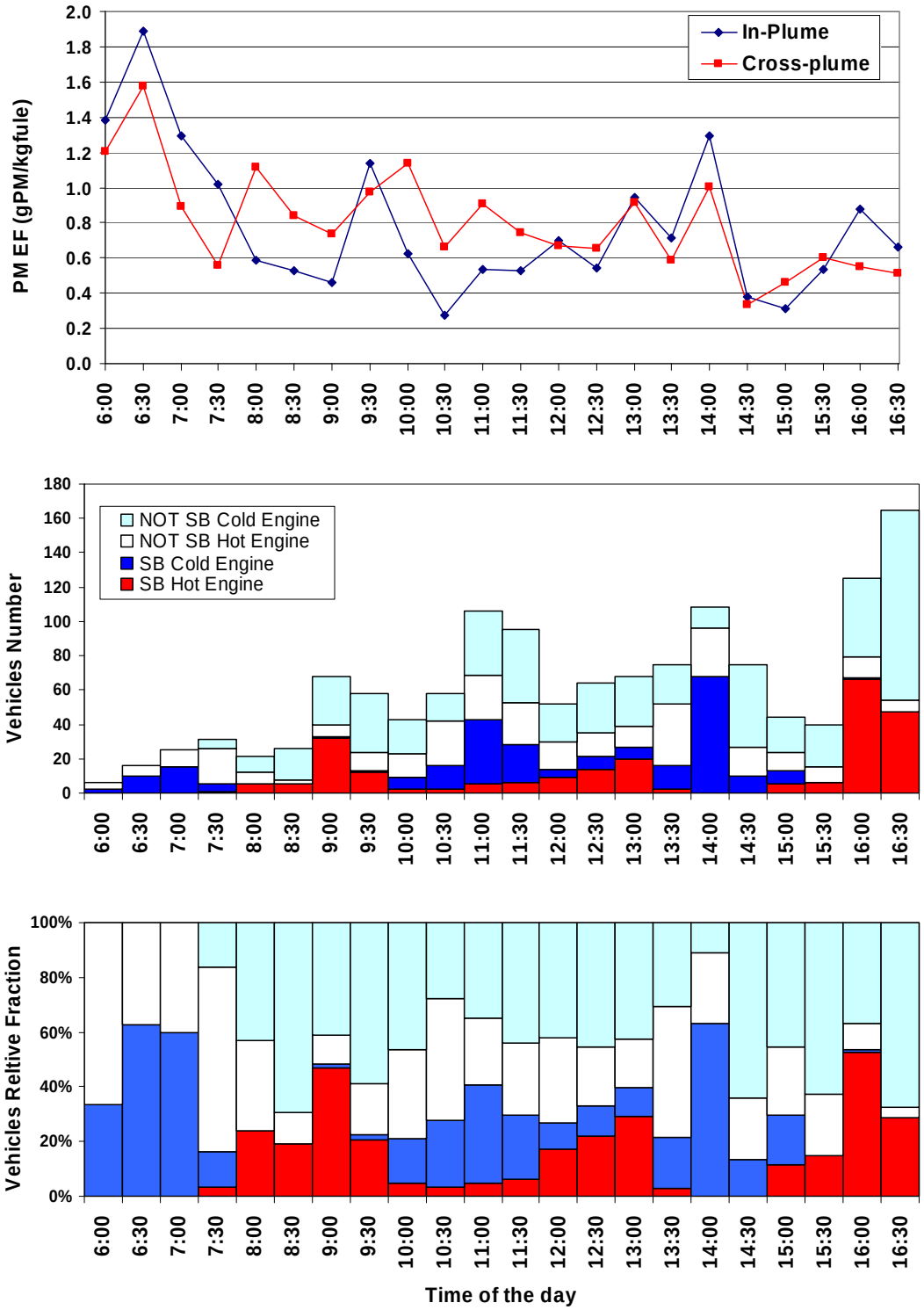

Figure 4-23. Comparison of PM measurements from in-plume and cross-plume monitors. Top graph: half hour averaged PM emissions factors as a function of time. Middle graph: half hour traffic composition. Lower graph: fraction of vehicles in each class. These data were collected in Boise, ID during March 4th 2004.

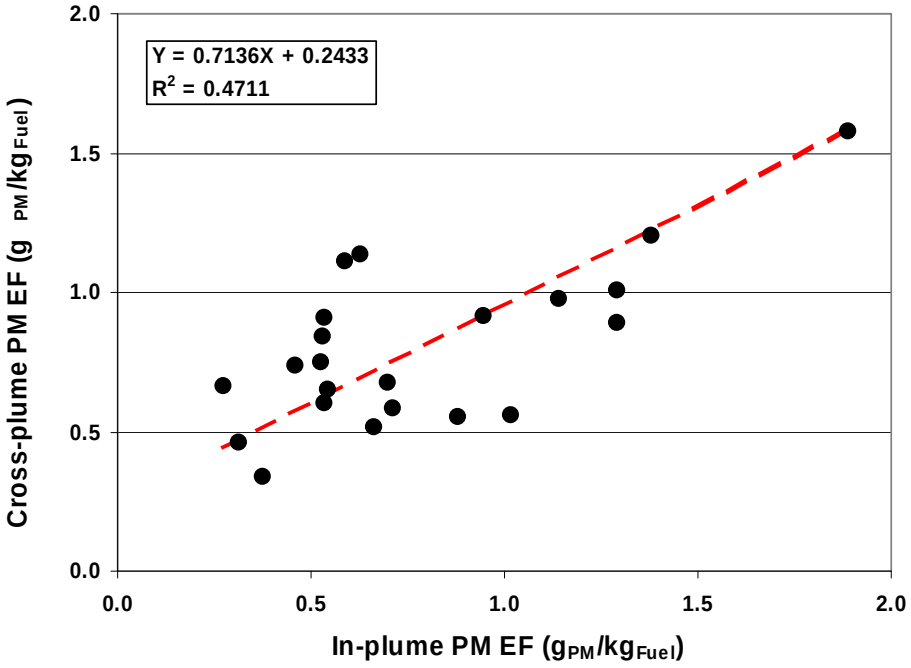

Figure 4-24. PM emission factor comparison for cross-plume VERSS with in-plume IPETS for 30 minute averages.

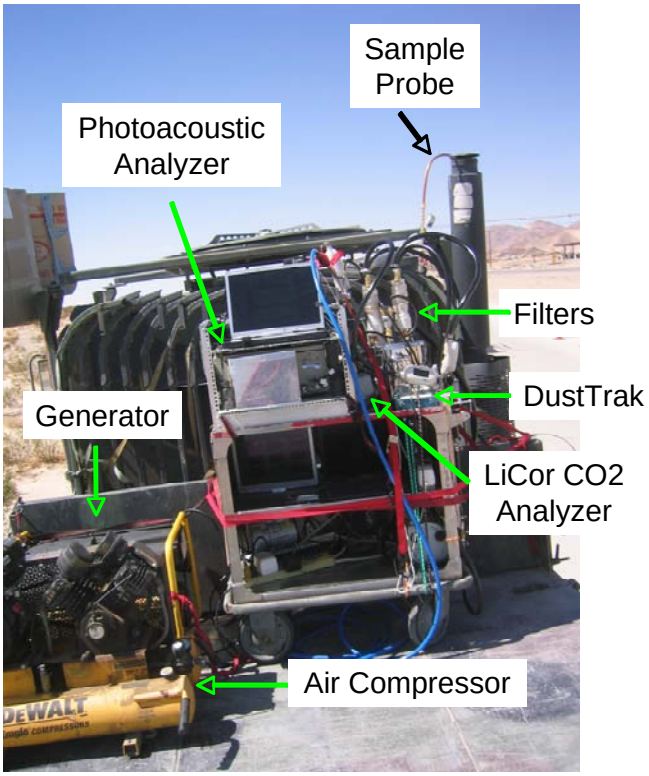

Figure 4-25. Photograph of on-board PM measurement system.

The Compact Exhaust Sampling and Dilution (CESD) system samples the vehicle exhaust with a 3/8" ID copper pipe that is inserted into the vehicle tailpipe. This pipe is

connected to an Air-Vac Engineering Company, Inc. model 260H ejector pump. This pump is based on the Venturi effect and is driven with compressed, HEPA-filtered air from a DeWalt D55270 gasoline engine powered portable compressor. The ejector pumps the exhaust through an 8' long, 1" ID conductive rubber hose into the sampling manifold and dilutes it with HEPA filtered air with a dilution ratio of 2.9. The sampling manifold is a 11 l volume stainless steel container (Figure 4-26) that is continuously filled by the ejector pump through its inlet with diluted exhaust.

Six of seven outlets are available for sampling by the instruments and filter samplers at a combined flow rate that is much smaller than the input flow rate from the ejector pump. Excess diluted exhaust is vented through a seventh outlet. The dilution ratio of the ejector pump has been determined by using the CESD system to sample compressed gas with a constant and elevated CO_2 concentration of about 2500 ppm. Alternate measurements of the CO_2 concentration of undiluted and diluted gas, taking into account the also measured CO_2 concentration of the dilution air, yielded a dilution ratio of 2.9.

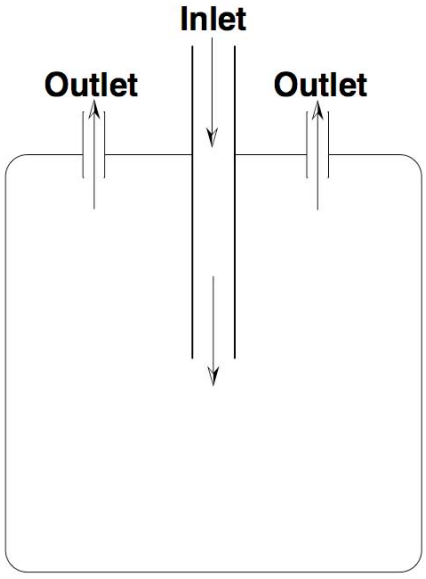

Figure 4-26. Diagram of Compact Exhaust Sampling and Dilution (CESD).

The DustTrak PM optical scattering and Licor CO2 systems area identical to those described in Section 4.3 for the IPETS. As the calibration of the DT with A1 test dust may not be adequate for the much smaller (sub-micron) diesel PM encountered in this study, gravimetric PM mass concentrations are obtained from Teflon filter measurements were used to calibrate the DT for this application. Filter calibration data include measurements with the on-board system for M TVR, LVS, and AAV military off-road diesel vehicles, as shown in Figure 4-27. There is a good (R^2=0.98) correlation between gravimetric filter PM mass concentrations and DT PM mass concentrations. The uncalibrated slope of 1.14 signifies that the uncalibrated DT measures 14% higher PM mass concentrations than the gravimetric filter method. This slope is used in the following to calibrate the DT and to bring its measurements in better agreement with the gravimetric filter method.

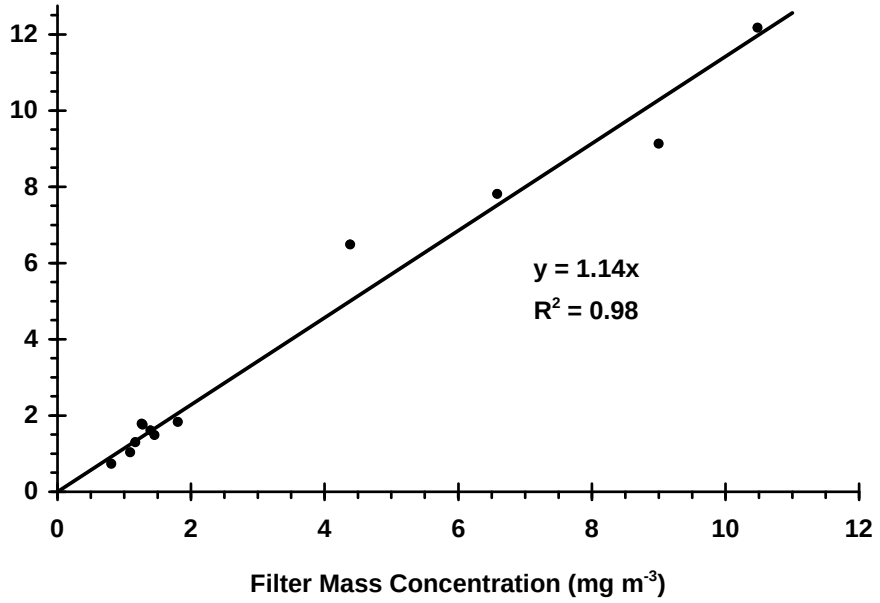

Figure 4-27. Relationship between DustTrak reading and filter mass concentration.

The DRI Photoacoustic Analyzer (PA) directly measures the optical absorption (B_{abs}) by PM at a wavelength of 1047 nm (Arnott et al., 1999; Arnott et al., 2003; Arnott et al., 2005; Moosmüller et al., 1997; Moosmüller et al., 1998; Moosmüller et al., 2001b; Raspet et al., 2003). Light absorption of a power-modulated 1047 nm laser beam by PM converts light energy to an acoustic pressure wave in the DRI PA instrument. A microphone detects the acoustic signal, and hence a measure of light absorption is produced (Arnott et al., 1999; Arnott et al., 2000). The DRI PA does not use filters for absorption measurements, is calibrated from first principles, and its dynamic range is large enough to allow for the characterization of samples ranging from raw diesel exhaust to ambient air in unpolluted settings.

An empirical absorption efficiency of 5 m^2/g for the 1047 nm is used to convert PA B_{abs} to BC concentration with $BC = B_{abs}/(5 m^2/g)$. This value was recommended based on previous comparisons of IMPROVE EC and PA B_{abs} measurements of diesel emissions at Hill Air Force Base, UT (Arnott et al., 2005). Limited comparisons of IMPROVE EC and PA B_{abs} obtained with the on-board system for MTVRs at the 29-Palms marine base yield a value of 4.4±0.8 m^2/g, in agreement of the 5 m^2/g value suggested by Arnott et al. (2005).

Filter sampling is similar to that for the IPETS, consisting of four parallel lines. The first channel contains a Teflon-membrane filter with a quartz fiber backup filter (to evaluate organic gas adsorption on quartz). The second channel contains a front quartz fiber filter with a potassium carbonate-impregnated cellulose-fiber filter to adsorb SO_2 gas. The third channel has a quartz fiber filter followed by a citric acid-impregnated cellulose-fiber filter that adsorbs NH_3., The fourth channel contains a Nuclepore polycarbonate filter. Teflon-membrane filters are submitted for mass by gravimetry and 51 elements by X-ray fluorescence (Watson et al., 1999). Half of the quartz-fiber filters are submitted for chloride (Cl^-), nitrate (NO_3^-), and sulfate ($SO_4^=$) by ion chromatography (IC; Chow and Watson, 1999) and water-soluble sodium (Na^+) and potassium (K^+) by atomic absorption spectroscopy. The second half of the quartz-fiber filters is submitted for ammonium (NH_4^+) by automated colorimetry (AC); for organic carbon (OC),

elemental carbon (EC), and their eight fractions (OC1-OC4, OP, EC1-EC3) by the IMPROVE_A thermal/optical protocol (Chow et al., 1993; 2001; 2004b; 2005a; 2007b); and for 125 non-polar speciated organic carbon compounds by thermal desorption-gas chromatography/mass spectrometry (Chow et al., 2007e; 2008; TD-GC/MS; Ho and Yu, 2004). The backup citric acidimpregnated cellulose-fiber filters were analyzed for ammonia (NH_3) by AC and the backup potassium carbonate-impregnated cellulose-fiber filters were analyzed for sulfur dioxide (SO_2) by IC.

4.6 Summary of SERDP Diesel Engine Emission Test Methods

The MEL, IPETS, VERSS, gas PEMS, and on-board PM systems all represent advances in measurement systems over the certification engine and chassis dynamometer tests. The MEL is the most well established technology, replicating the sampling, dilution system, and measurement devices that are usually confined to an emission testing laboratory. It offers the advantage of mobility, but its large size makes it difficult to position in a location to record realworld source emissions. For real-world mobile source emissions, the MELS is only applicable to sampling the exhaust of the tractor that is towing it. The MEL, however, is the only instrument that can provide a bridge between certification tests expressed in g/bhp-hr and the g/kgfuel fuelbased emission factors that are more useful for air quality planning inventories.

The gas PEMS show promise for NO_x and CO_2 emissions, but their current detection limits are too imprecise for quantifying VOC, CO, and PM emissions from diesel engines. PEMS have the advantage of being less costly to procure than other methods and being located on engines without causing interference with the routine operations. Though available commercial units were not found useful for further use in this study, continuing development of new portable gas sensing systems for homeland security and other applications will make gas PEMS a viable future technology. On-board PM emission monitoring was also an experimental technology for which the feasibility was demonstrated.

The IPETS is intermediate between the MEL and the PEMS, offering a movable platform that can be used in field situations, but is still too large and requires too much power to be mounted on the engine. IPETS is oriented toward real-world emissions, allowing exhaust samples to dilute and cool to ambient conditions prior to measurement. Simultaneous CO_2 measurements allow emissions concentrations in the plume to be related to the fuel consumption, resulting in a fuel-based emission factor. The current IPETS design has multiple measurements for CO_2 and PM mass concentrations. Particle number measurements in different size fractions allow the important UP fraction to be determined. The FTIR is capable of quantify non-criteria pollutants such as NH_3 along with the normal certification pollutants. As with the MEL, the IPETS challenge is being able to extract a portion of the plume for analysis. While this is relatively straightforward for stationary sources such as generators where a probe can be located in the plume, it is more difficult for mobile sources.

The VERSS remote sensing system is applicable to mobile sources following a set path. However, many non-road sources don't follow such paths. VERSS is a cutting edge technology that takes advantage of recent advances in lasers, radiation detection, and high speed data acquisition. VERSS feasibility was proven in this project, but it was not deemed practical for taking many measurements. A major limitation is the lack of commercial replacement parts, as several components were produced specifically for the system. Although many advances were

made in the technology as part of the project, time and budget limitations did not permit the development and implementation of the system as envisioned at the project onset.

Various comparison tests among the different methods on the same emissions showed promising results, typically within ±30% for fuel-based emissions factors, but sometimes as high as a factor of two or more. PM was the most difficult observable to measure, owing to its many different measurement methods and the fact that its semi-volatile components are susceptible to temperature differences as the plume ages and cools.

5. ENGINE TESTS AND RESULTS

Emission tests were performed on a variety of non-road military diesels using the MEL, IPETS, VERSS, and on-board PM monitor. A systematic selection of engines, fuels and operating modes from those with the largest number of units or highest fuel consumption as identified in Section 3 was not possible owing to access and logistical activities at military bases. The engines tested were those that could be made available by California military bases. Owing to its large size, it was difficult to move the MEL onto the bases. For mobile sources, the engine must be in a vehicle capable of towing the MEL trailer or operated on a chassis dynamometer. Backup generators were more easily moved to the UCR test facility than moving the large MEL van into the generator storage areas. Owing to its smaller size and portability, the IPETS could be located near stationary sources and some mobile sources. The VERSS and portable PM monitor were only useful for mobile sources traveling well-defined routes.

Due to training and combat requirements, military equipment use was at a maximum during the 2004 to 2007 period when tests were finally arranged. Frequent personnel turnover at the bases worked against optimal scheduling of emission tests that might interfere with normal base operations. These difficulties are important considerations for further emission testing and added substantially to the cost of executing the tests.

5.1 MEL Stationary Source Tests

Table 5-1 summarizes the MEL backup generator engine tests. The Kamatzu/SA6, Deere RZJ, and the CUM/NT855 engine were tested on several different fuels using the same engine and cycle, allowing fuel effects on emissions to be evaluated.

Test fuels were mixtures (Holden et al., 2006) of: 1) an in-use, on-road ARB-certified Ultralow sulfur diesel (ULSD), 2) a used vegetable oil/yellow-grease biodiesel fuel prepared at the Port Hueneme Naval Base using the Biodiesel Industries Inc. pilot plant biodiesel production facility (YGA), 3) a soy-based biodiesel obtained from World Energy (SOY); and a military JP8 fuel. Neat biodiesel fuels were made from typical methyl esterification processes and met ASTM D6751 specifications. The ULSD and the neat biodiesel fuels all had cetane number in the low 50s, while the cetane number for the JP-8 was _36. The cetane number for the B100-YGA increased from 52.7 to 53.2 for the 1200 ppm dose and from 52.7 to 57 for the 3000 ppm dose (Durbin et al., 2007).

Table 5-1. Backup generator diesel engines tested by the MEL using different fuels.

Unit	CARB	CA/ULSD	JP-8	B20/Soy	B20/YGA	B100/YGA	E-Diesel
DDC 6V92 (350kW)	X						
CAT 3406B (300kW)	X						
Cummins 6BT (100kW)	X						
Deere TBG (60kW)	X						
Deere 6076 (125kW)	X		X				
Kamatzu/SA6D125E (250kW)		X	X		X	X	X
Deere RZJ-01978 (60kW)		X	X		X		X
Deere 6059T (60kW)	X						
CUM/NT855 (200)	X					X	
CUM/NT855 (200)	X						
CAT/D343(200kW)	X						

Two different CUM/NT engines were tested, which allowed the precision of the emissions among similar engines and test cycles to be evaluated. The generators were provided by Camp Pendleton, Twenty-nine Palms Training Grounds, Vandenberg AFB, and Miramar Station. Table 5-2 describes the steady state engine loads and sample durations at which emission rates were quantified. The overall emission factor is determined by a weighted average of these emissions, with the weighting given in the final column of Table 5-2.

Data were collected at each mode from duplicate runs, as illustrated in Figure 5-1. For this modern unit with electronic controls, emissions were highest under the maximum load.

Table 5-2. Test loads for backup generator tests.

Mode number	Engine Speed[1]	Observed Torque[2]	Minimum time in mode, min.	Weighting factors
1	Rated	100	5.0	0.05
2	Rated	75	5.0	0.25
3	Rated	50	5.0	0.30
4	Rated	25	5.0	0.30
5	Rated	10	5.0	0.10

Notes: (1) Engine speed: ± 2% of point. (2) Torque: Throttle fully open for 100% point. Other points: ±2% of engine maximum.

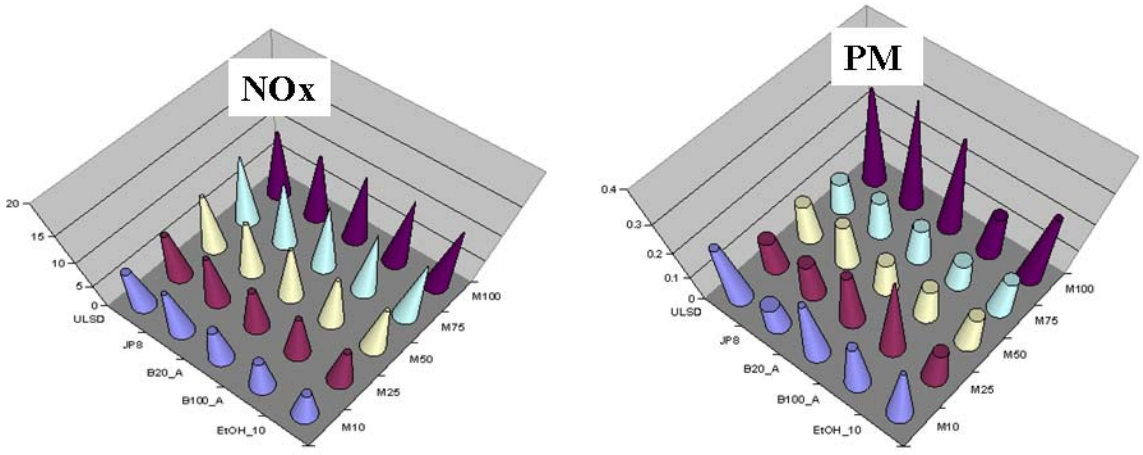

Figure 5-1. NO_x and PM emissions (g/kW-hr) for the Kamatzu 250 kW generator operating at different loads with different fuels.

Weighted emission factor for any component was calculated from the measured modal emission values as follows:

$$WE_c = \frac{\sum_{i=1}^{i=n} SE_c(i) \times Power(i) \times WF(i)}{\sum_{i=1}^{i=n} Power(i) \times WF(i)} \quad (5\text{-}1)$$

where:

WE_c : total weighed emission for component c
n : number of modes in cycle
i : mode number (specific load point in test cycle)
SE_c : specific emission for component c at specified load point (g/kWh)

Power : brake power (kWh) at specific load point
WF : weight factor (for specific load point and given cycle)

Tables 5-3 and 5-4 summarize the weighted emission factors for criteria pollutants and selected carbonyls, several of which are designated as Hazardous Air Pollutants (HAPs).

5.2 MEL Mobile Source Tests

Table 5-5 summarizes the MEL mobile source tests on vehicles provided by Port Hueneme, Camp Pendleton and Cheyenne Mountain Complex. Testing followed the AVL driving schedule as the AVL 8-Mode test is a steady-state engine test procedure, designed to closely correlate with the exhaust emission results over the US FTP heavy-duty engine transient cycle as outlined in Table 5-6.

Duplicate tests were carried out at each mode. For example, the modal results of a test with multiple fuels are plotted below for a truck with a 250 hp diesel engine. Figure 5-2 illustrates emissions for the different modes and fuels used in these tests. These results indicate that the emissions from EPA low-sulfur diesel exceeded those for the ARB ULSD.

Figure 5-3 compares emission factors for three of the tests as the weighted average over the entire AVL 8-mode cycle. PM emissions are slightly lower for biodiesel fuels, but the NO_x emissions are higher. Emission differences for different fuels are more evident for the heavy-duty diesel engine compared with the medium-duty diesel engine.

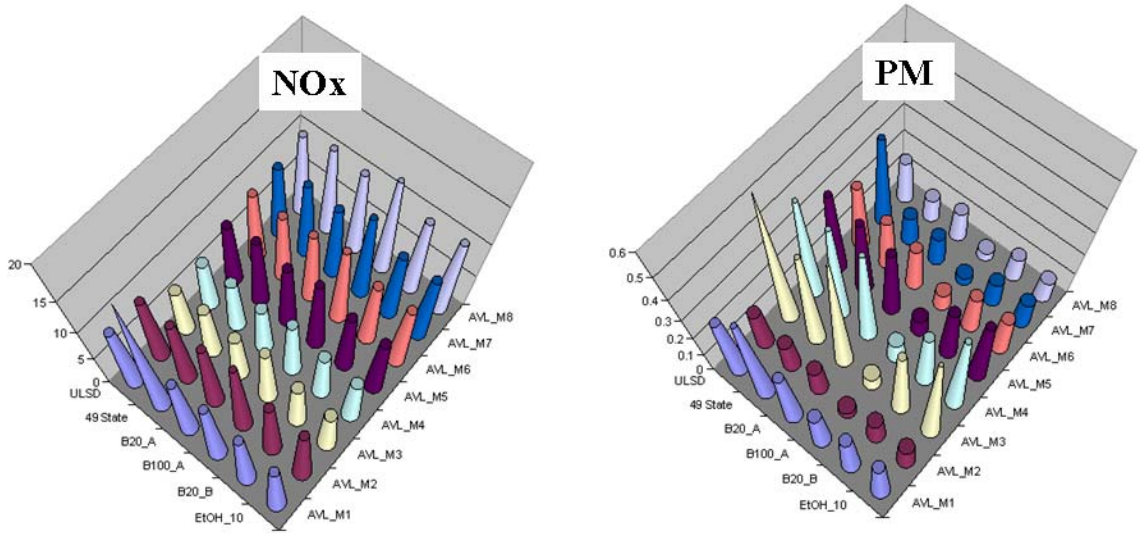

Figure 5-2. NO_x and PM emissions (g/bhp-hr) for a 250 hp truck engine as a function of AVL mode and fuel.

Table 5-3. Weighted CH_4, NMHC, NO_x, NO_2, CO_2, PM, EC, and OC emission factors for diesel generators tested by the MEL.

Mfg/Model/Yr	Fuel	Emission Factors g/kW-hr								
		CH4	NMHC	CO	NOx	NO2	CO_2	PM	EC	OC
CAT/3406B/90	CARB	0.03	0.12	1.21	12.96	nd	777	0.13		
DDC/V92/86	CARB	0.05	0.59	1.26	10.48	nd	868	0.29		
CUM/6BT/90	CARB	0.15	1.41	1.96	13.25	0.49	830	0.24	0.12	0.10
JD/KOHLER/01	CARB	0.11	1.12	1.25	9.02	0.32	878	0.26	0.16	0.08
JD/KOHLER/91	CARB	0.08	1.10	1.19	17.40	0.28	797	0.21	0.07	0.12
JD/KOHLER/91	JP8	0.10	1.06	1.23	17.48	0.15	783	0.17	0.03	0.07
Kamatzu/SA6D125E-2/2000	B20 YGA	0.03	0.33	0.53	7.80	0.27	752	0.12	0.06	0.04
Kamatzu/SA6D125E-2/2000	B100YGA	0.03	0.12	0.50	8.22	0.30	760	0.11	0.03	0.05
Kamatzu/SA6D125E-2/2000	JP8	0.03	0.48	0.65	7.70	0.33	753	0.11	0.08	0.04
Kamatzu/SA6D125E-2/2000	ULSD	0.03	0.36	0.50	7.59	0.31	754	0.10	0.07	0.03
Kamatzu/SA6D125E-2/2000	EtOH Diesel	0.03	0.38	0.50	7.64	0.34	744	0.12	0.06	0.05
Libby/MEP-806A/95	ULSD	nd	nd	1.71	9.06	0.81	940	0.28	0.10	0.11
Libby/MEP-806A/95	JP8	0.16	2.02	3.38	10.48	1.10	933	0.14	0.08	0.06
Libby/MEP-806A/95	B20YGA	0.09	1.33	1.68	9.23	0.76	937	0.28	0.12	0.09
Libby/MEP-806A/95	EtOH Diesel	0.09	1.39	1.58	9.36	0.77	944	0.26	0.11	0.14
JohnDeere/6059T/91	CARB	0.01	1.81	1.90	8.03	0.61	914	0.26		
CUM/NT-855-G3/91	CARB	0.01	0.78	1.34	8.62	0.45	906	0.77		
CUM/NT-855-G3/91	B20YGA	0.01	0.71	1.25	9.15	0.45	907	0.56		
CUM/NT-855-G3/91	CARB	0.01	0.66	1.12	9.87	0.41	906	0.41		
CAT/D343/85	CARB	0.01	1.59	4.46	9.75	1.99	1032	0.83		

CH_4=Methane, NMHC=Non-methane Hydrocarbons, NO_x=Oxides of Nitrogen, NO_2=Nitrogen Dioxide, CO_2= carbon dioxide, PM=Particulate Matter, PM EC=Elemental Carbon by Thermal Optical Transmittance (TOT), PM OC=Organic Carbon by TOT.

Table 5-4. Weighted carbonyl emission factors for diesel generators tested by the MEL.

Mfg/Model/Yr	Fuel	Emission Factors mg/kW-hr													
		Formal	Acetal	Acetone	Acrolein	Propional	Crotonal	MEK	Methac	Butyral	Benzal	Valeral	Tolual	Hexanal	Total
CAT/3406B/90	CARB	18.0	5.2	3.3	0.5	0.3	0.0	0.1	0.4	0.4	0.0	0.0	0.0	0.0	28.2
DDC/V92/86	CARB	19.0	6.8	3.7	0.3	1.2	0.3	0.4	0.1	2.1	0.6	0.8	0.0	0.3	35.6
CUM/6BT/90	CARB	66.2	12.7	6.3	3.1	3.5	1.8	1.9	1.0	3.2	3.7	1.4	1.2	3.8	109.9
JD/KOHLER/01	CARB	48.3	10.0	6.2	2.5	2.7	1.0	1.8	0.8	3.0	3.1	1.0	0.8	3.0	84.1
JD/KOHLER/91	CARB	50.5	10.6	5.8	1.6	2.8	0.7	1.2	1.4	4.3	2.4	1.2	0.7	4.1	87.5
JD/KOHLER/91	JP8														
Kamatzu/SA6D125E-2/2000	B20 YGA	36.6	13.3	3.8	2.2	2.1	1.2	1.1	0.3	1.6	2.1	1.4	0.5	2.6	68.8
Kamatzu/SA6D125E-2/2000	B100YGA	21.7	7.3	2.4	1.2	1.7	0.6	0.7	0.1	0.9	1.0	0.6	0.4	1.5	40.1
Kamatzu/SA6D125E-2/2000	JP8	16.4	6.0	3.3	0.7	0.8	0.4	0.7	0.2	0.7	1.1	0.4	0.2	1.3	32.2
Kamatzu/SA6D125E-2/2000	ULSD	16.7	6.0	2.3	1.2	0.9	0.5	0.7	0.3	0.6	1.1	0.4	0.4	1.2	32.2
Kamatzu/SA6D125E-2/2000	EtOH Diesel	26.8	10.9	2.2	2.2	1.3	0.3	0.3	0.3	0.7	0.9	0.5	0.4	1.6	48.4
Libby/MEP-806A/95	ULSD	56.2	24.8	7.4	1.8	3.6	1.6	2.0	0.4	2.5	3.3	1.6	1.1	3.8	110.1
Libby/MEP-806A/95	JP8	81.0	24.1	7.6	2.4	3.1	1.5	1.3	0.3	1.6	3.8	1.4	1.3	4.2	133.6
Libby/MEP-806A/95	B20YGA	59.4	19.1	6.9	2.3	3.5	1.5	1.7	0.2	2.1	4.1	2.2	0.9	1.9	105.8

Table 5-5. MEL Mobile source emissions test engines and fuel types.

				Soy		YGA			YGB	
Unit	EPA	CA/ULSD	JP-8	B20	B20	B50	B70	B100	B20	E-Diesel
Ford F-350 (Nav 7.4L		X			X					X
Ford F-700 (Cum 5.9L)		X		X	X					X
Ford F-9000 (Cat 34	X	X			X					X
Thomas Bus (Cat 3126)		X			X			X	X	X
Bus (Cum ISB245)	X	X		X						
Bus (Cum plus catal	X			X						
Humvee (GM6.5L)		X	X	X	X	X	X	X	X	X

Table 5-6. AVL8-mode test cycle specifications.

Mode	% Engine Speed[a]	% Load	Weight Factor[b]
1	0	0	35.00
2	11	25	6.34
3	21	63	2,91
4	32	84	3.34
5	100	18	8.40
6	95	40	10.45
7	95	69	10.21
8	81	95	7.34

[a]Normalized speed: 0%=low idle, 100% = rated speed.
[b]Relative weight factors, not normalized (they do not add to 100%).

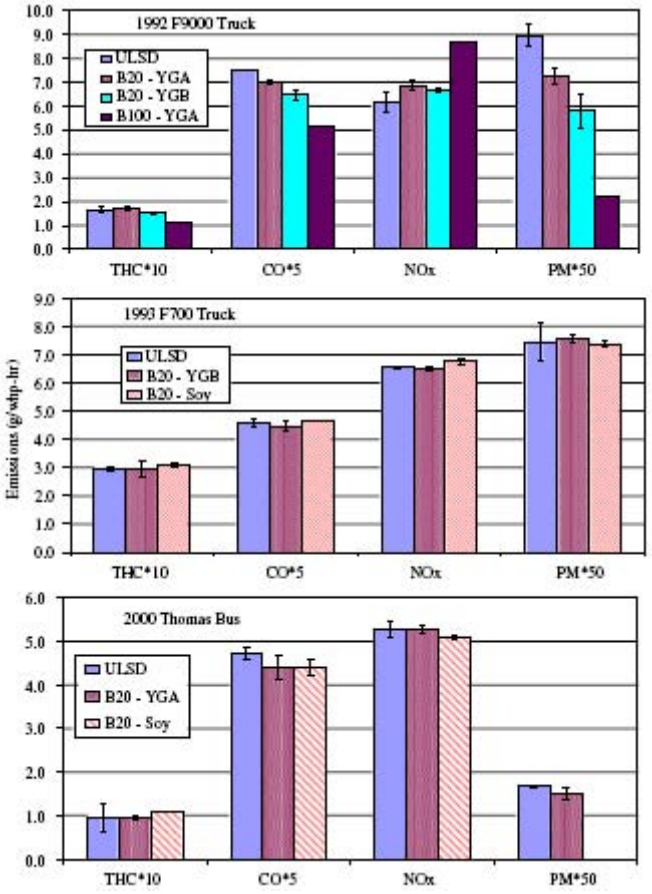

Figure 5-3. Weighted emission factors (g/bhp-hr) for the F9000, F700, and bus diesel engines.

5.3 IPETS Stationary Source Tests

Diesel generators described in Table 5-7 were tested with the IPETS at the Camp Pendleton Marine November 14-16, 2005. Test engines were selected based on a wide range of operating hours, engine manufacturers, generator manufacturers, and year of manufacture as recorded at the time of sampling. Test engines were situated in an open lot and were operated for ~ 5 minutes each at 100%, 75%, 50%, 25% and 10% of full capacity. A resistance load cell provided the engine load. Emissions from cold start (within 5 minutes of engine start up) were measured after an overnight cold soak of at least 16 hours.

Fuel samples were drawn from jerrycans and the fuel tanks of the 60 kW and 100 kW generator tanks and analyzed at Intertek Caleb Brett Laboratorie (Deerborne, TX), with results in Table 5-8. Fuel parameters from the jerrycans were consistent with the California No. 2 Diesel specification, with sulfur content between 148 and 139 ppmw, while the generator tank samples were consistent with the JP-8 characteristics with sulfur content ranging between 311 and 349 ppmw. Communications with the maintenance staff indicated that the base was temporarily unable to obtain JP-8 fuel for the generators and that they were using California No. 2 Diesel to refuel the generators when needed.

Table 5-7. Diesel generators tested at Camp Pendleton.

Generator	Test date	Generator Model	Hours used	Engine year	Serial Number	Rated power (kW)
1	11/14/05	MEP803A	2618	1999	FZ30644	10
2	11/14/05	MEP803A	3103	1995	RZCO2845	10
3	11/14/05	MEP803A	2154	1994	RZCO2061	10
4[a]	11/15/05	MEP805A	1943	1995	RZH01043	30 (1)
5	11/15/05	MEP805A	3374	1995	RZH01023	30 (2)
6	11/15/05	MEP805A	1641	1995	RZH00999	30 (3)
7	11/15/05	MEP805B	636	2002	HX32455	30 (4)
8	11/15/05	MEP805B	85	2002	HX33185	30 (5)
9	11/15/05	MEP806B	1017	2002	HX62471	60 (1)
10	11/15/05	MEP806B	1084	2001	HX62182	60 (2)
11	11/15/05	MEP806A	947	1995	RZJ02059	60 (3)
12	11/15/05	MEP806B	366	2001	HX62178	60 (4)
13	11/16/05	MEP007B	1874	n/a	n/a	100
14[b]	11/16/05	MEP805B	29	2002	RZ02630	30

a. Unit tested five distinct loads only
b. Unit tested cold start only.

Ambient PM samples were collected each day to evaluate the effects of atmospheric mixing with the diesel exhaust plumes using two parallel filter packs: 1) 47 mm PTFE filter (gravimetric mass) followed by quartz-fiber filter (volatilized PM organic carbon), and 2) quartz fiber filter (water soluble ions, OC/EC) followed by sodium carbonate coated cellulous fiber filter (for SO_2). The filter pack flow rate was monitored and adjusted to the specified flow rate at least every 30 minutes to assure accurate $PM_{2.5}$ size selection. Ambient temperature and RH were monitored and recorded every hour. Average ambient temperature and relative humidity during the sampling period were 28.5 ± 4.5°C and 25.8 ± 10.1%, respectively.

Figure 5-4 displays the background-corrected time series of pollutants as recorded on November 15, 2005 for five 30 kW and four 60 kW generators. During data reduction process CO_2 readings less than 300 ppm (0.28% of all data) were removed since these levels are well below the ambient CO_2 concentration. After examining background-corrected data time-series, all NH_3 data points with a standard error concentration (SEC) greater than 0.5 ppm were filtered out. SO_2 and ethylene, NO_2, and around 20% of NO data also showed high variation indicating system instabilities. NO data less than -2 ppm and all NO data with a SEC higher than 20 ppm were filtered out, all NO_2 data greater than 20 ppm and less than -20 ppm were filtered out.

Fuel-based emission factors (EF_i) were calculated using a variation of Equation 5-2:

$$EF_i = CMF_{diesel} \frac{\frac{\rho_i}{\rho_{CO_2}}}{CMF_{CO_2} + (CMF_{CO} \frac{\rho_{CO}}{\rho_{CO_2}} + CMF_{HC} \frac{\rho_{HC}}{\rho_{CO2}})} \quad , \qquad (5\text{-}2)$$

where ρ_i, ρ_{CO2}, ρ_{CO}, ρ_{HC} are the excess (i.e., above ambient) mass concentrations of the pollutant i, CO_2, CO, and HC, respectively, *CMF* is the carbon mass fraction with CMF_{CO} = 42.9%,

CMF_{CO2} = 27.3%, and CMF_{diesel} = 85.6% (assuming the empirical formula C_nH_{2n} for diesel fuel). For most engines with the exception of some gross CO or HC emitters, the terms in parentheses in Eq. 5-2 can be neglected.

Table 5-8. Fuel parameters. Measurements outside of the JP-8 specification are shown in italics whereas measurements outside of the California D2 specification are shown in bold.

		Date Sampled:	11/14/2005	11/15/2005	11/16/2005	11/16/2005	JP-8 Spec (MIL-DTL-831333E)	California Diesel Fuel Regs (CCR Title 13, Division 3, Ch. 5, Art. 2)
		Sampled From:	Refueling Jerrycan	Refueling Jerrycan	60KW, HX62178	100KW, RZ02630		
		Sample Number:	2005-007152-DRPK-001	2005-007152-DRPK-002	2005-007152-DRPK-003	2005-007152-DRPK-004		
Method	**Test**	**Units**						
ASTM D2500	Cloud Point	¡C	-11	-12	-56	-56		
	Cloud Point	¡F	12.2	10.4	-68.8	-68.8		
ASTM D2622	Sulfur	ppm (Wt)	148	139	311	349	*<3000*	**<500**
ASTM D2709	Sediment and Water	Vol %	0	0	0	0		
ASTM D4052 (IP 365)	API Gravity 15.56¡C, 60¡F	¡API	35.0	35.3	41.0	41.2	*37<x<51*	**33<x<39**
ASTM D86	Initial Boiling Point	¡F	372.5	366.1	392.2	**312.5**		**340<x<420**
	5% Recovery	¡F	415.0	407.4	358.4	353.7		
	10% Recovery	¡F	*433.4*	*427.6*	**362.0**	**355.2**	*<401*	**400<x<490**
	20% Recovery	¡F	467.3	455.7	376.8	370.5		
	30% Recovery	¡F	495.5	484.3	386.8	382.3		
	40% Recovery	¡F	523.8	514.3	398.6	393.6		
	50% Recovery	¡F	549.7	541.4	**410.4**	**405.3**		**470<x<560**
	60% Recovery	¡F	573.5	568.4	421.9	417.7		
	70% Recovery	¡F	596.9	592.9	436.5	432.1		
	80% Recovery	¡F	617.8	614.2	454.4	449.1		
	90% Recovery	¡F	**638.0**	**635.5**	**483.1**	**475.1**		**550<x<610**
	95% Recovery	¡F	654.4	655.5	513.6	498.3		
	Final Boiling Point	¡F	*658.1*	*663.7*	**546.4**	**530.4**	*<572*	**580<x<660**
	% Recovered	Vol %	96.6	97.8	97.7	98.5		
	% Residue	Vol %	*1.9*	1.1	*2.0*	1.4	*<1.5*	
	% Loss	Vol %	1.5	1.1	0.3	0.1	*<1.5*	
ASTM D93 (IP 34) Method A	Corrected Flash Point	¡C	96.5	**52**	**51**	71	*>38*	**>55**
	Corrected Flash Point	¡F	205.5	**125.5**	**123.5**	159.5	*>100*	**>130**
ASTM D976 (IP 364)	Calculated Cetane Index		51.1	50.9	**40.6**	**39.8**		**>48**

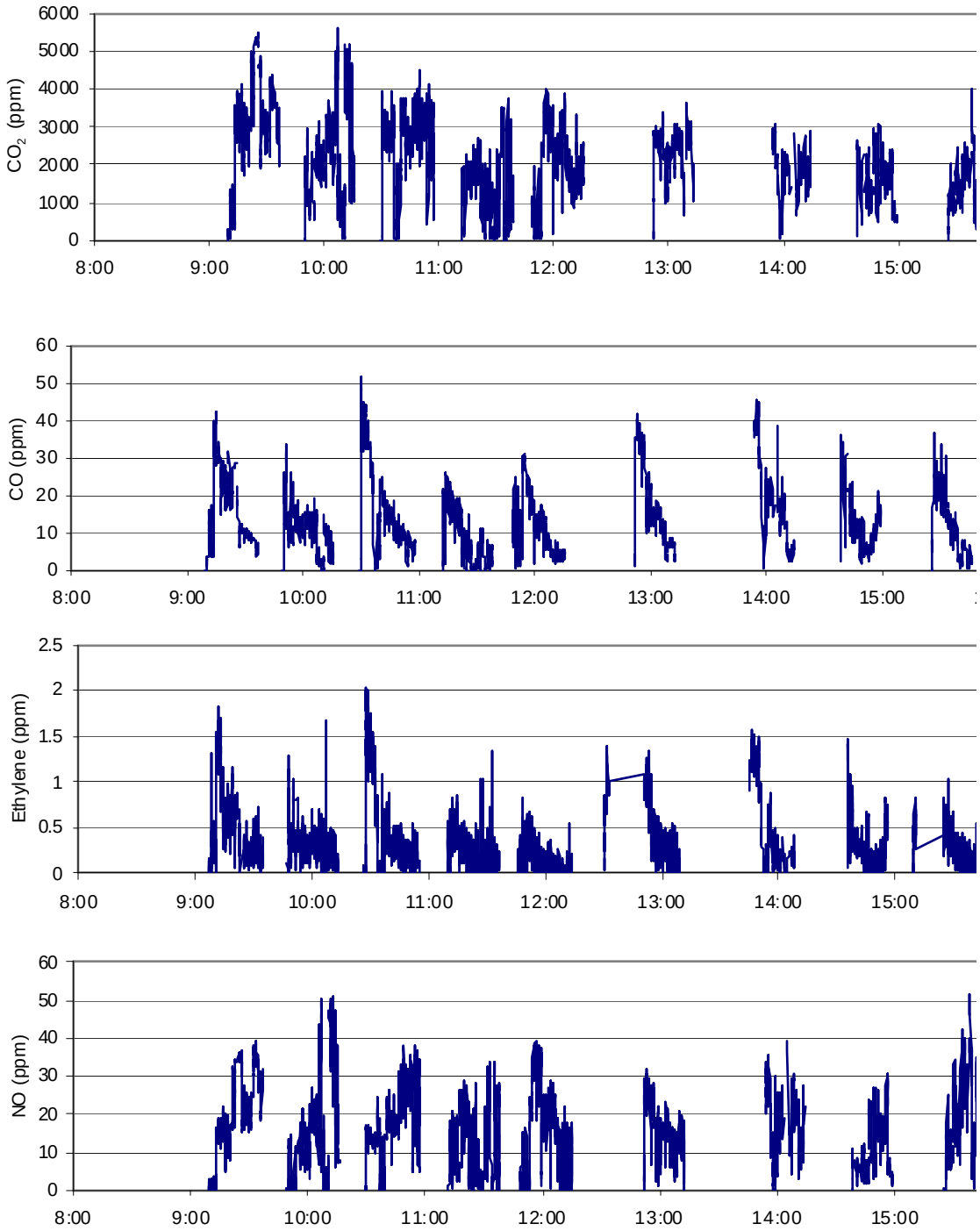

Figure 5-4. Time series of background corrected CO_2, CO, Ethylene, and NO from 11/15/2005.

Calculation of EFs from in-plume measurements relies upon the coincidence of the excess concentration of the pollutant of interest with the excess CO_2 and CO concentrations. As an example, Figure 5-5 shows that the excess NO concentration was well correlated with the excess CO_2+CO concentration in a generator sampling cycle.

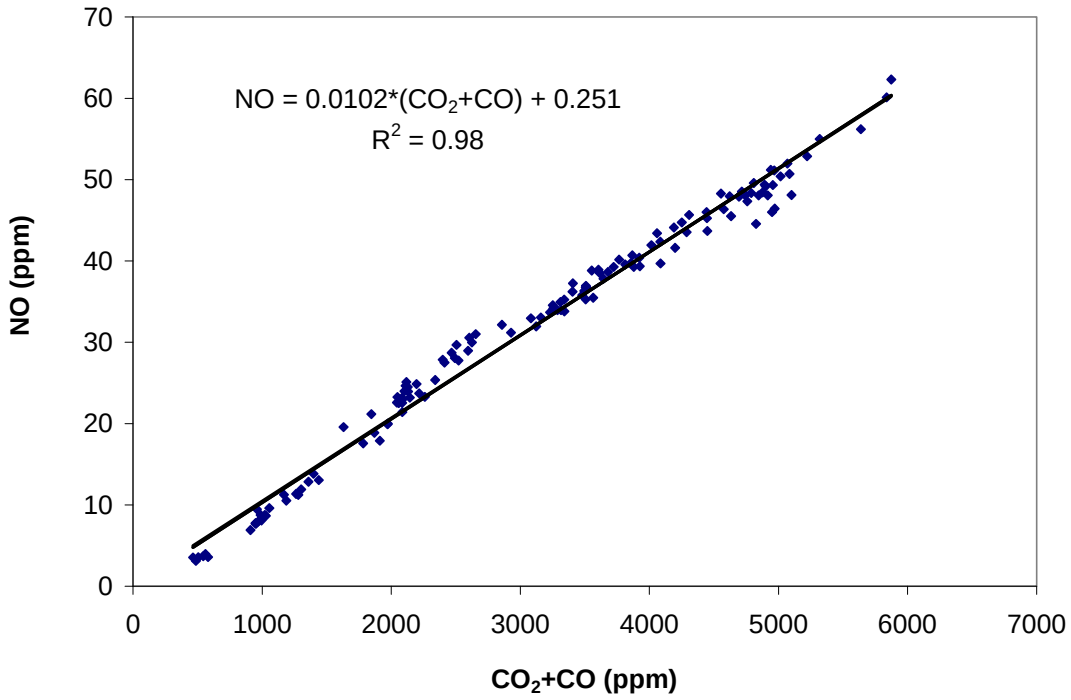

Figure 5-5. Correlation of FTIR NO with $CO+CO_2$ concentration over a sampling cycle

These time-resolved data are integrated over the sampling time of each operating mode to obtain average gas concentrations for each engine at every operating mode. Concentrations of CO_2 and CO were very well resolved while concentrations of other species (e.g., propane and NH_3) were close to or below the detection limits of the instrument. Mode independent EFs for a specific engine were calculated using weighting factors for each engine mode 0.10, 0.30, 0.30, 0.25, and 0.05 for the 10%, 25%, 50%, 75% and 100% loads, respectively. Average EFs for each engine type are summarized in Figures 5-6 and 5-7.

Gaseous EFs are consistent across engine types with CO, ethylene, and NO_2 all decreasing with increasing engine load. Moreover, the no-load cold start emissions of these species (measured during the first 5 minutes of operation after an overnight cold soak) were higher than those for the hot stabilized steady-state (running for at least 20 minutes) modes. The ethylene EF behavior is consistent with the transmission of unburned fuel through the exhaust system during the initial fuel-rich combustion. CO EFs reflect changes in combustion efficiency: as the engine cylinders heat up, the combustion efficiency improves, and less CO is produced.

NO EFs increased by <50% with increasing engine loads of 10% to 50% load, leveling off at the 100% load. At the high temperatures of the combustion environment, a fraction of the nitrogen and oxygen can dissociate, forming radicals, which then combine through a series of reactions to form NO, the primary NO_x constituent in fresh, untreated diesel exhaust. This rate of NO formation increases with engine temperature and therefore cold start NO EFs are lower than hot stabilized NO EFs. Except for the 30 kW generators, NO EFs were highest at the 50% load. As the engine load neared 100%, NO EFs increased slightly over the 75% load EF, except

for the 60 kW generators. This change is likely due to the higher fuel to air ratio at the highest load.

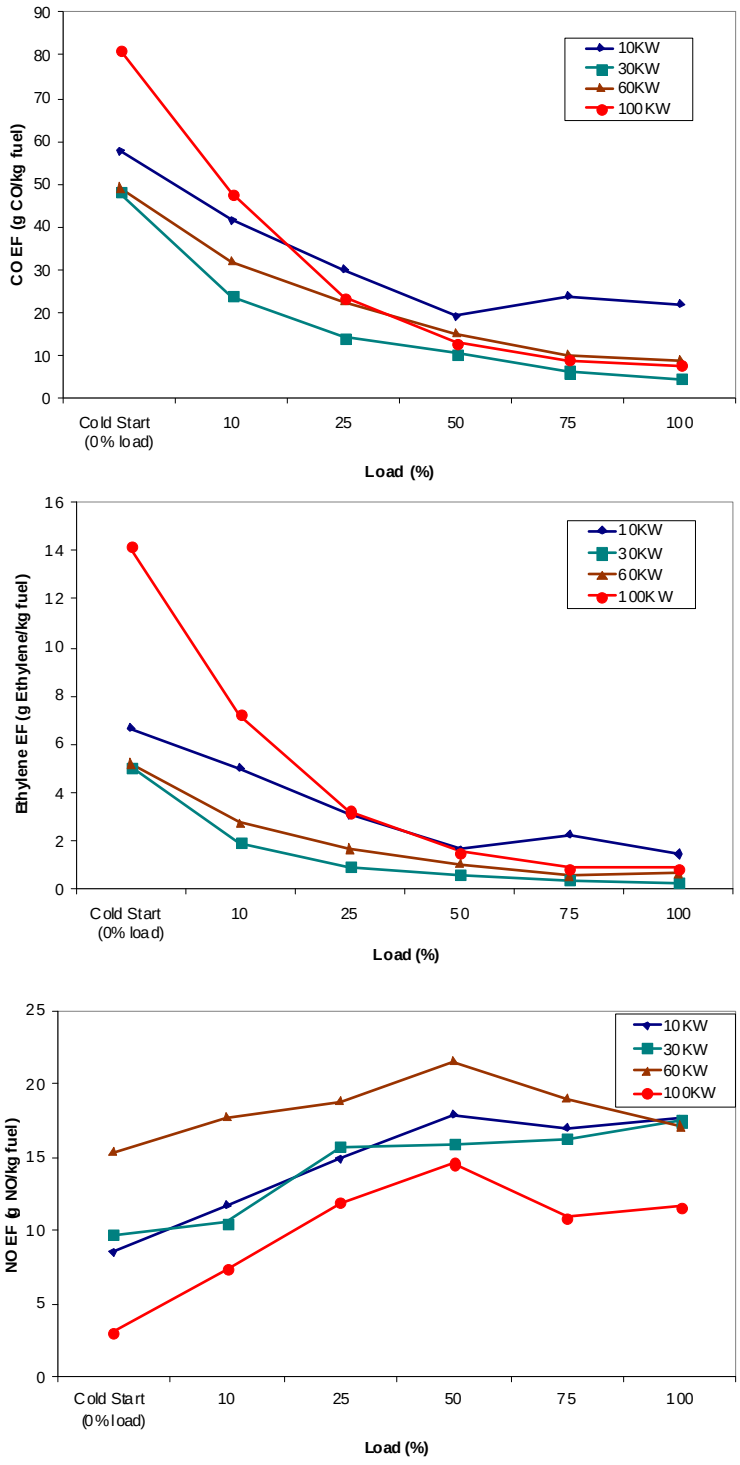

Figure 5-6. Average EFs for CO, ethylene, and NO for different size generators and power loads.

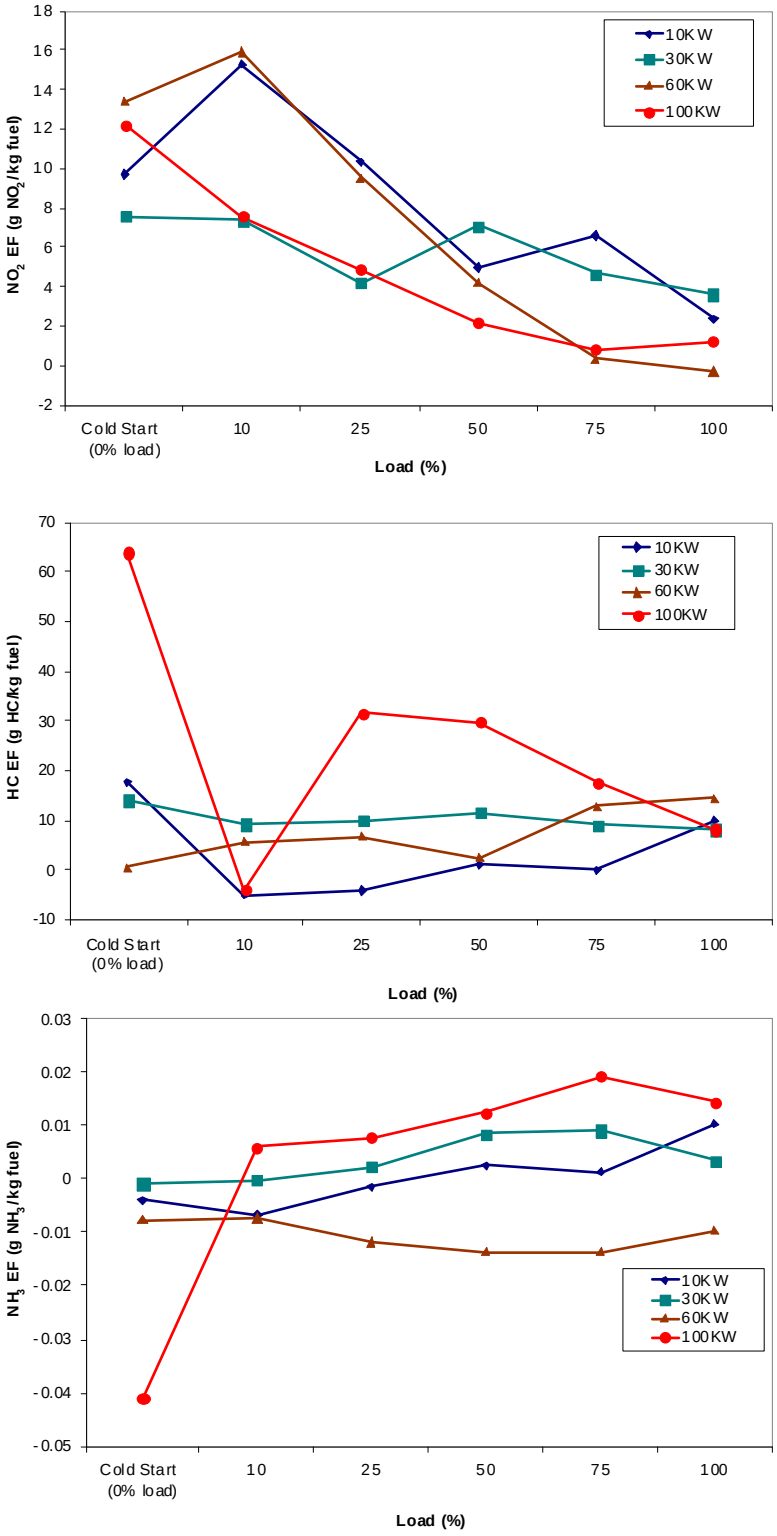

Figure 5-7. Average EFs for NO_2, HC (propane+hexane), and NH_3 for different size generators and power loads.

HC EFs are estimated as the sum of propane and hexane measured by the IPETS FTIR, and therefore represent a lower limit of NMHC emissions. HC EFs were low (< 20 g HC/kg fuel) and increased moderately with engine load. Except for the 60 kW generators, the average cold start HC EFs were 6.5 times higher than those for the hot stabilized modes. This trend is consistent with the presence of unburned fuel during the initial fuel-rich combustion. NH_3 EFs were low (<0.2 g NH_3/kg fuel), usually below the IPETS detection limits.

PM EFs were calculated when valid measurements were available for CO, CO_2, DT $PM_{2.5}$, and ELPI $PM_{0.263}$. The GRIMM optical particle counter's internal pump failed after the first 5 hours of testing, so these are not reported as part of the IPETS results. The ELPI was initially configured in its most sensitive sampling mode on the first day of testing, and exhaust concentrations exceeded its upper limit, so these data are considered invalid. A less sensitive ELPI setting was used for the remainder of the tests.

Figure 5-8 compares PM EFs. The benefit of testing multiple engines of the same type is shown in the bar chart for the 60 kW generators. Emissions of the 60 kW – S/N# HX62182 unit were more than 3 times higher than those of the other 3 units at 50% and 75% loads. PM EFs are compared based on generator rated load in Figure 5-9. The fleet average PM EF was 2.8 ± 3.0 g PM/kg fuel, 54% less than EPA's AP 42 estimates of 5.98 g PM/kg fuel. With the exception of the 100 kW generator, all engines showed an increase in PM EF as the load increased to 75%. EFs for the 10 kW generators were highest at 100% load.

The 100 kW engines yielded the highest PM EFs (load-weighted average of 12.0 g PM/kg fuel) and showed a steady decrease in EF as the load increased. These EFs were more than 4 times higher than those of the 60 kW engines (overall 3.0 g PM/kg fuel). This may be due to older 1987 model year of the 100 kW generators with a high number of operating hours (>1500 hours). Variable increases in PM EFs were observed for cold starts on <60 kW engines. For the 10, 30 and 60 kW engines, cold start PM EFs were 439%, 16% and 27% higher than 10% and 25% load PM EFs, typical of initial fuel rich conditions. The 100 kW generator cold start PM EF was 22% lower than the 10% and 25% load PM EFs. Cold starts are real-world occurrences that are not captured by certification tests.

Fuel-based emissions from the largest 100 kW generator quantified in this study are compared with corresponding measurements from a larger 350 kW generator tested with the MEL in Table 5-9. It is clear that engine power output is a poor indicator of real-world emissions, as all but the NO_x EFs are higher for the smaller engine. The differences are far greater than the ±~30% differences that might exist between the MEL and IPETS measurements. Table 5-10 compares IPETS and MEL fuel-based EFS for four 60 kW engines, again showing substantial differences, especially for PM. The fleet average of CO EF was 5% lower, NO_x EF was 63% lower, and PM EF was 25% lower than EPA's AP 42 estimates. Again, the EF differences are much larger than can be accounted for by differences in the measurement methods.

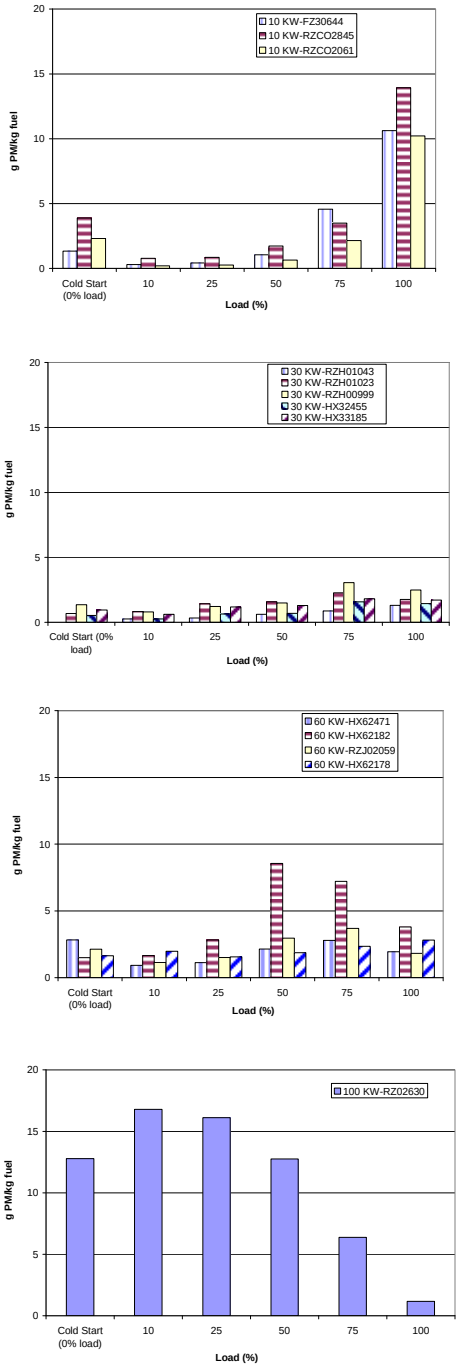

Figure 5-8. PM EFs for diesel generators operating under different loads.

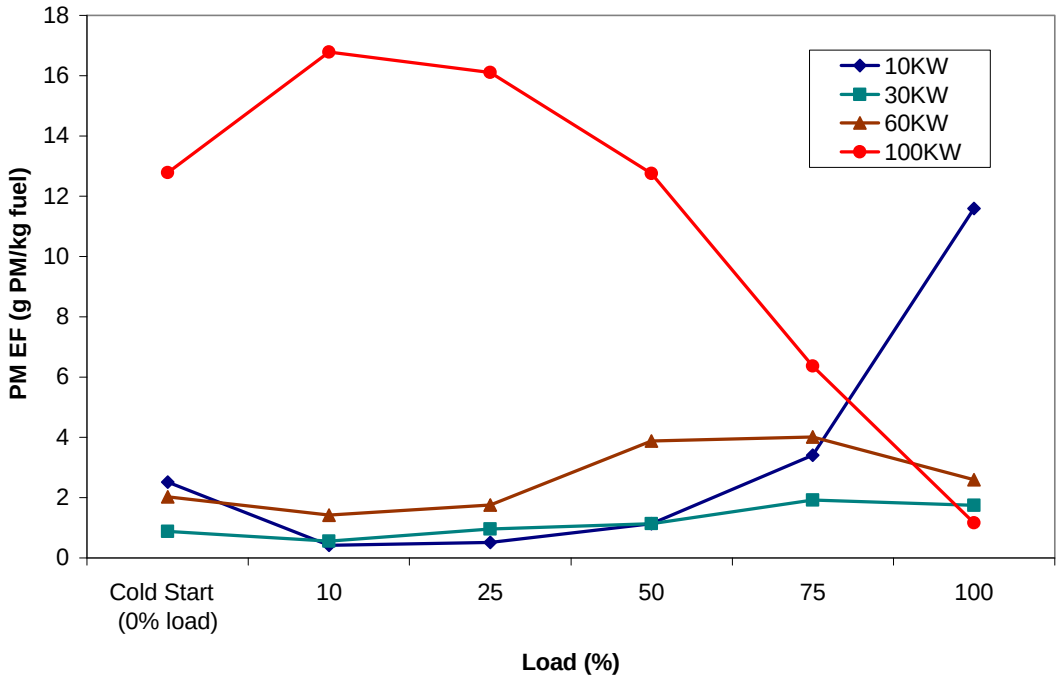

Figure 5-9. Average PM EFs based on generator rated load.

Table 5-9. Comparison of fuel-based emission factors (g pollutant/kg fuel) from a 100 kW generator measured with IPETS with emission factors from a 350 kW generator measured with the MEL (Cocker et al., 2004.)

	100kW Generator-IPETS (LIBBY MEP007B, year unknown)						350kW Generator-MEL (CAT 3406C, 2000)					
Load	**10%**	**25%**	**50%**	**75%**	**100%**	**Overall**	**10%**	**25%**	**50%**	**75%**	**100%**	**Overall**
EF CO	46.65	23.80	12.74	8.11	6.88	18.00	6.53	4.74	8.00	9.59	7.24	7.24
EF NO	8.05	12.92	15.49	11.44	12.07	12.79	24.58	31.77	37.58	36.37	30.84	33.90
EF NO_2	5.93	4.09	1.42	-0.46	0.16	2.14	2.02	1.30	1.47	1.00	1.53	1.36
EF HC	12.64	-0.25	5.19	30.47	21.70	11.45	2.23	1.19	0.63	0.50	0.66	0.93

Table 5-10. Comparison of fuel-based emission factors (g pollutant/kg fuel) from similar-sized engines measured with IPETS with emission factors from a 350 kW generator measured with the MEL (Shah et al., 2006)

	MEL 60 kW John Deer, 2001						IPETS 60 kW Average (1995,2001,2001,2002)						
% Load	**10**	**25**	**50**	**75**	**100**	**Overall**	**10**	**25**	**50**	**75**	**100**	**Overall**	**AP 42**
THC	33.10	11.74	5.24	3.16	2.08	9.30	5.61	6.80	2.54	12.80	14.54	7.29	6.76
CO	35.76	12.78	4.56	2.44	6.28	9.70	32.05	22.84	15.29	10.42	9.04	17.70	18.34
NOx	49.67	32.47	34.59	43.53	54.64	38.70	43.13	38.38	37.32	29.51	25.99	35.70	85.11
PM	1.99	1.58	0.99	0.99	1.76	1.31	1.42	1.75	3.88	4.01	2.60	2.96	5.98
	MEL 100 kW Cummins 6BT, 1990						**IPETS 100 kW (LIBBY MEP007B, year unknown)**						
THC	30.93	15.62	6.59	4.06	1.90	10.87	12.64	-0.25	5.19	30.47	21.70	11.45	
CO	32.29	14.31	3.52	5.01	26.42	11.15	46.65	23.80	12.74	8.11	6.88	18.00	
NOx	53.74	48.77	47.87	67.74	79.48	55.27	18.88	23.18	24.58	17.50	19.04	21.54	
PM	2.98	2.30	0.81	0.63	1.49	1.47	16.78	16.11	12.76	6.37	1.17	11.99	
	MEL 125 kW John Deer 6076, 1991												
THC	26.19	9.26	5.01	3.52	3.03	7.93							
CO	30.48	8.58	4.15	3.75	5.96	8.10							
NOx	151.28	88.51	77.22	73.61	74.06	86.95							
PM	3.93	1.54	0.81	0.72	0.81	1.32							

5.4 IPETS Mobile Source Tests

The IPETS was quantified emissions from tactical military vehicles along with the VERSS and portable PM system at the 29-Palms Marine Corps Training Facility from 04/16/2007 to 04/20/2007. Tests took place at a Marine Corps Training Facility and vehicles were recruited for testing as they traveled to and from field training sites. A four-meter high sampling inlet pipe was set up across a paved tank trail and suspended on each end using two scissor-jacks (Figure 5-9). A wrought iron pipe (0.75 inch ID) with inlets mounted at ~ 1 m intervals was connected to the IPETS system via a flexible conductive tubing (1 inch ID). The flexible tube was connected to a plenum within a cargo van on the side of the road to duct the exhaust to gas and particle measurement instrumentation.

The VERSS took a picture and logged the passage time of each vehicle by the test system. The vehicle exhaust signal peaks were identified from the CO_2 time series of the FTIR and Licor instruments from IPETS and were cross referenced with the vehicle passing time recorded by the RSD system. The standard deviations of the gaseous and particulate matter (PM) measurements between vehicle exhaust peaks were calculated to characterize ambient variability of each measurement. To calculate typical emission factor (EF) detection limits for the measured gas species and PM concentrations, the standard error of the non-exhaust concentrations were calculated over a period of 21 seconds (the average CO_2 peak duration for the passage of one vehicle). These standard errors were then propagated into the emission factor calculation. The CO_2 concentration used in the calculation was 239 ppm representing the average CO_2 plume concentration from all measured vehicles during the campaign. The resulting detection limits are shown in Table 5-11.

Figure 5-10. Picture of sampling system of In-Plume and Cross-Plume sampling.

Several gaseous species that were detected in the diesel generator exhaust (NH_3, SO_2, hexane, and propane) were below the limits of detection for mobile source sampling owing to the shorter sample durations and greater dilution ratios for mobile sources.

Table 5-11. Detection limits of FTIR gaseous components and PM by ELPI and DustTrak.

Components	Detection limit (ppm) for gas (mg/m^3) for PM	Corresponding EF detection limit (g/kg fuel)
NH_3	0.12	0.61
CO_2	2.8	
CO	1.1	9.04
Ethylene	0.2	4.06
Hexane	0.1	3.46
N_2O	0.005	0.03
NO	0.5	4.23
NO_2	0.1	1.48
Propane	0.2	4.54
SO_2	0.9	17.84
H_2O	366	
$PM_{0.263}$ by ELPI	0.000067	0.00049
$PM_{2.5}$ by DustTrak	0.0011	0.0082

The signal peaks detected from a single tactical military vehicle passing the sampling system were typically less than 25 seconds. Peaks durations in excess of 30 seconds were excluded from this analysis since they represented a coincidence of emissions from multiple vehicles.

The time resolution of the Licor CO_2 analyzer is 1 second, while the FTIR has a sampling time resolution of 2.4 seconds. In addition, the analytical volume and flow rate of the Licor is 1 L/min and 10 ml whereas the FTIR has a sample flow rate of 50 L/min and an analytical volume of 2 liters. As such, the FTIR responds to exhaust peaks more slowly and with less amplitude than the Licor. An example time series of the CO_2 concentrations measured by the Licor and FTIR are shown in Figure 5-11. The integrated vehicle exhaust CO_2 peak areas (used for emission factor calculation) from the Licor and FTIR showed negligible systematic bias (within 20% for the 95% confidence intervals) for the entire dataset (Figure 5-12).

One of the IPETS limitations for mobile sources is that a plume from a passing vehicle may not be drawn into the sampling line. Factors that are independent of emission factor such as exhaust pipe position with respect to the sampling inlet, wind speed, and wind direction can preclude the quantification of the vehicle's emission factors. Figures 5-13 through 5-15 compare calculated emission factors with the peak CO_2 area (ppm.s). For low CO_2 peak areas, the range of emission factors is larger than at higher concentrations. This behavior is expected since the uncertainty on the NO_x, CO, and PM concentrations are constant near their detection limits. At low CO_2 exhaust concentrations, the contribution of the analytical uncertainty of CO, NO_x, and PM to the EF is larger. The emission factors are more stable for higher CO_2 peak areas, reflecting the true EF from the vehicles rather than the instrument uncertainty.

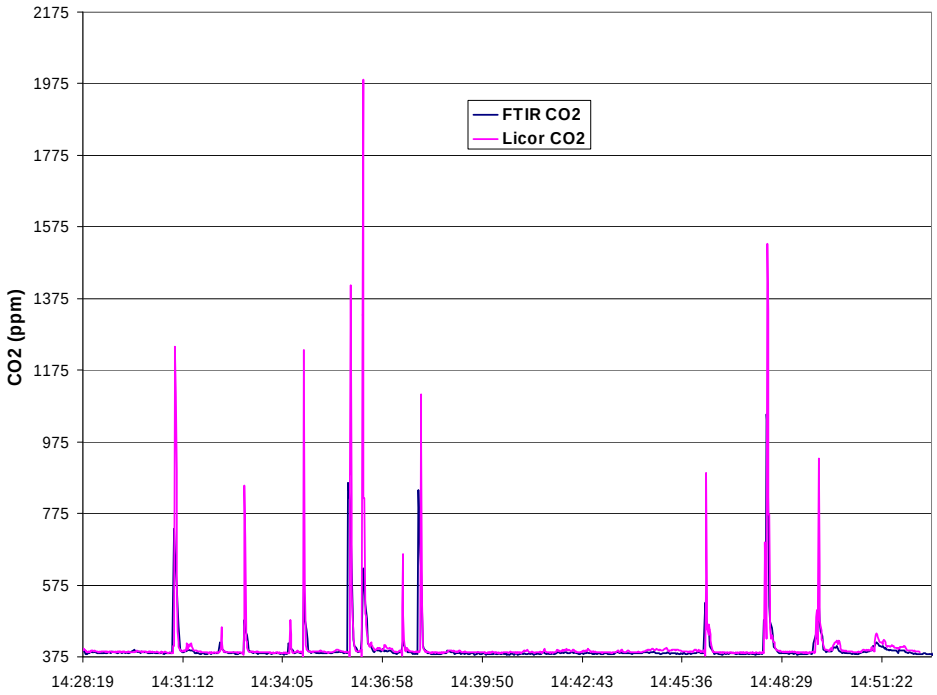

Figure 5-11. Time series of CO_2 readings by FTIR and Licor in April 19, 2007.

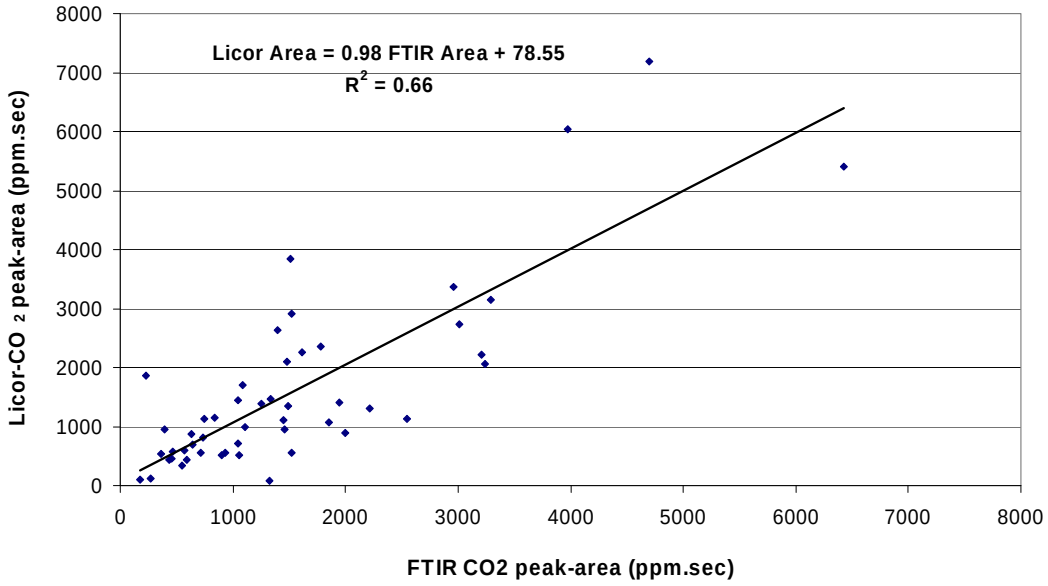

Figure 5-12. Correlation between CO_2 peak area (ppm.s) by FTIR and Licor.

A CO_2 peak area of 400 ppm.s was selected for NO_x, CO, and PM EF calculations to reduce the influences of the CO, NO_x, and PM analytical uncertainties on the average calculated EFs.

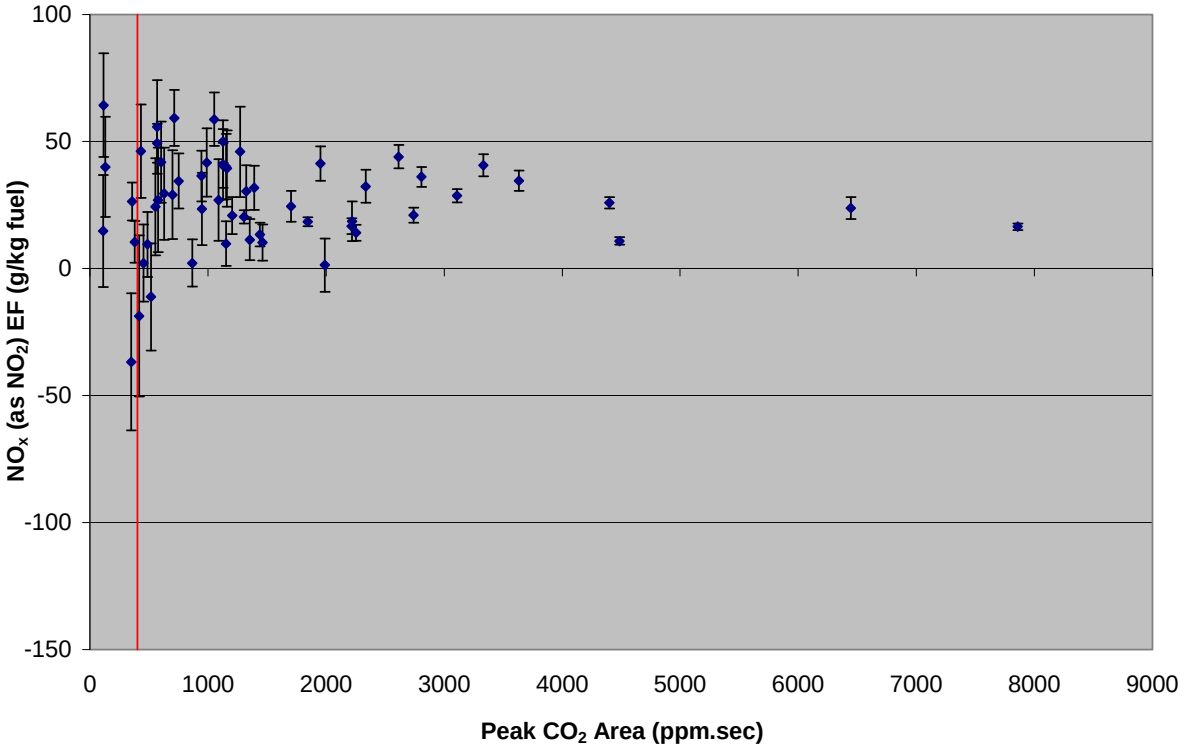

Figure 5-13. NO_x emission factors vs. peak CO_2 area for each vehicle pass. Error bars represent the propagated analytical uncertainty of the EF calculation. The 400 pmm s CO_2 criterion for EF validation is shown as a vertical bar on the figure.

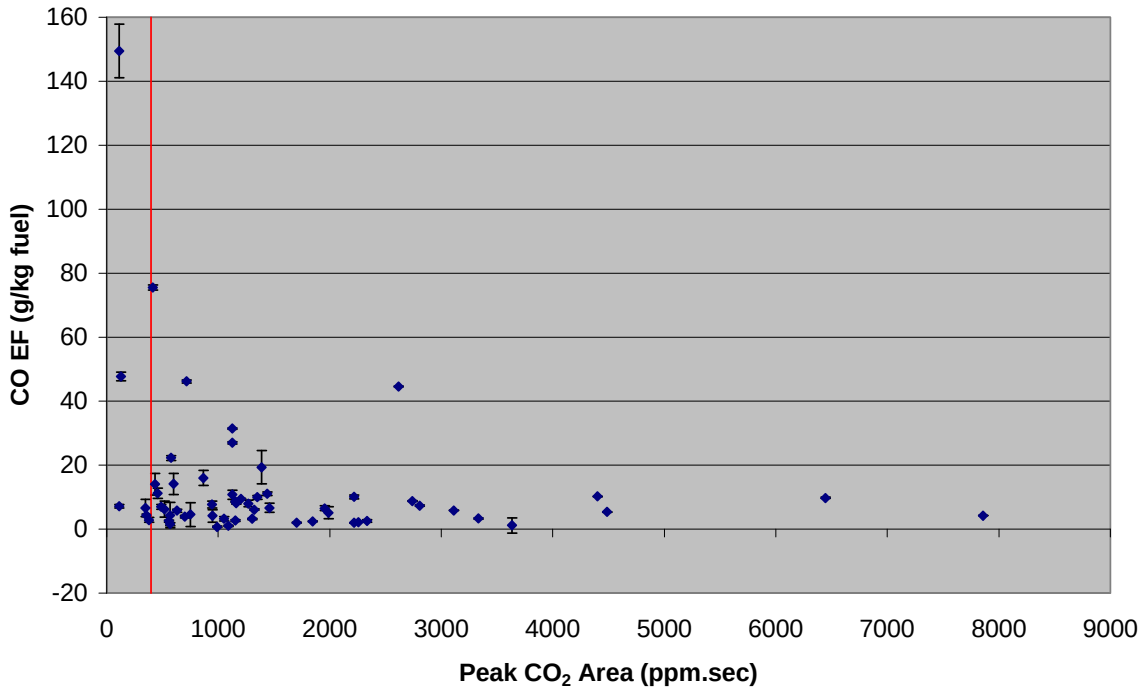

Figure 5-14. CO emission factors vs. peak CO_2 area for each vehicle pass Error bars represent the propagated analytical uncertainty of the EF calculation. The 400 pmm s CO_2 criterion for EF validation is shown as a vertical bar on the figure.

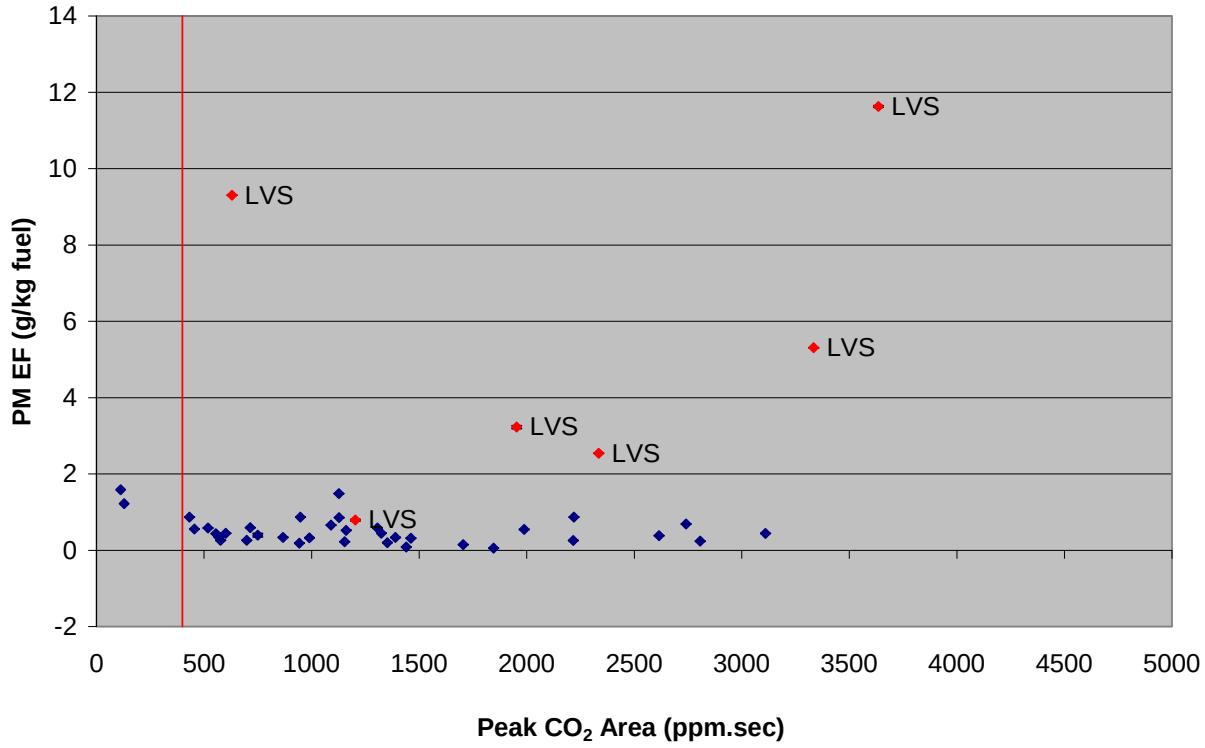

Figure 5-15. PM emission factor distribution vs. peak CO_2 area for each vehicle pass. Error bars represent the propagated analytical uncertainty of the EF calculation. The 400 pmm s CO_2 criterion for EF validation is shown as a vertical bar on the figure. The PM emission factor data points from the LVS vehicles are shown in red and are consistently higher than those measured from the 7-ton MTVR trucks.

Data recovery statistics for both the In-Plume and VERSS measurements are shown in Table 5-12.

Table 5-12. Data Recovery by date for FTIR And RSD counts and (percentage)

Date	Number of Vehicle Passes		CO_2		CO		NO	
	FTIR	RSD	FTIR	RSD	FTIR	RSD	FTIR	RSD
4/17/2007	26	26	15 (58%)	3 (12%)	15 (58%)	1 (4%)	11 (42%)	0 (0%)
4/19/2007	103	103	32 (31%)	43 (42%)	38 (37%)	28 (27%)	33 (32%)	38 (37%)
4/20/2007	129	129	11 (9%)	19 (15%)	11 (9%)	15 (12%)	10 (8%)	9 (7%)
Total	258	258	58 (22%)	65 (25%)	64 (25%)	44 (17%)	54 (21%)	47 (18%)

The fixed height of the IPETS inlet resulted in a range of data recoveries for the different types of vehicles passing the systems. For example, Humvees (HMMWV) have exhaust pipes at ~2 m above ground level (AGL), preventing sufficient exhaust to reach the elevated sampling inlet. The 7-ton trucks MTVR (Medium Tactical Vehicle Replacement) and Logistics Vehicle System (LVS) had the highest exhaust pipes (3 m to 3.5 m) of the vehicles tested and represented the majority of valid IPETS measurements.

Several vehicles passed through the test section multiple times. EFs from a single vehicle are expected to vary based on the mode of operation (i.e. slight, moderate, hard accelerations) and road grade (~1% at this test location. The EF variation for individual vehicles is shown in Figures 5-16 to 5-18.

For CO EFs (Figure 5-16), the variability of repeated measurements of the same vehicles (i.e. MTVRs 593901 and 543901 with coefficients of variation of ~1) are on the same order as the variation of vehicle average emission factors for the fleet. This indicates that mode of operation of a single engine has as large an impact on CO EFs as does specific engine being tested. Strong consistency was observed for the average NO_x EFs for all vehicles tested (Figure 5-17)). These results imply that fewer NO_x EFs are needed than CO EFs to produce reliable real-world estimates.

PM EF variability (Figure 5-18) was larger between vehicle types than between operating modes. The LVS emitted ~10 times more PM than the average MTVR. Because multiple measurements of only one LVS were acquired, it would be speculative to attribute this difference to engine type. It is possible that the LVS tested had much higher PM EFs than the fleet of LVSs.

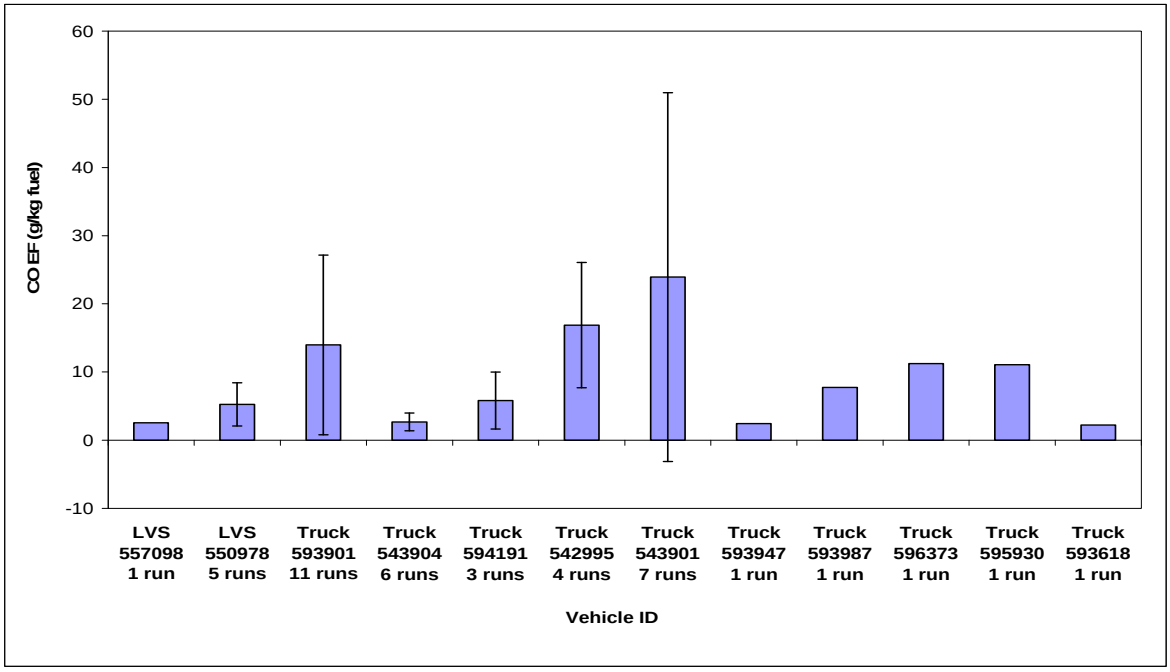

Figure 5-16. CO EF distribution for individual vehicles measured by IPETS. Error bars indicate the standard deviation of measurements of the same vehicle.

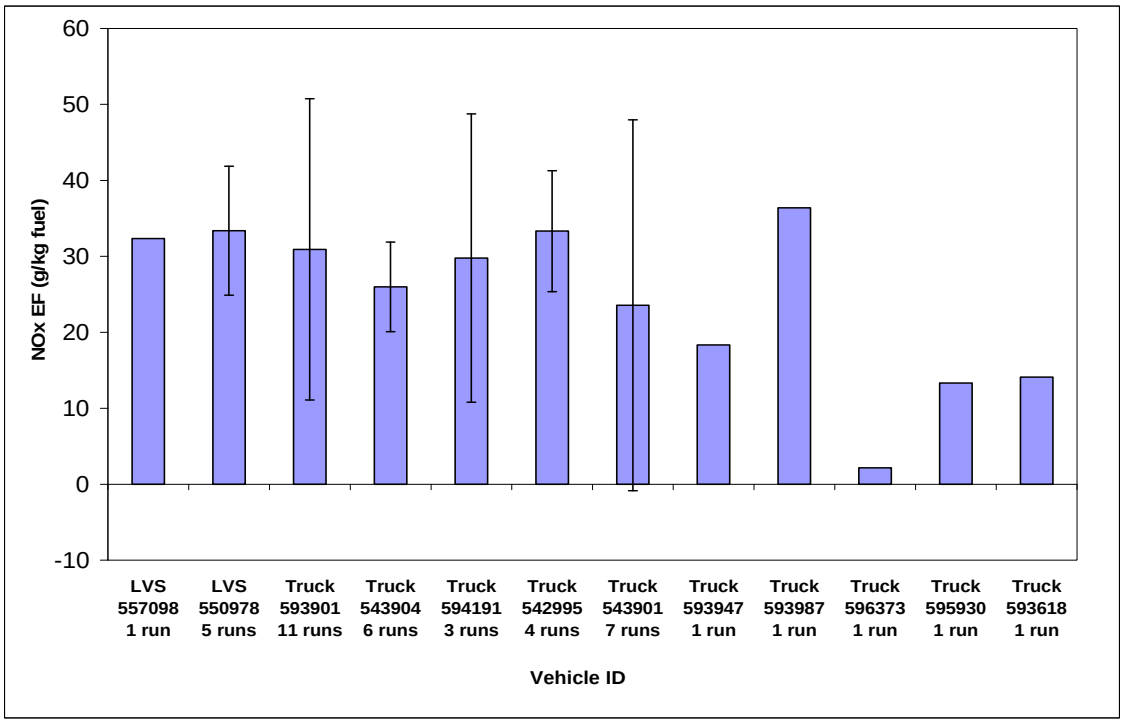

Figure 5-17. NO_x EF distribution for individual vehicles measured by IPETS. Error bars indicate the standard deviation of measurements of the same vehicle.

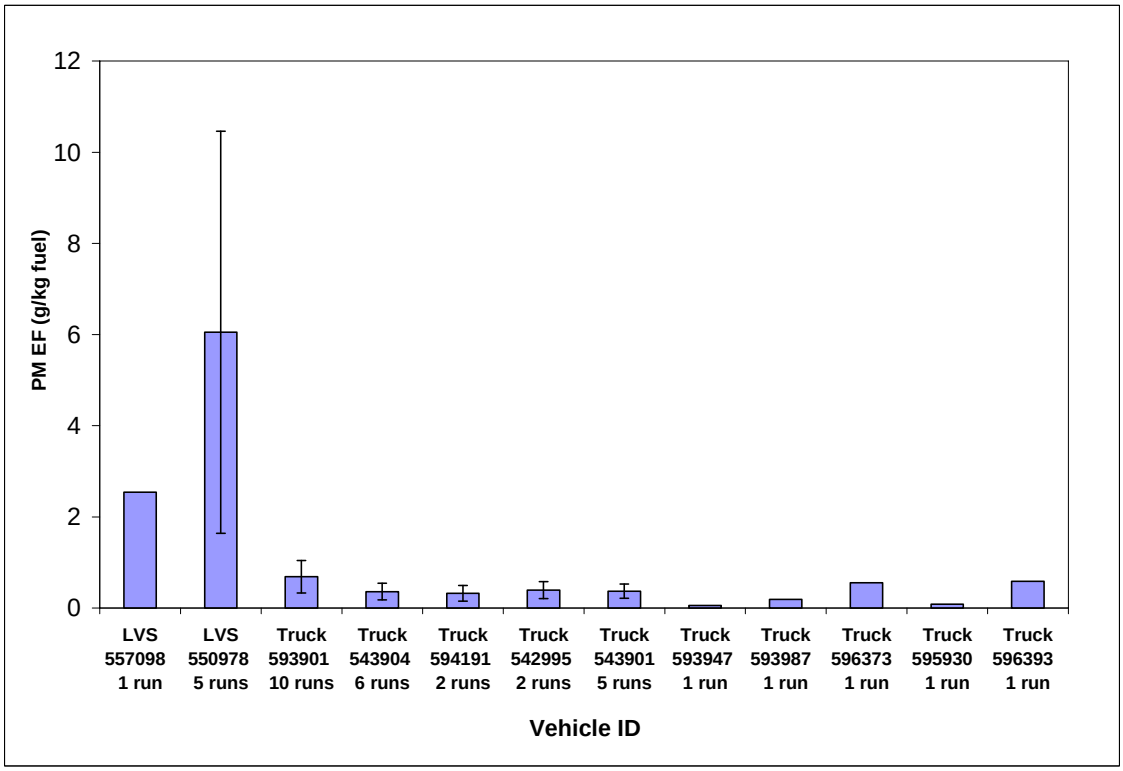

Figure 5-18. PM EF distribution for individual vehicles measured by IPETS. Error bars indicate the standard deviation of measurements of the same vehicle.

ELPI impactor stage 4 has a 50% cutpoint of 0.1 μm (100 nm), so ultrafine particle (UP) EFs are estimated in Table 5-13. 96% of the PM number remissions from diesel trucks and LVS vehicles are in the UP fraction. Table 5-14 summarizes the UP PM EF mass emissions, assuming a particle density of 1 g/cm^3.

Table 5-13. Fleet UP number emission factors.

Vehicle	Number of vehicles	Fine (< 263 nm) PM EF (# particles/kg fuel)	Ultrafine (< 100 nm) PM EF (# particles/kg fuel)
MTVR (7-ton Truck)	10	$(1.11 \pm 1.14) \times 10^{15}$	$(1.05 \pm 1.09) \times 10^{15}$
LVS	2	$(2.47 \pm 1.19) \times 10^{16}$	$(2.35 \pm 1.12) \times 10^{16}$
HDV[a]			$(6.3 \pm 1.9) \times 10^{15}$
On-road vehicles[b]		$(1.0\text{-}3.1) \times 10^{15}$	
On-Road Measurement[c]		8.3×10^{15}	

a. Tunnel study of HDV using CNC, (Kirchstetter et al., 1999; Kirchstetter et al., 2002).
b. On-road measurement with SMPS particle sampling range 8-300 nm, on Minnesota highways with diesel vehicles to gasoline vehicles ratio of about 0.09, (Kittelson et al., 2004a).
c. On-road measurement with ELPI particle range 7-960 nm, Helsinki metropolitan areas, Finland (Yli-Tuomi et al., 2005).

Table 5-14. Fleet average UP mass emission factors.

	Number of vehicles	Average UP EF (g/kg fuel)
7-ton Truck	10	0.06 ± 0.04
LVS	2	1.26 ± 0.64

As noted Section 2, certification emissions are expressed g/hp-hr that must be converted to fuel-based EFs for use in air quality planning. For this conversion, it is assumed that average brake-specific fuel consumption (BSFC) is 7000 Btu/hp-hr and that diesel fuel has a heating value of 19,300 Btu/lb. With these assumptions, Tables 5-15 and 5-16 summarize the average CO, NO_x and PM emission factors for the MTVR and LVS in fuel-based and certification units. The MTVR had average CO EFs more than twice those of the LVS. Average EFs of NO_x for both vehicles were within 20% of each other. The LVS had average PM EFs that were more than 10 times larger than those of the MTVR.

Table 5-15. Fleet average CO, NO_x and PM emission factors fuel-based units. Uncertainty terms are standard deviations of all measurements of each vehicle type.

Vehicle Type	Average CO EF (Number of vehicles) (g /kg fuel)	Average NO_x EF (Number of Vehicles) (g/kg fuel)	Average PM EF (Number of Vehicles) (g/kg fuel)
MTVR	9.8 $\pm$7.1 (10)	22.8 $\pm$ 10.7 (10)	0.36 $\pm$ 0.21 (10)
LVS	3.9 $\pm$ 1.9 (2)	32.9 $\pm$ 0.7 (2)	4.30 $\pm$ 2.48 (2)

Table 5-16. Fleet average CO, NO_x and PM emission factors power-based units Uncertainty terms are standard deviations of all measurements of each vehicle type.

Vehicle Type	Average CO EF (Number of Vehicles) (g/hp-hr)	Average NO_x EF (Number of Vehicles) (g/hp-hr)	Average PM EF (Number of Vehicles) (g/hp-hr)
MTVR	1.6 $\pm$1.2 (10)	3.7 $\pm$ 1.8 (10)	0.06 $\pm$ 0.03 (10)
LVS	0.6 $\pm$ 0.3 (9)	5.4 $\pm$ 0.1 (2)	0.71 $\pm$ 0.41 (2)

A military engine emission factor database was provided by the Environmental Manager at the Marine Base. This database incorporates emission factors from wheeled and tracked construction vehicles based on EPAs NONROAD model with bhp ratings for military vehicles. derived from Jane's Tank & Combat Vehicle Recognition Guide, the Encyclopedia of Modern U.S. Military Weapons, and Modern U.S. Military Vehicles.

EFs measured with the IPETS showed MTVR and LVS vehicles having lower CO EFs than the NONROAD values (9.8 g CO/kg fuel for MTVR and 3.9 g CO/kg fuel for LVS versus the 17 g/kg fuel in NONROAD). IPETS NO_x EFs were also lower (22.8 g NO_x/kg fuel for MTVR and 32.9 g NO_x/kg fuel for LVS vs 58 g NO_x/kg fuel). For PM, the IPETS LVS $PM_{0.263}$ EF was 12% less than that from the NONROAD database (4.3 g PM/kg fuel vs 4.9 g PM/kg fuel), whereas the truck $PM_{0.263}$ EF was an order of magnitude less than the NONROAD database value (0.36 g PM/kg fuel vs 4.9 g PM/kg fuel)

For heavy duty diesel vehicles with model year of 1998 and later, EFs should be less than 94 g CO/kg fuel, 24 g NO_x/kg fuel, and 0.61 g PM/kg fuel. Compared with these 1997 EPA emission standards, the CO EF for Trucks and LVS tested with IPETS were lower by nearly a factor of 10. NO_x EFs for the MTVR were 5% less than the EPA standard and the NO_x EF from the LVS was 37% higher than the EPA standard. The PM EF of from the MTVR were within 40% of EPA's highway truck EF standard, while the measured LVS PM EF was much higher than EPA highway EF (4.30 g PM/kg fuel vs 0.61 g/kg fuel).

As noted in Section 2, ARB's EMFAC emission model estimates diesel emissions in g/mile. There is uncertainty in converting from power-output EF (g/hp-hr) to a distance-based (g/mile) EF since the fuel economy (mi/gal) is unknown. For example, in the HDDV EF conversion factor settings for Medium Heavy-Duty Diesel Vehicles with model year after 1996, EPA suggest a 2.409 hp-hr/mile for all vehicles with GVW range from 26,001 lbs to 33,000 lbs.

Heavier vehicles typically have poorer fuel economy, and a constant factor 2.4 hp-hr/mile can't reflect such variation of 25% or more. With a conversion factor of 2.8 from g/mile to g/hp-hr for HDDV class 8 (> 33,000 lbs) and model years after 1996, EFs from the EMFAC model for model years 1999-2002 HDDV are 2.2 g CO/mile (4.9 g CO/kg fuel), 14.1 g NO_x/mile (31.0 g NO_x/kg fuel), and 0.39 g PM/mile (0.86 g PM/kg fuel). The MTVR emission factors of CO from this test were 100% higher than EMFAC estimates, PM was 58% less than the EMFAC model, and NO_x was 26% less than the EMFAC model. The LVS emission factor of CO in this test was 20% less than EMFAC model, PM was 400% higher than EMFAC model, and NO_x was 6% more than EMFAC model.

In summary, fleet average EFs for the MTVR trucks tested were 9.8 g CO/kg fuel, 22.8 g NO_x/kg fuel and 0.36 g PM/kg fuel. Fleet average emission factors for LVS vehicles were 3.9 g CO/kg fuel, 32.9 g NO_x/kg fuel and 4.30 g PM/kg fuel. Driving conditions varied, with slight, medium and hard accelerations and cruises at a target speed of 10-15 mph passing the sampling inlet. Test results were comparable to emission model results.

5.5 VERSS Cross-Plume Mobile Source Measurements

The VERSS was used in conjunction with the IPETS to quantify mobile source emissions at the 29 Palms Marine Training Facility. As shown in Figure5-10, the main unit and the retro unit were placed on individual scissor jacks located on opposite road sites. While the retro unit is not powered and does not acquire data, power, control, and signal cables for the main unit had to be adapted. The mechanical stability of the elevated scissor jacks was not sufficient to maintain optical alignment and to sufficiently reduce vibrations as needed for operation of the cross plume system. Stabilizing the scissor jack platforms with guy-wires anchored to the ground solved these problems. Even with this additional stabilization, system alignment had to be done from ladders as additional weight on either scissor jack platform would disturb the optical system alignment. A pipe between the two scissor jacks being used as inlet for in-plume sampling. Also note the traffic cones used to confine vehicle traffic between the scissor jacks.

System triggering had to be adapted. In normal operation for vehicles with low exhaust pipes such as passenger vehicles and buses, the vehicle body blocks and unblocks the remote sensing beams, thereby triggering data acquisition. For vehicles with elevated exhaust, the remote sensing beams had to be located above the highest part of the vehicle. Therefore, the remote sensing beams are not blocked when the vehicle passes by and the system is not triggered. In these tests, the remote sensing system was either triggered by a beam-block mounted on top of the vehicle or manually. Mounting a beam block was only efficient for vehicles with multiple passes through the remote sensing system, while manual triggering had to be used for vehicles doing only individual passes. Inconsistent manual triggering contributed to reduced rates of valid remote sensing data during the 29-Palms study.

In normal operation of the remote sensing system for passenger vehicles, valid data rates are in the 80-90% range. However, for the military vehicles tested at the 29-Palms Marine Base, only 46 (22% of total) gaseous measurements and 9 (4% of total) particulate matter (PM) measurements were valid. This low fraction of valid measurements can largely be attributed to the difficulty of capturing the exhaust plume and its dilution for the elevated exhaust stacks encountered. The elevated exhaust pipes ejected the exhaust plumes in vertical or near vertical directions into the ambient air, which is perpendicular to both the vehicle velocity and the remote sensing beams. To make a valid measurement, the remote sensing system measures the temporal

decay of exhaust constituents over 0.5 second after a vehicle passes by. For the vertical exhaust pipes combined with a large variation of stack heights and some variation of vehicle speed, the exhaust plumes frequently didn't intersect the remote sensing beams at all or only temporarily. No intersection was most common for the HMMWVs with ground-level exhausts, while for the taller vehicles, the plume was frequently ejected above the height of the remote sensing beams allowing for only temporary (i.e., when the stack is below the beams) intersection with the beams. For the gaseous remote sensing device, this problem was less due to the large (~30 cm) beam width used, while it was exacerbated for the PM remote sensing device due to its narrow (~ 0.3 cm) laser beam.

VERSS EFs are summarized in Table 5-17. PM EFs were on the order of 1 g_{PM}/kg_{fuel} for the MTVRs and the LVSs with LVS PM EFs being larger. NO EFs ranged from 14 g_{NO}/kg_{fuel} for the MTVR to 42 g_{NO}/kg_{fuel} for the AAV with HUMMWV and LVS EFs around 20 g_{NO}/kg_{fuel}. As typical for lean burning diesel engines CO and HC emission factors were considerably lower ranging from 1 to 5 g/kg_{fuel}. An extremely large variation of CO EFs for the MTVRs is evident.

Table 5-17. Remote sensing emission factors (EF) for different vehicle types.

Vehicle	PM EF (g_{PM}/kg_{fuel})	Valid PM Measurements	NO EF (g_{NO}/kg_{fuel})	CO EF (gCO/kgfuel)	HC EF (gHC/kgfuel)	Valid Gaseous Measurements
MTVR	0.72±0.26	3	14.2±5.1	3.8±22.8	1.05±3.02	28
LVS	1.27±0.5	6	23.9±3.0	3.55±1.85	3.71±1.77	13
AAV	NA	0	42.3±6.3	5.21±2.23	2.79±1.56	3
HUMMWV	NA	0	19.2	-0.05	1.21	2

Given the types of sources and the difficulty of the logistics, it is concluded that the VERSS in its present form is not a practical method of quantifying emissions from military diesel. It is more suited for on-road applications where most exhaust emissions are near ground level, vehicles are already channeled into traffic lanes, and a large volume of traffic disperses the plume in a predictable manner. As explained in Section 4, the lack of commercially available components also limits the reproduction of VERSS for these measurements. Further development and miniaturization may make a VERSS more applicable to this situation in the future, but it is not likely to meet immediate needs for quantifying non-road engine emissions.

5.6 On-Board PM Mobile Source Measurements

The on-board PM system described in Section 4 was mounted on the vehicles specified in Table 5-18. The Detroit Diesel 8V92TA engine accounts for the third highest (17% of total) diesel fuel consumption within the US Army and the fourth highest (9% of total) diesel fuel consumption within the US Marine Corps for 2003, as shown in Section 3.

The **MTVR** (Medium Tactical Vehicle Replacement) is a six-wheel drive all-terrain vehicle used by the United States Marine Corps and United States Navy. It is designed to replace the old M900 series of tactical trucks, and was first fielded in 1998, after the contract was awarded to Oshkosh Truck Corporation. The MTVR comes in several variants, for a wide spectrum of tasks. It offers a major improvement in off-road capability with an advanced suspension, a condition adaptable Central Tire Inflation System (CTIS), and a potent engine/drive train combination utilizing the Caterpillar C-12 engine. The Caterpillar C-12 engine is a turbo-charged, four-stroke, 6-cylinder, 12 l displacement diesel engine. The MTVR is the Marine Corps prime mover for the M777 howitzer, fuel and water assets, troops and a wide

variety of equipment. Its wide versatility and off-road capability make the MTVR an integral part of the Marine Corps logistical backbone.

Table 5-18. Vehicles tested with on-board system

Vehicle Type	USMC	Model Year	Engine	GVWR (lbs)	Engine Age (Miles/Hours)	Test
MTVR	593901	10/2002	Caterpillar C-12 (four stroke)	62,200	6637 / 661	Driving Cycle
MTVR	592995	4/2002	Caterpillar C-12 (four stroke)	62,200	5306 / 491	Driving Cycle
LVS	550978	8/2006	Detroit Diesel 8V92TA (two stroke)	32,000	377 / 122	Driving Cycle
AAVP7A1	523294		Cummings VT400 (four stroke)	61,158	2332 / 162	Idle

The **LVS** (Logistics Vehicle System) is a modular assortment of eight-wheel drive all-terrain vehicles used by the United States Marine Corps. It is powered by a Detroit Diesel 8V92TA engine, which is a turbo-charged, two-stroke, 8-cylinder, 12 l displacement diesel engine. The LVS was fielded in 1985 as the Marine Corps heavy tactical vehicle system. It was designed and manufactured by the Oshkosh Truck Corporation. The United States Army has a similar tactical vehicle called the Heavy Expanded Mobility Tactical Truck (HEMTT). The key difference between the two is the LVS's ability to interchange Front Power Units with Rear Body Units. The LVS also steers through both standard wheel pivoting (as on a typical automobile) and hydraulic yaw steering (by articulating the Front Power Unit against the Rear Body Unit). This gives the LVS remarkable maneuverability for its size.

The **AAVP7A1** (Amphibious Assault Vehicle) is a fully tracked amphibious landing vehicle manufactured by FMC Corporation (now BAE Systems Land and Armaments). It is powered by a Cummings VT400 engine, which is a turbo-charged, four-stroke, 8-cylinder, 14.8 l displacement diesel engine. The AAVP7A1 is the current amphibious troop transport of the United States Marine Corps. It is used by USMC Assault Amphibian Battalions to land the surface assault elements of the landing force and their equipment in a single lift from assault shipping during amphibious operations to inland objectives and to conduct mechanized operations and related combat support in subsequent mechanized operations ashore. It is also operated by other forces.

An 1.8 km roundtrip loop (Figure 5-19) over paved and concrete surfaces was followed in each of the tests. Driving started at the location of the in-plume and cross-plume systems on a tank track paralleling Rainbow Canyon Road in northwest direction. Turning right onto the connector road between the tank track and Rainbow Canyon Road and again right onto Rainbow Canyon Road, the vehicles traveled in southeast direction on Rainbow Canyon Road, turned

right onto Berkeley Avenue and immediately right onto the tank track, completing a round trip at the location of the in-plume and cross-plume systems. The whole area of this test loop has an approximately uniform slope resulting in a 1.1° uphill slope on the tank track and a 1.1° downhill slope on Rainbow Canyon Road with fairly level driving on the connector road and Berkeley road. The sharp turns between the tank track and Rainbow Canyon Road included stop signs and facilitated repeated decelerations and accelerations.

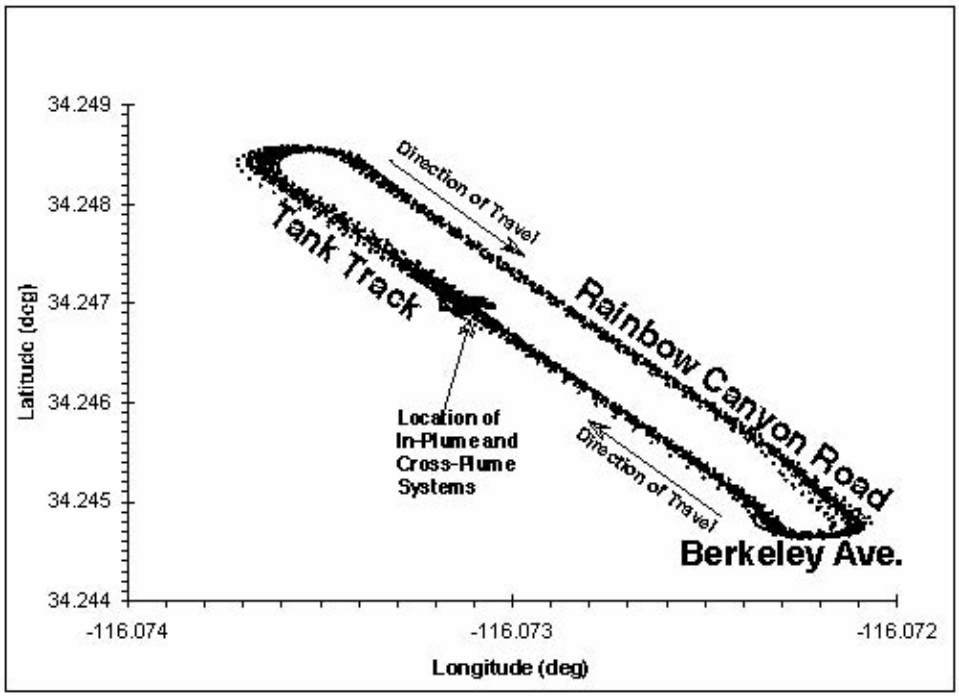

Figure 5-19. Labeled plot of GPS coordinates on test loop (cycle #1).

The length of the roundtrip loop was 1.8 km and it took 100 – 130 seconds to drive this loop. The MTVRs drove five sequential loops, resulting in a total distance of 9 km driven during 10 – 16 minutes with the total time depending on the individual driver and on idle time during change of on-board filters. LVSs drove either 5 or 3 loops with the total time for 3 loops ranging from 9 to 19 minutes.

In addition to driving on the test loop (Figure 5-19), more extended drives (10 – 21 minutes) with more high speed cruising and less frequent acceleration and deceleration were performed on a longer section of Rainbow Canyon Road that included most of the test loop, as documented in Figure 5-20.

An example of raw data from the on-board system is shown in Figure 5-21. The system was placed on-board of the MTVR with the Marine Corps identification code USMC593901 and recorded data for five test loops (cycle #1) on April 19, 2007. Data shown in Figure 5-21 include uncalibrated PM mass concentration as measured by the TSI DustTrak (DT), PM light absorption coefficients Babs (i.e., light absorption cross-section concentration) measured by the DRI Photoacoustic Analyzer, carbon dioxide (CO_2) concentrations measured by the LiCor LI-840, and vehicle speed measured by the GPS system. PM, Babs, and CO_2 concentrations are those in the sampling manifold after dilution.

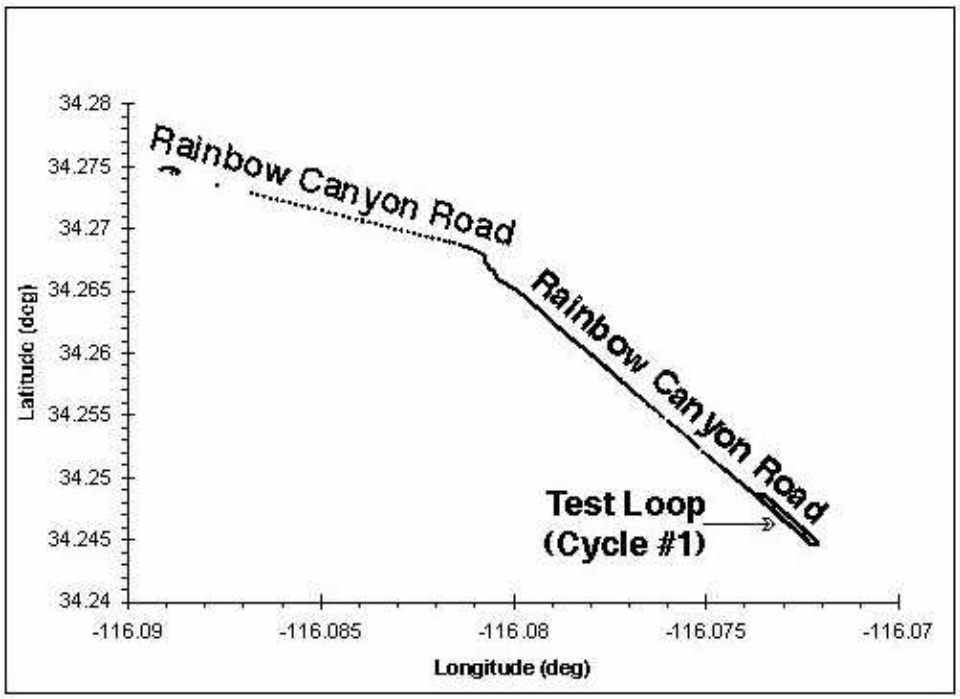

Figure 5-20. Labeled plot of GPS coordinates on extended drive (cycle #2).

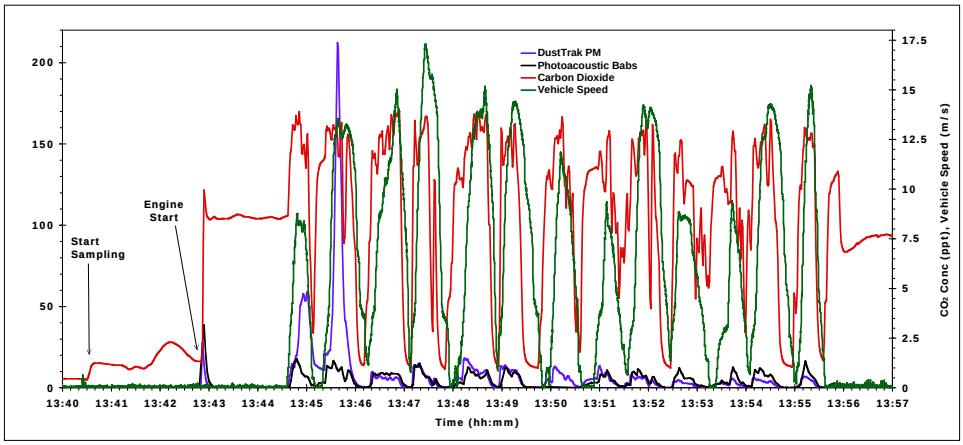

Figure 5-21. Raw on-board data for an MTVR driving five test loops (cycle #1).

The measured concentrations can be used without any knowledge of the dilution factor to determine the fuel-based emission factor EF_P for pollutant P under the assumption that virtually all carbon mass emissions are contained in the CO_2 emissions. The fuel-based emission factor EF_P for pollutant P can be written as (Moosmüller et al., 2003)

$$EF_P = \frac{CMF_{fuel}}{CMF_{CO2}} \frac{C_P}{C_{CO2}} , \qquad (5\text{-}3a)$$

where C_p and C_{CO2} are the mass concentration of pollutant P and CO_2, respectively and CMF_{fuel} and CMF_{CO2} are the carbon mass fractions of diesel fuel and CO_2, respectively.

CMF_{CO2} can be calculated directly from the respective atomic masses of carbon and oxygen as CMF_{CO2} =12/(12+2×16) = 12/44 = 27.3%. For diesel fuel, one may assume the empirical formula of C_nH_{2n}, resulting in CMF_{diesel} = 12/(12+2) = 85.6%.

$$EF_P = \frac{CMF_{diesel}}{CMF_{CO2}} \frac{C_P}{C_{CO2}} = \frac{22}{7} \frac{C_P}{C_{CO2}} = 3.14 \frac{C_P}{C_{CO2}} \ , \qquad (5\text{-}3b)$$

In the following, equation 5-3 is used to calculate fuel based emission factors for particulate matter (PM) and black carbon (BC) after application of the calibration factors for the TSI DustTrak (DT) and the DRI Photoacoustic Analyzer (PA).

Vehicle Specific Power (*VSP*, unit of kW/Mg) is a surrogate for actual engine power that can be calculated from vehicle speed, acceleration, and slope of the terrain as (Kuhns et al., 2004)

$$VSP = va(1+\varepsilon) + g(grade)v + gC_R v + C_{if} v + 0.5\rho_a C_D \frac{A}{Mass} v^3 \ , \qquad (5\text{-}4)$$

where v and a are the vehicle speed and acceleration is m/s and m/s^2, respectively. The variable ε is the 'mass factor' (unit of 1) that accounts for the translational mass of the rotating components. The variable g is the gravitational acceleration (9.8 m/s^2) and *grade* is the rise/run of the roadway. C_R, C_D, and C_{if} are the coefficients of rolling resistance (unit of 1), drag (unit of 1), and the internal friction factor (unit of m s^{-2}), respectively. The variable ρ_a is the density of air (unit of kg m^{-3}). The variables A and *Mass* are the vehicle frontal area (unit of m^2) and mass (unit of kg), respectively.

Fuel-based emission factors in units of gram of pollutant (PM or BC) emitted per kg of fuel consumed are shown for combinations of cycle #1 and cycle #2 driving cycles in Figures 5-22a-f as function of *VSP*. Individual data point have been boxcar averaged over 5 seconds and are displayed a small black dots. To display trends more clearly as function of *VSP*, individual data points have also been binned over *VSP* bins with a width of 2 kW/Mg. These averages are displayed as squares with error bars indicating the variation of the data points over each *VSP* bin. Averages over all data points are summarized together with their standard deviations in Table 5-19.

Table 5-19. Average emission factors (EFs) from real time instruments.

	DT PM EF (g_{PM}/kg_{fuel})	PA BC EF (g_{BC}/kg_{fuel})
MTVR (USMC 593901)	0.31 ± 0.92	0.09 ± 0.16
MTVR (USMC 592995)	0.37 ± 2.75	NA
LVS (USMC 592995)	4.98 ± 23.7	NA
AAVP7A1 (USMC 523294; idle)	1.19 ± 1.73	NA

Most figures show a large number of data points at VSP = 0 kW/Mg corresponding to the vehicles standing still and their engines idling. The corresponding emission factors have the largest variation due to the inclusion of engine start and idling at widely varying rpm (i.e., gunning the engine at idle). In general emission factors at positive *VSP*s are relative independent of *VSP* as can be seen from the binned data. The larger variation at negative *VSP*s is due to the fact that vehicles are decelerating with widely varying and poorly quantified negative engine loads.

Results for the MTVR (USMC 593901) are shown in Figures 5-22a (PM) and b (BC). Average PM emission factors are lower, but have larger variations at negative *VSP*s, while at positive *VSP*s they are larger and fairly constant. Note that some outlier data at positive *VSP* with very high PM *EF*s happened sequentially. Average BC emission factors are nearly identical for positive and negative VSPs with a minimum near idle (VSP = 0 kW/Mg) with very little dependence on VSP. Results for the MTVR (USMC 592995) are shown in Figures 5-22c (PM) and 5-22d (BC). Trends for average PM emission factors are very similar to USMC 593901 with the exception of less outlier data at positive *VSP* and more outlier data at small negative *VSP*s with extremely high PM *EF*s. Average BC emission factors decrease for increasing *VSP*s. However, the availability of valid BC data is rather poor for this vehicle, which makes this trend rather questionable. Results for the LVS (USMC 592995) are shown in Figures 5-22e (PM) and 10f (BC). Average PM emission factors are extremely high and have larger variations at negative *VSP*s, while at positive *VSP*s they are much smaller and decrease for increasing *VSP*s. The availability of valid BC data is extremely poor for this vehicle and no conclusions should be drawn from figure 5-22f.

The AAVP7A1 (USMC 523294) could only be tested at idle as the on-board system could not be mounted on this vehicle. Idle data are summarized together with the average data from the other vehicles in Table 5-19. MTVR PM emission factors are comparable to each other but those of MTVR (USMC 592995) have much higher variation than those of MTVR (USMC 592995). LVS PM emission factors are about an order of magnitude higher in their values and variations than those of the MTVRs.

The on-board PM monitor appears to function well. Although this unit was in prototype form, it could be more efficiently packaged for a large number of field measurements. Coupled with portable gas monitors with greater sensitivity to lower emissions levels than those detected by the gas PEMS, the on-board system could be more practical for mobile sources than the MELS, IPETS, or VERSS.

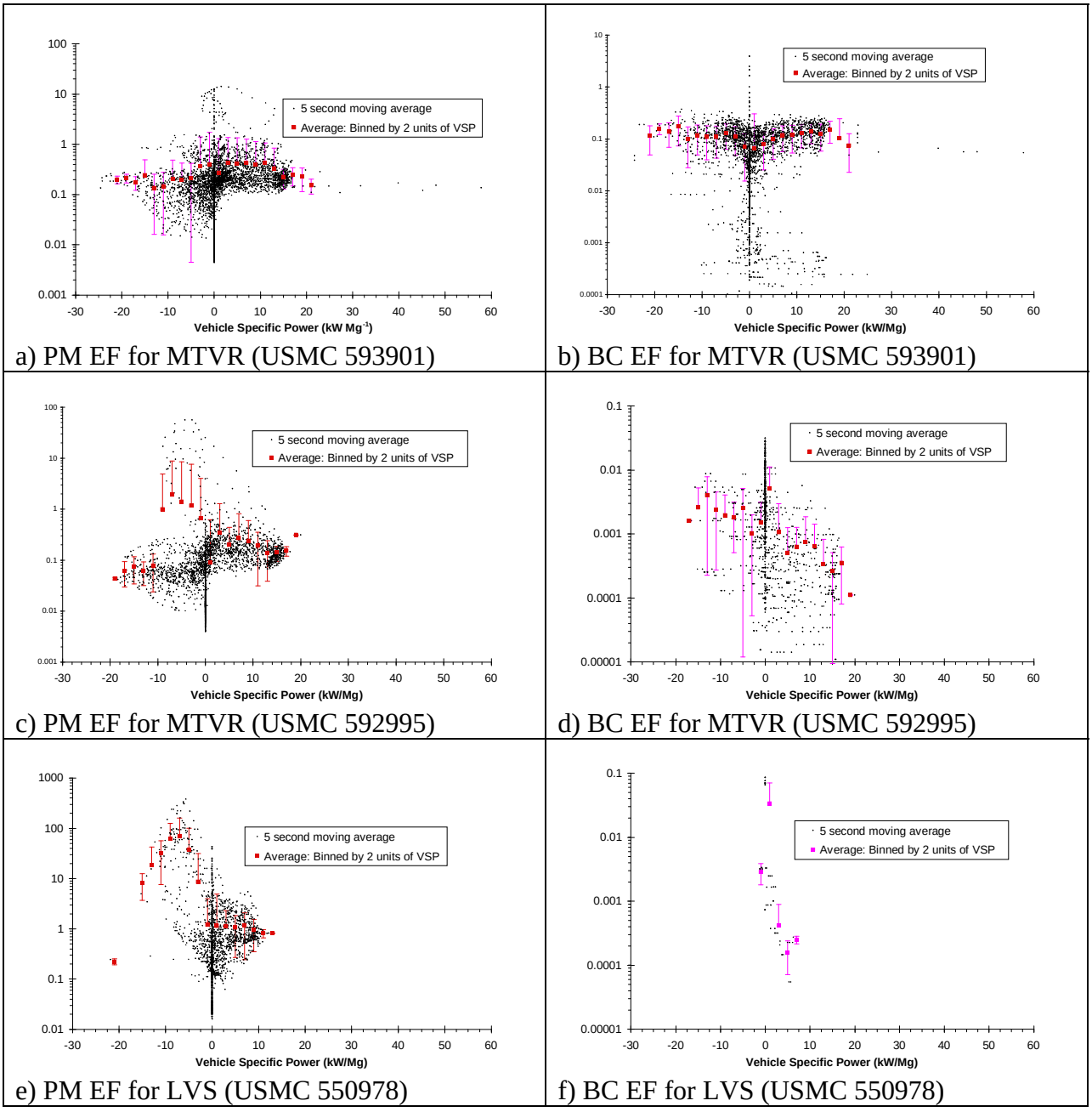

Figure 5-22. Emission factors for different vehicles measured with the on-board monitoring system. PM EFs were measured with the DustTrak and BC EFs were measured with the photoacoustic analyzer.

6. SOURCE PROFILES

PM filters were taken during the diesel generator tests at Camp Pendleton and the IPETS and on-board tests at 29 Palms, and these were submitted to chemical analysis to obtain source profiles, as described in Section 2. Table 6-1 lists the $PM_{2.5}$ source profiles mnemonic name along with a description of the sources.

Sample durations ranged from 22 to 82 minutes for the warm starts and 21 to 53 minutes for the cold starts for stationary diesel sources. Diesel vehicle tests included the two MTVRs, which are powered by Caterpillar 729 cubic inch six-cylinder turbocharged diesel engines. The LVS and AAVs are powered by Detroit Diesel 8V92TA and Cummins VT400 eight-cylinder turbocharged diesel engines, respectively.

6.1 Inorganic and Organic Chemical Speciation

Teflon-membrane filters were submitted for mass by gravimetry and 51 elements by X-ray fluorescence (Watson et al., 1999). Half of the quartz-fiber filters were submitted for chloride (Cl^-), nitrate (NO_3^-), and sulfate ($SO_4^=$) by ion chromatography (IC; Chow and Watson, 1999) and water-soluble sodium (Na^+) and potassium (K^+) by atomic absorption spectroscopy. The second half of the quartz-fiber filters were submitted for ammonium (NH_4^+) by automated colorimetry (AC); for organic carbon (OC), elemental carbon (EC), and their eight fractions (OC1-OC4, OP, EC1-EC3) by the IMPROVE_A thermal/optical protocol (Chow et al., 1993; 2001; 2004b; 2005a; 2007b); and for 125 non-polar speciated organic carbon compounds by thermal desorption-gas chromatography/mass spectrometry (Chow et al., 2007e; 2008; TD-GC/MS; Ho and Yu, 2004). The backup citric acid-impregnated cellulose-fiber filters were analyzed for ammonia (NH_3) by AC and the backup potassium carbonate-impregnated cellulose-fiber filters were analyzed for sulfur dioxide (SO_2) by IC. Table 6-2 summarizes the species measured for mass, elements, ions (including gaseous species), and carbon along with their minimum detection limits (MDLs) and lower quantifiable limits (LQLs). Similar information is given in Table 6-3 for 125 non-polar organic species.

6.2 $PM_{2.5}$ Source Profiles

Source profiles reported in this section are normalized by $PM_{2.5}$ mass. Since emissions from diesel exhaust consists of abundant volatile organic compounds (VOCs), some of the profiles report total carbon (TC) levels that exceed mass concentrations.

$PM_{2.5}$ source profiles for the diesel generators for the warm and cold starts are listed in Tables 6-4 and 6-5, respectively, while the diesel vehicle source profiles for MTVR and LVS are listed in Tables 6-6 and 6-7, respectively. Table 6-8 summarizes the composite profiles for the diesel generators as well as for MTVR and LVS. Only a single test was performed for AAV on idle mode; the AAV profile is compared with the composite profiles in Table 6-8. In these Tables, the 125 non-polar organic compounds are grouped into ten categories (i.e., polycylic aromatic hydrocarbons [PAHs], n-alkanes, iso- and anteiso-alkanes, hopanes, steranes, methyl-alkanes, branched alkanes, cyclo-alkanes, alkenes, and phthalates). For comparison, the abundances of individual organic species for the warm start, cold start, MTVRs, LVS, and composites (including AAV) are given in Tables 6-9 to 6-12, respectively.

6.3 $PM_{2.5}$ Diesel Generator Profiles

Figures 6-1 and 6-2 illustrate the abundances of source profiles for diesel generators and vehicles, respectively. The error bars on these Figures are the standard deviation of each measured species. Larger error bars suggest the large variations from each individual test.

Carbon is the most abundant species by far for all 25 test runs. For the diesel generators, TC accounts for 57 ± 25% and 85 ± 63% of $PM_{2.5}$ under various warm and cold start conditions, respectively. Large variations were found among the 13 generators. TC varied by ~twofold for warm starts, ranging from 38% (10 kW and 100 kW) to 95% (60 kW), and varied by ~sixfold for cold starts, ranging from 29% (100 kW) to 175% (60 kW) for $PM_{2.5}$. On average, the EC/TC ratio for warm starts (0.31) were approximately twice those for cold starts (0.14). Approximately 82% of EC reported in this study was present in the high-temperature EC2 fraction (740 °C at 98% helium [He]/2% oxygen [O_2] atmosphere) with 0.1 – 0.3% of EC in the EC3 fraction (840 °C at 98% He/2% O_2 atmosphere). On average, $PM_{2.5}$ OC accounts for 20 – 70% of $PM_{2.5}$ mass, with ~28% of OC found in the low-temperature OC1 (140 °C at 100% He atmosphere) and 44% of OC found in the OC2 fraction (280 °C at 100% He atmosphere) in warm starts; over twice those found in cold starts (22%).

The most noticeable abundance in organic compounds are the n-alkanes, averaging 0.7 ± 0.7% for warm starts and 1.1 ± 1.4% for cold starts, followed by hopanes (~0.12%) with low PAHs (0.02 – 0.08%). Levels of trace elements were low (typically < 0.05%) with elevated iron (Fe; 0.1 – 0.2%), calcium (Ca; 0.07 – 0.10%), and phosphorous (P; 0.07 – 0.13%). $PM_{2.5}$ $SO_4^=$ was low and variable, averaging 1.3 ± 1.1% for warm starts and 0.5 ± 0.5% for cold starts. Higher SO_2 (41 ± 37%) was reported for cold starts than warm starts (24 ± 19%). $PM_{2.5}$ $SO_4^=$ and SO_2 levels are also lower than the 2.4 ± 1% and 67 ± 24% reported by Watson et al. (1994). This reflects the reduction of sulfur content in diesel fuel over the past two decades. Low levels of NH_3 were detected, with 0.05 ± 0.05% for warm starts and 0.3 ± 0.6% for cold starts.

6.4 $PM_{2.5}$ Diesel Vehicle Profiles

Most of the diesel vehicle tests reported carbon concentrations higher than the corresponding gravimetric mass. With on-board testing, OC represents both gaseous VOCs and particulate OC. The abundance of VOCs is expected to be higher for on-board testing as compared to the more diluted in-plume testing.

Average TC accounts for 80 ± 13% (LVS) to 121 ± 18% (MTVR) of $PM_{2.5}$ mass. These TC levels are 30 – 50% higher than those found in diesel generators, ranging from 88 ± 12% for AAV (idle), 82 – 155% for MTVR, and 62 – 93% for LVS. Lower TC is found for the LVS Driving Cycle #2 test (TNP19, 62 ± 18%) and the MTVR Driving Cycle #1 test (TNP09, 83 ± 12%). On average, the EC/TC ratios are 0.70 for AAV (idle), 0.46 for MTVR, and 0.53 for LVS, much higher than the 0.14 – 0.31 found for diesel generators. The abundance of EC in $PM_{2.5}$ is also two to three times those of the diesel generators: 62 ± 14% for AAV, 55 ± 14% for MTVR, and 42 ± 15% for LVS. The most abundant EC is in the EC2 fraction, which accounts for 93%, 77%, and 68% of EC for AAV, MTVR, and LVS, respectively.

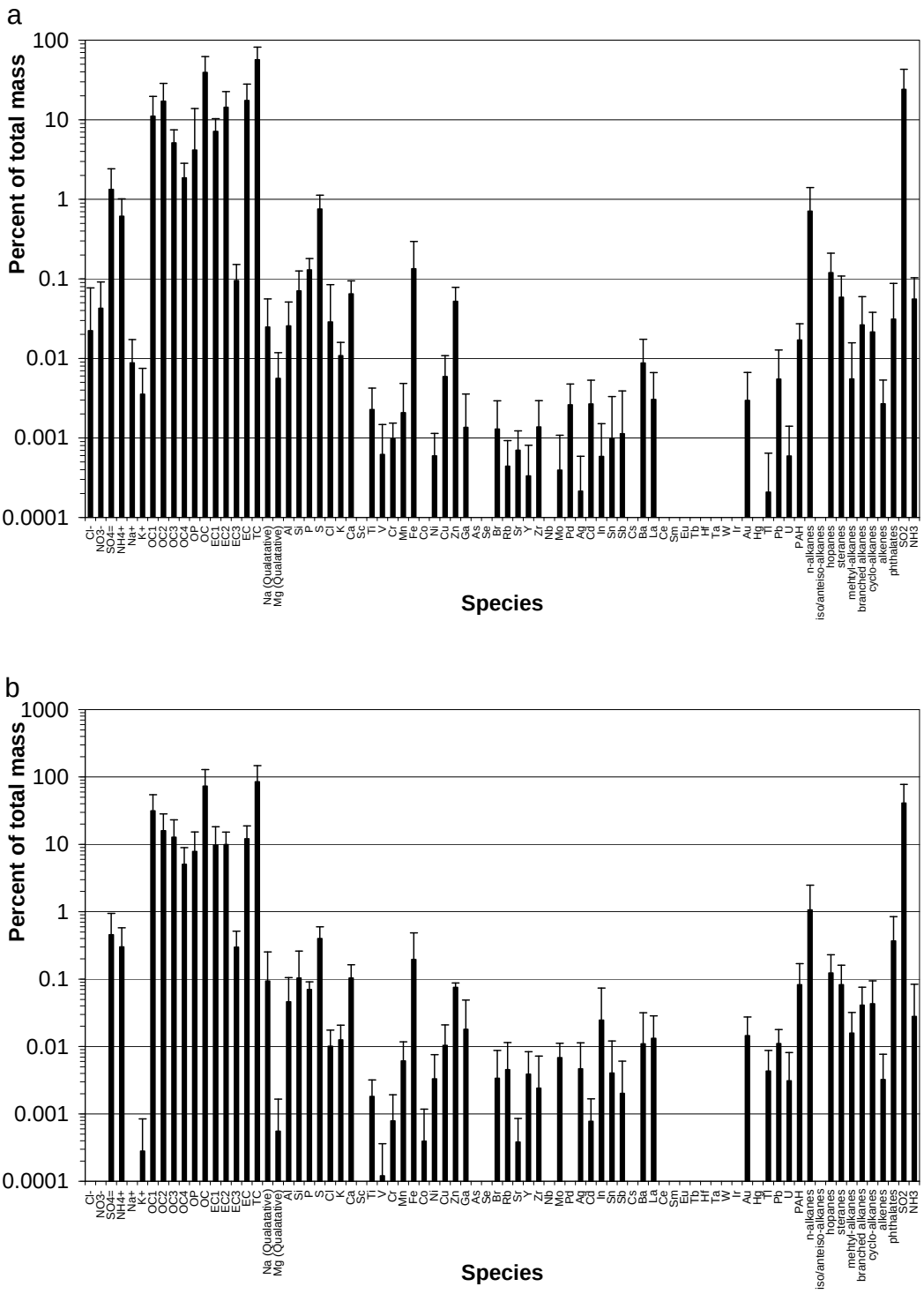

Figure 6-1. Composite $PM_{2.5}$ source profiles for the emissions tests performed on 13 military diesel generators operated under: a) warm start (running at 10, 25, 50, 75, and 100% load) and b) cold start modes.

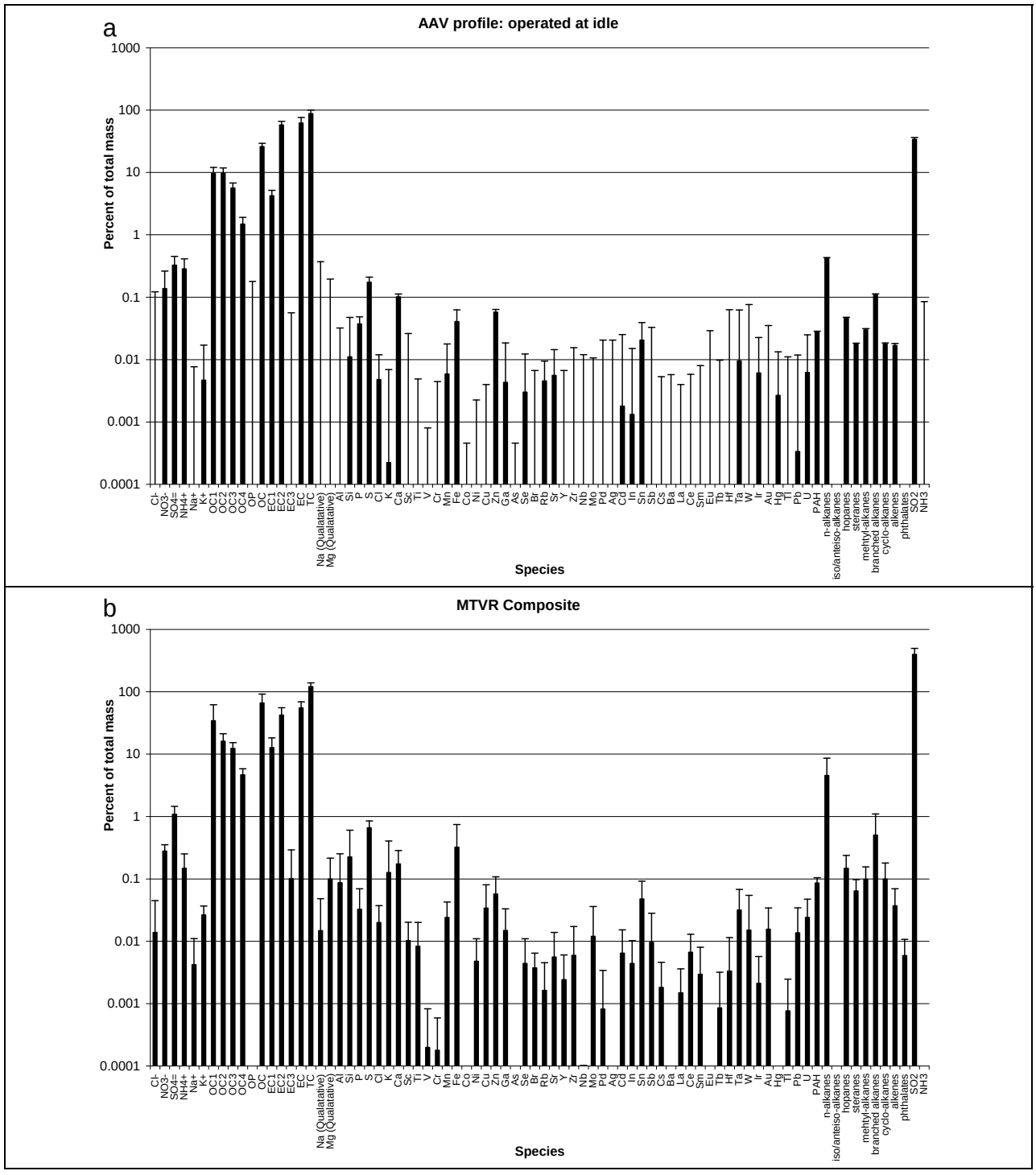

Figure 6-2. Source profiles of the military diesel vehicle emissions for: a) single test of the idle mode for the assault amphibious vehicle, b) composite test of the medium tactical vehicle replacement (MTVR), and c) composite test of the logistical vehicle system (LVS).

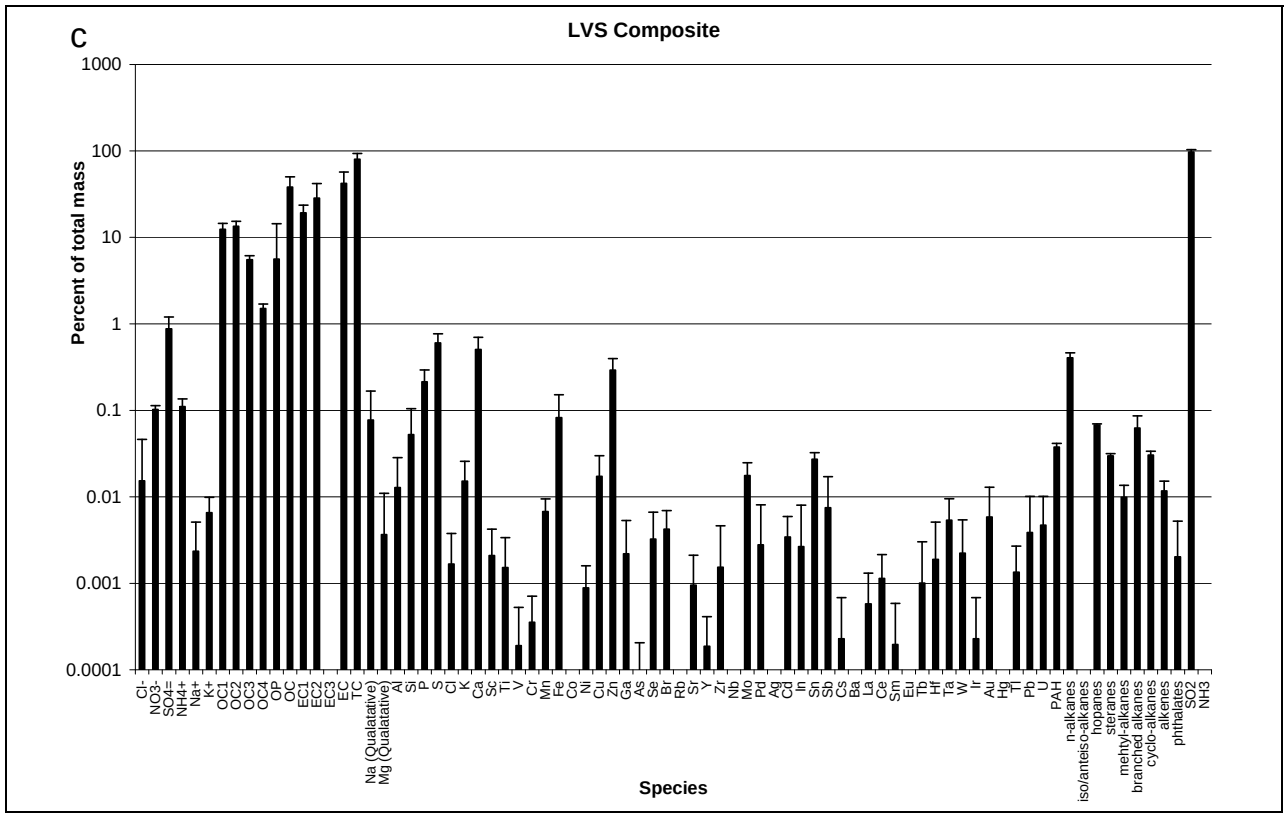

Figure 6-2. Continued

On average, $PM_{2.5}$ OC accounts for 26 – 66% of $PM_{2.5}$, with 30 – 52% of OC found in the OC1 fraction. Elevated n-alkanes (4.6 ± 4.1%) were found for MTVR, with ~0.4% found for LVS and AAV. Branched n-alkanes were less than 0.04% for the generators, and ranged from 0.5 ± 0.59% (MTVR) to 0.1 ± 0.008% (AAV) in vehicles. PAHs were low, in the range of 0.03 to 0.08%. Levels of trace elements were low, but ~3 – 10 times higher than those found for diesel generators. Elevated potassium (K; 0.13 ± 0.28%), Ca (0.17 ± 0.11%), and Fe (0.32 ± 0.4%) were found for MTVR. Elevated Ca (0.5 ± 0.2%) was also reported for LVS. $PM_{2.5}$ $SO_4^{=}$ was comparable to the generators, in the range of 0.3 – 1.1%. Elevated SO_2 is apparent, 97 ± 6% for LVS and 398 ± 98% for MTVR. SO_2 in AAV idle (34 ± 3%) is comparable to the 24 – 41% reported for generators. NH_3 is not detectable for any of the vehicles tested.

6.5 Comparison with Past Studies

Table 6-14 compares the carbon abundance of 118 profiles from the diesel engine tests conducted over the past two decades. This data demonstrates that TC typically accounts for 80 – 90% of $PM_{2.5}$ mass, with some exceptions ranging from 10% to >1,000% Test results are affected by the type and size of the engine tested, fuel composition, engine mode, dilution ratios, and sampling duration. The TC/$PM_{2.5}$ ratio of 57 – 85% for diesel generators and 80 – 121% for diesel vehicles found in this study fall into the nominal range of previous studies.

EC/TC ratios found from the diesel generators (0.14 to 0.31) are 40 – 70% lower than the 0.46 for MTVR and 0.53 for LVS. As shown in Table 6-14, EC/TC of 0.45 was reported from the 1990 test at the centralized State of Arizona Motor Vehicle Inspection and Maintenance Station (Watson et al., 1994). EC/TC ratios were 0.42 – 0.50 and 0.65 – 0.85 for the Northern

Front Range Air Quality Study (NFRAQS) in summer 1996 and winter 1997, respectively (Watson et al., 1998). The gas/diesel split project conducted in fall of 2001 at West Virginia for the 30 heavy-duty diesel trucks reported EC/TC ratios of 0.1 – 0.78 (Fujita et al., 2007a; 2007b). Most diesel engine tests yield EC/TC of 0.5 – 0.8. The low values (0.14 to 0.31) found for the diesel generators in this study are atypical.

High temperature EC (i.e., EC2) has been the dominant fraction in diesel exhaust consistently over the past two decades. Abundances of EC2 in EC were 69 – 93% for this study, 85% for the Phoenix study (Watson et al., 1994), 67 – 74% during NFRAQS (Watson et al., 1998), and 60 – 96% for the gas/diesel split project (Fujita et al., 2007a; 2007b). These data demonstrate that carbon abundances and the $PM_{2.5}$ diesel emission source profiles from the military generators and vehicles are similar to those found in other on-road emissions.

Table 6-1. Summary of 25 tests conducted for $PM_{2.5}$emissions from 13 military diesel generators and four military diesel vehicles.

Mnemonic ID	Generator / Vehicle Type	Sampling Mode	Sampling Load / driving condition	Sampling Location	Sampling Date	Sample Duration (min)
PEN_04	Two 10kW Generators	DRI in-plume	10, 25, 50, 75, 100% load / warm start	Camp Pendleton, CA	11/14/2005	82
PEN_05	One 10kW Generator	DRI in-plume	10, 25, 50, 75, 100% load / warm start	Camp Pendleton, CA	11/14/2005	25
PEN_06	Two 30kW Generators	DRI in-plume	10, 25, 50, 75, 100% load / warm start	Camp Pendleton, CA	11/15/2005	67
PEN_08	Three 60kW Generators	DRI in-plume	10, 25, 50, 75, 100% load / warm start	Camp Pendleton, CA	11/15/2005	66
PEN_09	Two 60kW Generators	DRI in-plume	10, 25, 50, 75, 100% load / warm start	Camp Pendleton, CA	11/15/2005	69
PEN_13	One 100kW Generator	DRI in-plume	10, 25, 50, 75, 100% load / warm start	Camp Pendleton, CA	11/16/2005	22
PEN_14	Three 10kW Generators	DRI in-plume	cold start idle	Camp Pendleton, CA	11/16/2005	21
PEN_11	Five 30kW Generators	DRI in-plume	cold start idle	Camp Pendleton, CA	11/16/2005	53
PEN_10	Four 60kW Generators	DRI in-plume	cold start idle	Camp Pendleton, CA	11/16/2005	34
PEN_12	One 100kW Generator	DRI in-plume	cold start idle	Camp Pendleton, CA	11/16/2005	21
TNP_04	MTVR[a] #1	DRI on-board	Driving Cycle #1[d]	Camp Wilson, CA	4/19/2007	16
TNP_05	MTVR[a] #1	DRI on-board	Driving Cycle #1[d]	Camp Wilson, CA	4/19/2007	11
TNP_06	MTVR[a] #1	DRI on-board	Driving Cycle #1[d]	Camp Wilson, CA	4/19/2007	12
TNP_07	MTVR[a] #1	DRI on-board	Driving Cycle #1[d]	Camp Wilson, CA	4/19/2007	12
TNP_08	MTVR[a] #1	DRI on-board	Driving Cycle #1[d]	Camp Wilson, CA	4/19/2007	11
TNP_09	MTVR[a] #1	DRI on-board	Driving Cycle #2[e]	Camp Wilson, CA	4/19/2007	21
TNP_10	MTVR[a] #2	DRI on-board	Driving Cycle #1[d]	Camp Wilson, CA	4/19/2007	11
TNP_11	MTVR[a] #2	DRI on-board	Driving Cycle #1[d]	Camp Wilson, CA	4/19/2007	14
TNP_12	MTVR[a] #2	DRI on-board	Driving Cycle #1[d]	Camp Wilson, CA	4/19/2007	10
TNP_13	MTVR[a] #2	DRI on-board	Driving Cycle #2[e]	Camp Wilson, CA	4/19/2007	12
TNP_14	LVS[b]	DRI on-board	Driving Cycle #1[d]	Camp Wilson, CA	4/20/2007	19
TNP_16	LVS[b]	DRI on-board	Driving Cycle #1[d]	Camp Wilson, CA	4/20/2007	9
TNP_17	LVS[b]	DRI on-board	Driving Cycle #1[d]	Camp Wilson, CA	4/20/2007	11
TNP_19	LVS[b]	DRI on-board	Driving Cycle #2[e]	Camp Wilson, CA	4/20/2007	10
TNP_15	AAV[c]	DRI on-board	idle	Camp Wilson, CA	4/20/2007	5

[a] Medium tactical vehicle replacement with a Caterpillar 729 cubic inch six-cylinder turbocharged diesel engine
[b] Logistics vehicle system with a Detroit Diesel 8V92TA eight-cylinder turbocharged diesel engine
[c] Assault amphibian vehicle with a Cummins VT400 eight-cylinder turbocharged diesel engine
[d] Driving Cycle #1 is characterized by frequent accelerations and decelerations (as shown in Figure 1)
[e] Driving Cycle #2 is characterized by cruising speeds of 15 – 19 m/s and some accelerations and decelerations (as shown in Figure 1)

Table 6-2. Summary of analytical detection limits for mass, elements, ions (including gaseous NH_3 and SO_2), and carbon applied to this study.

Species	Analysis Method[a]	MDL[b] (µg/filter[c])	LQL[d] (µg/filter)
Mass	GRAV	1.0000	5.1962
Ammonia (NH_3)	AC	1.5005	1.5005
Sulfur Dioxide (SO_2)	IC	1.5005	1.5005
Chloride (Cl^-)	IC	1.5005	1.5005
Nitrate (NO_3^-)	IC	1.5005	1.5005
Sulfate ($SO_4^=$)	IC	1.5005	1.5005
Ammonium ($NH4^+$)	AC	1.5005	1.5005
Soluble Sodium (Na^+)	AAS	0.2362	0.2362
Soluble Potassium (K^+)	AAS	0.1498	0.8350
Organic Carbon (OC) Fraction 1 (OC1)[e]	TOR	0.0516	1.0241
Organic Carbon (OC) Fraction 2 (OC2)[e]	TOR	1.2900	1.3369
Organic Carbon (OC) Fraction 3 (OC3)[e]	TOR	3.8700	3.8700
Organic Carbon (OC) Fraction 4 (OC4)[e]	TOR	0.1290	0.1290
Pyrolyzed organic carbon via transmittance (OPR)[e]	TOR	0.1290	0.1290
Pyrolyzed organic carbon via reflectance (OPT)[e]	TOR	0.1290	0.7071
Organic Carbon (OC)[e]	TOR	5.0310	5.0310
Elemental Carbon (EC) Fraction 1 (EC1)[e]	TOR	0.0387	0.0387
Elemental Carbon (EC) Fraction 2 (EC2)[e]	TOR	0.0387	0.0387
Elemental Carbon (EC) Fraction 3 (EC3)[e]	TOR	0.0387	0.0387
Elemental Carbon (EC)[e]	TOR	0.1290	0.7071
Total Carbon (TC)[e]	TOR	5.4180	5.4180
Sodium (Na)	XRF	3.7541	3.7541
Magnesium (Mg)	XRF	1.1341	1.1341
Aluminum (Al)	XRF	0.4483	0.4483
Silicon (Si)	XRF	0.3613	0.3613
Phosphorus (P)	XRF	0.1177	0.4295
Sulfur (S)	XRF	0.0506	0.0506
Chlorine (Cl)	XRF	0.0487	0.0487
Potassium (K)	XRF	0.0459	0.0646
Calcium (Ca)	XRF	0.0727	0.0754
Scandium (Sc)	XRF	0.1938	0.1938
Titanium (Ti)	XRF	0.0346	0.0346
Vanadium (V)	XRF	0.0082	0.0135

Table 6-2. Continued.

Species	Analysis Method[a]	MDL (µg/filter)	LQL (µg/filter)
Chromium (Cr)	XRF	0.0382	0.1603
Manganese (Mn)	XRF	0.0834	0.3217
Iron (Fe)	XRF	0.0760	0.0760
Cobalt (Co)	XRF	0.0041	0.0143
Nickel (Ni)	XRF	0.0131	0.0251
Copper (Cu)	XRF	0.0442	0.0442
Zinc (Zn)	XRF	0.0391	0.0391
Gallium (Ga)	XRF	0.1281	0.1281
Arsenic (As)	XRF	0.0147	0.0147
Selenium (Se)	XRF	0.0290	0.0574
Bromine (Br)	XRF	0.0412	0.0412
Rubidium (Rb)	XRF	0.0271	0.0395
Strontium (Sr)	XRF	0.0633	0.0633
Yttrium (Y)	XRF	0.0376	0.1263
Zirconium (Zr)	XRF	0.1012	0.1012
Niobium (Nb)	XRF	0.0667	0.0744
Molybdenum (Mo)	XRF	0.0640	0.1827
Palladium (Pd)	XRF	0.1549	0.2542
Silver (Ag)	XRF	0.1473	0.1473
Cadmium (Cd)	XRF	0.1152	0.1152
Indium (In)	XRF	0.1271	0.2225
Tin (Sn)	XRF	0.1372	0.1372
Antimony (Sb)	XRF	0.2063	0.2063
Cesium (Cs)	XRF	0.0585	0.0869
Barium (Ba)	XRF	0.0632	0.0632
Lanthanum (La)	XRF	0.0433	0.0433
Cerium (Ce)	XRF	0.0417	0.0417
Samarium (Sm)	XRF	0.0862	0.1906
Europium (Eu)	XRF	0.1325	0.1325
Terbium (Tb)	XRF	0.0976	0.5363
Hafnium (Hf)	XRF	0.3950	0.3950
Tantalum (Ta)	XRF	0.2579	0.5442
Wolfram (W)	XRF	0.3610	0.3610
Iridium (Ir)	XRF	0.1192	0.2678
Gold (Au)	XRF	0.1960	0.1960
Mercury (Hg)	XRF	0.0971	0.1118

Table 6-2. Continued.

Species	Analysis Method[a]	MDL (µg/filter)	LQL (µg/filter)
Thallium (Tl)	XRF	0.0654	0.0654
Lead (Pb)	XRF	0.0945	0.1088
Uranium (U)	XRF	0.1648	0.1648

[a] GRAV = gravimetry.

OP = optical density.

IC = ion chromatography.

AC = automated colorimetry.

AAS = atomic absorption spectrophotometry.

TOR = thermal/optical reflectance.

XRF = x-ray fluorescence.

[b] MDL (minimum detectable limit) is the concentration at which instrument response equals three times the standard deviation of the response to a known concentration of zero.

[c] Filter assumed to be a 47 mm filter with 11.9 square centimeter deposit area

[d] LQL (lower quantifiable limit) is the large of three times the standard deviation of the concentrations measured on field blanks or MDL.

[e] OC1, OC2, OC3, and OC4 are organic carbon evolved at 140, 280, 480, and 580 °C, respectively, in a 100% He atmosphere

EC1, EC2, and EC3 are elemental carbon evolved at 580, 740, and 840 °C, respectively, in a 98% He / 2% O_2 atmosphere

OP is pyrolyzed organic carbon by reflectance (OPR) or transmittance (OPT)

OC = (OC1 + OC2 + OC3 + OC4) + OPR

EC = (EC1 + EC2 + EC3) – OPR

TC = OC + EC

Table 6-3. Summary of analytical detection limits for 125 non-polar organic compounds.

Compounds	Analysis Method[a]	MDL[b] ng/filter[c]	LQL[d] ng/filter
PAHs			
acenaphthylene	TD-GC/MS	10.764	10.764
acenaphthene	TD-GC/MS	5.842	5.842
fluorene	TD-GC/MS	4.048	4.048
phenanthrene	TD-GC/MS	1.932	1.932
anthracene	TD-GC/MS	0.782	1.192
fluoranthene	TD-GC/MS	1.150	1.150
pyrene	TD-GC/MS	1.840	1.840
benzo[a]anthracene	TD-GC/MS	3.496	3.496
chrysene	TD-GC/MS	1.840	1.840
benzo[b]fluoranthene	TD-GC/MS	3.772	3.772
benzo[k]fluoranthene	TD-GC/MS	1.288	1.443
benzo[a]fluoranthene	TD-GC/MS	1.886	1.886
benzo[e]pyrene	TD-GC/MS	4.048	4.048
benzo[a]pyrene	TD-GC/MS	4.140	4.140
perylene	TD-GC/MS	4.462	4.462
indeno[1,2,3-cd]pyrene	TD-GC/MS	1.932	1.932
dibenzo[a,h]anthracene	TD-GC/MS	4.324	4.324
benzo[ghi]perylene	TD-GC/MS	2.852	2.852
coronene	TD-GC/MS	3.358	3.358
dibenzo[a,e]pyrene	TD-GC/MS	1.288	1.288
1-methylnaphthalene	TD-GC/MS	2.070	2.070
2-methylnaphthalene	TD-GC/MS	0.690	0.690
2,6-dimethylnaphthalene	TD-GC/MS	4.002	4.002
9-fluorenone	TD-GC/MS	4.508	4.508
9-methylanthracene	TD-GC/MS	4.186	4.186
anthraquinone	TD-GC/MS	5.060	5.060
methylfluoranthene	TD-GC/MS	1.288	1.288
retene	TD-GC/MS	5.566	5.566
cyclopenta[cd]pyrene	TD-GC/MS	1.288	1.288
benz[a]anthracene-7,12-dione	TD-GC/MS	4.692	4.692
methylchrysene	TD-GC/MS	1.932	1.932
picene	TD-GC/MS	4.784	4.784
Alkane/Alkene/Phthalate			
***n*-alkane**			
pentadecane (*n*-C15)	TD-GC/MS	3.956	22.500
hexadecane (*n*-C16)	TD-GC/MS	4.094	32.956
heptadecane (*n*-C17)	TD-GC/MS	3.496	17.322
octadecane (*n*-C18)	TD-GC/MS	3.036	14.275
nonadecane (*n*-C19)	TD-GC/MS	2.346	11.411
icosane (*n*-C20)	TD-GC/MS	2.346	20.124
heneicosane (*n*-C21)	TD-GC/MS	3.910	16.139

Table 6-3. Continued

Compounds	Analysis Method[a]	MDL[b] ng/filter[c]	LQL[d] ng/filter
Alkane/Alkene/Phthalate (continued)			
***n*-alkane (continued)**			
docosane (*n*-C22)	TD-GC/MS	2.944	12.686
tricosane (*n*-C23)	TD-GC/MS	3.404	15.957
tetracosane (*n*-C24)	TD-GC/MS	2.530	22.520
pentacosane (*n*-C25)	TD-GC/MS	2.714	32.318
hexacosane (*n*-C26)	TD-GC/MS	2.714	27.930
heptacosane (*n*-C27)	TD-GC/MS	1.334	22.946
octacosane (*n*-C28)	TD-GC/MS	3.358	10.552
nonacosane (*n*-C29)	TD-GC/MS	3.772	5.321
triacontane (*n*-C30)	TD-GC/MS	4.416	4.416
hentriacotane (*n*-C31)	TD-GC/MS	3.588	3.588
dotriacontane (*n*-C32)	TD-GC/MS	4.140	4.140
tritriactotane (*n*-C33)	TD-GC/MS	2.622	2.622
tetratriactoane (*n*-C34)	TD-GC/MS	3.082	3.082
pentatriacontane (*n*-C35)	TD-GC/MS	3.312	3.312
hexatriacontane (*n*-C36)	TD-GC/MS	3.956	3.956
heptatriacontane (*n*-C37)	TD-GC/MS	4.002	4.002
octatriacontane (*n*-C38)	TD-GC/MS	3.956	3.956
nonatriacontane (*n*-C39)	TD-GC/MS	3.772	3.772
tetracontane (*n*-C40)	TD-GC/MS	3.864	3.864
hentetracontane (*n*-C41)	TD-GC/MS	4.048	4.048
dotetracontane (*n*-C42)	TD-GC/MS	4.140	4.140
iso/anteiso-alkane			
iso-nonacosane (iso-C29)	TD-GC/MS	3.680	3.680
anteiso-nonacosane (anteiso-C29)	TD-GC/MS	3.588	3.588
iso-triacontane (iso-C30)	TD-GC/MS	3.726	3.726
anteiso-triacontane (anteiso-C30)	TD-GC/MS	3.864	3.864
iso-hentriacotane (iso-C31)	TD-GC/MS	4.002	4.002
anteiso-hentriacotane (anteiso-C31)	TD-GC/MS	4.048	4.048
iso-dotriacontane (iso-C32)	TD-GC/MS	3.588	3.588
anteiso-dotriacontane (anteiso-C32)	TD-GC/MS	3.496	3.496
iso-tritriactotane (iso-C33)	TD-GC/MS	3.726	3.726
anteiso-tritriactotane (anteiso-C33)	TD-GC/MS	3.910	3.910
iso-tetratriactoane (iso-C34)	TD-GC/MS	3.864	3.864
anteiso-tetratriactoane (anteiso-C34)	TD-GC/MS	3.818	3.818
iso-pentatriacontane (iso-C35)	TD-GC/MS	4.048	4.048
anteiso-pentatriacontane (anteiso-C35)	TD-GC/MS	3.956	3.956
iso-hexatriacontane (iso-C36)	TD-GC/MS	4.002	4.002
anteiso-hexatriacontane (anteiso-C36)	TD-GC/MS	3.588	3.588
iso-heptatriacontane (iso-37)	TD-GC/MS	3.772	3.772
anteiso-heptatriacontane (anteiso-37)	TD-GC/MS	3.910	3.910

Table 6-3. Continued

Compounds	Analysis Method[a]	MDL[b] ng/filter[c]	LQL[d] ng/filter
Alkane/Alkene/Phthalate (continued)			
hopane			
22,29,30-trisnorneophopane (Ts)	TD-GC/MS	2.070	2.070
22,29,30-trisnorphopane (Tm)	TD-GC/MS	2.346	2.346
αβ-norhopane (C29αβ-hopane)	TD-GC/MS	1.472	1.472
22,29,30-norhopane (29Ts)	TD-GC/MS	2.530	2.530
αα- + βα-norhopane (C29αα- + βα -hopane)	TD-GC/MS	2.806	2.806
αβ-hopane (C30αβ -hopane)	TD-GC/MS	2.392	2.392
αα-hopane (30αα-hopane)	TD-GC/MS	2.070	2.070
βα-hopane (C30βα -hopane)	TD-GC/MS	2.208	2.208
αβS-homohopane (C31αβS-hopane)	TD-GC/MS	3.864	3.864
αβR-homohopane (C31αβR-hopane)	TD-GC/MS	3.818	3.818
αβS-bishomohopane (C32αβS-hopane)	TD-GC/MS	3.588	3.588
αβR-bishomohopane (C32αβR-hopane)	TD-GC/MS	3.726	3.726
22S-trishomohopane (C33)	TD-GC/MS	3.680	3.680
22R-trishomohopane (C33)	TD-GC/MS	4.048	4.048
22S-tretrahomohopane (C34)	TD-GC/MS	3.726	3.726
22R-tetrashomohopane (C34)	TD-GC/MS	3.772	3.772
22S-pentashomohopane(C35)	TD-GC/MS	3.680	3.680
22R-pentashomohopane(C35)	TD-GC/MS	3.726	3.726
sterane			
ααα 20S-Cholestane	TD-GC/MS	2.990	2.990
αββ 20R-Cholestane	TD-GC/MS	3.036	3.036
αββ 20s-Cholestane	TD-GC/MS	2.530	2.530
ααα 20R-Cholestane	TD-GC/MS	1.150	1.150
ααα 20S 24S-Methylcholestane	TD-GC/MS	2.070	2.070
αββ 20R 24S-Methylcholestane	TD-GC/MS	2.024	2.024
αββ 20S 24S-Methylcholestane	TD-GC/MS	2.346	2.346
ααα 20R 24R-Methylcholestane	TD-GC/MS	2.668	2.668
ααα 20S 24R/S-Ethylcholestane	TD-GC/MS	3.588	3.588
αββ 20R 24R-Ethylcholestane	TD-GC/MS	1.610	1.610
αββ 20S 24R-Ethylcholestane	TD-GC/MS	1.748	1.748
ααα 20R 24R-Ethylcholestane	TD-GC/MS	1.702	1.702
methyl-alkane			
2-methylnonadecane	TD-GC/MS	4.048	4.048
3-methylnonadecane	TD-GC/MS	4.324	4.324
branched-alkane			
pristane	TD-GC/MS	4.554	35.768
phytane	TD-GC/MS	4.554	47.343
squalane	TD-GC/MS	4.600	4.600
cycloalkane			
octylcyclohexane	TD-GC/MS	4.324	4.860
decylcyclohexane	TD-GC/MS	3.220	3.220

Table 6-3. Continued

Compounds	Analysis Method[a]	MDL[b] ng/filter[c]	LQL[d] ng/filter
Alkane/Alkene/Phthalate (continued)			
tridecylcyclohexane	TD-GC/MS	6.072	6.072
n-heptadecylcyclohexane	TD-GC/MS	3.864	3.864
nonadecylcyclohexane	TD-GC/MS	3.220	3.220
alkene	TD-GC/MS		
1-octadecene	TD-GC/MS	3.680	3.680
phthalate	TD-GC/MS		
dimethylphthalate	TD-GC/MS	2.622	5.453
diethyl phthalate	TD-GC/MS	4.002	5.871
di-n-butyl phthalate	TD-GC/MS	2.116	3.788
butyl benzyl phthalate	TD-GC/MS	3.956	3.956
bis(2-ethylhexyl)phthalate	TD-GC/MS	3.450	3.450
di-n-octyl phthalate	TD-GC/MS	3.910	3.910

[a] TD-GC/MS = thermal desorption-gas chromatography/mass spectrometry

[b] MDL (minimum detectable limit) is the concentration at which instrument response equals three times the standard deviation of the response to a known concentration of zero.

[c] Filter assumed to be a 47 mm filter with 11.9 square centimeter deposit area

[d] LQL (lower quantifiable limit) is the large of three times the standard deviation of the concentrations measured on field blanks or MDL.

Table 6-4. Summary of the $PM_{2.5}$ source profiles for the six emissions test conducted for the 13 diesel generators using warm start.

Chemical Species	10kW[a] PEN_04[b]	10kW[a] PEN_05[b]	30kW[a] PEN_06[b]	60kW[a] PEN_08[b]	60kW[a] PEN_09[b]	100kW[a] PEN_13[b]
Cl^-	0.0000 ± 0.0206	0.0000 ± 0.0214	0.1339 ± 0.0254	0.0000 ± 0.0487	0.0000 ± 0.0273	0.0000 ± 0.0057
NO_3^-	0.0645 ± 0.0165	0.1087 ± 0.0201	0.0000 ± 0.0195	0.0830 ± 0.0359	0.0000 ± 0.0273	0.0010 ± 0.0040
$SO_4^=$	1.4670 ± 0.1186	0.6917 ± 0.0590	1.3359 ± 0.1098	3.3264 ± 0.2696	1.0044 ± 0.0845	0.1609 ± 0.0140
NH_4^+	0.8287 ± 0.0625	0.5855 ± 0.0468	0.5149 ± 0.0458	1.2336 ± 0.1005	0.5036 ± 0.0450	0.0283 ± 0.0061
Na^+	0.0094 ± 0.0015	0.0076 ± 0.0015	0.0023 ± 0.0017	0.0241 ± 0.0036	0.0093 ± 0.0019	0.0001 ± 0.0003
K^+	0.0049 ± 0.0021	0.0021 ± 0.0022	0.0009 ± 0.0028	0.0109 ± 0.0050	0.0026 ± 0.0028	0.0000 ± 0.0006
OC1	27.6825 ± 8.9092	8.8072 ± 2.8627	5.0592 ± 1.6742	12.2451 ± 4.0175	8.0267 ± 2.6242	4.9740 ± 1.6046
OC2	13.0411 ± 1.9615	5.4899 ± 0.8328	12.4821 ± 1.8816	35.9626 ± 5.4071	9.8093 ± 1.4819	26.1624 ± 3.9149
OC3	6.8586 ± 0.9520	3.5901 ± 0.5131	4.0065 ± 0.5790	9.1008 ± 1.2926	3.9364 ± 0.5694	3.3083 ± 0.4548
OC4	2.4047 ± 0.6019	1.7517 ± 0.4395	1.6319 ± 0.4113	3.1959 ± 0.8042	1.9580 ± 0.4920	0.2674 ± 0.0678
OP	23.8736 ± 7.6362	0.0286 ± 0.0328	0.0214 ± 0.0411	1.1145 ± 0.3637	0.0000 ± 0.0402	0.0000 ± 0.0084
OC	73.8523 ± 7.4343	19.6590 ± 1.9979	23.1903 ± 2.3607	61.5998 ± 6.2432	23.7196 ± 2.4132	34.7099 ± 3.4880
EC1	8.0961 ± 1.5063	6.3157 ± 1.1750	7.5907 ± 1.4123	12.2170 ± 2.2740	6.2518 ± 1.1633	2.4962 ± 0.4643
EC2	23.9859 ± 8.8703	12.4843 ± 4.6168	12.7709 ± 4.7229	22.6597 ± 8.3808	13.3972 ± 4.9546	1.0326 ± 0.3819
EC3	0.0310 ± 0.0257	0.1040 ± 0.0809	0.0951 ± 0.0746	0.1658 ± 0.1301	0.1457 ± 0.1133	0.0316 ± 0.0246
EC	8.2394 ± 2.1208	18.8754 ± 4.8576	20.4353 ± 5.2593	33.9279 ± 8.7334	19.7947 ± 5.0944	3.5604 ± 0.9163
TC	82.0917 ± 7.3905	38.5343 ± 3.4781	43.6256 ± 3.9422	95.5278 ± 8.6325	43.5144 ± 3.9319	38.2703 ± 3.4398
Nac	0.0026 ± 0.0409	0.0000 ± 0.0323	0.0801 ± 0.0432	0.0202 ± 0.0741	0.0044 ± 0.0414	0.0415 ± 0.0119
Mgc	0.0111 ± 0.0452	0.0000 ± 0.0356	0.0099 ± 0.0460	0.0126 ± 0.0814	0.0000 ± 0.0455	0.0000 ± 0.0120
Al	0.0129 ± 0.0306	0.0066 ± 0.0242	0.0164 ± 0.0312	0.0503 ± 0.0553	0.0650 ± 0.0315	0.0025 ± 0.0081
Si	0.0314 ± 0.0143	0.0213 ± 0.0113	0.0993 ± 0.0165	0.0902 ± 0.0265	0.1588 ± 0.0190	0.0240 ± 0.0042
P	0.1582 ± 0.0117	0.0777 ± 0.0060	0.1974 ± 0.0144	0.1244 ± 0.0103	0.1531 ± 0.0113	0.0698 ± 0.0050
S	0.6406 ± 0.0457	0.5883 ± 0.0420	1.1526 ± 0.0822	1.1551 ± 0.0827	0.8169 ± 0.0583	0.1870 ± 0.0133
Cl	0.0044 ± 0.0021	0.0049 ± 0.0017	0.0045 ± 0.0022	0.1433 ± 0.0110	0.0109 ± 0.0023	0.0042 ± 0.0006
K	0.0118 ± 0.0016	0.0058 ± 0.0011	0.0130 ± 0.0016	0.0123 ± 0.0025	0.0179 ± 0.0018	0.0040 ± 0.0004
Ca	0.0534 ± 0.0046	0.0217 ± 0.0025	0.0679 ± 0.0055	0.0552 ± 0.0060	0.0835 ± 0.0065	0.1085 ± 0.0077
Sc	N/A ± N/A	N/A ± N/A	N/A ± N/A	N/A ± N/A	N/A ± N/A	N/A ± N/A
Ti	0.0058 ± 0.0015	0.0028 ± 0.0012	0.0012 ± 0.0015	0.0022 ± 0.0026	0.0017 ± 0.0015	0.0000 ± 0.0004
V	0.0008 ± 0.0005	0.0000 ± 0.0004	0.0008 ± 0.0006	0.0022 ± 0.0010	0.0000 ± 0.0006	0.0000 ± 0.0001
Cr	0.0005 ± 0.0023	0.0004 ± 0.0018	0.0014 ± 0.0023	0.0016 ± 0.0041	0.0014 ± 0.0023	0.0006 ± 0.0006
Mn	0.0023 ± 0.0065	0.0000 ± 0.0051	0.0000 ± 0.0066	0.0033 ± 0.0117	0.0069 ± 0.0066	0.0000 ± 0.0017
Fe	0.0259 ± 0.0099	0.0137 ± 0.0077	0.2268 ± 0.0191	0.1116 ± 0.0193	0.4151 ± 0.0313	0.0117 ± 0.0027
Co	0.0000 ± 0.0011	0.0000 ± 0.0009	0.0000 ± 0.0011	0.0000 ± 0.0020	0.0000 ± 0.0011	0.0000 ± 0.0003
Ni	0.0014 ± 0.0017	0.0000 ± 0.0014	0.0005 ± 0.0018	0.0008 ± 0.0031	0.0009 ± 0.0018	0.0000 ± 0.0005
Cu	0.0052 ± 0.0014	0.0005 ± 0.0011	0.0113 ± 0.0016	0.0036 ± 0.0025	0.0126 ± 0.0017	0.0025 ± 0.0004
Zn	0.0426 ± 0.0036	0.0183 ± 0.0020	0.0541 ± 0.0043	0.0342 ± 0.0041	0.0813 ± 0.0061	0.0828 ± 0.0059
Ga	0.0052 ± 0.0056	0.0030 ± 0.0044	0.0000 ± 0.0057	0.0000 ± 0.0100	0.0000 ± 0.0056	0.0000 ± 0.0015
As	0.0000 ± 0.0015	0.0000 ± 0.0012	0.0000 ± 0.0015	0.0000 ± 0.0026	0.0000 ± 0.0015	0.0000 ± 0.0004
Se	0.0000 ± 0.0013	0.0000 ± 0.0010	0.0000 ± 0.0013	0.0000 ± 0.0023	0.0000 ± 0.0013	0.0000 ± 0.0003
Br	0.0000 ± 0.0015	0.0008 ± 0.0012	0.0000 ± 0.0015	0.0044 ± 0.0027	0.0015 ± 0.0015	0.0010 ± 0.0004
Rb	0.0009 ± 0.0014	0.0000 ± 0.0011	0.0009 ± 0.0014	0.0008 ± 0.0025	0.0000 ± 0.0014	0.0000 ± 0.0004
Sr	0.0015 ± 0.0032	0.0005 ± 0.0025	0.0006 ± 0.0033	0.0011 ± 0.0058	0.0000 ± 0.0032	0.0005 ± 0.0009
Y	0.0000 ± 0.0021	0.0000 ± 0.0017	0.0001 ± 0.0021	0.0011 ± 0.0038	0.0000 ± 0.0021	0.0008 ± 0.0006
Zr	0.0000 ± 0.0044	0.0040 ± 0.0035	0.0009 ± 0.0045	0.0025 ± 0.0079	0.0009 ± 0.0044	0.0000 ± 0.0012
Nb	N/A ± N/A	N/A ± N/A	N/A ± N/A	N/A ± N/A	N/A ± N/A	N/A ± N/A
Mo	0.0000 ± 0.0046	0.0017 ± 0.0037	0.0000 ± 0.0047	0.0000 ± 0.0084	0.0000 ± 0.0047	0.0007 ± 0.0012
Pd	0.0064 ± 0.0063	0.0029 ± 0.0050	0.0014 ± 0.0064	0.0016 ± 0.0113	0.0032 ± 0.0063	0.0001 ± 0.0017
Ag	0.0000 ± 0.0048	0.0000 ± 0.0038	0.0009 ± 0.0049	0.0000 ± 0.0087	0.0000 ± 0.0049	0.0004 ± 0.0013
Cd	0.0055 ± 0.0054	0.0014 ± 0.0042	0.0014 ± 0.0055	0.0066 ± 0.0097	0.0009 ± 0.0054	0.0002 ± 0.0014
In	0.0000 ± 0.0055	0.0023 ± 0.0044	0.0002 ± 0.0056	0.0000 ± 0.0099	0.0011 ± 0.0056	0.0000 ± 0.0015
Sn	0.0000 ± 0.0062	0.0000 ± 0.0049	0.0057 ± 0.0063	0.0003 ± 0.0112	0.0000 ± 0.0063	0.0000 ± 0.0016
Sb	0.0000 ± 0.0080	0.0000 ± 0.0063	0.0068 ± 0.0082	0.0000 ± 0.0144	0.0000 ± 0.0080	0.0000 ± 0.0021

Table6-4. Continued

Chemical Species	10kW[a] PEN_04[b]	10kW[a] PEN_05[b]	30kW[a] PEN_06[b]	60kW[a] PEN_08[b]	60kW[a] PEN_09[b]	100kW[a] PEN_13[b]
Cs	N/A ± N/A	N/A ± N/A	N/A ± N/A	N/A ± N/A	N/A ± N/A	N/A ± N/A
Ba	0.0199 ± 0.0140	0.0000 ± 0.0110	0.0008 ± 0.0141	0.0170 ± 0.0251	0.0118 ± 0.0141	0.0031 ± 0.0037
La	0.0049 ± 0.0280	0.0085 ± 0.0222	0.0049 ± 0.0285	0.0000 ± 0.0504	0.0000 ± 0.0283	0.0000 ± 0.0074
Ce	N/A ± N/A	N/A ± N/A	N/A ± N/A	N/A ± N/A	N/A ± N/A	N/A ± N/A
Sm	N/A ± N/A	N/A ± N/A	N/A ± N/A	N/A ± N/A	N/A ± N/A	N/A ± N/A
Eu	N/A ± N/A	N/A ± N/A	N/A ± N/A	N/A ± N/A	N/A ± N/A	N/A ± N/A
Tb	N/A ± N/A	N/A ± N/A	N/A ± N/A	N/A ± N/A	N/A ± N/A	N/A ± N/A
Hf	N/A ± N/A	N/A ± N/A	N/A ± N/A	N/A ± N/A	N/A ± N/A	N/A ± N/A
Ta	N/A ± N/A	N/A ± N/A	N/A ± N/A	N/A ± N/A	N/A ± N/A	N/A ± N/A
W	N/A ± N/A	N/A ± N/A	N/A ± N/A	N/A ± N/A	N/A ± N/A	N/A ± N/A
Ir	N/A ± N/A	N/A ± N/A	N/A ± N/A	N/A ± N/A	N/A ± N/A	N/A ± N/A
Au	0.0032 ± 0.0063	0.0004 ± 0.0050	0.0023 ± 0.0064	0.0000 ± 0.0113	0.0101 ± 0.0064	0.0018 ± 0.0017
Hg	0.0000 ± 0.0024	0.0000 ± 0.0019	0.0000 ± 0.0024	0.0000 ± 0.0043	0.0000 ± 0.0024	0.0000 ± 0.0006
Tl	0.0000 ± 0.0048	0.0000 ± 0.0038	0.0000 ± 0.0049	0.0011 ± 0.0087	0.0000 ± 0.0049	0.0002 ± 0.0013
Pb	0.0024 ± 0.0046	0.0196 ± 0.0039	0.0066 ± 0.0048	0.0000 ± 0.0084	0.0034 ± 0.0047	0.0009 ± 0.0012
U	0.0021 ± 0.0062	0.0000 ± 0.0049	0.0003 ± 0.0063	0.0000 ± 0.0112	0.0003 ± 0.0063	0.0008 ± 0.0016
PAH	0.0282 ± 0.0006	0.0312 ± 0.0006	0.0090 ± 0.0002	0.0155 ± 0.0003	0.0104 ± 0.0003	0.0081 ± 0.0002
n-alkanes	1.9227 ± 0.0459	0.2383 ± 0.0055	0.5472 ± 0.0099	1.1209 ± 0.0253	0.4031 ± 0.0073	0.0359 ± 0.0010
iso/anteiso-alkanes	0.0000 ± 0.0000	0.0000 ± 0.0000	0.0000 ± 0.0000	0.0000 ± 0.0000	0.0000 ± 0.0000	0.0000 ± 0.0000
hopanes	0.1546 ± 0.0037	0.0171 ± 0.0004	0.1964 ± 0.0047	0.2263 ± 0.0051	0.1127 ± 0.0027	0.0116 ± 0.0005
steranes	0.0718 ± 0.0018	0.0087 ± 0.0002	0.0736 ± 0.0019	0.1414 ± 0.0035	0.0482 ± 0.0012	0.0089 ± 0.0002
mehtyl-alkanes	0.0263 ± 0.0013	0.0010 ± 0.0001	0.0029 ± 0.0002	0.0018 ± 0.0001	0.0005 ± 0.0000	0.0007 ± 0.0000
branched alkanes	0.0906 ± 0.0044	0.0043 ± 0.0002	0.0263 ± 0.0014	0.0263 ± 0.0012	0.0050 ± 0.0002	0.0060 ± 0.0003
cyclo-alkanes	0.0413 ± 0.0018	0.0088 ± 0.0004	0.0193 ± 0.0009	0.0426 ± 0.0020	0.0109 ± 0.0005	0.0063 ± 0.0003
alkenes	0.0073 ± 0.0005	0.0004 ± 0.0000	0.0043 ± 0.0003	0.0023 ± 0.0002	0.0007 ± 0.0001	0.0012 ± 0.0001
phthalates	0.0147 ± 0.0006	0.1458 ± 0.0081	0.0162 ± 0.0006	0.0047 ± 0.0002	0.0020 ± 0.0001	0.0036 ± 0.0002
SO_2	21.0205 ± 1.5169	7.5790 ± 0.5466	34.0602 ± 2.4571	55.5407 ± 4.0156	24.0572 ± 1.7355	2.5221 ± 0.1818
NH_3	0.0808 ± 0.0862	0.0000 ± 0.0681	0.0832 ± 0.0879	0.1235 ± 0.1554	0.0347 ± 0.0870	0.0134 ± 0.0182

[a] Generator Size

[b] See Table 6-1 for Mnemonic ID definitions

[c] Quantitative

Table 6-5. Summary of the $PM_{2.5}$ source profiles for the four emission tests conducted for the 13 diesel generators using cold start.

Chemical Species	10kW[a] PEN_14[b]	30kW[a] PEN_11[b]	60kW[a] PEN_10[b]	100kW[a] PEN_12[b]
Cl^-	0.0000 ± 0.0719	0.0000 ± 0.0986	0.0000 ± 0.2874	0.0000 ± 0.0433
NO_3^-	0.0000 ± 0.0719	0.0000 ± 0.0986	0.0000 ± 0.2874	0.0000 ± 0.0433
$SO_4^=$	0.2771 ± 0.0753	0.3979 ± 0.1037	1.1525 ± 0.3043	0.0000 ± 0.0433
NH_4^+	0.1816 ± 0.0731	0.2531 ± 0.1003	0.7000 ± 0.2927	0.0738 ± 0.0436
Na^+	0.0000 ± 0.0044	0.0000 ± 0.0060	0.0000 ± 0.0174	0.0000 ± 0.0026
K^+	0.0000 ± 0.0072	0.0011 ± 0.0100	0.0000 ± 0.0290	0.0000 ± 0.0044
OC1	32.0702 ± 10.4163	22.5853 ± 7.4309	62.8788 ± 20.8131	8.3627 ± 2.7633
OC2	8.6836 ± 1.3432	14.6149 ± 2.2491	33.7482 ± 5.3456	6.8230 ± 1.0457
OC3	9.3755 ± 1.3713	9.9868 ± 1.5095	27.7595 ± 4.3211	4.0327 ± 0.6161
OC4	5.4717 ± 1.3747	3.5481 ± 0.9092	10.1768 ± 2.6305	1.1012 ± 0.2887
OP	5.2454 ± 1.6816	7.4883 ± 2.4011	18.0955 ± 5.8366	0.5942 ± 0.2005
OC	60.8181 ± 6.2096	58.1845 ± 6.0085	152.5449 ± 16.5601	20.8967 ± 2.1614
EC1	6.6913 ± 1.2483	8.0271 ± 1.4999	22.0646 ± 4.1859	2.3063 ± 0.4318
EC2	6.8507 ± 2.5360	9.3015 ± 3.4441	17.5541 ± 6.5315	5.9731 ± 2.2099
EC3	0.3487 ± 0.2715	0.3170 ± 0.2492	0.5219 ± 0.4251	0.0056 ± 0.0203
EC	8.6454 ± 2.2295	10.1573 ± 2.6223	22.0455 ± 5.7458	7.6908 ± 1.9809
TC	69.4634 ± 6.3364	68.3418 ± 6.3020	174.5904 ± 17.1235	28.5875 ± 2.6221
Na[c]	0.0408 ± 0.1096	0.0000 ± 0.1469	0.3327 ± 0.4411	0.0019 ± 0.0656
Mg[c]	0.0000 ± 0.1197	0.0022 ± 0.1647	0.0000 ± 0.4790	0.0000 ± 0.0722
Al	0.0101 ± 0.0814	0.0371 ± 0.1117	0.1325 ± 0.3259	0.0046 ± 0.0490
Si	0.0315 ± 0.0374	0.0333 ± 0.0511	0.3392 ± 0.1530	0.0117 ± 0.0224
P	0.0420 ± 0.0082	0.0909 ± 0.0123	0.0808 ± 0.0310	0.0669 ± 0.0067
S	0.2716 ± 0.0206	0.5420 ± 0.0402	0.5960 ± 0.0537	0.1889 ± 0.0141
Cl	0.0105 ± 0.0057	0.0177 ± 0.0078	0.0000 ± 0.0223	0.0122 ± 0.0035
K	0.0121 ± 0.0036	0.0067 ± 0.0048	0.0242 ± 0.0140	0.0073 ± 0.0022
Ca	0.0914 ± 0.0093	0.0970 ± 0.0115	0.1857 ± 0.0302	0.0418 ± 0.0050
Sc	N/A ± N/A	N/A ± N/A	N/A ± N/A	N/A ± N/A
Ti	0.0008 ± 0.0039	0.0028 ± 0.0053	0.0032 ± 0.0155	0.0005 ± 0.0023
V	0.0000 ± 0.0015	0.0000 ± 0.0020	0.0000 ± 0.0059	0.0005 ± 0.0009
Cr	0.0024 ± 0.0061	0.0000 ± 0.0083	0.0000 ± 0.0242	0.0007 ± 0.0036
Mn	0.0036 ± 0.0172	0.0033 ± 0.0236	0.0145 ± 0.0688	0.0029 ± 0.0104
Fe	0.0461 ± 0.0261	0.0865 ± 0.0360	0.6299 ± 0.1154	0.0219 ± 0.0156
Co	0.0000 ± 0.0029	0.0000 ± 0.0040	0.0016 ± 0.0116	0.0000 ± 0.0017
Ni	0.0012 ± 0.0046	0.0017 ± 0.0063	0.0097 ± 0.0184	0.0007 ± 0.0028
Cu	0.0077 ± 0.0037	0.0056 ± 0.0050	0.0258 ± 0.0147	0.0024 ± 0.0022
Zn	0.0614 ± 0.0066	0.0676 ± 0.0083	0.0856 ± 0.0207	0.0866 ± 0.0069
Ga	0.0000 ± 0.0148	0.0022 ± 0.0203	0.0646 ± 0.0596	0.0053 ± 0.0089
As	0.0000 ± 0.0039	0.0000 ± 0.0053	0.0000 ± 0.0155	0.0000 ± 0.0023
Se	0.0000 ± 0.0034	0.0000 ± 0.0047	0.0000 ± 0.0136	0.0000 ± 0.0020
Br	0.0000 ± 0.0039	0.0022 ± 0.0053	0.0113 ± 0.0156	0.0000 ± 0.0023
Rb	0.0036 ± 0.0036	0.0000 ± 0.0050	0.0145 ± 0.0146	0.0000 ± 0.0022
Sr	0.0000 ± 0.0086	0.0006 ± 0.0117	0.0000 ± 0.0342	0.0010 ± 0.0052
Y	0.0000 ± 0.0056	0.0088 ± 0.0077	0.0065 ± 0.0223	0.0002 ± 0.0034
Zr	0.0000 ± 0.0116	0.0000 ± 0.0160	0.0097 ± 0.0465	0.0000 ± 0.0070
Nb	N/A ± N/A	N/A ± N/A	N/A ± N/A	N/A ± N/A
Mo	0.0057 ± 0.0124	0.0061 ± 0.0170	0.0129 ± 0.0495	0.0027 ± 0.0074
Pd	0.0000 ± 0.0167	0.0000 ± 0.0229	0.0000 ± 0.0668	0.0000 ± 0.0101
Ag	0.0012 ± 0.0129	0.0000 ± 0.0176	0.0145 ± 0.0514	0.0029 ± 0.0077
Cd	0.0000 ± 0.0143	0.0017 ± 0.0196	0.0000 ± 0.0571	0.0015 ± 0.0086
In	0.0000 ± 0.0147	0.0000 ± 0.0201	0.0985 ± 0.0594	0.0000 ± 0.0088
Sn	0.0000 ± 0.0165	0.0000 ± 0.0226	0.0161 ± 0.0660	0.0000 ± 0.0099
Sb	0.0000 ± 0.0212	0.0000 ± 0.0291	0.0081 ± 0.0849	0.0000 ± 0.0128

Table 6-5. Continued.

Chemical Species	10kW[a] PEN_14[b]	30kW[a] PEN_11[b]	60kW[a] PEN_10[b]	100kW[a] PEN_12[b]
Cs	N/A ± N/A	N/A ± N/A	N/A ± N/A	N/A ± N/A
Ba	0.0000 ± 0.0369	0.0000 ± 0.0506	0.0420 ± 0.1479	0.0019 ± 0.0223
La	0.0263 ± 0.0747	0.0000 ± 0.1020	0.0000 ± 0.2972	0.0267 ± 0.0450
Ce	N/A ± N/A	N/A ± N/A	N/A ± N/A	N/A ± N/A
Sm	N/A ± N/A	N/A ± N/A	N/A ± N/A	N/A ± N/A
Eu	N/A ± N/A	N/A ± N/A	N/A ± N/A	N/A ± N/A
Tb	N/A ± N/A	N/A ± N/A	N/A ± N/A	N/A ± N/A
Hf	N/A ± N/A	N/A ± N/A	N/A ± N/A	N/A ± N/A
Ta	N/A ± N/A	N/A ± N/A	N/A ± N/A	N/A ± N/A
W	N/A ± N/A	N/A ± N/A	N/A ± N/A	N/A ± N/A
Ir	N/A ± N/A	N/A ± N/A	N/A ± N/A	N/A ± N/A
Au	0.0073 ± 0.0167	0.0266 ± 0.0230	0.0242 ± 0.0668	0.0000 ± 0.0101
Hg	0.0000 ± 0.0063	0.0000 ± 0.0087	0.0000 ± 0.0252	0.0000 ± 0.0038
Tl	0.0028 ± 0.0129	0.0105 ± 0.0176	0.0000 ± 0.0514	0.0039 ± 0.0077
Pb	0.0101 ± 0.0124	0.0072 ± 0.0170	0.0210 ± 0.0495	0.0061 ± 0.0075
U	0.0105 ± 0.0165	0.0000 ± 0.0226	0.0000 ± 0.0659	0.0019 ± 0.0099
PAH	0.0294 ± 0.0005	0.0309 ± 0.0006	0.0588 ± 0.0013	0.2124 ± 0.0043
n-alkanes	0.2156 ± 0.0047	0.5713 ± 0.0163	3.1757 ± 0.0829	0.2977 ± 0.0052
iso/anteiso-alkanes	0.0000 ± 0.0000	0.0000 ± 0.0000	0.0000 ± 0.0000	0.0000 ± 0.0000
hopanes	0.0499 ± 0.0014	0.0968 ± 0.0027	0.2809 ± 0.0082	0.0672 ± 0.0017
steranes	0.0118 ± 0.0003	0.1048 ± 0.0026	0.1848 ± 0.0051	0.0315 ± 0.0008
mehtyl-alkanes	0.0148 ± 0.0010	0.0088 ± 0.0006	0.0386 ± 0.0021	0.0012 ± 0.0001
branched alkanes	0.0623 ± 0.0033	0.0161 ± 0.0008	0.0787 ± 0.0047	0.0084 ± 0.0004
cyclo-alkanes	0.0124 ± 0.0007	0.0212 ± 0.0009	0.1202 ± 0.0062	0.0183 ± 0.0009
alkenes	0.0004 ± 0.0000	0.0016 ± 0.0001	0.0099 ± 0.0008	0.0012 ± 0.0001
phthalates	0.0483 ± 0.0021	0.3644 ± 0.0200	1.0456 ± 0.0656	0.0191 ± 0.0007
SO_2	20.0495 ± 1.4555	60.2045 ± 4.3968	82.0573 ± 6.5564	2.2493 ± 0.1636
NH_3	0.0000 ± 0.2292	0.1120 ± 0.3144	0.0000 ± 0.9160	0.0000 ± 0.1379

[a] Generator Size
[b] See Table 6-1 for Mnemonic ID definitions
[c] Quantitative

Table 6-6. Summary of the $PM_{2.5}$ source profiles from ten emission tests of medium tactical vehicle replacements (MTVRs).

Chemical Species	MTVR #1Driving Cycle #1[a] TNP_04[b]	MTVR #1Driving Cycle #1 TNP_05	MTVR #1Driving Cycle #1 TNP_06	MTVR #1Driving Cycle #1 TNP_07	MTVR #1Driving Cycle #1 TNP_08	MTVR #1Driving Cycle #2 TNP_09	MTVR #2 Driving Cycle #1 TNP_10	MTVR #2 Driving Cycle #1 TNP_11	MTVR #2 Driving Cycle #1 TNP_12	MTVR #2 Driving Cycle #2 TNP_13
Cl^-	0.0904 ± 0.2041	0.0000 ± 0.3943	0.0000 ± 0.2865	0.0000 ± 0.4517	0.0000 ± 0.4106	0.0489 ± 0.2384	0.0000 ± 0.4909	0.0000 ± 0.5701	0.0000 ± 0.5067	0.0000 ± 0.5038
NO_3^-	0.1545 ± 0.0988	0.2426 ± 0.3979	0.2297 ± 0.2903	0.2951 ± 0.4562	0.2805 ± 0.4149	0.2029 ± 0.2211	0.3811 ± 0.4974	0.3217 ± 0.5748	0.3031 ± 0.5112	0.3869 ± 0.5105
$SO_4^=$	0.5166 ± 0.1032	0.8851 ± 0.4031	0.8582 ± 0.2963	0.9353 ± 0.4610	0.9633 ± 0.4207	1.0604 ± 0.2351	1.7973 ± 0.5220	1.1634 ± 0.5839	1.5843 ± 0.5323	1.1094 ± 0.5162
NH_4^+	0.0467 ± 0.0957	0.0982 ± 0.3993	0.1248 ± 0.2906	0.0569 ± 0.4569	0.1144 ± 0.4158	0.2118 ± 0.2221	0.2617 ± 0.4986	0.1153 ± 0.5769	0.3712 ± 0.5163	0.0826 ± 0.5097
Na^+	0.0023 ± 0.0061	0.0011 ± 0.0250	0.0008 ± 0.0182	0.0000 ± 0.0284	0.0046 ± 0.0262	0.0191 ± 0.0150	0.0000 ± 0.0307	0.0000 ± 0.0359	0.0000 ± 0.0319	0.0143 ± 0.0326
K^+	0.0084 ± 0.0097	0.0268 ± 0.0402	0.0194 ± 0.0292	0.0230 ± 0.0459	0.0314 ± 0.0420	0.0332 ± 0.0230	0.0187 ± 0.0498	0.0290 ± 0.0579	0.0279 ± 0.0515	0.0470 ± 0.0518
OC1	111.9631 ± 25.9309	24.9629 ± 6.3590	32.7167 ± 7.9691	31.6682 ± 8.0551	27.0488 ± 6.8798	13.9131 ± 3.4929	24.2092 ± 6.3490	23.4814 ± 6.3707	27.9218 ± 7.2899	26.3694 ± 6.8997
OC2	11.4291 ± 2.3816	20.6151 ± 4.5502	16.5840 ± 3.5954	13.1280 ± 3.0751	17.0326 ± 3.8280	7.3137 ± 1.6441	13.1695 ± 3.1201	25.3430 ± 5.8174	16.7837 ± 3.9062	20.2063 ± 4.6060
OC3	7.7206 ± 1.3526	12.5403 ± 2.9554	11.5903 ± 2.4381	13.7349 ± 3.3314	11.3899 ± 2.8834	8.8168 ± 1.8403	11.9873 ± 3.2810	15.8932 ± 4.0974	17.5182 ± 4.0395	12.2414 ± 3.3714
OC4	3.3763 ± 0.7722	4.2189 ± 1.2462	4.4739 ± 1.1588	5.1215 ± 1.4852	3.9548 ± 1.2239	3.5019 ± 0.8962	5.6070 ± 1.6224	4.9252 ± 1.6282	7.3052 ± 1.9717	4.2158 ± 1.4065
OP	0.0000 ± 0.1388	0.0000 ± 0.5805	0.0000 ± 0.4217	0.0000 ± 0.6649	0.0000 ± 0.6044	0.0000 ± 0.3199	0.0000 ± 0.7226	0.0000 ± 0.8392	0.0000 ± 0.7458	0.0000 ± 0.7416
OC	134.1394 ± 15.0775	60.8751 ± 8.2601	64.3032 ± 8.0321	61.9779 ± 8.7668	57.9033 ± 8.0265	32.7397 ± 4.2458	53.1530 ± 7.9447	67.5299 ± 10.3303	67.6504 ± 9.8342	61.1657 ± 8.9926
EC1	6.4478 ± 1.4169	11.8052 ± 2.6845	6.0618 ± 1.3813	12.8374 ± 2.9459	10.5857 ± 2.4227	21.8228 ± 4.8170	21.4526 ± 4.8863	10.1722 ± 2.4303	15.8866 ± 3.6676	10.6625 ± 2.4880
EC2	14.9566 ± 2.1278	48.6224 ± 7.3113	38.7469 ± 5.6733	52.1262 ± 7.9775	56.9061 ± 8.5905	28.2363 ± 4.0773	40.3832 ± 6.2116	48.5373 ± 7.7754	39.8638 ± 6.2399	55.5617 ± 8.6098
EC3	0.0799 ± 0.0438	0.0000 ± 0.1814	0.0620 ± 0.1319	0.0000 ± 0.2078	0.1324 ± 0.1892	0.0793 ± 0.1002	0.0000 ± 0.2258	0.0000 ± 0.2622	0.6284 ± 0.2407	0.0271 ± 0.2318
EC	21.4843 ± 4.9304	60.4282 ± 14.1791	44.8706 ± 10.4176	64.9636 ± 15.3557	67.6243 ± 15.8948	50.1384 ± 11.5686	61.8357 ± 14.6347	58.7095 ± 14.1553	56.3781 ± 13.4465	66.2513 ± 15.7444
TC	155.6239 ± 20.5759	121.3033 ± 17.7237	109.1738 ± 15.3364	126.9414 ± 18.9960	125.5275 ± 18.4357	82.8782 ± 11.4649	114.9887 ± 17.4853	126.2393 ± 20.1131	124.0285 ± 19.1214	127.4170 ± 19.4537
Na^c	0.0490 ± 0.2779	0.0000 ± 1.2592	0.0000 ± 0.9127	0.0000 ± 1.4277	0.0992 ± 1.3034	0.0000 ± 0.6809	0.0000 ± 1.4484	0.0000 ± 1.8386	0.0000 ± 1.6256	0.0000 ± 1.5549
Mg^{ac}	0.0000 ± 0.1444	0.0000 ± 0.6577	0.1631 ± 0.4814	0.2942 ± 0.7533	0.0158 ± 0.6789	0.2366 ± 0.3571	0.2207 ± 0.7636	0.0138 ± 0.9654	0.0548 ± 0.8560	0.0000 ± 0.8157
Al	0.0352 ± 0.0241	0.0000 ± 0.1082	0.0000 ± 0.0788	0.0562 ± 0.1242	0.0331 ± 0.1121	0.5445 ± 0.0731	0.0000 ± 0.1255	0.0000 ± 0.1589	0.1221 ± 0.1417	0.0804 ± 0.1349
Si	0.1035 ± 0.0280	0.0000 ± 0.1216	0.1181 ± 0.0896	0.0843 ± 0.1392	0.0777 ± 0.1257	1.2887 ± 0.1202	0.2125 ± 0.1427	0.0743 ± 0.1786	0.1008 ± 0.1584	0.1912 ± 0.1523
P	0.0196 ± 0.0078	0.0283 ± 0.0351	0.0038 ± 0.0256	0.0000 ± 0.0400	0.0261 ± 0.0362	0.0201 ± 0.0190	0.1105 ± 0.0418	0.0000 ± 0.0514	0.0852 ± 0.0463	0.0333 ± 0.0435
S	0.2590 ± 0.0316	0.6136 ± 0.1262	0.5527 ± 0.0949	0.6944 ± 0.1454	0.5864 ± 0.1289	0.6180 ± 0.0783	0.8677 ± 0.1552	0.8055 ± 0.1871	0.8960 ± 0.1723	0.7453 ± 0.1584
Cl	0.0186 ± 0.0054	0.0034 ± 0.0239	0.0101 ± 0.0175	0.0039 ± 0.0273	0.0450 ± 0.0249	0.0054 ± 0.0129	0.0117 ± 0.0277	0.0225 ± 0.0351	0.0257 ± 0.0311	0.0532 ± 0.0300
K	0.0249 ± 0.0052	0.0127 ± 0.0224	0.0174 ± 0.0164	0.0000 ± 0.0256	0.0439 ± 0.0234	0.1869 ± 0.0187	0.0147 ± 0.0260	0.0306 ± 0.0330	0.0252 ± 0.0292	0.9065 ± 0.0903
Ca	0.0632 ± 0.0075	0.0946 ± 0.0281	0.0909 ± 0.0209	0.1013 ± 0.0321	0.1307 ± 0.0300	0.4317 ± 0.0359	0.2530 ± 0.0391	0.1432 ± 0.0421	0.2559 ± 0.0431	0.1747 ± 0.0372
Sc	0.0038 ± 0.0193	0.0179 ± 0.0879	0.0272 ± 0.0642	0.0119 ± 0.1004	0.0015 ± 0.0907	0.0020 ± 0.0475	0.0251 ± 0.1019	0.0055 ± 0.1290	0.0078 ± 0.1143	0.0000 ± 0.1090
Ti	0.0065 ± 0.0036	0.0049 ± 0.0164	0.0003 ± 0.0119	0.0089 ± 0.0187	0.0058 ± 0.0169	0.0401 ± 0.0093	0.0000 ± 0.0190	0.0083 ± 0.0240	0.0000 ± 0.0213	0.0088 ± 0.0203
V	0.0000 ± 0.0006	0.0000 ± 0.0027	0.0000 ± 0.0019	0.0000 ± 0.0030	0.0000 ± 0.0027	0.0020 ± 0.0014	0.0000 ± 0.0031	0.0000 ± 0.0039	0.0000 ± 0.0035	0.0000 ± 0.0033
Cr	0.0006 ± 0.0033	0.0000 ± 0.0148	0.0000 ± 0.0109	0.0000 ± 0.0170	0.0000 ± 0.0153	0.0000 ± 0.0080	0.0012 ± 0.0172	0.0000 ± 0.0218	0.0000 ± 0.0193	0.0000 ± 0.0184
Mn	0.0050 ± 0.0088	0.0026 ± 0.0400	0.0000 ± 0.0293	0.0515 ± 0.0460	0.0396 ± 0.0415	0.0268 ± 0.0217	0.0393 ± 0.0466	0.0115 ± 0.0588	0.0402 ± 0.0522	0.0245 ± 0.0497
Fe	0.0829 ± 0.0171	0.0443 ± 0.0729	0.0253 ± 0.0532	0.0856 ± 0.0838	0.1188 ± 0.0761	0.5394 ± 0.0569	1.3790 ± 0.1520	0.1284 ± 0.1080	0.5780 ± 0.1102	0.2388 ± 0.0933
Co	0.0000 ± 0.0003	0.0000 ± 0.0015	0.0000 ± 0.0011	0.0000 ± 0.0017	0.0000 ± 0.0015	0.0000 ± 0.0008	0.0000 ± 0.0017	0.0000 ± 0.0022	0.0000 ± 0.0020	0.0000 ± 0.0019
Ni	0.0019 ± 0.0017	0.0000 ± 0.0075	0.0008 ± 0.0055	0.0000 ± 0.0086	0.0050 ± 0.0078	0.0099 ± 0.0041	0.0038 ± 0.0087	0.0005 ± 0.0110	0.0198 ± 0.0100	0.0060 ± 0.0093
Cu	0.0000 ± 0.0029	0.0000 ± 0.0133	0.0000 ± 0.0098	0.0000 ± 0.0152	0.0000 ± 0.0138	0.1063 ± 0.0109	0.0518 ± 0.0162	0.0000 ± 0.0196	0.0776 ± 0.0189	0.1053 ± 0.0193
Zn	0.0032 ± 0.0029	0.0108 ± 0.0134	0.0150 ± 0.0098	0.0234 ± 0.0154	0.0366 ± 0.0141	0.0658 ± 0.0089	0.1249 ± 0.0196	0.0356 ± 0.0199	0.1255 ± 0.0216	0.1317 ± 0.0211
Ga	0.0019 ± 0.0105	0.0000 ± 0.0476	0.0057 ± 0.0348	0.0251 ± 0.0545	0.0000 ± 0.0492	0.0000 ± 0.0258	0.0358 ± 0.0553	0.0399 ± 0.0700	0.0411 ± 0.0621	0.0000 ± 0.0591
As	0.0000 ± 0.0003	0.0000 ± 0.0015	0.0000 ± 0.0011	0.0000 ± 0.0017	0.0000 ± 0.0015	0.0000 ± 0.0008	0.0000 ± 0.0017	0.0000 ± 0.0022	0.0000 ± 0.0020	0.0000 ± 0.0019
Se	0.0014 ± 0.0069	0.0182 ± 0.0313	0.0000 ± 0.0229	0.0000 ± 0.0358	0.0134 ± 0.0323	0.0000 ± 0.0169	0.0073 ± 0.0363	0.0038 ± 0.0459	0.0000 ± 0.0407	0.0000 ± 0.0388
Br	0.0018 ± 0.0049	0.0045 ± 0.0224	0.0011 ± 0.0163	0.0043 ± 0.0256	0.0092 ± 0.0231	0.0069 ± 0.0121	0.0035 ± 0.0259	0.0033 ± 0.0328	0.0029 ± 0.0291	0.0000 ± 0.0277
Rb	0.0000 ± 0.0036	0.0000 ± 0.0163	0.0000 ± 0.0119	0.0030 ± 0.0187	0.0000 ± 0.0169	0.0010 ± 0.0088	0.0091 ± 0.0190	0.0000 ± 0.0240	0.0000 ± 0.0213	0.0033 ± 0.0203
Sr	0.0043 ± 0.0066	0.0000 ± 0.0298	0.0011 ± 0.0218	0.0000 ± 0.0340	0.0000 ± 0.0307	0.0230 ± 0.0162	0.0130 ± 0.0346	0.0000 ± 0.0437	0.0000 ± 0.0388	0.0148 ± 0.0370
Y	0.0017 ± 0.0049	0.0000 ± 0.0224	0.0000 ± 0.0163	0.0000 ± 0.0256	0.0027 ± 0.0231	0.0054 ± 0.0121	0.0000 ± 0.0259	0.0116 ± 0.0328	0.0015 ± 0.0291	0.0014 ± 0.0277
Zr	0.0007 ± 0.0115	0.0011 ± 0.0521	0.0000 ± 0.0381	0.0000 ± 0.0596	0.0173 ± 0.0538	0.0062 ± 0.0282	0.0341 ± 0.0605	0.0000 ± 0.0765	0.0000 ± 0.0678	0.0000 ± 0.0647

Table 6-6. Continued

Chemical Species	MTVR #1Driving Cycle #1[a] TNP_04[b]	MTVR #1Driving Cycle #1 TNP_05	MTVR #1Driving Cycle #1 TNP_06	MTVR #1Driving Cycle #1 TNP_07	MTVR #1Driving Cycle #1 TNP_08	MTVR #1Driving Cycle #2 TNP_09	MTVR #2 Driving Cycle #1 TNP_10	MTVR #2 Driving Cycle #1 TNP_11	MTVR #2 Driving Cycle #1 TNP_12	MTVR #2 Driving Cycle #2 TNP_13
Nb	0.0002 ± 0.0088	0.0000 ± 0.0402	0.0000 ± 0.0294	0.0000 ± 0.0460	0.0000 ± 0.0415	0.0000 ± 0.0217	0.0000 ± 0.0466	0.0000 ± 0.0590	0.0000 ± 0.0523	0.0000 ± 0.0499
Mo	0.0022 ± 0.0078	0.0000 ± 0.0357	0.0000 ± 0.0261	0.0004 ± 0.0408	0.0034 ± 0.0369	0.0000 ± 0.0193	0.0609 ± 0.0418	0.0000 ± 0.0524	0.0537 ± 0.0467	0.0000 ± 0.0443
Pd	0.0000 ± 0.0151	0.0000 ± 0.0689	0.0082 ± 0.0503	0.0000 ± 0.0787	0.0000 ± 0.0711	0.0000 ± 0.0372	0.0000 ± 0.0798	0.0000 ± 0.1011	0.0000 ± 0.0896	0.0000 ± 0.0854
Ag	0.0000 ± 0.0152	0.0000 ± 0.0690	0.0000 ± 0.0504	0.0000 ± 0.0789	0.0000 ± 0.0713	0.0000 ± 0.0373	0.0000 ± 0.0800	0.0000 ± 0.1013	0.0000 ± 0.0898	0.0000 ± 0.0856
Cd	0.0079 ± 0.0173	0.0000 ± 0.0781	0.0000 ± 0.0574	0.0000 ± 0.0893	0.0193 ± 0.0811	0.0000 ± 0.0425	0.0225 ± 0.0911	0.0022 ± 0.1153	0.0127 ± 0.1022	0.0000 ± 0.0969
In	0.0116 ± 0.0103	0.0127 ± 0.0462	0.0103 ± 0.0338	0.0000 ± 0.0528	0.0000 ± 0.0477	0.0000 ± 0.0250	0.0000 ± 0.0536	0.0000 ± 0.0679	0.0097 ± 0.0601	0.0000 ± 0.0573
Sn	0.0166 ± 0.0138	0.0943 ± 0.0630	0.0000 ± 0.0454	0.1196 ± 0.0722	0.0381 ± 0.0646	0.0167 ± 0.0338	0.0471 ± 0.0726	0.0000 ± 0.0912	0.1081 ± 0.0819	0.0365 ± 0.0776
Sb	0.0000 ± 0.0242	0.0075 ± 0.1102	0.0000 ± 0.0805	0.0000 ± 0.1260	0.0062 ± 0.1138	0.0254 ± 0.0596	0.0000 ± 0.1278	0.0000 ± 0.1618	0.0572 ± 0.1435	0.0000 ± 0.1367
Cs	0.0000 ± 0.0039	0.0000 ± 0.0179	0.0030 ± 0.0130	0.0000 ± 0.0204	0.0027 ± 0.0184	0.0000 ± 0.0097	0.0000 ± 0.0207	0.0083 ± 0.0262	0.0000 ± 0.0232	0.0042 ± 0.0221
Ba	0.0000 ± 0.0042	0.0000 ± 0.0192	0.0000 ± 0.0140	0.0000 ± 0.0220	0.0000 ± 0.0198	0.0000 ± 0.0104	0.0000 ± 0.0223	0.0000 ± 0.0282	0.0000 ± 0.0250	0.0000 ± 0.0238
La	0.0000 ± 0.0029	0.0000 ± 0.0133	0.0000 ± 0.0098	0.0000 ± 0.0152	0.0027 ± 0.0138	0.0000 ± 0.0072	0.0022 ± 0.0155	0.0049 ± 0.0196	0.0000 ± 0.0174	0.0051 ± 0.0166
Ce	0.0005 ± 0.0043	0.0000 ± 0.0194	0.0076 ± 0.0142	0.0145 ± 0.0222	0.0070 ± 0.0200	0.0000 ± 0.0105	0.0138 ± 0.0225	0.0077 ± 0.0284	0.0155 ± 0.0252	0.0000 ± 0.0240
Sm	0.0000 ± 0.0059	0.0000 ± 0.0269	0.0000 ± 0.0196	0.0098 ± 0.0307	0.0000 ± 0.0277	0.0000 ± 0.0145	0.0000 ± 0.0312	0.0000 ± 0.0394	0.0063 ± 0.0350	0.0134 ± 0.0334
Eu	0.0000 ± 0.0214	0.0000 ± 0.0974	0.0000 ± 0.0711	0.0000 ± 0.1113	0.0000 ± 0.1005	0.0000 ± 0.0526	0.0000 ± 0.1129	0.0000 ± 0.1429	0.0000 ± 0.1266	0.0000 ± 0.1208
Tb	0.0000 ± 0.0072	0.0074 ± 0.0328	0.0000 ± 0.0242	0.0000 ± 0.0375	0.0000 ± 0.0338	0.0000 ± 0.0177	0.0000 ± 0.0384	0.0011 ± 0.0481	0.0000 ± 0.0427	0.0000 ± 0.0407
Hf	0.0079 ± 0.0467	0.0000 ± 0.2118	0.0253 ± 0.1553	0.0000 ± 0.2425	0.0000 ± 0.2190	0.0000 ± 0.1145	0.0000 ± 0.2455	0.0000 ± 0.3115	0.0000 ± 0.2755	0.0000 ± 0.2632
Ta	0.0211 ± 0.0392	0.0000 ± 0.1776	0.0245 ± 0.1298	0.0801 ± 0.2036	0.0000 ± 0.1833	0.0286 ± 0.0962	0.0700 ± 0.2065	0.0000 ± 0.2607	0.0000 ± 0.2320	0.0934 ± 0.2210
W	0.0000 ± 0.0561	0.0000 ± 0.2552	0.0000 ± 0.1865	0.0000 ± 0.2917	0.0062 ± 0.2639	0.0193 ± 0.1382	0.1253 ± 0.2966	0.0000 ± 0.3752	0.0000 ± 0.3320	0.0000 ± 0.3161
Ir	0.0042 ± 0.0122	0.0026 ± 0.0553	0.0000 ± 0.0404	0.0000 ± 0.0632	0.0000 ± 0.0571	0.0111 ± 0.0299	0.0000 ± 0.0641	0.0000 ± 0.0817	0.0034 ± 0.0719	0.0000 ± 0.0686
Au	0.0000 ± 0.0260	0.0429 ± 0.1183	0.0000 ± 0.0861	0.0000 ± 0.1347	0.0000 ± 0.1217	0.0308 ± 0.0640	0.0411 ± 0.1367	0.0000 ± 0.1736	0.0093 ± 0.1533	0.0319 ± 0.1462
Hg	0.0000 ± 0.0078	0.0000 ± 0.0357	0.0000 ± 0.0261	0.0000 ± 0.0408	0.0000 ± 0.0369	0.0000 ± 0.0193	0.0000 ± 0.0414	0.0000 ± 0.0524	0.0000 ± 0.0465	0.0000 ± 0.0443
Tl	0.0003 ± 0.0082	0.0000 ± 0.0372	0.0055 ± 0.0272	0.0009 ± 0.0425	0.0000 ± 0.0384	0.0000 ± 0.0201	0.0009 ± 0.0431	0.0000 ± 0.0546	0.0000 ± 0.0484	0.0000 ± 0.0462
Pb	0.0055 ± 0.0085	0.0116 ± 0.0387	0.0000 ± 0.0283	0.0000 ± 0.0442	0.0000 ± 0.0400	0.0231 ± 0.0210	0.0280 ± 0.0450	0.0028 ± 0.0568	0.0654 ± 0.0508	0.0000 ± 0.0480
U	0.0000 ± 0.0138	0.0417 ± 0.0628	0.0000 ± 0.0458	0.0298 ± 0.0717	0.0030 ± 0.0647	0.0157 ± 0.0339	0.0009 ± 0.0727	0.0514 ± 0.0921	0.0542 ± 0.0817	0.0462 ± 0.0778
PAH	0.1008 ± 0.0023	N/A ± N/A	N/A ± N/A	0.0946 ± 0.0019	N/A ± N/A	0.0697 ± 0.0016	0.0861 ± 0.0018	0.1061 ± 0.0028	N/A ± N/A	0.0580 ± 0.0020
n-alkanes	12.6578 ± 0.3048	N/A ± N/A	N/A ± N/A	3.2583 ± 0.0896	N/A ± N/A	3.4809 ± 0.0902	1.5902 ± 0.0361	4.3109 ± 0.1452	N/A ± N/A	2.0964 ± 0.0737
iso/anteiso-alkanes	0.0000 ± 0.0000	N/A ± N/A	N/A ± N/A	0.0000 ± 0.0000	N/A ± N/A	0.0000 ± 0.0000	0.0000 ± 0.0000	0.0000 ± 0.0000	N/A ± N/A	0.0000 ± 0.0000
hopanes	0.0885 ± 0.0026	N/A ± N/A	N/A ± N/A	0.1015 ± 0.0024	N/A ± N/A	0.1946 ± 0.0059	0.0840 ± 0.0021	0.3121 ± 0.0109	N/A ± N/A	0.1114 ± 0.0040
steranes	0.0772 ± 0.0022	N/A ± N/A	N/A ± N/A	0.0417 ± 0.0010	N/A ± N/A	0.0719 ± 0.0023	0.0349 ± 0.0007	0.1212 ± 0.0043	N/A ± N/A	0.0382 ± 0.0013
mehtyl-alkanes	0.2069 ± 0.0108	N/A ± N/A	N/A ± N/A	0.1081 ± 0.0049	N/A ± N/A	0.0665 ± 0.0042	0.0463 ± 0.0021	0.0970 ± 0.0071	N/A ± N/A	0.0667 ± 0.0045
branched alkanes	1.6720 ± 0.1003	N/A ± N/A	N/A ± N/A	0.2115 ± 0.0104	N/A ± N/A	0.1097 ± 0.0071	0.2254 ± 0.0103	0.5794 ± 0.0426	N/A ± N/A	0.2294 ± 0.0164
cyclo-alkanes	0.2587 ± 0.0130	N/A ± N/A	N/A ± N/A	0.0697 ± 0.0027	N/A ± N/A	0.0500 ± 0.0027	0.0488 ± 0.0018	0.1077 ± 0.0064	N/A ± N/A	0.0592 ± 0.0035
alkenes	0.0000 ± 0.0000	N/A ± N/A	N/A ± N/A	0.0404 ± 0.0025	N/A ± N/A	0.0209 ± 0.0018	0.0335 ± 0.0021	0.0964 ± 0.0098	N/A ± N/A	0.0313 ± 0.0029
phthalates	0.0130 ± 0.0006	N/A ± N/A	N/A ± N/A	0.0078 ± 0.0004	N/A ± N/A	0.0047 ± 0.0003	0.0004 ± 0.0000	0.0085 ± 0.0007	N/A ± N/A	0.0008 ± 0.0001
SO_2	143.9652 ± 10.3362	393.5385 ± 34.0267	354.0817 ± 28.1591	497.8870 ± 45.2812	416.7926 ± 36.5275	402.1100 ± 30.4330	408.3539 ± 37.3555	468.6416 ± 47.7745	435.9068 ± 41.7766	458.5815 ± 43.1298
NH_3	0.0000 ± 0.0626	0.0000 ± 0.2849	0.0000 ± 0.2088	0.0000 ± 0.3256	0.0000 ± 0.2943	0.0000 ± 0.1541	0.0000 ± 0.3304	0.0000 ± 0.4192	0.0000 ± 0.3718	0.0000 ± 0.3553

[a] See Figure 6-1 for Drive Cycles #1 and #2

[b] See Table 6-1 for Mnemonic ID definitions and test conditions

c Qualitative

Table 6-7. Summary of the $PM_{2.5}$ source profiles for the four tests conducted for the logistics vehicle system (LVS).

Chemical Species	LVS Driving Cycle #1[a] TNP_14[b]	LVS Driving Cycle #1 TNP_16	LVS Driving Cycle #1 TNP_17	LVS Driving Cycle #2 TNP_19
Cl^-	0.0000 ± 0.0393	0.0000 ± 0.1125	0.0000 ± 0.0893	0.0615 ± 0.1531
NO_3^-	0.0926 ± 0.0430	0.1107 ± 0.1146	0.0955 ± 0.0912	0.1125 ± 0.0937
$SO_4^=$	1.0197 ± 0.0909	0.6432 ± 0.1240	0.5830 ± 0.1010	1.2644 ± 0.1376
NH_4^+	0.0947 ± 0.0414	0.1053 ± 0.1148	0.0957 ± 0.0914	0.1476 ± 0.0942
Na^+	0.0041 ± 0.0028	0.0000 ± 0.0070	0.0000 ± 0.0056	0.0053 ± 0.0061
K^+	0.0067 ± 0.0042	0.0043 ± 0.0114	0.0042 ± 0.0091	0.0112 ± 0.0095
OC1	15.6313 ± 3.6476	11.3398 ± 2.7520	11.2085 ± 2.6914	11.4971 ± 2.7630
OC2	14.7731 ± 3.0298	15.4298 ± 3.2079	11.9011 ± 2.4739	11.9667 ± 2.4917
OC3	5.3051 ± 0.8886	6.1673 ± 1.1643	5.8221 ± 1.0571	4.7885 ± 0.9148
OC4	1.2670 ± 0.2916	1.6952 ± 0.4393	1.6350 ± 0.4049	1.4412 ± 0.3691
OP	18.4690 ± 3.8805	3.9962 ± 0.8570	0.0000 ± 0.1314	0.0000 ± 0.1342
OC	55.2998 ± 6.1909	38.2113 ± 4.4464	30.2355 ± 3.5110	29.3556 ± 3.4335
EC1	23.5739 ± 5.1610	20.9055 ± 4.5847	13.2324 ± 2.9007	19.5480 ± 4.2891
EC2	21.1621 ± 2.9978	38.0204 ± 5.4055	41.4260 ± 5.8795	13.2593 ± 1.8911
EC3	0.0000 ± 0.0181	0.0000 ± 0.0517	0.0000 ± 0.0411	0.0000 ± 0.0419
EC	26.2670 ± 6.0192	54.9297 ± 12.6043	54.6584 ± 12.5342	32.8073 ± 7.5326
TC	81.5668 ± 10.7383	93.1410 ± 12.4165	84.8941 ± 11.2746	62.1629 ± 8.3290
Na[c]	0.1538 ± 0.1178	0.0000 ± 0.3410	0.0000 ± 0.2741	0.1565 ± 0.3001
Mg[c]	0.0000 ± 0.0599	0.0146 ± 0.1781	0.0000 ± 0.1447	0.0000 ± 0.1549
Al	0.0316 ± 0.0102	0.0196 ± 0.0294	0.0000 ± 0.0238	0.0000 ± 0.0255
Si	0.1294 ± 0.0147	0.0335 ± 0.0331	0.0110 ± 0.0268	0.0352 ± 0.0289
P	0.2154 ± 0.0157	0.1664 ± 0.0155	0.1495 ± 0.0134	0.3252 ± 0.0253
S	0.6626 ± 0.0486	0.4809 ± 0.0471	0.4674 ± 0.0425	0.8102 ± 0.0655
Cl	0.0000 ± 0.0022	0.0023 ± 0.0065	0.0043 ± 0.0053	0.0000 ± 0.0056
K	0.0275 ± 0.0028	0.0065 ± 0.0061	0.0061 ± 0.0049	0.0206 ± 0.0055
Ca	0.5026 ± 0.0358	0.3602 ± 0.0270	0.3797 ± 0.0279	0.7818 ± 0.0571
Sc	0.0051 ± 0.0080	0.0000 ± 0.0238	0.0015 ± 0.0193	0.0018 ± 0.0207
Ti	0.0042 ± 0.0015	0.0013 ± 0.0044	0.0006 ± 0.0036	0.0000 ± 0.0039
V	0.0001 ± 0.0002	0.0000 ± 0.0007	0.0000 ± 0.0006	0.0007 ± 0.0006
Cr	0.0007 ± 0.0014	0.0001 ± 0.0040	0.0000 ± 0.0033	0.0006 ± 0.0035
Mn	0.0040 ± 0.0037	0.0104 ± 0.0109	0.0057 ± 0.0088	0.0069 ± 0.0095
Fe	0.1783 ± 0.0143	0.0310 ± 0.0199	0.0329 ± 0.0162	0.0875 ± 0.0184
Co	0.0000 ± 0.0001	0.0000 ± 0.0004	0.0000 ± 0.0003	0.0000 ± 0.0004
Ni	0.0000 ± 0.0007	0.0017 ± 0.0020	0.0011 ± 0.0017	0.0008 ± 0.0018
Cu	0.0329 ± 0.0026	0.0091 ± 0.0037	0.0053 ± 0.0030	0.0216 ± 0.0035
Zn	0.2787 ± 0.0198	0.2232 ± 0.0165	0.2236 ± 0.0163	0.4437 ± 0.0324
Ga	0.0021 ± 0.0043	0.0000 ± 0.0129	0.0066 ± 0.0105	0.0000 ± 0.0112
As	0.0003 ± 0.0001	0.0000 ± 0.0004	0.0000 ± 0.0003	0.0000 ± 0.0004
Se	0.0015 ± 0.0029	0.0033 ± 0.0085	0.0002 ± 0.0069	0.0080 ± 0.0074
Br	0.0070 ± 0.0021	0.0050 ± 0.0061	0.0005 ± 0.0049	0.0044 ± 0.0053
Rb	0.0000 ± 0.0015	0.0000 ± 0.0044	0.0000 ± 0.0036	0.0000 ± 0.0039
Sr	0.0024 ± 0.0027	0.0014 ± 0.0081	0.0000 ± 0.0066	0.0000 ± 0.0070
Y	0.0004 ± 0.0020	0.0003 ± 0.0061	0.0000 ± 0.0049	0.0000 ± 0.0053
Zr	0.0000 ± 0.0048	0.0061 ± 0.0141	0.0000 ± 0.0115	0.0000 ± 0.0123
Nb	0.0000 ± 0.0037	0.0000 ± 0.0109	0.0000 ± 0.0089	0.0000 ± 0.0095
Mo	0.0180 ± 0.0035	0.0181 ± 0.0098	0.0083 ± 0.0079	0.0259 ± 0.0087
Pd	0.0000 ± 0.0063	0.0004 ± 0.0186	0.0000 ± 0.0152	0.0107 ± 0.0164
Ag	0.0000 ± 0.0063	0.0000 ± 0.0187	0.0000 ± 0.0152	0.0000 ± 0.0163
Cd	0.0042 ± 0.0072	0.0036 ± 0.0213	0.0059 ± 0.0173	0.0000 ± 0.0184
In	0.0000 ± 0.0042	0.0000 ± 0.0125	0.0107 ± 0.0103	0.0000 ± 0.0109
Sn	0.0219 ± 0.0059	0.0342 ± 0.0171	0.0266 ± 0.0139	0.0263 ± 0.0149
Sb	0.0004 ± 0.0101	0.0000 ± 0.0298	0.0205 ± 0.0243	0.0091 ± 0.0260

Table 6-7. Continued

Chemical Species	LVS Driving Cycle #1[a] TNP_14[b]	LVS Driving Cycle #1 TNP_16	LVS Driving Cycle #1 TNP_17	LVS Driving Cycle #2 TNP_19
Cs	0.0000 ± 0.0016	0.0009 ± 0.0048	0.0000 ± 0.0039	0.0000 ± 0.0042
Ba	0.0000 ± 0.0018	0.0000 ± 0.0052	0.0000 ± 0.0042	0.0000 ± 0.0045
La	0.0000 ± 0.0012	0.0015 ± 0.0036	0.0000 ± 0.0029	0.0008 ± 0.0032
Ce	0.0006 ± 0.0018	0.0018 ± 0.0052	0.0000 ± 0.0043	0.0021 ± 0.0046
Sm	0.0008 ± 0.0025	0.0000 ± 0.0073	0.0000 ± 0.0059	0.0000 ± 0.0063
Eu	0.0000 ± 0.0089	0.0000 ± 0.0264	0.0000 ± 0.0214	0.0000 ± 0.0230
Tb	0.0000 ± 0.0030	0.0040 ± 0.0090	0.0000 ± 0.0072	0.0000 ± 0.0077
Hf	0.0009 ± 0.0194	0.0000 ± 0.0574	0.0066 ± 0.0467	0.0000 ± 0.0501
Ta	0.0054 ± 0.0162	0.0000 ± 0.0481	0.0061 ± 0.0391	0.0100 ± 0.0420
W	0.0000 ± 0.0233	0.0022 ± 0.0692	0.0067 ± 0.0563	0.0000 ± 0.0601
Ir	0.0000 ± 0.0050	0.0009 ± 0.0150	0.0000 ± 0.0122	0.0000 ± 0.0130
Au	0.0000 ± 0.0108	0.0000 ± 0.0319	0.0091 ± 0.0260	0.0143 ± 0.0279
Hg	0.0000 ± 0.0033	0.0000 ± 0.0097	0.0000 ± 0.0079	0.0000 ± 0.0084
Tl	0.0000 ± 0.0034	0.0004 ± 0.0101	0.0021 ± 0.0082	0.0028 ± 0.0088
Pb	0.0000 ± 0.0035	0.0000 ± 0.0105	0.0024 ± 0.0085	0.0131 ± 0.0092
U	0.0000 ± 0.0057	0.0095 ± 0.0170	0.0000 ± 0.0139	0.0093 ± 0.0148
PAH	0.0366 ± 0.0007	0.0433 ± 0.0012	0.0351 ± 0.0010	0.0356 ± 0.0010
n-alkanes	0.4223 ± 0.0051	0.4241 ± 0.0100	0.4533 ± 0.0091	0.3232 ± 0.0070
iso/anteiso-alkanes	0.0000 ± 0.0000	0.0000 ± 0.0000	0.0000 ± 0.0000	0.0000 ± 0.0000
hopanes	0.0698 ± 0.0013	0.0665 ± 0.0018	0.0664 ± 0.0018	0.0694 ± 0.0018
steranes	0.0316 ± 0.0005	0.0275 ± 0.0007	0.0307 ± 0.0008	0.0292 ± 0.0007
mehtyl-alkanes	0.0057 ± 0.0002	0.0079 ± 0.0005	0.0139 ± 0.0007	0.0119 ± 0.0006
branched alkanes	0.0375 ± 0.0013	0.0823 ± 0.0042	0.0834 ± 0.0042	0.0474 ± 0.0024
cyclo-alkanes	0.0263 ± 0.0008	0.0341 ± 0.0015	0.0318 ± 0.0014	0.0295 ± 0.0014
alkenes	0.0079 ± 0.0004	0.0150 ± 0.0011	0.0142 ± 0.0010	0.0097 ± 0.0007
phthalates	0.0000 ± 0.0000	0.0013 ± 0.0001	0.0000 ± 0.0000	0.0068 ± 0.0004
SO_2	88.4694 ± 6.2881	103.5506 ± 7.4583	96.7303 ± 6.9256	99.7063 ± 7.2183
NH_3	0.0000 ± 0.0261	0.0000 ± 0.0775	0.0000 ± 0.0630	0.0000 ± 0.0675

[a] See Figure 6-1 for Drive Cycles #1 and #2

[b] See Table 6-1 for Mnemonic ID definitions and test conditions

c Qualitative

Table 6-8. Composite $PM_{2.5}$ source profiles for the 13 military diesel generators and four military diesel vehicles.

Chemical Species	Warm Start[a] PEN_CP1	Cold Start PEN_CP2	AAV idle[b] TNP_15	MTVR[c] TNP_CP1	LVS[d] TNP_CP2
Cl^-	0.0223 ± 0.0547	0.0000 ± 0.0000	0.0000 ± 0.1223	0.0139 ± 0.0310	0.0154 ± 0.0307
NO_3^-	0.0429 ± 0.0487	0.0000 ± 0.0000	0.1375 ± 0.1252	0.2798 ± 0.0744	0.1028 ± 0.0103
$SO_4^=$	1.3311 ± 1.0849	0.4569 ± 0.4927	0.3258 ± 0.1251	1.0873 ± 0.3675	0.8776 ± 0.3222
NH_4^+	0.6158 ± 0.3990	0.3021 ± 0.2753	0.2841 ± 0.1286	0.1483 ± 0.1027	0.1108 ± 0.0250
Na^+	0.0088 ± 0.0084	0.0000 ± 0.0000	0.0000 ± 0.0076	0.0042 ± 0.0068	0.0023 ± 0.0028
K^+	0.0036 ± 0.0040	0.0003 ± 0.0006	0.0047 ± 0.0124	0.0265 ± 0.0103	0.0066 ± 0.0033
OC1	11.1324 ± 8.5441	31.4742 ± 23.0923	9.7087 ± 2.3898	34.4255 ± 27.7262	12.4192 ± 2.1447
OC2	17.1579 ± 11.5209	15.9674 ± 12.3107	9.7649 ± 2.0617	16.1605 ± 5.1710	13.5177 ± 1.8485
OC3	5.1335 ± 2.3295	12.7886 ± 10.3327	5.6479 ± 1.1202	12.3433 ± 2.9207	5.5208 ± 0.6032
OC4	1.8683 ± 0.9686	5.0745 ± 3.8431	1.4928 ± 0.4134	4.6701 ± 1.1590	1.5096 ± 0.1947
OP	4.1730 ± 9.6613	7.8559 ± 7.4057	0.0000 ± 0.1800	0.0000 ± 0.0000	5.6163 ± 8.7731
OC	39.4552 ± 22.8040	73.1110 ± 56.0059	26.1609 ± 3.1675	66.1437 ± 25.9345	38.2756 ± 12.0282
EC1	7.1613 ± 3.1599	9.7723 ± 8.5514	4.2432 ± 0.9403	12.7735 ± 5.4663	19.3150 ± 4.3863
EC2	14.3884 ± 8.3202	9.9199 ± 5.2808	57.9555 ± 8.2459	42.3941 ± 13.0479	28.4670 ± 13.4640
EC3	0.0955 ± 0.0562	0.2983 ± 0.2149	0.0000 ± 0.0562	0.1009 ± 0.1909	0.0000 ± 0.0000
EC	17.4722 ± 10.6369	12.1347 ± 6.6848	62.1989 ± 14.2773	55.2684 ± 13.8480	42.1656 ± 14.8249
TC	56.9274 ± 25.1653	85.2458 ± 62.5232	88.3598 ± 11.8202	121.4122 ± 18.1355	80.4412 ± 13.1209
Na[e]	0.0248 ± 0.0312	0.0939 ± 0.1603	0.0000 ± 0.3730	0.0148 ± 0.0334	0.0776 ± 0.0896
Mg[e]	0.0056 ± 0.0062	0.0006 ± 0.0011	0.0000 ± 0.1958	0.0999 ± 0.1162	0.0037 ± 0.0073
Al	0.0256 ± 0.0257	0.0461 ± 0.0593	0.0000 ± 0.0321	0.0871 ± 0.1658	0.0128 ± 0.0156
Si	0.0708 ± 0.0550	0.1039 ± 0.1572	0.0111 ± 0.0362	0.2251 ± 0.3785	0.0523 ± 0.0526
P	0.1301 ± 0.0495	0.0701 ± 0.0212	0.0375 ± 0.0109	0.0327 ± 0.0368	0.2141 ± 0.0792
S	0.7567 ± 0.3703	0.3996 ± 0.1997	0.1739 ± 0.0364	0.6638 ± 0.1856	0.6053 ± 0.1631
Cl	0.0287 ± 0.0562	0.0101 ± 0.0074	0.0048 ± 0.0071	0.0199 ± 0.0173	0.0017 ± 0.0021
K	0.0108 ± 0.0051	0.0126 ± 0.0081	0.0002 ± 0.0067	0.1263 ± 0.2793	0.0151 ± 0.0106
Ca	0.0650 ± 0.0295	0.1040 ± 0.0599	0.1017 ± 0.0109	0.1739 ± 0.1120	0.5061 ± 0.1943
Sc	N/A ± N/A	N/A ± N/A	0.0000 ± 0.0262	0.0103 ± 0.0099	0.0021 ± 0.0022
Ti	0.0023 ± 0.0020	0.0018 ± 0.0014	0.0000 ± 0.0049	0.0083 ± 0.0117	0.0015 ± 0.0019
V	0.0006 ± 0.0009	0.0001 ± 0.0002	0.0000 ± 0.0008	0.0002 ± 0.0006	0.0002 ± 0.0003
Cr	0.0010 ± 0.0006	0.0008 ± 0.0011	0.0000 ± 0.0044	0.0002 ± 0.0004	0.0004 ± 0.0004
Mn	0.0021 ± 0.0027	0.0061 ± 0.0056	0.0059 ± 0.0119	0.0241 ± 0.0184	0.0067 ± 0.0027
Fe	0.1341 ± 0.1608	0.1961 ± 0.2905	0.0407 ± 0.0220	0.3221 ± 0.4208	0.0824 ± 0.0691
Co	0.0000 ± 0.0000	0.0004 ± 0.0008	0.0000 ± 0.0004	0.0000 ± 0.0000	0.0000 ± 0.0000
Ni	0.0006 ± 0.0005	0.0033 ± 0.0042	0.0000 ± 0.0022	0.0048 ± 0.0062	0.0009 ± 0.0007
Cu	0.0059 ± 0.0049	0.0104 ± 0.0105	0.0000 ± 0.0040	0.0341 ± 0.0465	0.0172 ± 0.0126
Zn	0.0522 ± 0.0259	0.0753 ± 0.0127	0.0576 ± 0.0058	0.0573 ± 0.0514	0.2923 ± 0.1042
Ga	0.0014 ± 0.0022	0.0180 ± 0.0311	0.0043 ± 0.0142	0.0149 ± 0.0182	0.0022 ± 0.0031
As	0.0000 ± 0.0000	0.0000 ± 0.0000	0.0000 ± 0.0004	0.0000 ± 0.0000	0.0001 ± 0.0001
Se	0.0000 ± 0.0000	0.0000 ± 0.0000	0.0030 ± 0.0093	0.0044 ± 0.0066	0.0033 ± 0.0034
Br	0.0013 ± 0.0016	0.0034 ± 0.0054	0.0000 ± 0.0067	0.0037 ± 0.0027	0.0042 ± 0.0027
Rb	0.0004 ± 0.0005	0.0045 ± 0.0069	0.0045 ± 0.0049	0.0016 ± 0.0029	0.0000 ± 0.0000
Sr	0.0007 ± 0.0005	0.0004 ± 0.0005	0.0056 ± 0.0089	0.0056 ± 0.0083	0.0010 ± 0.0012
Y	0.0003 ± 0.0005	0.0039 ± 0.0045	0.0000 ± 0.0067	0.0024 ± 0.0036	0.0002 ± 0.0002
Zr	0.0014 ± 0.0016	0.0024 ± 0.0048	0.0000 ± 0.0155	0.0060 ± 0.0113	0.0015 ± 0.0031
Nb	N/A ± N/A	N/A ± N/A	0.0000 ± 0.0120	0.0000 ± 0.0001	0.0000 ± 0.0000
Mo	0.0004 ± 0.0007	0.0068 ± 0.0043	0.0000 ± 0.0106	0.0121 ± 0.0239	0.0176 ± 0.0072
Pd	0.0026 ± 0.0022	0.0000 ± 0.0000	0.0000 ± 0.0205	0.0008 ± 0.0026	0.0028 ± 0.0053
Ag	0.0002 ± 0.0004	0.0047 ± 0.0067	0.0000 ± 0.0206	0.0000 ± 0.0000	0.0000 ± 0.0000
Cd	0.0027 ± 0.0026	0.0008 ± 0.0009	0.0018 ± 0.0234	0.0065 ± 0.0088	0.0034 ± 0.0025
In	0.0006 ± 0.0009	0.0246 ± 0.0493	0.0013 ± 0.0138	0.0044 ± 0.0058	0.0027 ± 0.0053
Sn	0.0010 ± 0.0023	0.0040 ± 0.0081	0.0205 ± 0.0187	0.0477 ± 0.0443	0.0273 ± 0.0051
Sb	0.0011 ± 0.0028	0.0020 ± 0.0040	0.0000 ± 0.0328	0.0096 ± 0.0185	0.0075 ± 0.0096

Table 6-8. Continued

Chemical Species	Warm Start[a] PEN_CP1	Cold Start PEN_CP2	AAV idle[b] TNP_15	MTVR[c] TNP_CP1	LVS[d] TNP_CP2
Cs	N/A ± N/A	N/A ± N/A	0.0000 ± 0.0053	0.0018 ± 0.0028	0.0002 ± 0.0005
Ba	0.0088 ± 0.0086	0.0110 ± 0.0207	0.0000 ± 0.0057	0.0000 ± 0.0000	0.0000 ± 0.0000
La	0.0031 ± 0.0036	0.0133 ± 0.0153	0.0000 ± 0.0040	0.0015 ± 0.0021	0.0006 ± 0.0007
Ce	N/A ± N/A	N/A ± N/A	0.0000 ± 0.0058	0.0067 ± 0.0064	0.0011 ± 0.0010
Sm	N/A ± N/A	N/A ± N/A	0.0000 ± 0.0080	0.0030 ± 0.0050	0.0002 ± 0.0004
Eu	N/A ± N/A	N/A ± N/A	0.0000 ± 0.0290	0.0000 ± 0.0000	0.0000 ± 0.0000
Tb	N/A ± N/A	N/A ± N/A	0.0000 ± 0.0098	0.0009 ± 0.0023	0.0010 ± 0.0020
Hf	N/A ± N/A	N/A ± N/A	0.0000 ± 0.0632	0.0033 ± 0.0081	0.0019 ± 0.0032
Ta	N/A ± N/A	N/A ± N/A	0.0096 ± 0.0529	0.0318 ± 0.0362	0.0054 ± 0.0041
W	N/A ± N/A	N/A ± N/A	0.0000 ± 0.0760	0.0151 ± 0.0392	0.0022 ± 0.0032
Ir	N/A ± N/A	N/A ± N/A	0.0061 ± 0.0165	0.0021 ± 0.0035	0.0002 ± 0.0005
Au	0.0030 ± 0.0037	0.0145 ± 0.0130	0.0000 ± 0.0351	0.0156 ± 0.0187	0.0059 ± 0.0071
Hg	0.0000 ± 0.0000	0.0000 ± 0.0000	0.0027 ± 0.0106	0.0000 ± 0.0000	0.0000 ± 0.0000
Tl	0.0002 ± 0.0004	0.0043 ± 0.0045	0.0000 ± 0.0111	0.0008 ± 0.0017	0.0013 ± 0.0014
Pb	0.0055 ± 0.0073	0.0111 ± 0.0068	0.0003 ± 0.0115	0.0136 ± 0.0209	0.0039 ± 0.0063
U	0.0006 ± 0.0008	0.0031 ± 0.0050	0.0062 ± 0.0187	0.0243 ± 0.0228	0.0047 ± 0.0054
PAH	0.0170 ± 0.0102	0.0829 ± 0.0874	0.0276 ± 0.0007	0.0859 ± 0.0187	0.0376 ± 0.0038
n-alkanes	0.7113 ± 0.6981	1.0650 ± 1.4153	0.4212 ± 0.0100	4.5658 ± 4.0837	0.4057 ± 0.0568
iso/anteiso-alkanes	0.0000 ± 0.0000	0.0000 ± 0.0000	0.0000 ± 0.0000	0.0000 ± 0.0000	0.0000 ± 0.0000
hopanes	0.1198 ± 0.0903	0.1237 ± 0.1066	0.0465 ± 0.0012	0.1487 ± 0.0897	0.0680 ± 0.0018
steranes	0.0588 ± 0.0496	0.0832 ± 0.0787	0.0179 ± 0.0004	0.0642 ± 0.0332	0.0298 ± 0.0018
mehtyl-alkanes	0.0055 ± 0.0102	0.0159 ± 0.0162	0.0299 ± 0.0016	0.0986 ± 0.0576	0.0099 ± 0.0038
branched alkanes	0.0264 ± 0.0331	0.0413 ± 0.0344	0.1077 ± 0.0055	0.5046 ± 0.5939	0.0626 ± 0.0237
cyclo-alkanes	0.0215 ± 0.0164	0.0430 ± 0.0516	0.0177 ± 0.0008	0.0990 ± 0.0811	0.0304 ± 0.0033
alkenes	0.0027 ± 0.0027	0.0033 ± 0.0044	0.0169 ± 0.0012	0.0371 ± 0.0323	0.0117 ± 0.0035
phthalates	0.0312 ± 0.0565	0.3694 ± 0.4772	0.0000 ± 0.0000	0.0059 ± 0.0048	0.0020 ± 0.0032
SO_2	24.1299 ± 19.1612	41.1401 ± 36.4919	34.0577 ± 2.4626	397.9859 ± 98.3386	97.1142 ± 6.4038
NH_3	0.0559 ± 0.0476	0.0280 ± 0.0560	0.0000 ± 0.0852	0.0000 ± 0.0000	0.0000 ± 0.0000

[a] Warm start includes running at 10, 25, 50, 75, and 100% load
[b] Based on a single idle test for the assault amphibious vehicle (AAV)
[c] Medium tactical vehicle replacement with a Caterpillar 729 cubic inch six-cylinder turbocharged diesel engine
[d] Logistics vehicle system with a Detroit Diesel 8V92TA eight-cylinder turbocharged diesel engine
[e] Qualitative

Table 6-9. Summary of the organic species source profiles for the six emissions test conducted for the 13 diesel generators using warm start.

PAHs	MW	10kW[a] PEN_04[b]	10kW PEN_05	30kW PEN_06	60kW PEN_08	60kW PEN_09	100kW PEN_13
acenaphthylene	152	0.00009 ± 0.00001	0.00012 ± 0.00001	0.00008 ± 0.00001	0.00009 ± 0.00001	0.00004 ± 0.00000	0.00003 ± 0.00000
acenaphthene	154	0.00017 ± 0.00001	0.00012 ± 0.00001	0.00005 ± 0.00000	0.00002 ± 0.00000	0.00000 ± 0.00000	0.00001 ± 0.00000
fluorene	166	0.00008 ± 0.00001	0.00006 ± 0.00000	0.00003 ± 0.00000	0.00009 ± 0.00001	0.00003 ± 0.00000	0.00002 ± 0.00000
phenanthrene	178	0.00020 ± 0.00001	0.00008 ± 0.00001	0.00015 ± 0.00001	0.00016 ± 0.00001	0.00007 ± 0.00001	0.00010 ± 0.00001
anthracene	178	0.00010 ± 0.00001	0.00008 ± 0.00001	0.00009 ± 0.00001	0.00017 ± 0.00001	0.00008 ± 0.00001	0.00004 ± 0.00000
fluoranthene	202	0.00238 ± 0.00017	0.00238 ± 0.00017	0.00072 ± 0.00005	0.00027 ± 0.00002	0.00013 ± 0.00001	0.00083 ± 0.00006
pyrene	202	0.00438 ± 0.00031	0.00462 ± 0.00033	0.00147 ± 0.00010	0.00050 ± 0.00004	0.00024 ± 0.00002	0.00124 ± 0.00009
benzo[a]anthracene	228	0.00132 ± 0.00009	0.00151 ± 0.00011	0.00027 ± 0.00002	0.00050 ± 0.00004	0.00021 ± 0.00001	0.00041 ± 0.00003
chrysene	228	0.00334 ± 0.00024	0.00331 ± 0.00023	0.00080 ± 0.00006	0.00159 ± 0.00011	0.00064 ± 0.00005	0.00095 ± 0.00007
benzo[b]fluoranthene	252	0.00189 ± 0.00013	0.00308 ± 0.00022	0.00043 ± 0.00003	0.00143 ± 0.00010	0.00082 ± 0.00006	0.00032 ± 0.00002
benzo[k]fluoranthene	252	0.00202 ± 0.00014	0.00252 ± 0.00018	0.00066 ± 0.00005	0.00139 ± 0.00010	0.00062 ± 0.00004	0.00038 ± 0.00003
benzo[a]fluoranthene	252	0.00017 ± 0.00001	0.00017 ± 0.00001	0.00006 ± 0.00000	0.00072 ± 0.00005	0.00008 ± 0.00001	0.00003 ± 0.00000
benzo[e]pyrene	252	0.00354 ± 0.00025	0.00311 ± 0.00022	0.00088 ± 0.00006	0.00211 ± 0.00015	0.00128 ± 0.00009	0.00049 ± 0.00003
benzo[a]pyrene	252	0.00068 ± 0.00005	0.00149 ± 0.00011	0.00027 ± 0.00002	0.00045 ± 0.00003	0.00129 ± 0.00009	0.00011 ± 0.00001
perylene	252	0.00013 ± 0.00001	0.00019 ± 0.00001	0.00006 ± 0.00000	0.00005 ± 0.00000	0.00005 ± 0.00000	0.00005 ± 0.00000
indeno[1,2,3-cd]pyrene	276	0.00053 ± 0.00004	0.00104 ± 0.00007	0.00011 ± 0.00001	0.00036 ± 0.00003	0.00019 ± 0.00001	0.00057 ± 0.00004
dibenzo[a,h]anthracene	278	0.00002 ± 0.00000	0.00011 ± 0.00001	0.00005 ± 0.00000	0.00031 ± 0.00002	0.00007 ± 0.00000	0.00004 ± 0.00000
benzo[ghi]perylene	276	0.00091 ± 0.00006	0.00128 ± 0.00009	0.00026 ± 0.00002	0.00042 ± 0.00003	0.00048 ± 0.00003	0.00149 ± 0.00011
coronene	300	0.00039 ± 0.00003	0.00047 ± 0.00003	0.00000 ± 0.00000	0.00000 ± 0.00000	0.00016 ± 0.00001	0.00000 ± 0.00000
dibenzo[a,e]pyrene	302	0.00000 ± 0.00000	0.00000 ± 0.00000	0.00000 ± 0.00000	0.00000 ± 0.00000	0.00000 ± 0.00000	0.00000 ± 0.00000
2-methylnaphthalene	142	0.00102 ± 0.00007	0.00108 ± 0.00008	0.00005 ± 0.00000	0.00248 ± 0.00018	0.00270 ± 0.00019	0.00021 ± 0.00001
1-methylnaphthalene	142	0.00010 ± 0.00001	0.00014 ± 0.00001	0.00085 ± 0.00006	0.00002 ± 0.00000	0.00003 ± 0.00000	0.00001 ± 0.00000
2,6-dimethylnaphthalene	156	0.00039 ± 0.00003	0.00079 ± 0.00006	0.00038 ± 0.00003	0.00059 ± 0.00004	0.00038 ± 0.00003	0.00017 ± 0.00001
9-fluorenone	180	0.00021 ± 0.00002	0.00028 ± 0.00002	0.00012 ± 0.00001	0.00020 ± 0.00001	0.00012 ± 0.00001	0.00013 ± 0.00001
9-methylanthracene	192	0.00070 ± 0.00005	0.00020 ± 0.00001	0.00024 ± 0.00002	0.00028 ± 0.00002	0.00010 ± 0.00001	0.00014 ± 0.00001
anthraquinone	208	0.00031 ± 0.00002	0.00096 ± 0.00007	0.00017 ± 0.00001	0.00015 ± 0.00001	0.00009 ± 0.00001	0.00010 ± 0.00001
methylfluoranthene	216	0.00082 ± 0.00006	0.00037 ± 0.00003	0.00011 ± 0.00001	0.00006 ± 0.00000	0.00003 ± 0.00000	0.00014 ± 0.00001
retene	234	0.00060 ± 0.00004	0.00007 ± 0.00000	0.00016 ± 0.00001	0.00034 ± 0.00002	0.00013 ± 0.00001	0.00004 ± 0.00000
cyclopenta[cd]pyrene	226	0.00039 ± 0.00003	0.00011 ± 0.00001	0.00011 ± 0.00001	0.00006 ± 0.00000	0.00003 ± 0.00000	0.00000 ± 0.00000
benz[a]anthracene-7,12-dione	258	0.00114 ± 0.00008	0.00141 ± 0.00010	0.00023 ± 0.00002	0.00036 ± 0.00003	0.00025 ± 0.00002	0.00000 ± 0.00000
methylchrysene	242	0.00012 ± 0.00001	0.00001 ± 0.00000	0.00003 ± 0.00000	0.00014 ± 0.00001	0.00003 ± 0.00000	0.00000 ± 0.00000
picene	278	0.00006 ± 0.00000	0.00007 ± 0.00001	0.00006 ± 0.00000	0.00019 ± 0.00001	0.00000 ± 0.00000	0.00000 ± 0.00000
Alkane/Alkene/Phthalate							
***n*-alkane**							
n-pentadecane (*n*-C15)	212	0.00223 ± 0.00016	0.00055 ± 0.00004	0.00127 ± 0.00009	0.00167 ± 0.00012	0.00075 ± 0.00005	0.00116 ± 0.00008
n-hexadecane (*n*-C16)	226	0.00289 ± 0.00020	0.00086 ± 0.00006	0.00222 ± 0.00016	0.00264 ± 0.00019	0.00090 ± 0.00006	0.00181 ± 0.00013
n-heptadecane (*n*-C17)	240	0.00442 ± 0.00031	0.00087 ± 0.00006	0.00471 ± 0.00033	0.00382 ± 0.00027	0.00140 ± 0.00010	0.00232 ± 0.00016
n-octadecane (*n*-C18)	254	0.02547 ± 0.00180	0.00176 ± 0.00012	0.01583 ± 0.00112	0.00725 ± 0.00051	0.00262 ± 0.00019	0.00364 ± 0.00026
n-nonadecane (*n*-C19)	268	0.13831 ± 0.00979	0.00363 ± 0.00026	0.02991 ± 0.00212	0.01174 ± 0.00083	0.00350 ± 0.00025	0.00518 ± 0.00037
n-icosane (*n*-C20)	282	0.31009 ± 0.02195	0.01338 ± 0.00095	0.03585 ± 0.00254	0.02404 ± 0.00171	0.00667 ± 0.00047	0.00645 ± 0.00046
n-heneicosane (*n*-C21)	296	0.26656 ± 0.01887	0.00884 ± 0.00063	0.04706 ± 0.00333	0.05450 ± 0.00387	0.01020 ± 0.00072	0.00708 ± 0.00050
n-docosane (*n*-C22)	310	0.31867 ± 0.02256	0.04298 ± 0.00304	0.03905 ± 0.00276	0.09849 ± 0.00699	0.01557 ± 0.00110	0.00611 ± 0.00043
n-tricosane (*n*-C23)	324	0.25116 ± 0.01778	0.03998 ± 0.00283	0.03186 ± 0.00226	0.13951 ± 0.00990	0.01743 ± 0.00123	0.00209 ± 0.00015
n-tetracosane (*n*-C24)	338	0.19820 ± 0.01403	0.03160 ± 0.00224	0.02466 ± 0.00175	0.14875 ± 0.01055	0.01768 ± 0.00125	0.00000 ± 0.00000

Table 6-9. Continued.

PAHs	MW	10kW[a] PEN_04[b]	10kW PEN_05	30kW PEN_06	60kW PEN_08	60kW PEN_09	100kW PEN_13
Alkane/Alkene/Phthalate (continued)							
***n*-alkane (continued)**							
n-pentacosane (*n*-C25)	352	0.12220 ± 0.00865	0.02435 ± 0.00172	0.03319 ± 0.00235	0.15261 ± 0.01083	0.02430 ± 0.00172	0.00000 ± 0.00000
n-hexacosane (*n*-C26)	366	0.09123 ± 0.00646	0.01153 ± 0.00082	0.04862 ± 0.00344	0.16415 ± 0.01165	0.01335 ± 0.00094	0.00000 ± 0.00000
n-heptacosane (*n*-C27)	380	0.04473 ± 0.00317	0.00758 ± 0.00054	0.06629 ± 0.00469	0.09776 ± 0.00694	0.01240 ± 0.00088	0.00000 ± 0.00000
n-octacosane (*n*-C28)	394	0.02477 ± 0.00175	0.00183 ± 0.00013	0.03018 ± 0.00214	0.06523 ± 0.00463	0.04515 ± 0.00320	0.00000 ± 0.00000
n-nonacosane (*n*-C29)	408	0.02972 ± 0.00210	0.01398 ± 0.00099	0.02025 ± 0.00143	0.03783 ± 0.00268	0.04516 ± 0.00320	0.00000 ± 0.00000
n-triacontane (*n*-C30)	422	0.03096 ± 0.00219	0.01132 ± 0.00080	0.01076 ± 0.00076	0.07542 ± 0.00535	0.02844 ± 0.00201	0.00000 ± 0.00000
n-hentriacotane (*n*-C31)	436	0.04243 ± 0.00300	0.00866 ± 0.00061	0.00845 ± 0.00060	0.03545 ± 0.00252	0.02662 ± 0.00188	0.00000 ± 0.00000
n-dotriacontane (*n*-C32)	450	0.01866 ± 0.00132	0.00636 ± 0.00045	0.01410 ± 0.00100	0.00000 ± 0.00000	0.01249 ± 0.00088	0.00000 ± 0.00000
n-tritriactotane (*n*-C33)	464	0.00000 ± 0.00000	0.00400 ± 0.00028	0.02545 ± 0.00180	0.00000 ± 0.00000	0.01684 ± 0.00119	0.00000 ± 0.00000
n-tetratriactoane (*n*-C34)	478	0.00000 ± 0.00000	0.00122 ± 0.00009	0.02612 ± 0.00185	0.00000 ± 0.00000	0.03426 ± 0.00243	0.00000 ± 0.00000
n-pentatriacontane (*n*-C35)	492	0.00000 ± 0.00000	0.00009 ± 0.00001	0.03144 ± 0.00223	0.00000 ± 0.00000	0.03034 ± 0.00215	0.00000 ± 0.00000
n-hexatriacontane (*n*-C36)	506	0.00000 ± 0.00000	0.00212 ± 0.00015	0.00000 ± 0.00000	0.00000 ± 0.00000	0.00636 ± 0.00045	0.00000 ± 0.00000
n-heptatriacontane (*n*-C37)	520	0.00000 ± 0.00000	0.00084 ± 0.00006	0.00000 ± 0.00000	0.00000 ± 0.00000	0.00414 ± 0.00029	0.00000 ± 0.00000
n-octatriacontane (*n*-C38)	534	0.00000 ± 0.00000	0.00000 ± 0.00000	0.00000 ± 0.00000	0.00000 ± 0.00000	0.01769 ± 0.00125	0.00000 ± 0.00000
n-nonatriacontane (*n*-C39)	548	0.00000 ± 0.00000	0.00000 ± 0.00000	0.00000 ± 0.00000	0.00000 ± 0.00000	0.00884 ± 0.00063	0.00000 ± 0.00000
n-tetracontane (*n*-C40)	562	0.00000 ± 0.00000	0.00000 ± 0.00000	0.00000 ± 0.00000	0.00000 ± 0.00000	0.00000 ± 0.00000	0.00000 ± 0.00000
n-hentetracontane (*n*-C41)	576	0.00000 ± 0.00000	0.00000 ± 0.00000	0.00000 ± 0.00000	0.00000 ± 0.00000	0.00000 ± 0.00000	0.00000 ± 0.00000
n-dotetracontane (*n*-C42)	590	0.00000 ± 0.00000	0.00000 ± 0.00000	0.00000 ± 0.00000	0.00000 ± 0.00000	0.00000 ± 0.00000	0.00000 ± 0.00000
iso/anteiso-alkane							
iso-nonacosane (iso-C29)	408	0.00000 ± 0.00000	0.00000 ± 0.00000	0.00000 ± 0.00000	0.00000 ± 0.00000	0.00000 ± 0.00000	0.00000 ± 0.00000
anteiso-nonacosane (anteiso-C29)	408	0.00000 ± 0.00000	0.00000 ± 0.00000	0.00000 ± 0.00000	0.00000 ± 0.00000	0.00000 ± 0.00000	0.00000 ± 0.00000
iso-triacontane (iso-C30)	422	0.00000 ± 0.00000	0.00000 ± 0.00000	0.00000 ± 0.00000	0.00000 ± 0.00000	0.00000 ± 0.00000	0.00000 ± 0.00000
anteiso-triacontane (anteiso-C30)	422	0.00000 ± 0.00000	0.00000 ± 0.00000	0.00000 ± 0.00000	0.00000 ± 0.00000	0.00000 ± 0.00000	0.00000 ± 0.00000
iso-hentriacotane (iso-C31)	436	0.00000 ± 0.00000	0.00000 ± 0.00000	0.00000 ± 0.00000	0.00000 ± 0.00000	0.00000 ± 0.00000	0.00000 ± 0.00000
anteiso-hentriacotane (anteiso-C31)	436	0.00000 ± 0.00000	0.00000 ± 0.00000	0.00000 ± 0.00000	0.00000 ± 0.00000	0.00000 ± 0.00000	0.00000 ± 0.00000
iso-dotriacontane (iso-C32)	450	0.00000 ± 0.00000	0.00000 ± 0.00000	0.00000 ± 0.00000	0.00000 ± 0.00000	0.00000 ± 0.00000	0.00000 ± 0.00000
anteiso-dotriacontane (anteiso-C32)	450	0.00000 ± 0.00000	0.00000 ± 0.00000	0.00000 ± 0.00000	0.00000 ± 0.00000	0.00000 ± 0.00000	0.00000 ± 0.00000
iso-tritriactotane (iso-C33)	464	0.00000 ± 0.00000	0.00000 ± 0.00000	0.00000 ± 0.00000	0.00000 ± 0.00000	0.00000 ± 0.00000	0.00000 ± 0.00000
anteiso-tritriactotane (anteiso-C33)	464	0.00000 ± 0.00000	0.00000 ± 0.00000	0.00000 ± 0.00000	0.00000 ± 0.00000	0.00000 ± 0.00000	0.00000 ± 0.00000
iso-tetratriactoane (iso-C34)	478	0.00000 ± 0.00000	0.00000 ± 0.00000	0.00000 ± 0.00000	0.00000 ± 0.00000	0.00000 ± 0.00000	0.00000 ± 0.00000
anteiso-tetratriactoane (anteiso-C34)	478	0.00000 ± 0.00000	0.00000 ± 0.00000	0.00000 ± 0.00000	0.00000 ± 0.00000	0.00000 ± 0.00000	0.00000 ± 0.00000
iso-pentatriacontane (iso-C35)	492	0.00000 ± 0.00000	0.00000 ± 0.00000	0.00000 ± 0.00000	0.00000 ± 0.00000	0.00000 ± 0.00000	0.00000 ± 0.00000
anteiso-pentatriacontane (anteiso-C35)	492	0.00000 ± 0.00000	0.00000 ± 0.00000	0.00000 ± 0.00000	0.00000 ± 0.00000	0.00000 ± 0.00000	0.00000 ± 0.00000
iso-hexatriacontane (iso-C36)	506	0.00000 ± 0.00000	0.00000 ± 0.00000	0.00000 ± 0.00000	0.00000 ± 0.00000	0.00000 ± 0.00000	0.00000 ± 0.00000
anteiso-hexatriacontane (anteiso-C36)	506	0.00000 ± 0.00000	0.00000 ± 0.00000	0.00000 ± 0.00000	0.00000 ± 0.00000	0.00000 ± 0.00000	0.00000 ± 0.00000
iso-heptatriacontane (iso-37)	520	0.00000 ± 0.00000	0.00000 ± 0.00000	0.00000 ± 0.00000	0.00000 ± 0.00000	0.00000 ± 0.00000	0.00000 ± 0.00000
anteiso-heptatriacontane (anteiso-37)	520	0.00000 ± 0.00000	0.00000 ± 0.00000	0.00000 ± 0.00000	0.00000 ± 0.00000	0.00000 ± 0.00000	0.00000 ± 0.00000
hopane							
22,29,30-trisnorneophopane (Ts)	370	0.00559 ± 0.00040	0.00078 ± 0.00006	0.00795 ± 0.00056	0.00770 ± 0.00055	0.00385 ± 0.00027	0.00064 ± 0.00005
22,29,30-trisnorphopane (Tm)	370	0.00642 ± 0.00045	0.00075 ± 0.00005	0.00802 ± 0.00057	0.01200 ± 0.00085	0.00500 ± 0.00035	0.00135 ± 0.00010
αβ-norhopane (C29αβ-hopane)	398	0.03290 ± 0.00233	0.00334 ± 0.00024	0.04025 ± 0.00285	0.03112 ± 0.00221	0.02374 ± 0.00168	0.00514 ± 0.00036
22,29,30-norhopane (29Ts)	398	0.01023 ± 0.00072	0.00087 ± 0.00006	0.01247 ± 0.00088	0.01832 ± 0.00130	0.00691 ± 0.00049	0.00006 ± 0.00000
αα- + βα-norhopane (C29αα- + βα -hopane)	398	0.00261 ± 0.00018	0.00036 ± 0.00003	0.00299 ± 0.00021	0.00373 ± 0.00026	0.00194 ± 0.00014	0.00029 ± 0.00002

Table 6-9. Continued.

PAHs	MW	10kW[a] PEN_04[b]	10kW PEN_05	30kW PEN_06	60kW PEN_08	60kW PEN_09	100kW PEN_13
Alkane/Alkene/Phthalate (continued)							
hopanes (continued)							
αβ-hopane (C30αβ -hopane)	412	0.02149 ± 0.00152	0.00286 ± 0.00020	0.02951 ± 0.00209	0.03352 ± 0.00238	0.01538 ± 0.00109	0.00412 ± 0.00029
αα-hopane (30αα-hopane)	412	0.00069 ± 0.00005	0.00009 ± 0.00001	0.00069 ± 0.00005	0.00080 ± 0.00006	0.00041 ± 0.00003	0.00000 ± 0.00000
βα-hopane (C30βα -hopane)	412	0.00153 ± 0.00011	0.00031 ± 0.00002	0.00198 ± 0.00014	0.00284 ± 0.00020	0.00138 ± 0.00010	0.00000 ± 0.00000
αβS-homohopane (C31αβS-hopane)	426	0.02162 ± 0.00153	0.00219 ± 0.00015	0.02813 ± 0.00199	0.03245 ± 0.00230	0.01587 ± 0.00112	0.00000 ± 0.00000
αβR-homohopane (C31αβR-hopane)	426	0.01847 ± 0.00131	0.00220 ± 0.00016	0.02494 ± 0.00177	0.03238 ± 0.00230	0.01347 ± 0.00095	0.00000 ± 0.00000
αβS-bishomohopane (C32αβS-hopane)	440	0.00723 ± 0.00051	0.00081 ± 0.00006	0.00986 ± 0.00070	0.01187 ± 0.00084	0.00569 ± 0.00040	0.00000 ± 0.00000
αβR-bishomohopane (C32αβR-hopane)	440	0.00497 ± 0.00035	0.00058 ± 0.00004	0.00677 ± 0.00048	0.00808 ± 0.00057	0.00385 ± 0.00027	0.00000 ± 0.00000
22S-trishomohopane (C33)	454	0.00536 ± 0.00038	0.00059 ± 0.00004	0.00648 ± 0.00046	0.00900 ± 0.00064	0.00404 ± 0.00029	0.00000 ± 0.00000
22R-trishomohopane (C33)	454	0.00348 ± 0.00025	0.00036 ± 0.00003	0.00409 ± 0.00029	0.00570 ± 0.00040	0.00253 ± 0.00018	0.00000 ± 0.00000
22S-tretrahomohopane (C34)	468	0.00341 ± 0.00024	0.00032 ± 0.00002	0.00366 ± 0.00026	0.00534 ± 0.00038	0.00245 ± 0.00017	0.00000 ± 0.00000
22R-tetrashomohopane (C34)	468	0.00222 ± 0.00016	0.00021 ± 0.00001	0.00217 ± 0.00015	0.00299 ± 0.00021	0.00167 ± 0.00012	0.00000 ± 0.00000
22S-pentashomohopane(C35)	482	0.00386 ± 0.00027	0.00031 ± 0.00002	0.00423 ± 0.00030	0.00487 ± 0.00035	0.00294 ± 0.00021	0.00000 ± 0.00000
22R-pentashomohopane(C35)	482	0.00254 ± 0.00018	0.00016 ± 0.00001	0.00226 ± 0.00016	0.00356 ± 0.00025	0.00162 ± 0.00011	0.00000 ± 0.00000
sterane							
ααα 20S-Cholestane	372	0.00378 ± 0.00027	0.00030 ± 0.00002	0.00357 ± 0.00025	0.00510 ± 0.00036	0.00180 ± 0.00013	0.00051 ± 0.00004
αββ 20R-Cholestane	372	0.00451 ± 0.00032	0.00057 ± 0.00004	0.00398 ± 0.00028	0.00913 ± 0.00065	0.00294 ± 0.00021	0.00080 ± 0.00006
αββ 20s-Cholestane	372	0.00362 ± 0.00026	0.00046 ± 0.00003	0.00437 ± 0.00031	0.00842 ± 0.00060	0.00264 ± 0.00019	0.00094 ± 0.00007
ααα 20R-Cholestane	372	0.00330 ± 0.00023	0.00046 ± 0.00003	0.00360 ± 0.00025	0.00602 ± 0.00043	0.00192 ± 0.00014	0.00065 ± 0.00005
ααα 20S 24S-Methylcholestane	386	0.00466 ± 0.00033	0.00049 ± 0.00003	0.00215 ± 0.00015	0.00711 ± 0.00050	0.00227 ± 0.00016	0.00017 ± 0.00001
αββ 20R 24S-Methylcholestane	386	0.00244 ± 0.00017	0.00026 ± 0.00002	0.00206 ± 0.00015	0.00381 ± 0.00027	0.00167 ± 0.00012	0.00034 ± 0.00002
αββ 20S 24S-Methylcholestane	386	0.00271 ± 0.00019	0.00033 ± 0.00002	0.00295 ± 0.00021	0.00648 ± 0.00046	0.00187 ± 0.00013	0.00065 ± 0.00005
ααα 20R 24R-Methylcholestane	386	0.00891 ± 0.00063	0.00120 ± 0.00008	0.00764 ± 0.00054	0.01326 ± 0.00094	0.00609 ± 0.00043	0.00070 ± 0.00005
ααα 20S 24R/S-Ethylcholestane	400	0.01685 ± 0.00119	0.00227 ± 0.00016	0.01951 ± 0.00138	0.03177 ± 0.00225	0.01125 ± 0.00080	0.00211 ± 0.00015
αββ 20R 24R-Ethylcholestane	400	0.00778 ± 0.00055	0.00101 ± 0.00007	0.00724 ± 0.00051	0.02466 ± 0.00175	0.00585 ± 0.00041	0.00090 ± 0.00006
αββ 20S 24R-Ethylcholestane	400	0.01004 ± 0.00071	0.00090 ± 0.00006	0.01212 ± 0.00086	0.01722 ± 0.00122	0.00668 ± 0.00047	0.00071 ± 0.00005
ααα 20R 24R-Ethylcholestane	400	0.00318 ± 0.00022	0.00041 ± 0.00003	0.00442 ± 0.00031	0.00841 ± 0.00060	0.00325 ± 0.00023	0.00042 ± 0.00003
methyl-alkane							
2-methylnonadecane	282	0.01101 ± 0.00078	0.00066 ± 0.00005	0.00256 ± 0.00018	0.00125 ± 0.00009	0.00035 ± 0.00002	0.00063 ± 0.00004
3-methylnonadecane	282	0.01533 ± 0.00109	0.00029 ± 0.00002	0.00034 ± 0.00002	0.00050 ± 0.00004	0.00018 ± 0.00001	0.00008 ± 0.00001
branched-alkane							
pristane	268	0.00691 ± 0.00049	0.00201 ± 0.00014	0.00701 ± 0.00050	0.00510 ± 0.00036	0.00223 ± 0.00016	0.00257 ± 0.00018
phytane	282	0.02918 ± 0.00207	0.00228 ± 0.00016	0.01802 ± 0.00128	0.00665 ± 0.00047	0.00260 ± 0.00018	0.00324 ± 0.00023
squalane	422	0.05452 ± 0.00386	0.00000 ± 0.00000	0.00128 ± 0.00009	0.01457 ± 0.00103	0.00014 ± 0.00001	0.00021 ± 0.00001
cycloalkane							
octylcyclohexane	196	0.00067 ± 0.00005	0.00046 ± 0.00003	0.00033 ± 0.00002	0.00040 ± 0.00003	0.00004 ± 0.00000	0.00041 ± 0.00003
decylcyclohexane	224	0.00052 ± 0.00004	0.00022 ± 0.00002	0.00040 ± 0.00003	0.00110 ± 0.00008	0.00034 ± 0.00002	0.00028 ± 0.00002
tridecylcyclohexane	266	0.00937 ± 0.00066	0.00053 ± 0.00004	0.00197 ± 0.00014	0.00093 ± 0.00007	0.00029 ± 0.00002	0.00048 ± 0.00003
n-heptadecylcyclohexane	322	0.02268 ± 0.00161	0.00501 ± 0.00035	0.01026 ± 0.00073	0.02050 ± 0.00145	0.00592 ± 0.00042	0.00292 ± 0.00021
nonadecylcyclohexane	350	0.00808 ± 0.00057	0.00259 ± 0.00018	0.00632 ± 0.00045	0.01968 ± 0.00140	0.00430 ± 0.00030	0.00219 ± 0.00015
alkene							
1-octadecene	252.000	0.00729 ± 0.00052	0.00042 ± 0.00003	0.00427 ± 0.00030	0.00229 ± 0.00016	0.00072 ± 0.00005	0.00115 ± 0.00008
phthalate							
dimethylphthalate	194	0.00037 ± 0.00003	0.00455 ± 0.00032	0.00367 ± 0.00026	0.00001 ± 0.00000	0.00001 ± 0.00000	0.00042 ± 0.00003
diethyl phthalate	222	0.00071 ± 0.00005	0.00112 ± 0.00008	0.00096 ± 0.00007	0.00003 ± 0.00000	0.00000 ± 0.00000	0.00004 ± 0.00000
di-n-butyl phthalate	278	0.00334 ± 0.00024	0.00923 ± 0.00065	0.00355 ± 0.00025	0.00011 ± 0.00001	0.00008 ± 0.00001	0.00026 ± 0.00002

Table 6-9. Continued.

PAHs	MW	10kW[a] PEN_04[b]	10kW PEN_05	30kW PEN_06	60kW PEN_08	60kW PEN_09	100kW PEN_13
Alkane/Alkene/Phthalate (continued)							
phthalate (continued)							
butyl benzyl phthalate	312	0.00000 ± 0.00000	0.00245 ± 0.00017	0.00000 ± 0.00000	0.00033 ± 0.00002	0.00000 ± 0.00000	0.00000 ± 0.00000
bis(2-ethylhexyl)phthalate	390	0.00679 ± 0.00048	0.11335 ± 0.00802	0.00560 ± 0.00040	0.00164 ± 0.00012	0.00043 ± 0.00003	0.00289 ± 0.00020
di-n-octyl phthalate	390	0.00350 ± 0.00025	0.01506 ± 0.00107	0.00242 ± 0.00017	0.00255 ± 0.00018	0.00145 ± 0.00010	0.00000 ± 0.00000

[a] Generator Size
[b] See Table 6-1 for Mnemonic ID definitions

Table 6-10. Summary of the organic species source profiles for the four emission tests conducted for the 13 diesel generators using cold start.

PAHs	MW	10kW[a] PEN_14[b]	30kW PEN_11	60kW PEN_10	100kW PEN_12
acenaphthylene	152	0.00029 ± 0.00002	0.00039 ± 0.00003	0.00103 ± 0.00008	0.00034 ± 0.00002
acenaphthene	154	0.00011 ± 0.00001	0.00015 ± 0.00001	0.00017 ± 0.00001	0.00000 ± 0.00000
fluorene	166	0.00012 ± 0.00001	0.00018 ± 0.00001	0.00033 ± 0.00003	0.00010 ± 0.00001
phenanthrene	178	0.00022 ± 0.00002	0.00025 ± 0.00002	0.00053 ± 0.00004	0.00049 ± 0.00003
anthracene	178	0.00013 ± 0.00001	0.00017 ± 0.00001	0.00019 ± 0.00002	0.00039 ± 0.00003
fluoranthene	202	0.00132 ± 0.00009	0.00118 ± 0.00008	0.00136 ± 0.00011	0.00463 ± 0.00033
pyrene	202	0.00026 ± 0.00002	0.00238 ± 0.00017	0.00107 ± 0.00008	0.00789 ± 0.00056
benzo[a]anthracene	228	0.00184 ± 0.00013	0.00077 ± 0.00005	0.00167 ± 0.00013	0.01045 ± 0.00074
chrysene	228	0.00012 ± 0.00001	0.00153 ± 0.00011	0.00392 ± 0.00031	0.01555 ± 0.00110
benzo[b]fluoranthene	252	0.00149 ± 0.00011	0.00030 ± 0.00002	0.00305 ± 0.00024	0.01361 ± 0.00097
benzo[k]fluoranthene	252	0.00219 ± 0.00016	0.00253 ± 0.00018	0.00251 ± 0.00020	0.00300 ± 0.00021
benzo[a]fluoranthene	252	0.00025 ± 0.00002	0.00043 ± 0.00003	0.00035 ± 0.00003	0.01070 ± 0.00076
benzo[e]pyrene	252	0.00307 ± 0.00022	0.00158 ± 0.00011	0.00404 ± 0.00032	0.01726 ± 0.00122
benzo[a]pyrene	252	0.00148 ± 0.00011	0.00139 ± 0.00010	0.00193 ± 0.00015	0.02510 ± 0.00178
perylene	252	0.00019 ± 0.00001	0.00048 ± 0.00003	0.00024 ± 0.00002	0.00462 ± 0.00033
indeno[1,2,3-cd]pyrene	276	0.00113 ± 0.00008	0.00098 ± 0.00007	0.00165 ± 0.00013	0.01778 ± 0.00126
dibenzo[a,h]anthracene	278	0.00008 ± 0.00001	0.00016 ± 0.00001	0.00012 ± 0.00001	0.00125 ± 0.00009
benzo[ghi]perylene	276	0.00214 ± 0.00015	0.00232 ± 0.00017	0.00361 ± 0.00028	0.02416 ± 0.00171
coronene	300	0.00134 ± 0.00010	0.00212 ± 0.00015	0.00238 ± 0.00019	0.03034 ± 0.00215
dibenzo[a,e]pyrene	302	0.00000 ± 0.00000	0.00023 ± 0.00002	0.00000 ± 0.00000	0.01129 ± 0.00080
2-methylnaphthalene	142	0.00235 ± 0.00017	0.00227 ± 0.00016	0.00941 ± 0.00074	0.00158 ± 0.00011
1-methylnaphthalene	142	0.00038 ± 0.00003	0.00041 ± 0.00003	0.00037 ± 0.00003	0.00008 ± 0.00001
2,6-dimethylnaphthalene	156	0.00195 ± 0.00014	0.00398 ± 0.00029	0.00857 ± 0.00067	0.00104 ± 0.00007
9-fluorenone	180	0.00059 ± 0.00004	0.00039 ± 0.00003	0.00098 ± 0.00008	0.00020 ± 0.00001
9-methylanthracene	192	0.00033 ± 0.00002	0.00041 ± 0.00003	0.00121 ± 0.00010	0.00028 ± 0.00002
anthraquinone	208	0.00170 ± 0.00012	0.00266 ± 0.00019	0.00382 ± 0.00030	0.00023 ± 0.00002
methylfluoranthene	216	0.00040 ± 0.00003	0.00037 ± 0.00003	0.00074 ± 0.00006	0.00189 ± 0.00013
retene	234	0.00002 ± 0.00000	0.00024 ± 0.00002	0.00075 ± 0.00006	0.00009 ± 0.00001
cyclopenta[cd]pyrene	226	0.00052 ± 0.00004	0.00054 ± 0.00004	0.00084 ± 0.00007	0.00613 ± 0.00043
benz[a]anthracene-7,12-dione	258	0.00298 ± 0.00021	0.00000 ± 0.00000	0.00176 ± 0.00014	0.00058 ± 0.00004
methylchrysene	242	0.00031 ± 0.00002	0.00004 ± 0.00000	0.00023 ± 0.00002	0.00022 ± 0.00002
picene	278	0.00008 ± 0.00001	0.00006 ± 0.00000	0.00000 ± 0.00000	0.00113 ± 0.00008
Alkane/Alkene/Phthalate					
***n*-alkane**					
n-pentadecane (*n*-C15)	212	0.00098 ± 0.00007	0.00119 ± 0.00009	0.00347 ± 0.00027	0.00093 ± 0.00007
n-hexadecane (*n*-C16)	226	0.00189 ± 0.00013	0.00191 ± 0.00014	0.00611 ± 0.00048	0.00253 ± 0.00018
n-heptadecane (*n*-C17)	240	0.00303 ± 0.00022	0.00302 ± 0.00022	0.00988 ± 0.00078	0.00230 ± 0.00016
n-octadecane (*n*-C18)	254	0.00709 ± 0.00051	0.00785 ± 0.00056	0.03672 ± 0.00289	0.00416 ± 0.00029
n-nonadecane (*n*-C19)	268	0.03686 ± 0.00263	0.03674 ± 0.00263	0.24188 ± 0.01903	0.00647 ± 0.00046
n-icosane (*n*-C20)	282	0.00236 ± 0.00017	0.10112 ± 0.00725	0.56141 ± 0.04416	0.01497 ± 0.00106
n-heneicosane (*n*-C21)	296	0.00529 ± 0.00038	0.13560 ± 0.00972	0.13827 ± 0.01088	0.02366 ± 0.00168
n-docosane (*n*-C22)	310	0.02735 ± 0.00195	0.11640 ± 0.00835	0.55769 ± 0.04387	0.02116 ± 0.00150
n-tricosane (*n*-C23)	324	0.02495 ± 0.00178	0.06025 ± 0.00432	0.43503 ± 0.03422	0.01455 ± 0.00103
n-tetracosane (*n*-C24)	338	0.00989 ± 0.00070	0.03172 ± 0.00227	0.31361 ± 0.02467	0.01396 ± 0.00099
n-pentacosane (*n*-C25)	352	0.02234 ± 0.00159	0.05604 ± 0.00402	0.24280 ± 0.01910	0.01981 ± 0.00140
n-hexacosane (*n*-C26)	366	0.02252 ± 0.00160	0.00275 ± 0.00020	0.19237 ± 0.01513	0.00356 ± 0.00025
n-heptacosane (*n*-C27)	380	0.00241 ± 0.00017	0.00581 ± 0.00042	0.07308 ± 0.00575	0.00433 ± 0.00031
n-octacosane (*n*-C28)	394	0.00697 ± 0.00050	0.01085 ± 0.00078	0.06325 ± 0.00498	0.03241 ± 0.00230
n-nonacosane (*n*-C29)	408	0.00855 ± 0.00061	0.00000 ± 0.00000	0.05658 ± 0.00445	0.00865 ± 0.00061
n-triacontane (*n*-C30)	422	0.01008 ± 0.00072	0.00000 ± 0.00000	0.06381 ± 0.00502	0.02425 ± 0.00172
n-hentriacotane (*n*-C31)	436	0.00495 ± 0.00035	0.00000 ± 0.00000	0.02432 ± 0.00191	0.01471 ± 0.00104
n-dotriacontane (*n*-C32)	450	0.00158 ± 0.00011	0.00000 ± 0.00000	0.01495 ± 0.00118	0.01479 ± 0.00105
n-tritriactotane (*n*-C33)	464	0.00504 ± 0.00036	0.00000 ± 0.00000	0.00934 ± 0.00073	0.00856 ± 0.00061
n-tetratriactoane (*n*-C34)	478	0.00746 ± 0.00053	0.00000 ± 0.00000	0.03717 ± 0.00292	0.01735 ± 0.00123
n-pentatriacontane (*n*-C35)	492	0.00397 ± 0.00028	0.00000 ± 0.00000	0.03155 ± 0.00248	0.02279 ± 0.00162
n-hexatriacontane (*n*-C36)	506	0.00000 ± 0.00000	0.00000 ± 0.00000	0.00471 ± 0.00037	0.00068 ± 0.00005
n-heptatriacontane (*n*-C37)	520	0.00000 ± 0.00000	0.00000 ± 0.00000	0.01127 ± 0.00089	0.00793 ± 0.00056
n-octatriacontane (*n*-C38)	534	0.00000 ± 0.00000	0.00000 ± 0.00000	0.00908 ± 0.00071	0.00741 ± 0.00053
n-nonatriacontane (*n*-C39)	548	0.00000 ± 0.00000	0.00000 ± 0.00000	0.01239 ± 0.00097	0.00576 ± 0.00041
n-tetracontane (*n*-C40)	562	0.00000 ± 0.00000	0.00000 ± 0.00000	0.02497 ± 0.00196	0.00000 ± 0.00000
n-hentetracontane (*n*-C41)	576	0.00000 ± 0.00000	0.00000 ± 0.00000	0.00000 ± 0.00000	0.00000 ± 0.00000
n-dotetracontane (*n*-C42)	590	0.00000 ± 0.00000	0.00000 ± 0.00000	0.00000 ± 0.00000	0.00000 ± 0.00000

Table 6-10. Continued.

PAHs	MW	10kW[a] PEN_14[b]	30kW PEN_11	60kW PEN_10	100kW PEN_12
Alkane/Alkene/Phthalate (continued)					
iso/anteiso-alkane					
iso-nonacosane (iso-C29)	408	0.00000 ± 0.00000	0.00000 ± 0.00000	0.00000 ± 0.00000	0.00000 ± 0.00000
anteiso-nonacosane (anteiso-C29)	408	0.00000 ± 0.00000	0.00000 ± 0.00000	0.00000 ± 0.00000	0.00000 ± 0.00000
iso-triacontane (iso-C30)	422	0.00000 ± 0.00000	0.00000 ± 0.00000	0.00000 ± 0.00000	0.00000 ± 0.00000
anteiso-triacontane (anteiso-C30)	422	0.00000 ± 0.00000	0.00000 ± 0.00000	0.00000 ± 0.00000	0.00000 ± 0.00000
iso-hentriacotane (iso-C31)	436	0.00000 ± 0.00000	0.00000 ± 0.00000	0.00000 ± 0.00000	0.00000 ± 0.00000
anteiso-hentriacotane (anteiso-C31)	436	0.00000 ± 0.00000	0.00000 ± 0.00000	0.00000 ± 0.00000	0.00000 ± 0.00000
iso-dotriacontane (iso-C32)	450	0.00000 ± 0.00000	0.00000 ± 0.00000	0.00000 ± 0.00000	0.00000 ± 0.00000
anteiso-dotriacontane (anteiso-C32)	450	0.00000 ± 0.00000	0.00000 ± 0.00000	0.00000 ± 0.00000	0.00000 ± 0.00000
iso-tritriactotane (iso-C33)	464	0.00000 ± 0.00000	0.00000 ± 0.00000	0.00000 ± 0.00000	0.00000 ± 0.00000
anteiso-tritriactotane (anteiso-C33)	464	0.00000 ± 0.00000	0.00000 ± 0.00000	0.00000 ± 0.00000	0.00000 ± 0.00000
iso-tetratriactoane (iso-C34)	478	0.00000 ± 0.00000	0.00000 ± 0.00000	0.00000 ± 0.00000	0.00000 ± 0.00000
anteiso-tetratriactoane (anteiso-C34)	478	0.00000 ± 0.00000	0.00000 ± 0.00000	0.00000 ± 0.00000	0.00000 ± 0.00000
iso-pentatriacontane (iso-C35)	492	0.00000 ± 0.00000	0.00000 ± 0.00000	0.00000 ± 0.00000	0.00000 ± 0.00000
anteiso-pentatriacontane (anteiso-C35)	492	0.00000 ± 0.00000	0.00000 ± 0.00000	0.00000 ± 0.00000	0.00000 ± 0.00000
iso-hexatriacontane (iso-C36)	506	0.00000 ± 0.00000	0.00000 ± 0.00000	0.00000 ± 0.00000	0.00000 ± 0.00000
anteiso-hexatriacontane (anteiso-C36)	506	0.00000 ± 0.00000	0.00000 ± 0.00000	0.00000 ± 0.00000	0.00000 ± 0.00000
iso-heptatriacontane (iso-37)	520	0.00000 ± 0.00000	0.00000 ± 0.00000	0.00000 ± 0.00000	0.00000 ± 0.00000
anteiso-heptatriacontane (anteiso-37)	520	0.00000 ± 0.00000	0.00000 ± 0.00000	0.00000 ± 0.00000	0.00000 ± 0.00000
hopane					
22,29,30-trisnorneophopane (Ts)	370	0.00336 ± 0.00024	0.00690 ± 0.00049	0.01785 ± 0.00140	0.00344 ± 0.00024
22,29,30-trisnorphopane (Tm)	370	0.00349 ± 0.00025	0.00859 ± 0.00062	0.02081 ± 0.00164	0.00341 ± 0.00024
αβ-norhopane (C29αβ-hopane)	398	0.01494 ± 0.00106	0.02847 ± 0.00204	0.07542 ± 0.00593	0.01618 ± 0.00115
22,29,30-norhopane (29Ts)	398	0.00308 ± 0.00022	0.00089 ± 0.00006	0.01844 ± 0.00145	0.00327 ± 0.00023
αα- + βα-norhopane (C29αα- + βα -hopane)	398	0.00120 ± 0.00009	0.00170 ± 0.00012	0.00568 ± 0.00045	0.00142 ± 0.00010
αβ-hopane (C30αβ -hopane)	412	0.00964 ± 0.00069	0.01591 ± 0.00114	0.04404 ± 0.00346	0.00982 ± 0.00070
αα-hopane (30αα-hopane)	412	0.00051 ± 0.00004	0.00058 ± 0.00004	0.00168 ± 0.00013	0.00039 ± 0.00003
βα-hopane (C30βα -hopane)	412	0.00152 ± 0.00011	0.00138 ± 0.00010	0.00400 ± 0.00031	0.00105 ± 0.00007
αβS-homohopane (C31αβS-hopane)	426	0.00037 ± 0.00003	0.01180 ± 0.00085	0.03265 ± 0.00257	0.00917 ± 0.00065
αβR-homohopane (C31αβR-hopane)	426	0.00660 ± 0.00047	0.01020 ± 0.00073	0.02700 ± 0.00212	0.00779 ± 0.00055
αβS-bishomohopane (C32αβS-hopane)	440	0.00183 ± 0.00013	0.00332 ± 0.00024	0.00987 ± 0.00078	0.00278 ± 0.00020
αβR-bishomohopane (C32αβR-hopane)	440	0.00185 ± 0.00013	0.00220 ± 0.00016	0.00659 ± 0.00052	0.00194 ± 0.00014
22S-trishomohopane (C33)	454	0.00014 ± 0.00001	0.00173 ± 0.00012	0.00547 ± 0.00043	0.00181 ± 0.00013
22R-trishomohopane (C33)	454	0.00051 ± 0.00004	0.00106 ± 0.00008	0.00320 ± 0.00025	0.00121 ± 0.00009
22S-tretrahomohopane (C34)	468	0.00013 ± 0.00001	0.00073 ± 0.00005	0.00252 ± 0.00020	0.00104 ± 0.00007
22R-tetrashomohopane (C34)	468	0.00025 ± 0.00002	0.00046 ± 0.00003	0.00169 ± 0.00013	0.00068 ± 0.00005
22S-pentashomohopane(C35)	482	0.00030 ± 0.00002	0.00056 ± 0.00004	0.00237 ± 0.00019	0.00099 ± 0.00007
22R-pentashomohopane(C35)	482	0.00017 ± 0.00001	0.00032 ± 0.00002	0.00164 ± 0.00013	0.00079 ± 0.00006
sterane					
ααα 20S-Cholestane	372	0.00007 ± 0.00001	0.00522 ± 0.00037	0.00997 ± 0.00078	0.00132 ± 0.00009
αββ 20R-Cholestane	372	0.00027 ± 0.00002	0.00539 ± 0.00039	0.01629 ± 0.00128	0.00222 ± 0.00016
αββ 20s-Cholestane	372	0.00034 ± 0.00002	0.00742 ± 0.00053	0.01303 ± 0.00103	0.00165 ± 0.00012
ααα 20R-Cholestane	372	0.00039 ± 0.00003	0.00179 ± 0.00013	0.00604 ± 0.00048	0.00168 ± 0.00012
ααα 20S 24S-Methylcholestane	386	0.00319 ± 0.00023	0.00970 ± 0.00070	0.00645 ± 0.00051	0.00117 ± 0.00008
αββ 20R 24S-Methylcholestane	386	0.00069 ± 0.00005	0.00305 ± 0.00022	0.00762 ± 0.00060	0.00127 ± 0.00009
αββ 20S 24S-Methylcholestane	386	0.00069 ± 0.00005	0.00698 ± 0.00050	0.00739 ± 0.00058	0.00127 ± 0.00009
ααα 20R 24R-Methylcholestane	386	0.00258 ± 0.00018	0.01198 ± 0.00086	0.02349 ± 0.00185	0.00418 ± 0.00030
ααα 20S 24R/S-Ethylcholestane	400	0.00033 ± 0.00002	0.02510 ± 0.00180	0.04319 ± 0.00340	0.00807 ± 0.00057
αββ 20R 24R-Ethylcholestane	400	0.00137 ± 0.00010	0.01144 ± 0.00082	0.01912 ± 0.00150	0.00328 ± 0.00023
αββ 20S 24R-Ethylcholestane	400	0.00138 ± 0.00010	0.01226 ± 0.00088	0.02388 ± 0.00188	0.00363 ± 0.00026
ααα 20R 24R-Ethylcholestane	400	0.00047 ± 0.00003	0.00448 ± 0.00032	0.00838 ± 0.00066	0.00174 ± 0.00012
methyl-alkane					
2-methylnonadecane	282	0.00042 ± 0.00003	0.00798 ± 0.00057	0.01882 ± 0.00148	0.00088 ± 0.00006
3-methylnonadecane	282	0.01441 ± 0.00103	0.00084 ± 0.00006	0.01979 ± 0.00156	0.00031 ± 0.00002
branched-alkane					
pristane	268	0.00574 ± 0.00041	0.00541 ± 0.00039	0.01855 ± 0.00146	0.00376 ± 0.00027
phytane	282	0.01168 ± 0.00083	0.01030 ± 0.00074	0.05718 ± 0.00450	0.00462 ± 0.00033
squalane	422	0.04486 ± 0.00320	0.00036 ± 0.00003	0.00293 ± 0.00023	0.00000 ± 0.00000
cycloalkane					
octylcyclohexane	196	0.00084 ± 0.00006	0.00095 ± 0.00007	0.00233 ± 0.00018	0.00034 ± 0.00002
decylcyclohexane	224	0.00025 ± 0.00002	0.00092 ± 0.00007	0.00412 ± 0.00032	0.00030 ± 0.00002
tridecylcyclohexane	266	0.00141 ± 0.00010	0.00272 ± 0.00019	0.01363 ± 0.00107	0.00058 ± 0.00004

Table 6-10. Continued.

PAHs	MW	10kW[a] PEN_14[b]	30kW PEN_11	60kW PEN_10	100kW PEN_12
Alkane/Alkene/Phthalate (continued)					
cycloalkane (continued)					
n-heptadecylcyclohexane	322	0.00939 ± 0.00067	0.00997 ± 0.00071	0.07254 ± 0.00571	0.01175 ± 0.00083
nonadecylcyclohexane	350	0.00047 ± 0.00003	0.00665 ± 0.00048	0.02753 ± 0.00217	0.00535 ± 0.00038
alkene					
1-octadecene	252.000	0.00041 ± 0.00003	0.00159 ± 0.00011	0.00988 ± 0.00078	0.00115 ± 0.00008
phthalate					
dimethylphthalate	194	0.01601 ± 0.00114	0.03104 ± 0.00223	0.06487 ± 0.00510	0.00451 ± 0.00032
diethyl phthalate	222	0.00176 ± 0.00013	0.00221 ± 0.00016	0.01002 ± 0.00079	0.00168 ± 0.00012
di-n-butyl phthalate	278	0.00288 ± 0.00020	0.03273 ± 0.00235	0.08631 ± 0.00679	0.00746 ± 0.00053
butyl benzyl phthalate	312	0.00239 ± 0.00017	0.01406 ± 0.00101	0.02955 ± 0.00232	0.00000 ± 0.00000
bis(2-ethylhexyl)phthalate	390	0.02427 ± 0.00173	0.27478 ± 0.01970	0.82514 ± 0.06491	0.00481 ± 0.00034
di-n-octyl phthalate	390	0.00104 ± 0.00007	0.00959 ± 0.00069	0.02971 ± 0.00234	0.00062 ± 0.00004

[a] Generator Size
[b] See Table 6-1 for Mnemonic ID definitions

Table 6-11. Summary of the organic species source profiles from the ten emission tests conducted for the medium tactical vehicle replacements (MTVRs).

PAHs	MW	MTVR #1 Driving Cycle #1[a] TNP_04[b]	MTVR #1 Driving Cycle #1 TNP_05	MTVR #1 Driving Cycle #1 TNP_06	MTVR #1 Driving Cycle #1 TNP_07	MTVR #1 Driving Cycle #1 TNP_08	MTVR #1 Driving Cycle #2 TNP_09	MTVR #2 Driving Cycle #1 TNP_10	MTVR #2 Driving Cycle #1 TNP_11	MTVR #2 Driving Cycle #1 TNP_12	MTVR #2 Driving Cycle #2 TNP_13
acenaphthylene	152	0.00063 ± 0.00005	N/A ± N/A	N/A ± N/A	0.00105 ± 0.00007	N/A ± N/A	0.00045 ± 0.00004	0.00144 ± 0.00009	0.00095 ± 0.00010	N/A ± N/A	0.00074 ± 0.00007
acenaphthene	154	0.00000 ± 0.00000	N/A ± N/A	N/A ± N/A	0.00000 ± 0.00000	N/A ± N/A	0.00000 ± 0.00000	0.00000 ± 0.00000	0.00000 ± 0.00000	N/A ± N/A	0.00000 ± 0.00000
fluorene	166	0.00024 ± 0.00002	N/A ± N/A	N/A ± N/A	0.00070 ± 0.00004	N/A ± N/A	0.00097 ± 0.00008	0.00067 ± 0.00004	0.00045 ± 0.00005	N/A ± N/A	0.00038 ± 0.00004
phenanthrene	178	0.00150 ± 0.00011	N/A ± N/A	N/A ± N/A	0.00584 ± 0.00037	N/A ± N/A	0.00291 ± 0.00026	0.00665 ± 0.00042	0.00354 ± 0.00036	N/A ± N/A	0.00491 ± 0.00046
anthracene	178	0.00049 ± 0.00003	N/A ± N/A	N/A ± N/A	0.00237 ± 0.00015	N/A ± N/A	0.00058 ± 0.00005	0.00271 ± 0.00017	0.00055 ± 0.00006	N/A ± N/A	0.00056 ± 0.00005
fluoranthene	202	0.00829 ± 0.00059	N/A ± N/A	N/A ± N/A	0.01343 ± 0.00084	N/A ± N/A	0.00481 ± 0.00042	0.01282 ± 0.00081	0.00604 ± 0.00061	N/A ± N/A	0.00754 ± 0.00071
pyrene	202	0.02163 ± 0.00155	N/A ± N/A	N/A ± N/A	0.01905 ± 0.00120	N/A ± N/A	0.00846 ± 0.00074	0.01468 ± 0.00093	0.00984 ± 0.00100	N/A ± N/A	0.01165 ± 0.00110
benzo[a]anthracene	228	0.00150 ± 0.00011	N/A ± N/A	N/A ± N/A	0.00083 ± 0.00005	N/A ± N/A	0.00034 ± 0.00003	0.00070 ± 0.00004	0.00047 ± 0.00005	N/A ± N/A	0.00000 ± 0.00000
chrysene	228	0.00441 ± 0.00032	N/A ± N/A	N/A ± N/A	0.00410 ± 0.00026	N/A ± N/A	0.00126 ± 0.00011	0.00261 ± 0.00016	0.00123 ± 0.00013	N/A ± N/A	0.00000 ± 0.00000
benzo[b]fluoranthene	252	0.00270 ± 0.00019	N/A ± N/A	N/A ± N/A	0.00124 ± 0.00008	N/A ± N/A	0.00351 ± 0.00031	0.00040 ± 0.00003	0.00648 ± 0.00066	N/A ± N/A	0.00000 ± 0.00000
benzo[k]fluoranthene	252	0.00263 ± 0.00019	N/A ± N/A	N/A ± N/A	0.00133 ± 0.00008	N/A ± N/A	0.00265 ± 0.00023	0.00050 ± 0.00003	0.00422 ± 0.00043	N/A ± N/A	0.00000 ± 0.00000
benzo[a]fluoranthene	252	0.00045 ± 0.00003	N/A ± N/A	N/A ± N/A	0.00025 ± 0.00002	N/A ± N/A	0.00032 ± 0.00003	0.00013 ± 0.00001	0.00053 ± 0.00005	N/A ± N/A	0.00000 ± 0.00000
benzo[e]pyrene	252	0.00514 ± 0.00037	N/A ± N/A	N/A ± N/A	0.00230 ± 0.00014	N/A ± N/A	0.00659 ± 0.00058	0.00072 ± 0.00005	0.01062 ± 0.00108	N/A ± N/A	0.00000 ± 0.00000
benzo[a]pyrene	252	0.00248 ± 0.00018	N/A ± N/A	N/A ± N/A	0.00074 ± 0.00005	N/A ± N/A	0.00440 ± 0.00039	0.00011 ± 0.00001	0.00652 ± 0.00066	N/A ± N/A	0.00000 ± 0.00000
perylene	252	0.00026 ± 0.00002	N/A ± N/A	N/A ± N/A	0.00008 ± 0.00001	N/A ± N/A	0.00058 ± 0.00005	0.00000 ± 0.00000	0.00173 ± 0.00018	N/A ± N/A	0.00000 ± 0.00000
indeno[1,2,3-cd]pyrene	276	0.00225 ± 0.00016	N/A ± N/A	N/A ± N/A	0.00031 ± 0.00002	N/A ± N/A	0.00278 ± 0.00024	0.00000 ± 0.00000	0.00514 ± 0.00052	N/A ± N/A	0.00000 ± 0.00000
dibenzo[a,h]anthracene	278	0.00034 ± 0.00002	N/A ± N/A	N/A ± N/A	0.00000 ± 0.00000	N/A ± N/A	0.00000 ± 0.00000	0.00000 ± 0.00000	0.00056 ± 0.00006	N/A ± N/A	0.00000 ± 0.00000
benzo[ghi]perylene	276	0.00361 ± 0.00026	N/A ± N/A	N/A ± N/A	0.00080 ± 0.00005	N/A ± N/A	0.00527 ± 0.00046	0.00000 ± 0.00000	0.00978 ± 0.00100	N/A ± N/A	0.00000 ± 0.00000
coronene	300	0.01457 ± 0.00104	N/A ± N/A	N/A ± N/A	0.00000 ± 0.00000	N/A ± N/A	0.00127 ± 0.00011	0.00000 ± 0.00000	0.00046 ± 0.00005	N/A ± N/A	0.00000 ± 0.00000
dibenzo[a,e]pyrene	302	0.00000 ± 0.00000	N/A ± N/A	N/A ± N/A	0.00000 ± 0.00000	N/A ± N/A	0.00000 ± 0.00000	0.00000 ± 0.00000	0.00000 ± 0.00000	N/A ± N/A	0.00000 ± 0.00000
2-methylnaphthalene	142	0.00074 ± 0.00005	N/A ± N/A	N/A ± N/A	0.01064 ± 0.00067	N/A ± N/A	0.00565 ± 0.00050	0.00783 ± 0.00049	0.01209 ± 0.00123	N/A ± N/A	0.00968 ± 0.00091
1-methylnaphthalene	142	0.00017 ± 0.00001	N/A ± N/A	N/A ± N/A	0.00000 ± 0.00000	N/A ± N/A	0.00055 ± 0.00005	0.00100 ± 0.00006	0.00128 ± 0.00013	N/A ± N/A	0.00000 ± 0.00000
2,6-dimethylnaphthalene	156	0.00164 ± 0.00012	N/A ± N/A	N/A ± N/A	0.00612 ± 0.00038	N/A ± N/A	0.00321 ± 0.00028	0.00767 ± 0.00048	0.00789 ± 0.00080	N/A ± N/A	0.00862 ± 0.00081
9-fluorenone	180	0.00205 ± 0.00015	N/A ± N/A	N/A ± N/A	0.00663 ± 0.00042	N/A ± N/A	0.00446 ± 0.00039	0.01180 ± 0.00074	0.00609 ± 0.00062	N/A ± N/A	0.00515 ± 0.00048
9-methylanthracene	192	0.01128 ± 0.00081	N/A ± N/A	N/A ± N/A	0.01075 ± 0.00068	N/A ± N/A	0.00507 ± 0.00044	0.00935 ± 0.00059	0.00657 ± 0.00067	N/A ± N/A	0.00629 ± 0.00059
anthraquinone	208	0.00334 ± 0.00024	N/A ± N/A	N/A ± N/A	0.00387 ± 0.00024	N/A ± N/A	0.00206 ± 0.00018	0.00241 ± 0.00015	0.00154 ± 0.00016	N/A ± N/A	0.00128 ± 0.00012
methylfluoranthene	216	0.00230 ± 0.00016	N/A ± N/A	N/A ± N/A	0.00097 ± 0.00006	N/A ± N/A	0.00037 ± 0.00003	0.00080 ± 0.00005	0.00029 ± 0.00003	N/A ± N/A	0.00012 ± 0.00001
retene	234	0.00300 ± 0.00021	N/A ± N/A	N/A ± N/A	0.00124 ± 0.00008	N/A ± N/A	0.00069 ± 0.00006	0.00109 ± 0.00007	0.00113 ± 0.00012	N/A ± N/A	0.00107 ± 0.00010
cyclopenta[cd]pyrene	226	0.00000 ± 0.00000	N/A ± N/A	N/A ± N/A	0.00000 ± 0.00000	N/A ± N/A	0.00002 ± 0.00000	0.00000 ± 0.00000	0.00011 ± 0.00001	N/A ± N/A	0.00000 ± 0.00000
benz[a]anthracene-7,12-dione	258	0.00306 ± 0.00022	N/A ± N/A	N/A ± N/A	0.00000 ± 0.00000	N/A ± N/A	0.00051 ± 0.00004	0.00000 ± 0.00000	0.00000 ± 0.00000	N/A ± N/A	0.00000 ± 0.00000
methylchrysene	242	0.00012 ± 0.00001	N/A ± N/A	N/A ± N/A	0.00000 ± 0.00000	N/A ± N/A	0.00000 ± 0.00000	0.00000 ± 0.00000	0.00003 ± 0.00000	N/A ± N/A	0.00000 ± 0.00000
picene	278	0.00000 ± 0.00000	N/A ± N/A	N/A ± N/A	0.00000 ± 0.00000	N/A ± N/A	0.00000 ± 0.00000	0.00000 ± 0.00000	0.00000 ± 0.00000	N/A ± N/A	0.00000 ± 0.00000
Alkane/Alkene/Phthalate											
***n*-alkane**											
n-pentadecane (*n*-C15)	212	0.01235 ± 0.00088	N/A ± N/A	N/A ± N/A	0.00858 ± 0.00054	N/A ± N/A	0.01058 ± 0.00093	0.01148 ± 0.00072	0.02877 ± 0.00293	N/A ± N/A	0.01708 ± 0.00161
n-hexadecane (*n*-C16)	226	0.04455 ± 0.00319	N/A ± N/A	N/A ± N/A	0.01662 ± 0.00104	N/A ± N/A	0.01738 ± 0.00152	0.02556 ± 0.00161	0.06317 ± 0.00643	N/A ± N/A	0.02459 ± 0.00231
n-heptadecane (*n*-C17)	240	0.33627 ± 0.02406	N/A ± N/A	N/A ± N/A	0.03815 ± 0.00240	N/A ± N/A	0.03336 ± 0.00292	0.05553 ± 0.00350	0.15374 ± 0.01565	N/A ± N/A	0.04586 ± 0.00431
n-octadecane (*n*-C18)	254	1.51939 ± 0.10871	N/A ± N/A	N/A ± N/A	0.14011 ± 0.00880	N/A ± N/A	0.07567 ± 0.00663	0.11737 ± 0.00741	0.35151 ± 0.03577	N/A ± N/A	0.11724 ± 0.01102
n-nonadecane (*n*-C19)	268	2.10069 ± 0.15030	N/A ± N/A	N/A ± N/A	0.62964 ± 0.03954	N/A ± N/A	0.25484 ± 0.02232	0.23166 ± 0.01462	0.55703 ± 0.05668	N/A ± N/A	0.29430 ± 0.02767
n-icosane (*n*-C20)	282	2.10346 ± 0.15050	N/A ± N/A	N/A ± N/A	0.96717 ± 0.06073	N/A ± N/A	0.58843 ± 0.05155	0.30453 ± 0.01922	0.74449 ± 0.07576	N/A ± N/A	0.44460 ± 0.04180
n-heneicosane (*n*-C21)	296	1.76008 ± 0.12593	N/A ± N/A	N/A ± N/A	0.70854 ± 0.04449	N/A ± N/A	0.58208 ± 0.05099	0.28667 ± 0.01809	0.75536 ± 0.07687	N/A ± N/A	0.42586 ± 0.04004
n-docosane (*n*-C22)	310	1.46713 ± 0.10497	N/A ± N/A	N/A ± N/A	0.38005 ± 0.02386	N/A ± N/A	0.34342 ± 0.03008	0.23008 ± 0.01452	0.53701 ± 0.05465	N/A ± N/A	0.30725 ± 0.02889
n-tricosane (*n*-C23)	324	0.95929 ± 0.06864	N/A ± N/A	N/A ± N/A	0.16004 ± 0.01005	N/A ± N/A	0.16756 ± 0.01468	0.13195 ± 0.00833	0.27653 ± 0.02814	N/A ± N/A	0.15414 ± 0.01449
n-tetracosane (*n*-C24)	338	0.59304 ± 0.04243	N/A ± N/A	N/A ± N/A	0.07056 ± 0.00443	N/A ± N/A	0.10037 ± 0.00879	0.07952 ± 0.00502	0.18655 ± 0.01898	N/A ± N/A	0.08932 ± 0.00840
n-pentacosane (*n*-C25)	352	0.36577 ± 0.02617	N/A ± N/A	N/A ± N/A	0.04471 ± 0.00281	N/A ± N/A	0.07631 ± 0.00668	0.05410 ± 0.00341	0.11645 ± 0.01185	N/A ± N/A	0.06833 ± 0.00642
n-hexacosane (*n*-C26)	366	0.30580 ± 0.02188	N/A ± N/A	N/A ± N/A	0.02997 ± 0.00188	N/A ± N/A	0.05839 ± 0.00511	0.02400 ± 0.00151	0.07919 ± 0.00806	N/A ± N/A	0.01797 ± 0.00169
n-heptacosane (*n*-C27)	380	0.13727 ± 0.00982	N/A ± N/A	N/A ± N/A	0.01218 ± 0.00076	N/A ± N/A	0.06440 ± 0.00564	0.00929 ± 0.00059	0.08406 ± 0.00855	N/A ± N/A	0.01931 ± 0.00182
n-octacosane (*n*-C28)	394	0.11251 ± 0.00805	N/A ± N/A	N/A ± N/A	0.01145 ± 0.00072	N/A ± N/A	0.05670 ± 0.00497	0.01366 ± 0.00086	0.03332 ± 0.00339	N/A ± N/A	0.00947 ± 0.00089
n-nonacosane (*n*-C29)	408	0.06984 ± 0.00500	N/A ± N/A	N/A ± N/A	0.00805 ± 0.00051	N/A ± N/A	0.04678 ± 0.00410	0.00835 ± 0.00053	0.05483 ± 0.00558	N/A ± N/A	0.02680 ± 0.00252
n-triacontane (*n*-C30)	422	0.03788 ± 0.00271	N/A ± N/A	N/A ± N/A	0.01249 ± 0.00078	N/A ± N/A	0.04880 ± 0.00428	0.00641 ± 0.00040	0.04267 ± 0.00434	N/A ± N/A	0.01842 ± 0.00173
n-hentriacotane (*n*-C31)	436	0.03337 ± 0.00239	N/A ± N/A	N/A ± N/A	0.01157 ± 0.00073	N/A ± N/A	0.02770 ± 0.00243	0.00000 ± 0.00000	0.03350 ± 0.00341	N/A ± N/A	0.01036 ± 0.00097
n-dotriacontane (*n*-C32)	450	0.04980 ± 0.00356	N/A ± N/A	N/A ± N/A	0.00686 ± 0.00043	N/A ± N/A	0.02384 ± 0.00209	0.00000 ± 0.00000	0.05059 ± 0.00515	N/A ± N/A	0.00556 ± 0.00052
n-tritriactotane (*n*-C33)	464	0.08146 ± 0.00583	N/A ± N/A	N/A ± N/A	0.00159 ± 0.00010	N/A ± N/A	0.03513 ± 0.00308	0.00000 ± 0.00000	0.03283 ± 0.00334	N/A ± N/A	0.00000 ± 0.00000
n-tetratriactoane (*n*-C34)	478	0.19221 ± 0.01375	N/A ± N/A	N/A ± N/A	0.00000 ± 0.00000	N/A ± N/A	0.06953 ± 0.00609	0.00000 ± 0.00000	0.03174 ± 0.00323	N/A ± N/A	0.00000 ± 0.00000
n-pentatriacontane (*n*-C35)	492	0.20900 ± 0.01495	N/A ± N/A	N/A ± N/A	0.00000 ± 0.00000	N/A ± N/A	0.06091 ± 0.00534	0.00000 ± 0.00000	0.09753 ± 0.00992	N/A ± N/A	0.00000 ± 0.00000
n-hexatriacontane (*n*-C36)	506	0.00000 ± 0.00000	N/A ± N/A	N/A ± N/A	0.00000 ± 0.00000	N/A ± N/A	0.01719 ± 0.00151	0.00000 ± 0.00000	0.00000 ± 0.00000	N/A ± N/A	0.00000 ± 0.00000
n-heptatriacontane (*n*-C37)	520	0.00000 ± 0.00000	N/A ± N/A	N/A ± N/A	0.00000 ± 0.00000	N/A ± N/A	0.00684 ± 0.00060	0.00000 ± 0.00000	0.00000 ± 0.00000	N/A ± N/A	0.00000 ± 0.00000

n-octatriacontane (*n*-C38)	534	0.00000 ± 0.00000	N/A ± N/A	N/A ± N/A	0.00000 ± 0.00000	N/A ± N/A	0.13494 ± 0.01182	0.00000 ± 0.00000	0.00000 ± 0.00000	N/A ± N/A	0.00000 ± 0.00000

Table 6-11. Continued

PAHs	MW	MTVR #1 Driving Cycle #1[a] TNP_04[b]	MTVR #1 Driving Cycle #1 TNP_05	MTVR #1 Driving Cycle #1 TNP_06	MTVR #1 Driving Cycle #1 TNP_07	MTVR #1 Driving Cycle #1 TNP_08	MTVR #1 Driving Cycle #2 TNP_09	MTVR #2 Driving Cycle #1 TNP_10	MTVR #2 Driving Cycle #1 TNP_11	MTVR #2 Driving Cycle #1 TNP_12	MTVR #2 Driving Cycle #2 TNP_13
Alkane/Alkene/Phthalate (continued)											
***n*-alkane (continued)**											
n-nonatriacontane (*n*-C39)	548	0.00000 ± 0.00000	N/A ± N/A	N/A ± N/A	0.00000 ± 0.00000	N/A ± N/A	0.10996 ± 0.00963	0.00000 ± 0.00000	0.00000 ± 0.00000	N/A ± N/A	0.00000 ± 0.00000
n-tetracontane (*n*-C40)	562	0.04648 ± 0.00333	N/A ± N/A	N/A ± N/A	0.00000 ± 0.00000	N/A ± N/A	0.21348 ± 0.01870	0.00000 ± 0.00000	0.00000 ± 0.00000	N/A ± N/A	0.00000 ± 0.00000
n-hentetracontane (*n*-C41)	576	0.02822 ± 0.00202	N/A ± N/A	N/A ± N/A	0.00000 ± 0.00000	N/A ± N/A	0.18397 ± 0.01612	0.00000 ± 0.00000	0.00000 ± 0.00000	N/A ± N/A	0.00000 ± 0.00000
n-dotetracontane (*n*-C42)	590	0.09197 ± 0.00658	N/A ± N/A	N/A ± N/A	0.00000 ± 0.00000	N/A ± N/A	0.07237 ± 0.00634	0.00000 ± 0.00000	0.00000 ± 0.00000	N/A ± N/A	0.00000 ± 0.00000
iso/anteiso-alkane											
iso-nonacosane (iso-C29)	408	0.00000 ± 0.00000	N/A ± N/A	N/A ± N/A	0.00000 ± 0.00000	N/A ± N/A	0.00000 ± 0.00000	0.00000 ± 0.00000	0.00000 ± 0.00000	N/A ± N/A	0.00000 ± 0.00000
anteiso-nonacosane (anteiso-C29)	408	0.00000 ± 0.00000	N/A ± N/A	N/A ± N/A	0.00000 ± 0.00000	N/A ± N/A	0.00000 ± 0.00000	0.00000 ± 0.00000	0.00000 ± 0.00000	N/A ± N/A	0.00000 ± 0.00000
iso-triacontane (iso-C30)	422	0.00000 ± 0.00000	N/A ± N/A	N/A ± N/A	0.00000 ± 0.00000	N/A ± N/A	0.00000 ± 0.00000	0.00000 ± 0.00000	0.00000 ± 0.00000	N/A ± N/A	0.00000 ± 0.00000
anteiso-triacontane (anteiso-C30)	422	0.00000 ± 0.00000	N/A ± N/A	N/A ± N/A	0.00000 ± 0.00000	N/A ± N/A	0.00000 ± 0.00000	0.00000 ± 0.00000	0.00000 ± 0.00000	N/A ± N/A	0.00000 ± 0.00000
iso-hentriacotane (iso-C31)	436	0.00000 ± 0.00000	N/A ± N/A	N/A ± N/A	0.00000 ± 0.00000	N/A ± N/A	0.00000 ± 0.00000	0.00000 ± 0.00000	0.00000 ± 0.00000	N/A ± N/A	0.00000 ± 0.00000
anteiso-hentriacotane (anteiso-C31)	436	0.00000 ± 0.00000	N/A ± N/A	N/A ± N/A	0.00000 ± 0.00000	N/A ± N/A	0.00000 ± 0.00000	0.00000 ± 0.00000	0.00000 ± 0.00000	N/A ± N/A	0.00000 ± 0.00000
iso-dotriacontane (iso-C32)	450	0.00000 ± 0.00000	N/A ± N/A	N/A ± N/A	0.00000 ± 0.00000	N/A ± N/A	0.00000 ± 0.00000	0.00000 ± 0.00000	0.00000 ± 0.00000	N/A ± N/A	0.00000 ± 0.00000
anteiso-dotriacontane (anteiso-C32)	450	0.00000 ± 0.00000	N/A ± N/A	N/A ± N/A	0.00000 ± 0.00000	N/A ± N/A	0.00000 ± 0.00000	0.00000 ± 0.00000	0.00000 ± 0.00000	N/A ± N/A	0.00000 ± 0.00000
iso-tritriactotane (iso-C33)	464	0.00000 ± 0.00000	N/A ± N/A	N/A ± N/A	0.00000 ± 0.00000	N/A ± N/A	0.00000 ± 0.00000	0.00000 ± 0.00000	0.00000 ± 0.00000	N/A ± N/A	0.00000 ± 0.00000
anteiso-tritriactotane (anteiso-C33)	464	0.00000 ± 0.00000	N/A ± N/A	N/A ± N/A	0.00000 ± 0.00000	N/A ± N/A	0.00000 ± 0.00000	0.00000 ± 0.00000	0.00000 ± 0.00000	N/A ± N/A	0.00000 ± 0.00000
iso-tetratriactoane (iso-C34)	478	0.00000 ± 0.00000	N/A ± N/A	N/A ± N/A	0.00000 ± 0.00000	N/A ± N/A	0.00000 ± 0.00000	0.00000 ± 0.00000	0.00000 ± 0.00000	N/A ± N/A	0.00000 ± 0.00000
anteiso-tetratriactoane (anteiso-C34)	478	0.00000 ± 0.00000	N/A ± N/A	N/A ± N/A	0.00000 ± 0.00000	N/A ± N/A	0.00000 ± 0.00000	0.00000 ± 0.00000	0.00000 ± 0.00000	N/A ± N/A	0.00000 ± 0.00000
iso-pentatriacontane (iso-C35)	492	0.00000 ± 0.00000	N/A ± N/A	N/A ± N/A	0.00000 ± 0.00000	N/A ± N/A	0.00000 ± 0.00000	0.00000 ± 0.00000	0.00000 ± 0.00000	N/A ± N/A	0.00000 ± 0.00000
anteiso-pentatriacontane (anteiso-C35)	492	0.00000 ± 0.00000	N/A ± N/A	N/A ± N/A	0.00000 ± 0.00000	N/A ± N/A	0.00000 ± 0.00000	0.00000 ± 0.00000	0.00000 ± 0.00000	N/A ± N/A	0.00000 ± 0.00000
iso-hexatriacontane (iso-C36)	506	0.00000 ± 0.00000	N/A ± N/A	N/A ± N/A	0.00000 ± 0.00000	N/A ± N/A	0.00000 ± 0.00000	0.00000 ± 0.00000	0.00000 ± 0.00000	N/A ± N/A	0.00000 ± 0.00000
anteiso-hexatriacontane (anteiso-C36)	506	0.00000 ± 0.00000	N/A ± N/A	N/A ± N/A	0.00000 ± 0.00000	N/A ± N/A	0.00000 ± 0.00000	0.00000 ± 0.00000	0.00000 ± 0.00000	N/A ± N/A	0.00000 ± 0.00000
iso-heptatriacontane (iso-37)	520	0.00000 ± 0.00000	N/A ± N/A	N/A ± N/A	0.00000 ± 0.00000	N/A ± N/A	0.00000 ± 0.00000	0.00000 ± 0.00000	0.00000 ± 0.00000	N/A ± N/A	0.00000 ± 0.00000
anteiso-heptatriacontane (anteiso-37)	520	0.00000 ± 0.00000	N/A ± N/A	N/A ± N/A	0.00000 ± 0.00000	N/A ± N/A	0.00000 ± 0.00000	0.00000 ± 0.00000	0.00000 ± 0.00000	N/A ± N/A	0.00000 ± 0.00000
hopane											
22,29,30-trisnorneophopane (Ts)	370	0.00101 ± 0.00007	N/A ± N/A	N/A ± N/A	0.00643 ± 0.00040	N/A ± N/A	0.01001 ± 0.00088	0.00656 ± 0.00041	0.01515 ± 0.00154	N/A ± N/A	0.00735 ± 0.00069
22,29,30-trisnorphopane (Tm)	370	0.00892 ± 0.00064	N/A ± N/A	N/A ± N/A	0.00689 ± 0.00043	N/A ± N/A	0.01118 ± 0.00098	0.00627 ± 0.00040	0.01772 ± 0.00180	N/A ± N/A	0.00869 ± 0.00082
αβ-norhopane (C29αβ-hopane)	398	0.00071 ± 0.00005	N/A ± N/A	N/A ± N/A	0.02943 ± 0.00185	N/A ± N/A	0.04640 ± 0.00406	0.02527 ± 0.00159	0.07127 ± 0.00725	N/A ± N/A	0.03220 ± 0.00303
22,29,30-norhopane (29Ts)	398	0.00070 ± 0.00005	N/A ± N/A	N/A ± N/A	0.00476 ± 0.00030	N/A ± N/A	0.01085 ± 0.00095	0.00392 ± 0.00025	0.01596 ± 0.00162	N/A ± N/A	0.00671 ± 0.00063
αα- + βα-norhopane (C29αα- + βα -hopane)	398	0.00260 ± 0.00019	N/A ± N/A	N/A ± N/A	0.00301 ± 0.00019	N/A ± N/A	0.00309 ± 0.00027	0.00240 ± 0.00015	0.00596 ± 0.00061	N/A ± N/A	0.00230 ± 0.00022
αβ-hopane (C30αβ -hopane)	412	0.00078 ± 0.00006	N/A ± N/A	N/A ± N/A	0.01588 ± 0.00100	N/A ± N/A	0.02716 ± 0.00238	0.01210 ± 0.00076	0.04496 ± 0.00458	N/A ± N/A	0.01528 ± 0.00144
αα-hopane (30αα-hopane)	412	0.00231 ± 0.00017	N/A ± N/A	N/A ± N/A	0.00047 ± 0.00003	N/A ± N/A	0.00206 ± 0.00018	0.00053 ± 0.00003	0.00106 ± 0.00011	N/A ± N/A	0.00083 ± 0.00008
βα-hopane (C30βα -hopane)	412	0.00220 ± 0.00016	N/A ± N/A	N/A ± N/A	0.00095 ± 0.00006	N/A ± N/A	0.00199 ± 0.00017	0.00132 ± 0.00008	0.00336 ± 0.00034	N/A ± N/A	0.00154 ± 0.00015
αβS-homohopane (C31αβS-hopane)	426	0.00166 ± 0.00012	N/A ± N/A	N/A ± N/A	0.01178 ± 0.00074	N/A ± N/A	0.02567 ± 0.00225	0.00986 ± 0.00062	0.04203 ± 0.00428	N/A ± N/A	0.01290 ± 0.00121
αβR-homohopane (C31αβR-hopane)	426	0.02977 ± 0.00213	N/A ± N/A	N/A ± N/A	0.01019 ± 0.00064	N/A ± N/A	0.02088 ± 0.00183	0.00770 ± 0.00049	0.03456 ± 0.00352	N/A ± N/A	0.01092 ± 0.00103
αβS-bishomohopane (C32αβS-hopane)	440	0.00947 ± 0.00068	N/A ± N/A	N/A ± N/A	0.00339 ± 0.00021	N/A ± N/A	0.00777 ± 0.00068	0.00236 ± 0.00015	0.01334 ± 0.00136	N/A ± N/A	0.00381 ± 0.00036
αβR-bishomohopane (C32αβR-hopane)	440	0.00901 ± 0.00064	N/A ± N/A	N/A ± N/A	0.00191 ± 0.00012	N/A ± N/A	0.00564 ± 0.00049	0.00182 ± 0.00011	0.00942 ± 0.00096	N/A ± N/A	0.00245 ± 0.00023
22S-trishomohopane (C33)	454	0.00152 ± 0.00011	N/A ± N/A	N/A ± N/A	0.00206 ± 0.00013	N/A ± N/A	0.00543 ± 0.00048	0.00166 ± 0.00010	0.00979 ± 0.00100	N/A ± N/A	0.00206 ± 0.00019
22R-trishomohopane (C33)	454	0.00039 ± 0.00003	N/A ± N/A	N/A ± N/A	0.00112 ± 0.00007	N/A ± N/A	0.00409 ± 0.00036	0.00091 ± 0.00006	0.00666 ± 0.00068	N/A ± N/A	0.00112 ± 0.00011
22S-tretrahomohopane (C34)	468	0.00073 ± 0.00005	N/A ± N/A	N/A ± N/A	0.00090 ± 0.00006	N/A ± N/A	0.00360 ± 0.00032	0.00078 ± 0.00005	0.00545 ± 0.00055	N/A ± N/A	0.00117 ± 0.00011
22R-tetrashomohopane (C34)	468	0.00407 ± 0.00029	N/A ± N/A	N/A ± N/A	0.00092 ± 0.00006	N/A ± N/A	0.00234 ± 0.00020	0.00049 ± 0.00003	0.00402 ± 0.00041	N/A ± N/A	0.00084 ± 0.00008
22S-pentashomohopane(C35)	482	0.00000 ± 0.00000	N/A ± N/A	N/A ± N/A	0.00099 ± 0.00006	N/A ± N/A	0.00437 ± 0.00038	0.00000 ± 0.00000	0.00683 ± 0.00069	N/A ± N/A	0.00074 ± 0.00007
22R-pentashomohopane(C35)	482	0.01267 ± 0.00091	N/A ± N/A	N/A ± N/A	0.00041 ± 0.00003	N/A ± N/A	0.00202 ± 0.00018	0.00000 ± 0.00000	0.00455 ± 0.00046	N/A ± N/A	0.00044 ± 0.00004
sterane											
ααα 20S-Cholestane	372	0.00000 ± 0.00000	N/A ± N/A	N/A ± N/A	0.00203 ± 0.00013	N/A ± N/A	0.00337 ± 0.00029	0.00171 ± 0.00011	0.00612 ± 0.00062	N/A ± N/A	0.00232 ± 0.00022
αββ 20R-Cholestane	372	0.00174 ± 0.00012	N/A ± N/A	N/A ± N/A	0.00334 ± 0.00021	N/A ± N/A	0.00601 ± 0.00053	0.00356 ± 0.00022	0.01024 ± 0.00104	N/A ± N/A	0.00353 ± 0.00033
αββ 20s-Cholestane	372	0.00173 ± 0.00012	N/A ± N/A	N/A ± N/A	0.00285 ± 0.00018	N/A ± N/A	0.00489 ± 0.00043	0.00276 ± 0.00017	0.00690 ± 0.00070	N/A ± N/A	0.00244 ± 0.00023
ααα 20R-Cholestane	372	0.00547 ± 0.00039	N/A ± N/A	N/A ± N/A	0.00050 ± 0.00003	N/A ± N/A	0.00398 ± 0.00035	0.00263 ± 0.00017	0.00603 ± 0.00061	N/A ± N/A	0.00217 ± 0.00020
ααα 20S 24S-Methylcholestane	386	0.01487 ± 0.00106	N/A ± N/A	N/A ± N/A	0.00298 ± 0.00019	N/A ± N/A	0.00164 ± 0.00014	0.00238 ± 0.00015	0.00374 ± 0.00038	N/A ± N/A	0.00032 ± 0.00003
αββ 20R 24S-Methylcholestane	386	0.00277 ± 0.00020	N/A ± N/A	N/A ± N/A	0.00136 ± 0.00009	N/A ± N/A	0.00193 ± 0.00017	0.00115 ± 0.00007	0.00462 ± 0.00047	N/A ± N/A	0.00145 ± 0.00014
αββ 20S 24S-Methylcholestane	386	0.00326 ± 0.00023	N/A ± N/A	N/A ± N/A	0.00115 ± 0.00007	N/A ± N/A	0.00204 ± 0.00018	0.00141 ± 0.00009	0.00450 ± 0.00046	N/A ± N/A	0.00151 ± 0.00014
ααα 20R 24R-Methylcholestane	386	0.00756 ± 0.00054	N/A ± N/A	N/A ± N/A	0.00500 ± 0.00031	N/A ± N/A	0.00741 ± 0.00065	0.00251 ± 0.00016	0.01497 ± 0.00152	N/A ± N/A	0.00451 ± 0.00042
ααα 20S 24R/S-Ethylcholestane	400	0.02155 ± 0.00154	N/A ± N/A	N/A ± N/A	0.01108 ± 0.00070	N/A ± N/A	0.01896 ± 0.00166	0.00739 ± 0.00047	0.02917 ± 0.00297	N/A ± N/A	0.01045 ± 0.00098
αββ 20R 24R-Ethylcholestane	400	0.00683 ± 0.00049	N/A ± N/A	N/A ± N/A	0.00540 ± 0.00034	N/A ± N/A	0.00935 ± 0.00082	0.00462 ± 0.00029	0.01562 ± 0.00159	N/A ± N/A	0.00367 ± 0.00035
αββ 20S 24R-Ethylcholestane	400	0.00623 ± 0.00045	N/A ± N/A	N/A ± N/A	0.00430 ± 0.00027	N/A ± N/A	0.00894 ± 0.00078	0.00361 ± 0.00023	0.01322 ± 0.00135	N/A ± N/A	0.00414 ± 0.00039
ααα 20R 24R-Ethylcholestane	400	0.00519 ± 0.00037	N/A ± N/A	N/A ± N/A	0.00172 ± 0.00011	N/A ± N/A	0.00338 ± 0.00030	0.00117 ± 0.00007	0.00611 ± 0.00062	N/A ± N/A	0.00168 ± 0.00016
methyl-alkane											

Table 6-11. Continued

PAHs	MW	MTVR #1 Driving Cycle #1[a] TNP_04[b]	MTVR #1 Driving Cycle #1 TNP_05	MTVR #1 Driving Cycle #1 TNP_06	MTVR #1 Driving Cycle #1 TNP_07	MTVR #1 Driving Cycle #1 TNP_08	MTVR #1 Driving Cycle #2 TNP_09	MTVR #2 Driving Cycle #1 TNP_10	MTVR #2 Driving Cycle #1 TNP_11	MTVR #2 Driving Cycle #1 TNP_12	MTVR #2 Driving Cycle #2 TNP_13
Alkane/Alkene/Phthalate (continued)											
2-methylnonadecane	282	0.07688 ± 0.00550	N/A ± N/A	N/A ± N/A	0.04369 ± 0.00274	N/A ± N/A	0.02710 ± 0.00237	0.02511 ± 0.00158	0.03887 ± 0.00396	N/A ± N/A	0.02785 ± 0.00262
3-methylnonadecane	282	0.13006 ± 0.00931	N/A ± N/A	N/A ± N/A	0.06439 ± 0.00404	N/A ± N/A	0.03938 ± 0.00345	0.02121 ± 0.00134	0.05812 ± 0.00591	N/A ± N/A	0.03884 ± 0.00365
branched-alkane											
pristane	268	0.30081 ± 0.02152	N/A ± N/A	N/A ± N/A	0.05478 ± 0.00344	N/A ± N/A	0.03685 ± 0.00323	0.08434 ± 0.00532	0.22534 ± 0.02293	N/A ± N/A	0.06898 ± 0.00648
phytane	282	1.36983 ± 0.09801	N/A ± N/A	N/A ± N/A	0.15623 ± 0.00981	N/A ± N/A	0.07229 ± 0.00633	0.14057 ± 0.00887	0.35324 ± 0.03595	N/A ± N/A	0.16029 ± 0.01507
squalane	422	0.00133 ± 0.00010	N/A ± N/A	N/A ± N/A	0.00052 ± 0.00003	N/A ± N/A	0.00060 ± 0.00005	0.00049 ± 0.00003	0.00087 ± 0.00009	N/A ± N/A	0.00011 ± 0.00001
cycloalkane											
octylcyclohexane	196	0.00105 ± 0.00008	N/A ± N/A	N/A ± N/A	0.00224 ± 0.00014	N/A ± N/A	0.00000 ± 0.00000	0.00000 ± 0.00000	0.00662 ± 0.00067	N/A ± N/A	0.00198 ± 0.00019
decylcyclohexane	224	0.00135 ± 0.00010	N/A ± N/A	N/A ± N/A	0.00463 ± 0.00029	N/A ± N/A	0.00165 ± 0.00014	0.00385 ± 0.00024	0.00385 ± 0.00039	N/A ± N/A	0.00121 ± 0.00011
tridecylcyclohexane	266	0.14085 ± 0.01008	N/A ± N/A	N/A ± N/A	0.03556 ± 0.00223	N/A ± N/A	0.01483 ± 0.00130	0.01560 ± 0.00098	0.03681 ± 0.00375	N/A ± N/A	0.01874 ± 0.00176
n-heptadecylcyclohexane	322	0.11481 ± 0.00821	N/A ± N/A	N/A ± N/A	0.02222 ± 0.00140	N/A ± N/A	0.02616 ± 0.00229	0.02300 ± 0.00145	0.04870 ± 0.00496	N/A ± N/A	0.03089 ± 0.00290
nonadecylcyclohexane	350	0.00059 ± 0.00004	N/A ± N/A	N/A ± N/A	0.00504 ± 0.00032	N/A ± N/A	0.00740 ± 0.00065	0.00640 ± 0.00040	0.01174 ± 0.00119	N/A ± N/A	0.00635 ± 0.00060
alkene											
1-octadecene	252.000	0.00000 ± 0.00000	N/A ± N/A	N/A ± N/A	0.04043 ± 0.00254	N/A ± N/A	0.02090 ± 0.00183	0.03353 ± 0.00212	0.09641 ± 0.00981	N/A ± N/A	0.03133 ± 0.00295
phthalate											
dimethylphthalate	194	0.00114 ± 0.00008	N/A ± N/A	N/A ± N/A	0.00000 ± 0.00000	N/A ± N/A	0.00000 ± 0.00000	0.00000 ± 0.00000	0.00034 ± 0.00004	N/A ± N/A	0.00046 ± 0.00004
diethyl phthalate	222	0.00454 ± 0.00032	N/A ± N/A	N/A ± N/A	0.00036 ± 0.00002	N/A ± N/A	0.00055 ± 0.00005	0.00000 ± 0.00000	0.00015 ± 0.00001	N/A ± N/A	0.00039 ± 0.00004
di-n-butyl phthalate	278	0.00728 ± 0.00052	N/A ± N/A	N/A ± N/A	0.00086 ± 0.00005	N/A ± N/A	0.00091 ± 0.00008	0.00041 ± 0.00003	0.00123 ± 0.00013	N/A ± N/A	0.00000 ± 0.00000
butyl benzyl phthalate	312	0.00000 ± 0.00000	N/A ± N/A	N/A ± N/A	0.00658 ± 0.00041	N/A ± N/A	0.00000 ± 0.00000	0.00000 ± 0.00000	0.00000 ± 0.00000	N/A ± N/A	0.00000 ± 0.00000
bis(2-ethylhexyl)phthalate	390	0.00000 ± 0.00000	N/A ± N/A	N/A ± N/A	0.00000 ± 0.00000	N/A ± N/A	0.00327 ± 0.00029	0.00000 ± 0.00000	0.00674 ± 0.00069	N/A ± N/A	0.00000 ± 0.00000
di-n-octyl phthalate	390	0.00000 ± 0.00000	N/A ± N/A	N/A ± N/A	0.00000 ± 0.00000	N/A ± N/A	0.00000 ± 0.00000	0.00000 ± 0.00000	0.00000 ± 0.00000	N/A ± N/A	0.00000 ± 0.00000

[a] See Figure 6-1 for Drive Cycles #1 and #2

[b] See Table 6-1 for Mnemonic ID definitions and test conditions

Table 6-12. Summary of the organic species source profiles for the four tests conducted for the logistics vehicle system (LVS).

PAHs	MW	LVS Driving Cycle #1[a] TNP_14[b]	LVS Driving Cycle #1 TNP_16	LVS Driving Cycle #1 TNP_17	LVS Driving Cycle #2 TNP_19
acenaphthylene	152	0.00063 ± 0.00003	0.00213 ± 0.00015	0.00092 ± 0.00007	0.00063 ± 0.00005
acenaphthene	154	0.00000 ± 0.00000	0.00000 ± 0.00000	0.00000 ± 0.00000	0.00000 ± 0.00000
fluorene	166	0.00042 ± 0.00002	0.00060 ± 0.00004	0.00070 ± 0.00005	0.00023 ± 0.00002
phenanthrene	178	0.00812 ± 0.00041	0.00925 ± 0.00067	0.00835 ± 0.00060	0.00635 ± 0.00046
anthracene	178	0.00150 ± 0.00008	0.00151 ± 0.00011	0.00142 ± 0.00010	0.00119 ± 0.00009
fluoranthene	202	0.00635 ± 0.00032	0.00613 ± 0.00044	0.00500 ± 0.00036	0.00620 ± 0.00045
pyrene	202	0.00798 ± 0.00040	0.01047 ± 0.00075	0.00734 ± 0.00053	0.00974 ± 0.00070
benzo[a]anthracene	228	0.00014 ± 0.00001	0.00007 ± 0.00000	0.00000 ± 0.00000	0.00000 ± 0.00000
chrysene	228	0.00047 ± 0.00002	0.00003 ± 0.00000	0.00004 ± 0.00000	0.00015 ± 0.00001
benzo[b]fluoranthene	252	0.00013 ± 0.00001	0.00010 ± 0.00001	0.00013 ± 0.00001	0.00016 ± 0.00001
benzo[k]fluoranthene	252	0.00027 ± 0.00001	0.00023 ± 0.00002	0.00019 ± 0.00001	0.00015 ± 0.00001
benzo[a]fluoranthene	252	0.00016 ± 0.00001	0.00014 ± 0.00001	0.00006 ± 0.00000	0.00010 ± 0.00001
benzo[e]pyrene	252	0.00015 ± 0.00001	0.00042 ± 0.00003	0.00036 ± 0.00003	0.00071 ± 0.00005
benzo[a]pyrene	252	0.00009 ± 0.00000	0.00020 ± 0.00001	0.00018 ± 0.00001	0.00030 ± 0.00002
perylene	252	0.00008 ± 0.00000	0.00015 ± 0.00001	0.00005 ± 0.00000	0.00020 ± 0.00001
indeno[1,2,3-cd]pyrene	276	0.00000 ± 0.00000	0.00000 ± 0.00000	0.00000 ± 0.00000	0.00049 ± 0.00004
dibenzo[a,h]anthracene	278	0.00000 ± 0.00000	0.00000 ± 0.00000	0.00000 ± 0.00000	0.00000 ± 0.00000
benzo[ghi]perylene	276	0.00012 ± 0.00001	0.00028 ± 0.00002	0.00048 ± 0.00003	0.00088 ± 0.00006
coronene	300	0.00000 ± 0.00000	0.00000 ± 0.00000	0.00000 ± 0.00000	0.00000 ± 0.00000
dibenzo[a,e]pyrene	302	0.00000 ± 0.00000	0.00000 ± 0.00000	0.00000 ± 0.00000	0.00000 ± 0.00000
2-methylnaphthalene	142	0.00052 ± 0.00003	0.00062 ± 0.00004	0.00103 ± 0.00007	0.00082 ± 0.00006
1-methylnaphthalene	142	0.00014 ± 0.00001	0.00038 ± 0.00003	0.00000 ± 0.00000	0.00000 ± 0.00000
2,6-dimethylnaphthalene	156	0.00205 ± 0.00010	0.00465 ± 0.00033	0.00398 ± 0.00028	0.00222 ± 0.00016
9-fluorenone	180	0.00319 ± 0.00016	0.00266 ± 0.00019	0.00197 ± 0.00014	0.00207 ± 0.00015
9-methylanthracene	192	0.00276 ± 0.00014	0.00254 ± 0.00018	0.00223 ± 0.00016	0.00226 ± 0.00016
anthraquinone	208	0.00061 ± 0.00003	0.00000 ± 0.00000	0.00017 ± 0.00001	0.00035 ± 0.00003
methylfluoranthene	216	0.00022 ± 0.00001	0.00000 ± 0.00000	0.00011 ± 0.00001	0.00013 ± 0.00001
retene	234	0.00034 ± 0.00002	0.00027 ± 0.00002	0.00034 ± 0.00002	0.00022 ± 0.00002
cyclopenta[cd]pyrene	226	0.00000 ± 0.00000	0.00051 ± 0.00004	0.00000 ± 0.00000	0.00001 ± 0.00000
benz[a]anthracene-7,12-dione	258	0.00022 ± 0.00001	0.00000 ± 0.00000	0.00000 ± 0.00000	0.00000 ± 0.00000
methylchrysene	242	0.00000 ± 0.00000	0.00000 ± 0.00000	0.00000 ± 0.00000	0.00000 ± 0.00000
picene	278	0.00000 ± 0.00000	0.00000 ± 0.00000	0.00000 ± 0.00000	0.00000 ± 0.00000
Alkane/Alkene/Phthalate					
***n*-alkane**					
n-pentadecane (*n*-C15)	212	0.00340 ± 0.00017	0.01090 ± 0.00078	0.01059 ± 0.00076	0.00413 ± 0.00030
n-hexadecane (*n*-C16)	226	0.01029 ± 0.00052	0.02309 ± 0.00166	0.02206 ± 0.00158	0.00939 ± 0.00068
n-heptadecane (*n*-C17)	240	0.01875 ± 0.00094	0.04642 ± 0.00334	0.04373 ± 0.00313	0.02402 ± 0.00173
n-octadecane (*n*-C18)	254	0.02827 ± 0.00142	0.05695 ± 0.00410	0.05045 ± 0.00361	0.03536 ± 0.00255
n-nonadecane (*n*-C19)	268	0.03400 ± 0.00170	0.05181 ± 0.00373	0.04070 ± 0.00291	0.02934 ± 0.00211
n-icosane (*n*-C20)	282	0.03607 ± 0.00181	0.06356 ± 0.00457	0.04991 ± 0.00357	0.03804 ± 0.00274
n-heneicosane (*n*-C21)	296	0.03106 ± 0.00156	0.05059 ± 0.00364	0.04367 ± 0.00312	0.03627 ± 0.00261
n-docosane (*n*-C22)	310	0.02309 ± 0.00116	0.03849 ± 0.00277	0.04020 ± 0.00288	0.02880 ± 0.00207
n-tricosane (*n*-C23)	324	0.01153 ± 0.00058	0.01912 ± 0.00138	0.01987 ± 0.00142	0.01815 ± 0.00131
n-tetracosane (*n*-C24)	338	0.02988 ± 0.00150	0.02113 ± 0.00152	0.01690 ± 0.00121	0.02229 ± 0.00161
n-pentacosane (*n*-C25)	352	0.02752 ± 0.00138	0.04205 ± 0.00303	0.03746 ± 0.00268	0.02800 ± 0.00202
n-hexacosane (*n*-C26)	366	0.03248 ± 0.00163	0.00000 ± 0.00000	0.00881 ± 0.00063	0.01787 ± 0.00129
n-heptacosane (*n*-C27)	380	0.02770 ± 0.00139	0.00000 ± 0.00000	0.01978 ± 0.00141	0.03158 ± 0.00228
n-octacosane (*n*-C28)	394	0.01994 ± 0.00100	0.00000 ± 0.00000	0.01510 ± 0.00108	0.00000 ± 0.00000
n-nonacosane (*n*-C29)	408	0.01542 ± 0.00077	0.00000 ± 0.00000	0.01454 ± 0.00104	0.00000 ± 0.00000
n-triacontane (*n*-C30)	422	0.02211 ± 0.00111	0.00000 ± 0.00000	0.01949 ± 0.00139	0.00000 ± 0.00000
n-hentriacotane (*n*-C31)	436	0.00565 ± 0.00028	0.00000 ± 0.00000	0.00000 ± 0.00000	0.00000 ± 0.00000
n-dotriacontane (*n*-C32)	450	0.00798 ± 0.00040	0.00000 ± 0.00000	0.00000 ± 0.00000	0.00000 ± 0.00000
n-tritriactotane (*n*-C33)	464	0.01190 ± 0.00060	0.00000 ± 0.00000	0.00000 ± 0.00000	0.00000 ± 0.00000
n-tetratriactoane (*n*-C34)	478	0.01091 ± 0.00055	0.00000 ± 0.00000	0.00000 ± 0.00000	0.00000 ± 0.00000
n-pentatriacontane (*n*-C35)	492	0.01436 ± 0.00072	0.00000 ± 0.00000	0.00000 ± 0.00000	0.00000 ± 0.00000
n-hexatriacontane (*n*-C36)	506	0.00000 ± 0.00000	0.00000 ± 0.00000	0.00000 ± 0.00000	0.00000 ± 0.00000
n-heptatriacontane (*n*-C37)	520	0.00000 ± 0.00000	0.00000 ± 0.00000	0.00000 ± 0.00000	0.00000 ± 0.00000
n-octatriacontane (*n*-C38)	534	0.00000 ± 0.00000	0.00000 ± 0.00000	0.00000 ± 0.00000	0.00000 ± 0.00000
n-nonatriacontane (*n*-C39)	548	0.00000 ± 0.00000	0.00000 ± 0.00000	0.00000 ± 0.00000	0.00000 ± 0.00000
n-tetracontane (*n*-C40)	562	0.00000 ± 0.00000	0.00000 ± 0.00000	0.00000 ± 0.00000	0.00000 ± 0.00000
n-hentetracontane (*n*-C41)	576	0.00000 ± 0.00000	0.00000 ± 0.00000	0.00000 ± 0.00000	0.00000 ± 0.00000
n-dotetracontane (*n*-C42)	590	0.00000 ± 0.00000	0.00000 ± 0.00000	0.00000 ± 0.00000	0.00000 ± 0.00000

Table 6-12. Continued.

PAHs	MW	LVS Driving Cycle #1[a] TNP_14[b]	LVS Driving Cycle #1 TNP_16	LVS Driving Cycle #1 TNP_17	LVS Driving Cycle #2 TNP_19
Alkane/Alkene/Phthalate (continued)					
iso/anteiso-alkane					
iso-nonacosane (iso-C29)	408	0.00000 ± 0.00000	0.00000 ± 0.00000	0.00000 ± 0.00000	0.00000 ± 0.00000
anteiso-nonacosane (anteiso-C29)	408	0.00000 ± 0.00000	0.00000 ± 0.00000	0.00000 ± 0.00000	0.00000 ± 0.00000
iso-triacontane (iso-C30)	422	0.00000 ± 0.00000	0.00000 ± 0.00000	0.00000 ± 0.00000	0.00000 ± 0.00000
anteiso-triacontane (anteiso-C30)	422	0.00000 ± 0.00000	0.00000 ± 0.00000	0.00000 ± 0.00000	0.00000 ± 0.00000
iso-hentriacotane (iso-C31)	436	0.00000 ± 0.00000	0.00000 ± 0.00000	0.00000 ± 0.00000	0.00000 ± 0.00000
anteiso-hentriacotane (anteiso-C31)	436	0.00000 ± 0.00000	0.00000 ± 0.00000	0.00000 ± 0.00000	0.00000 ± 0.00000
iso-dotriacontane (iso-C32)	450	0.00000 ± 0.00000	0.00000 ± 0.00000	0.00000 ± 0.00000	0.00000 ± 0.00000
anteiso-dotriacontane (anteiso-C32)	450	0.00000 ± 0.00000	0.00000 ± 0.00000	0.00000 ± 0.00000	0.00000 ± 0.00000
iso-tritriactotane (iso-C33)	464	0.00000 ± 0.00000	0.00000 ± 0.00000	0.00000 ± 0.00000	0.00000 ± 0.00000
anteiso-tritriactotane (anteiso-C33)	464	0.00000 ± 0.00000	0.00000 ± 0.00000	0.00000 ± 0.00000	0.00000 ± 0.00000
iso-tetratriactoane (iso-C34)	478	0.00000 ± 0.00000	0.00000 ± 0.00000	0.00000 ± 0.00000	0.00000 ± 0.00000
anteiso-tetratriactoane (anteiso-C34)	478	0.00000 ± 0.00000	0.00000 ± 0.00000	0.00000 ± 0.00000	0.00000 ± 0.00000
iso-pentatriacontane (iso-C35)	492	0.00000 ± 0.00000	0.00000 ± 0.00000	0.00000 ± 0.00000	0.00000 ± 0.00000
anteiso-pentatriacontane (anteiso-C35)	492	0.00000 ± 0.00000	0.00000 ± 0.00000	0.00000 ± 0.00000	0.00000 ± 0.00000
iso-hexatriacontane (iso-C36)	506	0.00000 ± 0.00000	0.00000 ± 0.00000	0.00000 ± 0.00000	0.00000 ± 0.00000
anteiso-hexatriacontane (anteiso-C36)	506	0.00000 ± 0.00000	0.00000 ± 0.00000	0.00000 ± 0.00000	0.00000 ± 0.00000
iso-heptatriacontane (iso-37)	520	0.00000 ± 0.00000	0.00000 ± 0.00000	0.00000 ± 0.00000	0.00000 ± 0.00000
anteiso-heptatriacontane (anteiso-37)	520	0.00000 ± 0.00000	0.00000 ± 0.00000	0.00000 ± 0.00000	0.00000 ± 0.00000
hopane					
22,29,30-trisnorneophopane (Ts)	370	0.00390 ± 0.00020	0.00392 ± 0.00028	0.00386 ± 0.00028	0.00395 ± 0.00028
22,29,30-trisnorphopane (Tm)	370	0.00361 ± 0.00018	0.00438 ± 0.00031	0.00427 ± 0.00031	0.00413 ± 0.00030
αβ-norhopane (C29αβ-hopane)	398	0.01751 ± 0.00088	0.01864 ± 0.00134	0.01829 ± 0.00131	0.01847 ± 0.00133
22,29,30-norhopane (29Ts)	398	0.00327 ± 0.00016	0.00351 ± 0.00025	0.00305 ± 0.00022	0.00384 ± 0.00028
αα- + βα-norhopane (C29αα- + βα -hopane)	398	0.00156 ± 0.00008	0.00146 ± 0.00011	0.00173 ± 0.00012	0.00142 ± 0.00010
αβ-hopane (C30αβ -hopane)	412	0.01070 ± 0.00054	0.00975 ± 0.00070	0.00984 ± 0.00070	0.01115 ± 0.00080
αα-hopane (30αα-hopane)	412	0.00028 ± 0.00001	0.00029 ± 0.00002	0.00033 ± 0.00002	0.00036 ± 0.00003
βα-hopane (C30βα -hopane)	412	0.00101 ± 0.00005	0.00109 ± 0.00008	0.00115 ± 0.00008	0.00103 ± 0.00007
αβS-homohopane (C31αβS-hopane)	426	0.00933 ± 0.00047	0.00852 ± 0.00061	0.00861 ± 0.00062	0.00886 ± 0.00064
αβR-homohopane (C31αβR-hopane)	426	0.00809 ± 0.00041	0.00670 ± 0.00048	0.00694 ± 0.00050	0.00704 ± 0.00051
αβS-bishomohopane (C32αβS-hopane)	440	0.00281 ± 0.00014	0.00235 ± 0.00017	0.00247 ± 0.00018	0.00263 ± 0.00019
αβR-bishomohopane (C32αβR-hopane)	440	0.00192 ± 0.00010	0.00165 ± 0.00012	0.00160 ± 0.00011	0.00170 ± 0.00012
22S-trishomohopane (C33)	454	0.00175 ± 0.00009	0.00129 ± 0.00009	0.00147 ± 0.00011	0.00141 ± 0.00010
22R-trishomohopane (C33)	454	0.00102 ± 0.00005	0.00081 ± 0.00006	0.00078 ± 0.00006	0.00086 ± 0.00006
22S-tretrahomohopane (C34)	468	0.00098 ± 0.00005	0.00078 ± 0.00006	0.00070 ± 0.00005	0.00085 ± 0.00006
22R-tetrashomohopane (C34)	468	0.00062 ± 0.00003	0.00046 ± 0.00003	0.00041 ± 0.00003	0.00053 ± 0.00004
22S-pentashomohopane(C35)	482	0.00100 ± 0.00005	0.00061 ± 0.00004	0.00054 ± 0.00004	0.00074 ± 0.00005
22R-pentashomohopane(C35)	482	0.00047 ± 0.00002	0.00029 ± 0.00002	0.00032 ± 0.00002	0.00043 ± 0.00003
sterane					
ααα 20S-Cholestane	372	0.00154 ± 0.00008	0.00122 ± 0.00009	0.00132 ± 0.00009	0.00122 ± 0.00009
αββ 20R-Cholestane	372	0.00263 ± 0.00013	0.00256 ± 0.00018	0.00260 ± 0.00019	0.00238 ± 0.00017
αββ 20s-Cholestane	372	0.00208 ± 0.00010	0.00193 ± 0.00014	0.00187 ± 0.00013	0.00177 ± 0.00013
ααα 20R-Cholestane	372	0.00139 ± 0.00007	0.00196 ± 0.00014	0.00189 ± 0.00014	0.00163 ± 0.00012
ααα 20S 24S-Methylcholestane	386	0.00228 ± 0.00011	0.00090 ± 0.00006	0.00088 ± 0.00006	0.00066 ± 0.00005
αββ 20R 24S-Methylcholestane	386	0.00118 ± 0.00006	0.00117 ± 0.00008	0.00128 ± 0.00009	0.00123 ± 0.00009
αββ 20S 24S-Methylcholestane	386	0.00149 ± 0.00007	0.00113 ± 0.00008	0.00128 ± 0.00009	0.00144 ± 0.00010
ααα 20R 24R-Methylcholestane	386	0.00422 ± 0.00021	0.00350 ± 0.00025	0.00308 ± 0.00022	0.00349 ± 0.00025
ααα 20S 24R/S-Ethylcholestane	400	0.00517 ± 0.00026	0.00551 ± 0.00040	0.00779 ± 0.00056	0.00644 ± 0.00046
αββ 20R 24R-Ethylcholestane	400	0.00461 ± 0.00023	0.00331 ± 0.00024	0.00362 ± 0.00026	0.00409 ± 0.00029
αββ 20S 24R-Ethylcholestane	400	0.00347 ± 0.00017	0.00336 ± 0.00024	0.00368 ± 0.00026	0.00356 ± 0.00026
ααα 20R 24R-Ethylcholestane	400	0.00154 ± 0.00008	0.00095 ± 0.00007	0.00145 ± 0.00010	0.00134 ± 0.00010
methyl-alkane					
2-methylnonadecane	282	0.00422 ± 0.00021	0.00684 ± 0.00049	0.00622 ± 0.00045	0.00506 ± 0.00036
3-methylnonadecane	282	0.00147 ± 0.00007	0.00104 ± 0.00007	0.00771 ± 0.00055	0.00688 ± 0.00050
branched-alkane					
pristane	268	0.01642 ± 0.00082	0.04402 ± 0.00317	0.04649 ± 0.00333	0.02372 ± 0.00171
phytane	282	0.02018 ± 0.00101	0.03771 ± 0.00271	0.03640 ± 0.00260	0.02322 ± 0.00167
squalane	422	0.00086 ± 0.00004	0.00057 ± 0.00004	0.00048 ± 0.00003	0.00042 ± 0.00003

Table 6-12. Continued.

PAHs	MW	LVS Driving Cycle #1[a] TNP_14[b]	LVS Driving Cycle #1 TNP_16	LVS Driving Cycle #1 TNP_17	LVS Driving Cycle #2 TNP_19
Alkane/Alkene/Phthalate (continued)					
cycloalkane					
octylcyclohexane	196	0.00105 ± 0.00005	0.00143 ± 0.00010	0.00221 ± 0.00016	0.00128 ± 0.00009
decylcyclohexane	224	0.00117 ± 0.00006	0.00126 ± 0.00009	0.00122 ± 0.00009	0.00061 ± 0.00004
tridecylcyclohexane	266	0.00392 ± 0.00020	0.00463 ± 0.00033	0.00473 ± 0.00034	0.00377 ± 0.00027
n-heptadecylcyclohexane	322	0.01508 ± 0.00076	0.01958 ± 0.00141	0.01673 ± 0.00120	0.01701 ± 0.00123
nonadecylcyclohexane	350	0.00503 ± 0.00025	0.00715 ± 0.00051	0.00693 ± 0.00050	0.00682 ± 0.00049
alkene					
1-octadecene	252.000	0.00789 ± 0.00040	0.01502 ± 0.00108	0.01419 ± 0.00102	0.00965 ± 0.00070
phthalate					
dimethylphthalate	194	0.00000 ± 0.00000	0.00003 ± 0.00000	0.00002 ± 0.00000	0.00012 ± 0.00001
diethyl phthalate	222	0.00000 ± 0.00000	0.00025 ± 0.00002	0.00000 ± 0.00000	0.00082 ± 0.00006
di-n-butyl phthalate	278	0.00000 ± 0.00000	0.00103 ± 0.00007	0.00000 ± 0.00000	0.00583 ± 0.00042
butyl benzyl phthalate	312	0.00000 ± 0.00000	0.00000 ± 0.00000	0.00000 ± 0.00000	0.00000 ± 0.00000
bis(2-ethylhexyl)phthalate	390	0.00000 ± 0.00000	0.00000 ± 0.00000	0.00000 ± 0.00000	0.00000 ± 0.00000
di-n-octyl phthalate	390	0.00000 ± 0.00000	0.00000 ± 0.00000	0.00000 ± 0.00000	0.00000 ± 0.00000

[a] See Figure 6-1 for Drive Cycles #1 and #2
[b] See Table 6-1 for Mnemonic ID definitions and test conditions

Table 6-13. Composite organic species source profiles for the 13 military diesel generators and four military diesel vehicles.

PAHs	MW	Warm Start[a] PEN_CP1	Cold Start PEN_CP2	AAV idle[b] TNP_15	MTVR[c] TNP_CP1	LVS[d] TNP_CP2
acenaphthylene	152	0.00007 ± 0.00003	0.00051 ± 0.00035	0.00070 ± 0.00005	0.00088 ± 0.00035	0.00108 ± 0.00071
acenaphthene	154	0.00006 ± 0.00007	0.00011 ± 0.00008	0.00000 ± 0.00000	0.00000 ± 0.00000	0.00000 ± 0.00000
fluorene	166	0.00005 ± 0.00003	0.00018 ± 0.00010	0.00064 ± 0.00005	0.00057 ± 0.00026	0.00049 ± 0.00021
phenanthrene	178	0.00013 ± 0.00005	0.00037 ± 0.00016	0.00720 ± 0.00052	0.00423 ± 0.00193	0.00802 ± 0.00122
anthracene	178	0.00009 ± 0.00004	0.00022 ± 0.00012	0.00114 ± 0.00008	0.00121 ± 0.00104	0.00140 ± 0.00015
fluoranthene	202	0.00112 ± 0.00101	0.00212 ± 0.00167	0.00249 ± 0.00018	0.00882 ± 0.00355	0.00592 ± 0.00062
pyrene	202	0.00207 ± 0.00194	0.00290 ± 0.00344	0.00292 ± 0.00021	0.01422 ± 0.00524	0.00888 ± 0.00147
benzo[a]anthracene	228	0.00070 ± 0.00056	0.00368 ± 0.00454	0.00000 ± 0.00000	0.00064 ± 0.00051	0.00005 ± 0.00006
chrysene	228	0.00177 ± 0.00125	0.00528 ± 0.00702	0.00004 ± 0.00000	0.00227 ± 0.00175	0.00017 ± 0.00020
benzo[b]fluoranthene	252	0.00133 ± 0.00105	0.00462 ± 0.00610	0.00017 ± 0.00001	0.00239 ± 0.00241	0.00013 ± 0.00002
benzo[k]fluoranthene	252	0.00127 ± 0.00086	0.00256 ± 0.00033	0.00011 ± 0.00001	0.00189 ± 0.00157	0.00021 ± 0.00005
benzo[a]fluoranthene	252	0.00021 ± 0.00026	0.00293 ± 0.00518	0.00016 ± 0.00001	0.00028 ± 0.00020	0.00012 ± 0.00004
benzo[e]pyrene	252	0.00190 ± 0.00124	0.00649 ± 0.00725	0.00008 ± 0.00001	0.00423 ± 0.00403	0.00041 ± 0.00023
benzo[a]pyrene	252	0.00071 ± 0.00056	0.00747 ± 0.01176	0.00006 ± 0.00000	0.00237 ± 0.00263	0.00019 ± 0.00009
perylene	252	0.00009 ± 0.00006	0.00138 ± 0.00216	0.00001 ± 0.00000	0.00044 ± 0.00067	0.00012 ± 0.00007
indeno[1,2,3-cd]pyrene	276	0.00047 ± 0.00033	0.00538 ± 0.00827	0.00008 ± 0.00001	0.00175 ± 0.00205	0.00012 ± 0.00024
dibenzo[a,h]anthracene	278	0.00010 ± 0.00011	0.00040 ± 0.00057	0.00000 ± 0.00000	0.00015 ± 0.00024	0.00000 ± 0.00000
benzo[ghi]perylene	276	0.00081 ± 0.00050	0.00806 ± 0.01076	0.00024 ± 0.00002	0.00324 ± 0.00385	0.00044 ± 0.00033
coronene	300	0.00017 ± 0.00021	0.00904 ± 0.01420	0.00000 ± 0.00000	0.00272 ± 0.00583	0.00000 ± 0.00000
dibenzo[a,e]pyrene	302	0.00000 ± 0.00000	0.00288 ± 0.00561	0.00000 ± 0.00000	0.00000 ± 0.00000	0.00000 ± 0.00000
2-methylnaphthalene	142	0.00126 ± 0.00112	0.00390 ± 0.00369	0.00209 ± 0.00015	0.00777 ± 0.00411	0.00075 ± 0.00023
1-methylnaphthalene	142	0.00019 ± 0.00033	0.00031 ± 0.00015	0.00044 ± 0.00003	0.00050 ± 0.00054	0.00013 ± 0.00018
2,6-dimethylnaphthalene	156	0.00045 ± 0.00021	0.00388 ± 0.00336	0.00289 ± 0.00021	0.00586 ± 0.00283	0.00322 ± 0.00129
9-fluorenone	180	0.00018 ± 0.00006	0.00054 ± 0.00033	0.00343 ± 0.00025	0.00603 ± 0.00325	0.00247 ± 0.00056
9-methylanthracene	192	0.00028 ± 0.00022	0.00056 ± 0.00044	0.00213 ± 0.00015	0.00822 ± 0.00258	0.00245 ± 0.00025
anthraquinone	208	0.00030 ± 0.00034	0.00210 ± 0.00152	0.00032 ± 0.00002	0.00242 ± 0.00102	0.00028 ± 0.00026
methylfluoranthene	216	0.00026 ± 0.00030	0.00085 ± 0.00071	0.00005 ± 0.00000	0.00081 ± 0.00080	0.00011 ± 0.00009
retene	234	0.00022 ± 0.00022	0.00027 ± 0.00033	0.00024 ± 0.00002	0.00137 ± 0.00082	0.00029 ± 0.00006
cyclopenta[cd]pyrene	226	0.00012 ± 0.00014	0.00201 ± 0.00275	0.00000 ± 0.00000	0.00002 ± 0.00004	0.00013 ± 0.00025
benz[a]anthracene-7,12-dione	258	0.00056 ± 0.00057	0.00133 ± 0.00132	0.00000 ± 0.00000	0.00059 ± 0.00122	0.00005 ± 0.00011
methylchrysene	242	0.00006 ± 0.00006	0.00020 ± 0.00011	0.00000 ± 0.00000	0.00003 ± 0.00005	0.00000 ± 0.00000
picene	278	0.00006 ± 0.00007	0.00032 ± 0.00054	0.00000 ± 0.00000	0.00000 ± 0.00000	0.00000 ± 0.00000
Alkane/Alkene/Phthalate						
***n*-alkane**						
n-pentadecane (*n*-C15)	212	0.00127 ± 0.00061	0.00164 ± 0.00122	0.00855 ± 0.00062	0.01481 ± 0.00740	0.00726 ± 0.00404
n-hexadecane (*n*-C16)	226	0.00189 ± 0.00086	0.00311 ± 0.00202	0.02439 ± 0.00176	0.03198 ± 0.01831	0.01621 ± 0.00737
n-heptadecane (*n*-C17)	240	0.00292 ± 0.00162	0.00456 ± 0.00356	0.06176 ± 0.00446	0.11049 ± 0.11935	0.03323 ± 0.01389
n-octadecane (*n*-C18)	254	0.00943 ± 0.00940	0.01395 ± 0.01526	0.06249 ± 0.00451	0.38688 ± 0.56337	0.04276 ± 0.01323
n-nonadecane (*n*-C19)	268	0.03204 ± 0.05301	0.08049 ± 0.10854	0.04954 ± 0.00358	0.67803 ± 0.71645	0.03896 ± 0.00975
n-icosane (*n*-C20)	282	0.06608 ± 0.12007	0.16996 ± 0.26463	0.05316 ± 0.00384	0.85878 ± 0.65205	0.04689 ± 0.01268
n-heneicosane (*n*-C21)	296	0.06571 ± 0.10056	0.07571 ± 0.07111	0.04264 ± 0.00308	0.75310 ± 0.52343	0.04039 ± 0.00854
n-docosane (*n*-C22)	310	0.08681 ± 0.11805	0.18065 ± 0.25510	0.03253 ± 0.00235	0.54416 ± 0.46345	0.03264 ± 0.00811
n-tricosane (*n*-C23)	324	0.08034 ± 0.09668	0.13370 ± 0.20184	0.02404 ± 0.00174	0.30825 ± 0.32294	0.01717 ± 0.00382
n-tetracosane (*n*-C24)	338	0.07015 ± 0.08222	0.09230 ± 0.14785	0.03854 ± 0.00278	0.18656 ± 0.20348	0.02255 ± 0.00541
n-pentacosane (*n*-C25)	352	0.05944 ± 0.06214	0.08525 ± 0.10633	0.02358 ± 0.00170	0.12095 ± 0.12247	0.03376 ± 0.00718
n-hexacosane (*n*-C26)	366	0.05481 ± 0.06311	0.05530 ± 0.09184	0.00000 ± 0.00000	0.08589 ± 0.11021	0.01479 ± 0.01387
n-heptacosane (*n*-C27)	380	0.03813 ± 0.03858	0.02141 ± 0.03448	0.00000 ± 0.00000	0.05442 ± 0.05079	0.01977 ± 0.01406
n-octacosane (*n*-C28)	394	0.02786 ± 0.02516	0.02837 ± 0.02581	0.00000 ± 0.00000	0.03952 ± 0.04005	0.00876 ± 0.01031
n-nonacosane (*n*-C29)	408	0.02449 ± 0.01650	0.01844 ± 0.02574	0.00000 ± 0.00000	0.03578 ± 0.02548	0.00749 ± 0.00866
n-triacontane (*n*-C30)	422	0.02615 ± 0.02682	0.02454 ± 0.02801	0.00000 ± 0.00000	0.02778 ± 0.01757	0.01040 ± 0.01206
n-hentriacotane (*n*-C31)	436	0.02027 ± 0.01701	0.01099 ± 0.01078	0.00000 ± 0.00000	0.01942 ± 0.01401	0.00141 ± 0.00283
n-dotriacontane (*n*-C32)	450	0.00860 ± 0.00774	0.00783 ± 0.00815	0.00000 ± 0.00000	0.02278 ± 0.02269	0.00199 ± 0.00399
n-tritriactotane (*n*-C33)	464	0.00772 ± 0.01086	0.00573 ± 0.00425	0.00000 ± 0.00000	0.02517 ± 0.03209	0.00297 ± 0.00595
n-tetratriactoane (*n*-C34)	478	0.01027 ± 0.01565	0.01549 ± 0.01610	0.00000 ± 0.00000	0.04891 ± 0.07541	0.00273 ± 0.00545
n-pentatriacontane (*n*-C35)	492	0.01031 ± 0.01594	0.01458 ± 0.01506	0.00000 ± 0.00000	0.06124 ± 0.08295	0.00359 ± 0.00718
n-hexatriacontane (*n*-C36)	506	0.00141 ± 0.00257	0.00135 ± 0.00226	0.00000 ± 0.00000	0.00287 ± 0.00702	0.00000 ± 0.00000
n-heptatriacontane (*n*-C37)	520	0.00083 ± 0.00166	0.00480 ± 0.00571	0.00000 ± 0.00000	0.00114 ± 0.00279	0.00000 ± 0.00000
n-octatriacontane (*n*-C38)	534	0.00295 ± 0.00722	0.00412 ± 0.00481	0.00000 ± 0.00000	0.02249 ± 0.05509	0.00000 ± 0.00000
n-nonatriacontane (*n*-C39)	548	0.00147 ± 0.00361	0.00454 ± 0.00590	0.00000 ± 0.00000	0.01833 ± 0.04489	0.00000 ± 0.00000
n-tetracontane (*n*-C40)	562	0.00000 ± 0.00000	0.00624 ± 0.01248	0.00000 ± 0.00000	0.04333 ± 0.08541	0.00000 ± 0.00000
n-hentetracontane (*n*-C41)	576	0.00000 ± 0.00000	0.00000 ± 0.00000	0.00000 ± 0.00000	0.03536 ± 0.07367	0.00000 ± 0.00000
n-dotetracontane (*n*-C42)	590	0.00000 ± 0.00000	0.00000 ± 0.00000	0.00000 ± 0.00000	0.02739 ± 0.04288	0.00000 ± 0.00000
iso/anteiso-alkane						
iso-nonacosane (iso-C29)	408	0.00000 ± 0.00000	0.00000 ± 0.00000	0.00000 ± 0.00000	0.00000 ± 0.00000	0.00000 ± 0.00000
anteiso-nonacosane (anteiso-C29)	408	0.00000 ± 0.00000	0.00000 ± 0.00000	0.00000 ± 0.00000	0.00000 ± 0.00000	0.00000 ± 0.00000
iso-triacontane (iso-C30)	422	0.00000 ± 0.00000	0.00000 ± 0.00000	0.00000 ± 0.00000	0.00000 ± 0.00000	0.00000 ± 0.00000
anteiso-triacontane (anteiso-C30)	422	0.00000 ± 0.00000	0.00000 ± 0.00000	0.00000 ± 0.00000	0.00000 ± 0.00000	0.00000 ± 0.00000
iso-hentriacotane (iso-C31)	436	0.00000 ± 0.00000	0.00000 ± 0.00000	0.00000 ± 0.00000	0.00000 ± 0.00000	0.00000 ± 0.00000
anteiso-hentriacotane (anteiso-C31)	436	0.00000 ± 0.00000	0.00000 ± 0.00000	0.00000 ± 0.00000	0.00000 ± 0.00000	0.00000 ± 0.00000
iso-dotriacontane (iso-C32)	450	0.00000 ± 0.00000	0.00000 ± 0.00000	0.00000 ± 0.00000	0.00000 ± 0.00000	0.00000 ± 0.00000
anteiso-dotriacontane (anteiso-C32)	450	0.00000 ± 0.00000	0.00000 ± 0.00000	0.00000 ± 0.00000	0.00000 ± 0.00000	0.00000 ± 0.00000
iso-tritriactotane (iso-C33)	464	0.00000 ± 0.00000	0.00000 ± 0.00000	0.00000 ± 0.00000	0.00000 ± 0.00000	0.00000 ± 0.00000

Table 6-13. Continued.

PAHs	MW	Warm Start[a] PEN_CP1	Cold Start PEN_CP2	AAV idle[b] TNP_15	MTVR[c] TNP_CP1	LVS[d] TNP_CP2
Alkane/Alkene/Phthalate (continued)						
iso/anteiso-alkane (continued)						
anteiso-tritriactotane (anteiso-C33)	464	0.00000 ± 0.00000	0.00000 ± 0.00000	0.00000 ± 0.00000	0.00000 ± 0.00000	0.00000 ± 0.00000
iso-tetratriactoane (iso-C34)	478	0.00000 ± 0.00000	0.00000 ± 0.00000	0.00000 ± 0.00000	0.00000 ± 0.00000	0.00000 ± 0.00000
anteiso-tetratriactoane (anteiso-C34)	478	0.00000 ± 0.00000	0.00000 ± 0.00000	0.00000 ± 0.00000	0.00000 ± 0.00000	0.00000 ± 0.00000
iso-pentatriacontane (iso-C35)	492	0.00000 ± 0.00000	0.00000 ± 0.00000	0.00000 ± 0.00000	0.00000 ± 0.00000	0.00000 ± 0.00000
anteiso-pentatriacontane (anteiso-C35)	492	0.00000 ± 0.00000	0.00000 ± 0.00000	0.00000 ± 0.00000	0.00000 ± 0.00000	0.00000 ± 0.00000
iso-hexatriacontane (iso-C36)	506	0.00000 ± 0.00000	0.00000 ± 0.00000	0.00000 ± 0.00000	0.00000 ± 0.00000	0.00000 ± 0.00000
anteiso-hexatriacontane (anteiso-C36)	506	0.00000 ± 0.00000	0.00000 ± 0.00000	0.00000 ± 0.00000	0.00000 ± 0.00000	0.00000 ± 0.00000
iso-heptatriacontane (iso-37)	520	0.00000 ± 0.00000	0.00000 ± 0.00000	0.00000 ± 0.00000	0.00000 ± 0.00000	0.00000 ± 0.00000
anteiso-heptatriacontane (anteiso-37)	520	0.00000 ± 0.00000	0.00000 ± 0.00000	0.00000 ± 0.00000	0.00000 ± 0.00000	0.00000 ± 0.00000
hopane						
22,29,30-trisnorneophopane (Ts)	370	0.00442 ± 0.00324	0.00789 ± 0.00684	0.00253 ± 0.00018	0.00775 ± 0.00466	0.00391 ± 0.00004
22,29,30-trisnorphopane (Tm)	370	0.00559 ± 0.00423	0.00908 ± 0.00819	0.00265 ± 0.00019	0.00995 ± 0.00418	0.00410 ± 0.00034
αβ-norhopane (C29αβ-hopane)	398	0.02275 ± 0.01528	0.03375 ± 0.02844	0.01239 ± 0.00089	0.03421 ± 0.02346	0.01823 ± 0.00050
22,29,30-norhopane (29Ts)	398	0.00814 ± 0.00702	0.00642 ± 0.00808	0.00186 ± 0.00013	0.00715 ± 0.00546	0.00342 ± 0.00034
αα- + βα-norhopane (C29αα- + βα -hopane)	398	0.00199 ± 0.00141	0.00250 ± 0.00213	0.00100 ± 0.00007	0.00323 ± 0.00137	0.00154 ± 0.00014
αβ-hopane (C30αβ -hopane)	412	0.01781 ± 0.01276	0.01985 ± 0.01639	0.00717 ± 0.00052	0.01936 ± 0.01512	0.01036 ± 0.00068
αα-hopane (30αα-hopane)	412	0.00045 ± 0.00034	0.00079 ± 0.00060	0.00014 ± 0.00001	0.00121 ± 0.00079	0.00031 ± 0.00004
βα-hopane (C30βα -hopane)	412	0.00134 ± 0.00105	0.00199 ± 0.00136	0.00081 ± 0.00006	0.00189 ± 0.00085	0.00107 ± 0.00006
αβS-homohopane (C31αβS-hopane)	426	0.01671 ± 0.01337	0.01350 ± 0.01367	0.00631 ± 0.00046	0.01732 ± 0.01436	0.00883 ± 0.00036
αβR-homohopane (C31αβR-hopane)	426	0.01524 ± 0.01268	0.01290 ± 0.00952	0.00513 ± 0.00037	0.01900 ± 0.01124	0.00719 ± 0.00062
αβS-bishomohopane (C32αβS-hopane)	440	0.00591 ± 0.00477	0.00445 ± 0.00367	0.00174 ± 0.00013	0.00669 ± 0.00427	0.00256 ± 0.00020
αβR-bishomohopane (C32αβR-hopane)	440	0.00404 ± 0.00326	0.00315 ± 0.00230	0.00125 ± 0.00009	0.00504 ± 0.00353	0.00172 ± 0.00014
22S-trishomohopane (C33)	454	0.00424 ± 0.00347	0.00229 ± 0.00226	0.00104 ± 0.00008	0.00375 ± 0.00330	0.00148 ± 0.00019
22R-trishomohopane (C33)	454	0.00269 ± 0.00221	0.00149 ± 0.00118	0.00079 ± 0.00006	0.00238 ± 0.00247	0.00087 ± 0.00011
22S-tretrahomohopane (C34)	468	0.00253 ± 0.00206	0.00110 ± 0.00102	0.00057 ± 0.00004	0.00211 ± 0.00197	0.00083 ± 0.00012
22R-tetrashomohopane (C34)	468	0.00154 ± 0.00119	0.00077 ± 0.00064	0.00042 ± 0.00003	0.00211 ± 0.00163	0.00051 ± 0.00009
22S-pentashomohopane(C35)	482	0.00270 ± 0.00207	0.00106 ± 0.00092	0.00047 ± 0.00003	0.00215 ± 0.00281	0.00072 ± 0.00020
22R-pentashomohopane(C35)	482	0.00169 ± 0.00140	0.00073 ± 0.00066	0.00028 ± 0.00002	0.00335 ± 0.00487	0.00038 ± 0.00008
sterane						
ααα 20S-Cholestane	372	0.00251 ± 0.00194	0.00415 ± 0.00446	0.00088 ± 0.00006	0.00259 ± 0.00205	0.00132 ± 0.00015
αββ 20R-Cholestane	372	0.00365 ± 0.00313	0.00604 ± 0.00715	0.00159 ± 0.00011	0.00474 ± 0.00302	0.00254 ± 0.00011
αββ 20s-Cholestane	372	0.00341 ± 0.00288	0.00561 ± 0.00582	0.00120 ± 0.00009	0.00359 ± 0.00193	0.00191 ± 0.00013
ααα 20R-Cholestane	372	0.00266 ± 0.00210	0.00247 ± 0.00246	0.00049 ± 0.00004	0.00346 ± 0.00210	0.00172 ± 0.00026
ααα 20S 24S-Methylcholestane	386	0.00281 ± 0.00265	0.00513 ± 0.00375	0.00066 ± 0.00005	0.00432 ± 0.00530	0.00118 ± 0.00074
αββ 20R 24S-Methylcholestane	386	0.00176 ± 0.00134	0.00316 ± 0.00314	0.00072 ± 0.00005	0.00221 ± 0.00131	0.00122 ± 0.00005
αββ 20S 24S-Methylcholestane	386	0.00250 ± 0.00222	0.00408 ± 0.00359	0.00078 ± 0.00006	0.00231 ± 0.00131	0.00133 ± 0.00016
ααα 20R 24R-Methylcholestane	386	0.00630 ± 0.00478	0.01056 ± 0.00955	0.00211 ± 0.00015	0.00699 ± 0.00434	0.00357 ± 0.00047
ααα 20S 24R/S-Ethylcholestane	400	0.01396 ± 0.01132	0.01917 ± 0.01906	0.00355 ± 0.00026	0.01643 ± 0.00826	0.00623 ± 0.00117
αββ 20R 24R-Ethylcholestane	400	0.00790 ± 0.00874	0.00880 ± 0.00815	0.00274 ± 0.00020	0.00758 ± 0.00441	0.00391 ± 0.00057
αββ 20S 24R-Ethylcholestane	400	0.00795 ± 0.00650	0.01029 ± 0.01020	0.00225 ± 0.00016	0.00674 ± 0.00373	0.00352 ± 0.00014
ααα 20R 24R-Ethylcholestane	400	0.00335 ± 0.00297	0.00377 ± 0.00350	0.00090 ± 0.00006	0.00321 ± 0.00205	0.00132 ± 0.00026
methyl-alkane						
2-methylnonadecane	282	0.00275 ± 0.00413	0.00703 ± 0.00859	0.01761 ± 0.00127	0.03992 ± 0.01955	0.00559 ± 0.00117
3-methylnonadecane	282	0.00278 ± 0.00615	0.00884 ± 0.00979	0.01229 ± 0.00089	0.05867 ± 0.03821	0.00427 ± 0.00351
branched-alkane						
pristane	268	0.00430 ± 0.00233	0.00837 ± 0.00685	0.06326 ± 0.00457	0.12851 ± 0.10807	0.03266 ± 0.01488
phytane	282	0.01033 ± 0.01098	0.02094 ± 0.02435	0.04317 ± 0.00312	0.37541 ± 0.49613	0.02938 ± 0.00897
squalane	422	0.01179 ± 0.02169	0.01204 ± 0.02192	0.00131 ± 0.00009	0.00065 ± 0.00041	0.00058 ± 0.00020
cycloalkane						
octylcyclohexane	196	0.00039 ± 0.00020	0.00112 ± 0.00085	0.00041 ± 0.00003	0.00198 ± 0.00246	0.00149 ± 0.00050
decylcyclohexane	224	0.00047 ± 0.00032	0.00140 ± 0.00184	0.00095 ± 0.00007	0.00275 ± 0.00152	0.00107 ± 0.00031
tridecylcyclohexane	266	0.00226 ± 0.00353	0.00458 ± 0.00609	0.00244 ± 0.00018	0.04373 ± 0.04858	0.00426 ± 0.00049
n-heptadecylcyclohexane	322	0.01121 ± 0.00841	0.02591 ± 0.03110	0.00950 ± 0.00069	0.04430 ± 0.03589	0.01710 ± 0.00186
nonadecylcyclohexane	350	0.00719 ± 0.00651	0.01000 ± 0.01199	0.00438 ± 0.00032	0.00625 ± 0.00360	0.00648 ± 0.00098
alkene						
1-octadecene	252.000	0.00269 ± 0.00265	0.00326 ± 0.00444	0.01688 ± 0.00122	0.03710 ± 0.03229	0.01169 ± 0.00346
phthalate						
dimethylphthalate	194	0.00150 ± 0.00205	0.02911 ± 0.02620	0.00003 ± 0.00000	0.00032 ± 0.00045	0.00004 ± 0.00005
diethyl phthalate	222	0.00048 ± 0.00051	0.00392 ± 0.00408	0.00000 ± 0.00000	0.00100 ± 0.00175	0.00027 ± 0.00039
di-n-butyl phthalate	278	0.00276 ± 0.00356	0.03234 ± 0.03830	0.00000 ± 0.00000	0.00178 ± 0.00273	0.00172 ± 0.00279
butyl benzyl phthalate	312	0.00046 ± 0.00098	0.01150 ± 0.01351	0.00000 ± 0.00000	0.00110 ± 0.00268	0.00000 ± 0.00000
bis(2-ethylhexyl)phthalate	390	0.02178 ± 0.04492	0.28225 ± 0.38224	0.00000 ± 0.00000	0.00167 ± 0.00281	0.00000 ± 0.00000
di-n-octyl phthalate	390	0.00416 ± 0.00547	0.01024 ± 0.01362	0.00000 ± 0.00000	0.00000 ± 0.00000	0.00000 ± 0.00000

[a] Warm start includes running at 10, 25, 50, 75, and 100% load

[b] Based on a single idle test for the assault amphibious vehicle (AAV)

[c] Medium tactical vehicle replacement with a Caterpillar 729 cubic inch six-cylinder turbocharged diesel engine

[d] Logistics vehicle system with a Detroit Diesel 8V92TA eight-cylinder turbocharged diesel engine

Table 6-14. Summary of carbon abundance[a] (%) in $PM_{2.5}$ fractions from the 118 diesel profiles[b].

ID	Source Profile Mnemonic	Test Year	Region	OC1	OC2	OC3	OC4	OP	OC	EC1	EC2	EC3	EC	TC	EC/TC	EC2/EC
01030	M-ND-CC	1988	DENVER, CO	NA	NA	NA	NA	NA	18.5371	NA	NA	NA	78.8270	97.3641	0.8096	NA
01031	M-ND-CH	1988	DENVER, CO	NA	NA	NA	NA	NA	25.7472	NA	NA	NA	72.5022	98.2494	0.7379	NA
01032	M-ND-CS	1988	DENVER, CO	NA	NA	NA	NA	NA	23.3335	NA	NA	NA	74.0359	97.3694	0.7604	NA
02026	MADIEC	1988	CA	NA	NA	NA	NA	NA	90.8000	NA	NA	NA	8.1400	98.9400	0.0823	NA
02027	MADIEC	1988	CA	NA	NA	NA	NA	NA	88.2000	NA	NA	NA	10.5400	98.7400	0.1067	NA
02028	MADIEC	1988	CA	NA	NA	NA	NA	NA	89.5600	NA	NA	NA	9.5100	99.0700	0.0960	NA
02029	MADIEC	1988	CA	NA	NA	NA	NA	NA	-99.0000	NA	NA	NA	NA	NA	NA	NA
02030	MADIEC	1988	CA	NA	NA	NA	NA	NA	89.5100	NA	NA	NA	8.9800	98.4900	0.0912	NA
02221	WHDIEC	1987	CA	NA	NA	NA	NA	NA	51.6300	NA	NA	NA	44.2900	95.9200	0.4617	NA
02222	WHDIEC	1987	CA	NA	NA	NA	NA	NA	49.5600	NA	NA	NA	41.6600	91.2200	0.4567	NA
02223	WHDIEC	1987	CA	NA	NA	NA	NA	NA	49.1400	NA	NA	NA	43.3700	92.5100	0.4688	NA
02224	WHDIEC	1987	CA	NA	NA	NA	NA	NA	-99.0000	NA	NA	NA	-99.0000	-99.0000	1.0000	NA
02225	WHDIEC	1987	CA	NA	NA	NA	NA	NA	47.9200	NA	NA	NA	42.4500	90.3700	0.4697	NA
05032	PHDIES	1989	PHOENIX, AZ	20.9685	9.0883	5.9017	4.0412	-99.0000	40.0956	4.4462	27.9093	0.6860	32.9189	73.0145	0.4509	0.8478
12002	DIESHEV1	1995	ANTARCTICA	27.7162	17.1261	11.1064	9.1233	0.0000	65.1007	19.1224	9.1470	0.1049	28.3480	93.4487	0.3034	0.3227
12003	DIESHEV2	1995	ANTARCTICA	8.7292	6.5247	6.2639	4.1070	0.0000	25.6558	44.3089	15.2530	0.8897	60.4331	86.0890	0.7020	0.2524
13013	NWHD	1997	N CO	9.5060	3.9386	3.9376	1.5448	0.0029	18.9289	5.2313	67.5131	2.2529	74.9982	93.9271	0.7985	0.9002
13014	NWHDmC	1997	N CO	6.9607	4.3335	4.3316	1.6932	0.0031	13.9480	5.7031	72.7051	2.3413	80.7506	94.6986	0.8527	0.9004
13015	NWHDpC	1997	N CO	11.5945	3.6248	3.6240	1.4251	0.0027	23.0403	4.8456	63.2258	2.1713	70.2437	93.2840	0.7530	0.9001
13044	NWLDCP1	1997	N CO	18.5411	5.3439	3.3307	1.8996	1.1660	30.2573	21.0248	41.0054	0.0670	60.9351	91.1924	0.6682	0.6729
13045	NWLDCP2	1997	N CO	19.5683	5.5325	2.7471	1.2227	1.3372	30.3828	11.0883	52.4600	0.0546	62.2708	92.6536	0.6721	0.8424
13046	NWLDCP3	1997	N CO	21.6398	5.4093	2.8053	1.3468	1.1122	32.2845	10.2029	50.7862	0.1012	59.9849	92.2694	0.6501	0.8466
13047	NWLDCPC	1997	N CO	19.7619	5.4698	2.9072	1.4279	1.1901	30.7311	13.7289	48.8497	0.0704	61.4641	92.1953	0.6667	0.7948
13048	NWHDc	1997	N CO	10.3060	3.7923	4.1061	1.6065	0.0000	19.8087	3.8504	69.6030	0.0536	73.5138	93.3226	0.7877	0.9468
13049	NWHDOc	1997	N CO	8.3426	3.8264	3.6918	1.6913	0.0062	17.5588	7.6059	65.7483	3.7719	77.1241	94.6829	0.8146	0.8525
13095	NSLDCP1	1996	N CO	NA	NA	NA	NA	NA	41.5870	NA	NA	NA	48.0380	89.6250	0.5360	NA
13096	NSLDCP2	1996	N CO	NA	NA	NA	NA	NA	51.7100	NA	NA	NA	36.8850	88.5950	0.4163	NA
13097	NSLDCP3	1996	N CO	NA	NA	NA	NA	NA	39.7440	NA	NA	NA	50.5850	90.3290	0.5600	NA
13098	NSLDCPC	1996	N CO	NA	NA	NA	NA	NA	44.1930	NA	NA	NA	45.3470	89.5400	0.5064	NA
16001	CCL1	1998	MEXICO CITY	NA	NA	NA	NA	NA	51.5341	NA	NA	NA	37.1467	88.0601	0.4218	NA
16002	CCL2	1998	MEXICO CITY	NA	NA	NA	NA	NA	37.5248	NA	NA	NA	37.5855	74.5946	0.5039	NA
16003	CCLC	1998	MEXICO CITY	NA	NA	NA	NA	NA	44.5294	NA	NA	NA	37.3661	81.3273	0.4595	NA
16040	TOL1	1998	MEXICO CITY	NA	NA	NA	NA	NA	66.7016	NA	NA	NA	22.6194	89.2210	0.2535	NA
16041	TOL2	1998	MEXICO CITY	NA	NA	NA	NA	NA	64.9835	NA	NA	NA	35.7275	100.5708	0.3552	NA
16042	TOL3	1998	MEXICO CITY	NA	NA	NA	NA	NA	85.8753	NA	NA	NA	17.3803	102.9417	0.1688	NA
16043	TOL4	1998	MEXICO CITY	NA	NA	NA	NA	NA	58.5246	NA	NA	NA	47.2183	105.5696	0.4473	NA
16044	TOLC	1998	MEXICO CITY	NA	NA	NA	NA	NA	69.0212	NA	NA	NA	30.7363	99.5757	0.3087	NA
16045	TOS1	1998	MEXICO CITY	NA	NA	NA	NA	NA	91.0556	NA	NA	NA	21.6710	112.6561	0.1924	NA
16046	TOS2	1998	MEXICO CITY	NA	NA	NA	NA	NA	42.8240	NA	NA	NA	48.4568	91.2121	0.5313	NA
16047	TOS3	1998	MEXICO CITY	NA	NA	NA	NA	NA	62.4181	NA	NA	NA	29.5399	91.8527	0.3216	NA
16048	TOS4	1998	MEXICO CITY	NA	NA	NA	NA	NA	68.0572	NA	NA	NA	11.5579	79.5468	0.1453	NA
16049	TOSC	1998	MEXICO CITY	NA	NA	NA	NA	NA	66.0887	NA	NA	NA	27.8064	93.8169	0.2964	NA

Table 6-14. Continued

ID	Source Profile Mnemonic	Test Year	Region	OC1	OC2	OC3	OC4	OP	OC	EC1	EC2	EC3	EC	TC	EC/TC	EC2/EC
18020	HDDV	1999	PA MTN TUNNEL	NA	NA	NA	NA	NA	-99.0000	NA	NA	NA	60.8450	97.7920	0.6222	NA
23009	LVOnRDIE1	2003	LAS VEGAS, NV	21.9723	9.1073	12.8356	5.2654	0.0217	49.2022	14.7253	14.8827	0.0000	29.5863	78.7885	0.3755	0.5030
23010	LVOnRDIE2	2003	LAS VEGAS, NV	14.3051	11.3311	9.0983	3.9771	0.0176	38.7293	14.3086	45.8307	0.1746	60.2963	99.0256	0.6089	0.7601
23011	LVOnRDIE3	2003	LAS VEGAS, NV	42.8223	12.5691	11.5804	3.6921	1.8911	72.5550	18.9562	32.5044	0.0000	49.5695	122.1245	0.4059	0.6557
23012	LVOnRDIE4	2003	LAS VEGAS, NV	23.4636	14.0521	8.7424	4.5060	0.0142	50.7784	11.4413	30.5749	0.1801	42.1821	92.9605	0.4538	0.7248
23013	LVOffRDIE1	2003	LAS VEGAS, NV	39.6414	6.9914	10.4047	4.3111	0.0084	61.3571	8.2258	12.4156	0.1189	20.7520	82.1090	0.2527	0.5983
23014	LVOffRDIE2	2003	LAS VEGAS, NV	44.3612	14.1522	17.0862	10.9579	2.4145	88.9720	16.2563	22.5924	0.0852	36.5194	125.4915	0.2910	0.6186
23015	LVOffRDIE3	2003	LAS VEGAS, NV	39.2958	11.1636	5.9720	2.6507	16.3035	75.3856	8.1255	35.5524	0.0000	27.3745	102.7601	0.2664	1.2987
23016	LVOffRDIE4	2003	LAS VEGAS, NV	31.8846	8.0214	13.3723	3.6160	2.2080	59.1023	10.6674	20.5531	0.0000	29.0126	88.1149	0.3293	0.7084
23026	LVOffRDIE5	2003	LAS VEGAS, NV	26.3109	3.5286	4.5806	1.8853	0.3845	36.6899	2.2869	3.0503	0.0081	4.9608	41.6506	0.1191	0.6149
23031	LVOnRDIE6	2003	LAS VEGAS, NV	3.6778	4.1093	9.0620	3.3620	0.0773	20.2014	7.6788	72.0902	0.0000	79.6885	99.8899	0.7978	0.9047
23032	LVOnRDIE7	2003	LAS VEGAS, NV	8.9893	6.9205	9.2991	4.3607	1.0107	30.2768	2.5357	55.6357	0.0500	57.2143	87.4911	0.6539	0.9724
23033	LVOnRDIE8	2003	LAS VEGAS, NV	9.5630	16.2763	21.7006	9.9160	0.0462	57.1744	9.4958	67.2731	0.6176	77.3529	134.4853	0.5752	0.8697
23036	LVOnRDIE9	2003	LAS VEGAS, NV	16.2083	8.0914	7.5498	5.9352	0.8750	38.2755	5.1250	13.5926	0.9398	18.7963	57.0718	0.3293	0.7232
23050	LVOnRDIE	2003	LAS VEGAS, NV	25.6408	11.7649	10.5642	4.3602	0.4862	52.8162	14.8578	30.9482	0.0887	45.4085	98.2248	0.4623	0.6815
23051	LVOffRDIE	2003	LAS VEGAS, NV	36.2988	8.7715	10.2832	4.6842	4.2638	64.3014	9.1124	18.8328	0.0425	23.7238	88.0252	0.2695	0.7938
23075	LVOnRDIEs	2003	LAS VEGAS, NV	9.6096	8.8494	11.9029	5.8935	0.5023	36.4820	6.2088	52.1479	0.4019	58.2630	94.7345	0.6150	0.8950
DSSplit	CCS-10	2001	DSSplit	25.0858	15.2480	20.2140	7.7518	0.6998	69.0396	7.7788	72.2426	0.5653	79.9405	148.8455	0.5371	0.9037
DSSplit	CCS-11N	2001	DSSplit	10.8363	6.3811	10.4445	7.2077	0.0177	34.8912	25.4863	39.7090	1.1170	66.2958	101.1870	0.6552	0.5990
DSSplit	CCS-12	2001	DSSplit	39.6761	14.5738	19.6443	10.9389	0.0570	84.8902	9.4234	89.1290	1.3673	99.8172	184.7074	0.5404	0.8929
DSSplit	CCS-9E	2001	DSSplit	11.3703	4.5239	6.6361	2.0613	1.2680	25.8692	2.4117	93.4606	0.3950	95.0025	120.8718	0.7860	0.9838
DSSplit	CCS-9N	2001	DSSplit	21.0800	3.5688	4.2438	1.9377	0.3611	31.1902	6.6533	52.0510	0.0000	58.3453	89.5355	0.6516	0.8921
DSSplit	CCSF-1	2001	DSSplit	17.5695	4.1644	5.8025	3.2940	1.9949	32.8267	11.4255	64.0266	0.0000	73.4584	106.2851	0.6911	0.8716
DSSplit	CCSF-4	2001	DSSplit	14.7941	4.9065	6.4811	6.6240	0.0168	32.8256	23.1660	48.9622	0.0000	72.1113	104.9370	0.6872	0.6790
DSSplit	CCS-IA	2001	DSSplit	59.3311	23.1554	35.4768	18.3082	0.4525	136.7440	13.5721	70.6897	2.6569	86.5196	223.1564	0.3877	0.8170
DSSplit	CCS-IB	2001	DSSplit	41.6993	31.7482	39.1120	17.9452	0.0291	130.5505	8.5049	70.2753	1.0685	79.8759	210.3140	0.3798	0.8798
DSSplit	CID-11E	2001	DSSplit	85.2815	27.4911	29.1763	18.0763	3.0446	163.0256	15.0610	28.4075	4.8038	45.2277	208.2532	0.2172	0.6281
DSSplit	CID-9E	2001	DSSplit	40.8845	18.6330	24.7630	7.9123	3.1325	95.3254	3.1325	52.6045	2.7544	55.3589	150.6842	0.3674	0.9502
DSSplit	CSJ-IIIE	2001	DSSplit	7.3517	6.1146	10.7884	2.5051	0.0000	26.7474	3.2023	95.1769	0.0123	98.3823	125.1606	0.7860	0.9674
DSSplit	HCS-10	2001	DSSplit	17.6082	8.5134	13.4094	5.6996	0.0202	45.2509	23.7846	54.5921	0.0302	78.4031	123.6326	0.6342	0.6963
DSSplit	HCS-11	2001	DSSplit	26.6290	15.7183	21.6965	10.1890	0.0603	74.2972	19.8807	61.9656	0.7478	82.5273	156.8232	0.5262	0.7508
DSSplit	HCS-11E	2001	DSSplit	13.4621	7.6879	10.1061	4.1182	10.0197	45.3939	21.8333	59.3833	0.6636	71.8636	117.2576	0.6129	0.8263
DSSplit	HCS-11N	2001	DSSplit	14.7550	6.7310	9.1031	4.3792	0.0265	35.0009	27.5398	61.2230	0.0000	88.7464	123.7269	0.7173	0.6899
DSSplit	HCS-12	2001	DSSplit	23.4110	29.4971	44.7840	12.9460	0.0199	110.6621	7.1120	97.4603	1.3949	105.9436	216.6055	0.4891	0.9199
DSSplit	HCS-13.1	2001	DSSplit	36.8578	10.6891	12.7187	4.2929	0.0216	64.5671	6.9284	61.7499	0.0000	68.6350	133.2453	0.5151	0.8997
DSSplit	HCS-13.2	2001	DSSplit	9.7779	7.0412	11.7183	4.3698	0.0106	32.9107	12.8200	71.7873	0.0000	84.5897	117.5180	0.7198	0.8487
DSSplit	HCS-4R	2001	DSSplit	39.6116	57.9846	72.0421	25.5873	0.0000	195.1916	9.9113	72.7504	10.2485	93.0446	288.2365	0.3228	0.7819
DSSplit	HCS-5	2001	DSSplit	14.9115	5.7422	8.0416	4.2492	0.0252	32.9791	28.9283	52.6374	0.0000	81.5499	114.4975	0.7122	0.6455
DSSplit	HCS-8R	2001	DSSplit	62.8795	28.2126	35.7598	19.8456	0.0000	146.7396	6.7483	55.2480	3.0484	64.9606	211.7003	0.3069	0.8505
DSSplit	HCS-9E	2001	DSSplit	10.2008	7.9943	18.9633	5.0882	0.0000	42.2711	4.0216	91.4944	0.0000	95.5013	137.7724	0.6932	0.9580
DSSplit	HCS-9N	2001	DSSplit	10.9228	2.5744	3.5055	2.4409	2.9967	22.4409	7.9217	67.8773	0.0120	72.8163	95.2572	0.7644	0.9322

Table 6-14. Continued

ID	Source Profile Mnemonic	Test Year	Region	OC1	OC2	OC3	OC4	OP	OC	EC1	EC2	EC3	EC	TC	EC/TC	EC2/EC
DSSplit	HCSF-3	2001	DSSplit	7.6699	6.3662	11.4147	2.5223	0.0000	27.9770	6.1660	72.0905	0.0000	78.2644	106.2217	0.7368	0.9211
DSSplit	HCSF-4	2001	DSSplit	17.0710	4.8079	6.2927	3.1927	0.0170	31.3786	13.8718	71.1480	0.0000	85.0028	116.3815	0.7304	0.8370
DSSplit	HCS-IA	2001	DSSplit	48.5657	20.7194	25.9711	16.2126	2.6119	114.0898	12.1890	33.9620	0.5219	44.0124	158.1801	0.2782	0.7716
DSSplit	HCS-IB	2001	DSSplit	46.9867	29.5459	43.8293	19.0781	0.0214	139.5072	9.6480	75.2485	1.4120	86.2624	225.7695	0.3821	0.8723
DSSplit	HCS-II	2001	DSSplit	56.5750	42.4097	54.3323	27.2847	0.2330	180.8063	13.4787	79.7541	3.5124	96.4549	277.3207	0.3478	0.8269
DSSplit	HCS-IIB	2001	DSSplit	16.5178	17.9242	31.1743	15.7669	0.0635	81.4254	10.0565	45.4078	0.2221	55.6230	137.0484	0.4059	0.8163
DSSplit	HW-10	2001	DSSplit	26.3326	13.2398	23.2539	10.1985	0.0260	73.0194	32.0136	57.7359	0.6086	90.3321	163.3775	0.5529	0.6392
DSSplit	HW-11	2001	DSSplit	22.4152	16.0876	22.3309	7.9281	0.0302	68.7955	17.9826	48.4924	0.7526	67.1906	135.9861	0.4941	0.7217
DSSplit	HW-11E	2001	DSSplit	27.6725	6.1135	8.5699	4.5218	0.0000	46.8777	34.4629	35.5131	0.0000	69.9782	116.8559	0.5988	0.5075
DSSplit	HW-11N	2001	DSSplit	7.2825	5.5368	9.7619	3.3307	0.0093	25.9227	19.8313	19.0481	0.0000	38.8686	64.7914	0.5999	0.4901
DSSplit	HW-12	2001	DSSplit	42.6298	30.2469	36.6870	16.4858	0.0197	126.0771	9.9333	94.7747	1.8744	106.5864	232.6237	0.4582	0.8892
DSSplit	HW-5	2001	DSSplit	11.0186	6.5717	9.6578	2.7201	0.0091	29.9803	13.0644	68.6829	0.0000	81.7397	111.7200	0.7316	0.8403
DSSplit	HW-9E	2001	DSSplit	14.0382	5.5399	7.9113	3.4461	0.0198	30.9712	7.9946	90.9547	0.0000	98.9414	129.8729	0.7618	0.9193
DSSplit	HW-9N	2001	DSSplit	16.9916	4.2290	6.7236	3.0783	0.0046	31.0272	8.4940	46.6336	0.0286	55.1518	86.1789	0.6400	0.8456
DSSplit	HW-IA	2001	DSSplit	50.1705	25.4334	32.4947	18.8871	1.7479	128.6785	11.4794	52.4690	0.9777	63.1321	191.9030	0.3290	0.8311
DSSplit	HW-IB	2001	DSSplit	44.3950	32.5323	42.9865	25.6776	0.0350	145.6498	12.1224	78.5073	1.4300	92.0602	237.6317	0.3874	0.8528
DSSplit	HW-II	2001	DSSplit	32.4159	29.1464	33.2408	23.5287	0.0795	118.3953	27.4527	48.4795	1.2922	77.1346	195.5633	0.3944	0.6285
DSSplit	HW-IIB	2001	DSSplit	34.4709	34.8287	52.6376	21.8420	0.0986	143.9270	14.3680	78.4754	6.4995	99.2812	243.0850	0.4084	0.7904
DSSplit	ID-11E	2001	DSSplit	13.0149	8.3463	12.0257	4.1000	0.0125	37.5025	17.2644	55.4379	0.0850	72.7683	110.2708	0.6599	0.7618
DSSplit	ID-11N	2001	DSSplit	51.3673	16.5790	24.1583	14.5786	4.8216	111.4721	19.9148	34.1369	0.0000	49.2629	160.7350	0.3065	0.6930
DSSplit	ID-9N	2001	DSSplit	15.5104	2.5139	3.7957	4.6559	0.0792	26.5569	17.6606	51.6701	0.0000	69.2540	95.8066	0.7229	0.7461
DSSplit	ID-I	2001	DSSplit	114.2145	44.5998	70.2489	30.5968	1.8021	261.4153	6.8824	22.4501	2.4079	29.9557	291.3711	0.1028	0.7494
DSSplit	ID-II	2001	DSSplit	284.2200	216.4179	312.4117	141.2494	10.0415	964.5603	37.1068	61.0847	1.9479	90.1430	1054.3302	0.0855	0.6776
DSSplit	ID-III	2001	DSSplit	106.9298	89.5603	137.9207	51.0578	0.9431	386.4398	13.6799	36.5308	6.3639	55.6835	441.9667	0.1260	0.6560
DSSplit	MC-13.1	2001	DSSplit	14.4684	11.8163	16.6123	4.3683	0.0208	47.2861	4.3631	87.0437	0.3033	91.6945	138.9806	0.6598	0.9493
DSSplit	MC-13.2	2001	DSSplit	16.5018	9.9204	13.4704	4.4989	0.0146	44.4033	3.2014	85.7575	0.9021	89.8610	134.2642	0.6693	0.9543
DSSplit	UD-IIIE	2001	DSSplit	15.6897	7.6484	11.2579	9.7456	0.0000	44.3644	20.5282	85.7954	0.0000	106.3191	150.6835	0.7056	0.8070
DSSplit	BLANK-3	2001	DSSplit	102.9275	74.2463	112.9496	36.9274	0.1202	327.1407	14.2654	17.7262	9.0286	40.9303	368.0710	0.1112	0.4331
DSSplit	BLANK-3M	2001	DSSplit	6.0713	2.2549	3.3740	1.1624	0.0000	12.8604	1.9318	72.8141	0.9309	75.6753	88.5356	0.8547	0.9622
DSSplit	BLANK-9	2001	DSSplit	35.9229	30.0528	44.3943	15.6767	0.0000	125.9609	6.2981	18.5861	0.0000	24.8155	150.9478	0.1644	0.7490
DSSplit	BLANK-I	2001	DSSplit	387.1588	270.0245	338.9757	152.5752	10.1085	1159.2073	4.7130	18.4759	0.0000	13.0716	1171.7219	0.0112	1.4134
DSSplit	BLANK-III	2001	DSSplit	190.6798	125.5259	173.7266	57.5741	5.1081	552.6905	2.3861	13.4015	0.0000	10.5165	563.6121	0.0187	1.2743
DSSplit	BLANK-IIIN	2001	DSSplit	41.1319	14.1686	20.3623	13.9574	1.2504	90.8905	21.5703	23.4976	0.0000	43.8230	134.6542	0.3254	0.5362
DSSplit	CI_11C1	2001	DSSplit	27.2603	3.7799	3.4944	1.2459	21.6994	57.4797	5.9800	46.4327	0.0032	30.7172	88.1969	0.3483	1.5116
DSSplit	CI_11W1	2001	DSSplit	26.3632	11.9578	8.6254	2.4173	14.7615	64.1237	7.5733	56.5236	0.2360	49.5749	113.6987	0.4360	1.1402

[a] Normalized to $PM_{2.5}$ mass

[b] SPECIATE database (U.S.EPA, 1999b; updated 2006)

7. INTEGRATION WITH EPA EMISSION MODELS

As shown in the previous sections, diesel exhaust emissions are influenced by many factors, including engine age, maintenance, fuel, engine type, engine temperature, and engine operating cycle. Given the unique history and usage of each piece of equipment, population emissions must be simulated using sparse matrices of data. The influence of engine age on emission factors has been previously determined based on just a few engine tests over their useful lifetimes. These patterns are then used to fill in engine degradation for the entire population of similar engines. While this gap-filling approach may be prone to errors, it generally produces the most realistic results with the available data. Due to the complexity and diversity of engine populations, all emissions models employ gap-filling as a means to most accurately estimate total emissions.

At the beginning of the project, it was thought that a separate emissions model could be created that would be applicable to individual military bases. An exploration of the available data sets in Section 3, and the inability to obtain examples of the major fuel users for testing indicated that this would be impractial. Improvemets in EPA's emissions models, along with their documentation and acceptance, suggested that integrating study results with those models would be a more useful endeavor.

During the course of the project, EPA developed the MOVES (MOtor Vehicle Emission Simulator) to encompass all pollutants and all mobile sources at the levels of resolution needed for the diverse applications. MOVES2006 includes HC (including non-exhaust emissions), CO, NO_x, PM, Toxics, CO_2, NH_3 and SO_2 emissions. MOVES2006 is the draft replacement for MOBILE6. Non-road sources are to be incorporated by the end of 2008 or early 2009.

An advantage of the MOVES platform is that engine modal cycles are used as an independent input. That is, emission factors collected during the Federal Test Procedurel (FTP) test cycle can be remapped for a domain that has a very different driving cycle than the FTP (e.g. urban stop and go or highway cruising). The same will be true for non-road emission simulations. For example, an operating cycle for a cement mixer would involve the engine operating at a variety of conditions that are not well represented by distances traveled or total engine hours. Rather, a modal cycle would account for the different engine loads associated with start up emissions, driving transients, and near constant loads during cruising.

EFs from generators are quantified for start up conditions and steady state loads at 10%, 25%, 50%, 75%, and 100% of the rated power. These emission factors can be tabulated in a MOVES ready format so more detailed simulations of emissions can be performed when additional data is available about usage activity.

For mobile sources such as trucks and HUMVEEs, emissions data can be tabulated based on vehicle speed and vehicle specific power. Gap-filling techniques will be used to fill in bins where measurements are sparse. For example, a dynamometer test of a HUMVEE operating on a known test cycle may produce second by second data that relates emissions to speed and vehicle specific power (VSP), a proxy for engine load. This data may not be available for 5-ton trucks, but remotely sensed data may exist for the truck operating over a very limited range of loads. The HUMVEE's emission's relationship with speed and VSP can then be used to scale the remotely sense emissions from the 5-ton truck. This gap filling technique will integrate all

emissions measurements and improve the accuracy and degree of representation of the model results.

For the currently available NONROAD model, data are stored in lookup tables within the DATA/EMFAC subdirectory of the NONROAD program directory. Each ASCII tables within the directory assembles the emissions from the type of source (i.e. crankcase, exhaust, spillage, evaporative) as well as a brake specific fuel consumption factor that permits the translation from bhp-hr emission factors to fuel based emissions factors.

NONROAD uses a set of deterioration factor lookup tables to simulate the emissions from aging engines. Since the dataset produced from the study will not be sufficiently large to quantify deterioration factors from the engines tested, we used the default deterioration factors from NONROAD and the age of the military engines tested to calculate the 0-hour emission factors.

Emission factors are defined in the NONROAD model by the Source Classification Code (SCC), the power level range in HP, and the engine technology type (i.e. 2-stroke gasoline, 4-stroke gasoline, diesel, etc.). The SCC is a hierarchical numbering system defined by the EPA and used to describe all types of emission sources. When less specific emission factors are available for a certain class of equipment, the NONROAD model defaults to the more general equipment classification. An example list of NONROAD SCCs is shown in Table 7-1. NONROAD files that can be modified are shown in Table 7-2. The results of this study can be appended to this file using units of g pollutant/gallon fuel consumed.

The 10 kW generators tested in this project had model years (MY) of 1994, 1995 and 1999, and represent Tier 0 (MY 1988-1999) EFs for engine power between 11 and 25 hp. The 30 kW generators included three MY 1995 and two MY 2002 engines, so the 3 MY 1995 EFs represent the Tier 0 (MY 1988-1998) EFs to be used in NONROAD model, the 2 MY 2002 EFs represent the Tier 1 (MY 1999-2003) with engine power between 25 and 50 hp. For 60 kW generators, one MY 1995 and two MY 2001 and one MY 2002 unites were tested. The MY 1995 EF represent the Tier 0 (MY 1988-1997) emission factor to be used in NONROAD model, the 3 MY 2001/2002 EFs represent the Tier 1 (MY 1998-2003) emission factors with engine power between 75 and 100 hp. The 100 kW MY 1987 generator represents the EF for Base (pre-1988 MY) engines.

For the mobile sources, valid EFs were obtained for the 425 hp engine MTVR and the 445 hp LVS engines. The MTVR has model year range from 1999 to 2005. Emissions data from MTVR represent Tier 1 (MY 1996-2000) and Tier 2 (MY 2001-2005) emission factor for engine power between 300 and 600 hp. The measured LVSs has model years of from 1985 to 1989. LVS emission data represent the EF for Base (pre-1988 MY) engines and Tier 0 (MY 1988-1995) for engine power between 300 and 600 hp.

Non-road EF were created as part of this project for these model year and Tier specifications. Additional data can be added to the files when available. To use these emission

factors in NONROAD, the user copies and pastes the format line by line, as shown in Figures 7-1 and 7-2.

After copying the format, it should be pasted into new line. Non applicable tiers (i.e. data gaps) have been changed from 0.000 values to -9999 so that if the software picks up the incorrect tier via the input options file, the output should be erroneous.

Table 7-1. SCCs for NONROAD equipment. The xx in the SCC number refers to the fuel/technology types of the equipment ('60' for 2 stroke gas, '65' for 4 stroke gas, and '70' for diesel). The 'yyy' and 'zzzzzz' refer to the specific equipment types as denoted in the examples and the numbers in parentheses.

SCC	Equipment Types	Examples
22xx001yyy	Recreational Vehicles	Snowmobiles (020), ATVs (030), Golf Carts (050)
22xx002yyy	Construction	Pavers (003), Surfacing equipment (024), Off-highway trucks (051)
22xx003yyy	Industrial	Forklifts (020), Sweepers (030), Refrigeration (060)
22xx004yyy	Lawn and Garden	Lawn mowers (010), Snow blowers residential (035), chippers and stump grinders (066)
22xx005yyy	Agricultural	Combines (020), Balers (025), Tillers (040)
22xx006yyy	Commercial	Generator set (005), Pumps (010), Welders (025)
22xx007yyy	Logging	Chainsaws (005), Shredders (010), Skidders (015)
22xx008005	Airport Ground Support	All types
22xx009010	Underground Mining	All types
22xx010010	Oil Field	All types
2282zzzzzz	Recreational Marine	Gasoline outboard (005010), Diesel inboard (020005), Diesel Sailboat Auxiliary (020025)

2285zzzzzz	Railway Maintenance	Diesel (002015), 4-stroke (004015), LPG (006015)
To be determined	Tactical Military	Generators, Humvees, 5-ton Trucks, etc.

Table 7-2. Files to be modified in the NONROAD model.

NONROAD Sub Directory	Filename	Description
\data\emfac	*Bsfc.emf*	Brake specific fuel consumption factors
\data\emfac	*Exhco.emf*	Emission factors data for exhaust CO emissions
\data\emfac	*Exhnox.emf*	Emission factors data for exhaust NO_x emissions
\data\emfac	*Exhpm.emf*	Emission factors data for exhaust PM emissions
\data\emfac	*Exhthc.emf*	Emission factors data for exhaust THC emissions

GENEXHCO.EMF - Notepad

File Edit Format View Help

```
This file contains emission factors data for exhaust CO
emissions.  The emission factors are specified by SCC code,
HP range and technology type.  An ALL in the tech type field
will apply to all technology types.  The model will use the
the emission factor for the closest year that is less than or
equal to the current model year.

11/30/05 s2pM, CI FRM & NR05y: add phs3 base SI rec marine from CO-42b.

-------------------------------------------------------------
The format is as follows:
Line 1:
       6-15  character     -- SCC Code
      21-25  real          -- beginning of HP range
      26-30  real          -- end of horsepower range
      35-44  character     -- technology type
      x5-x4  character     -- technology type (repeating fields of 10)
      x5-x4  character     -- units (10 characters max)
      x5-x4  character     -- pollutant (12 characters max)
Line 2:
       1-5   integer       -- year
      35-44  real          -- emission factors for technology type 1
      x5-x4  real          -- EF's for tech types (repeating fields of 10)

     2200000000     HpmnHpmax    techtyT1  techtyT2  techtyT3  techtyp4  techtyp5  techtyp6  techtyp7  techtyp8  techtyp9  techtyT10 g/hp-hr    CO
1900                             37.7      0         37.7      999.99    999.99    999.99    999.99    999.99    999.99    999.99
-------------------------------------------------------------

/EMSFAC/
     2270006006        11   25    Base      T0        T1        T2        T3        T3B       T4A       T4B       T4        T4N       g/hp-hr     CO
1988                             -9999     4.307     -9999     -9999     -9999     -9999     -9999     -9999     -9999     -9999
     2270006006        11   25    Base      T0        T1        T2        T3        T3B       T4A       T4B       T4        T4N       g/hp-hr     CO
1997                             -9999     4.307     -9999     -9999     -9999     -9999     -9999     -9999     -9999     -9999
     2270006006        25   50    Base      T0        T1        T2        T3        T3B       T4A       T4B       T4        T4N       g/hp-hr     CO
1988                             -9999     1.949     -9999     -9999     -9999     -9999     -9999     -9999     -9999     -9999
     2270006006        25   50    Base      T0        T1        T2        T3        T3B       T4A       T4B       T4        T4N       g/hp-hr     CO
1997                             -9999     1.949     -9999     -9999     -9999     -9999     -9999     -9999     -9999     -9999
     2270006006        25   50    Base      T0        T1        T2        T3        T3B       T4A       T4B       T4        T4N       g/hp-hr     CO
2003                             -9999     -9999     1.898     -9999     -9999     -9999     -9999     -9999     -9999     -9999
     2270006006        75  100    Base      T0        T1        T2        T3        T3B       T4A       T4B       T4        T4N       g/hp-hr     CO
1988                             -9999     2.303     -9999     -9999     -9999     -9999     -9999     -9999     -9999     -9999
     2270006006        75  100    Base      T0        T1        T2        T3        T3B       T4A       T4B       T4        T4N       g/hp-hr     CO
1997                             -9999     2.303     -9999     -9999     -9999     -9999     -9999     -9999     -9999     -9999
     2270006006       100  175    Base      T0        T1        T2        T3        T3B       T4A       T4B       T4        T4N       g/hp-hr     CO
1900                             3.026     -9999     -9999     -9999     -9999     -9999     -9999     -9999     -9999     -9999
/END/
```

Figure 7-1. Example of the NONROAD emission factor data file and the records that need to be inserted from the SERDP sample files.

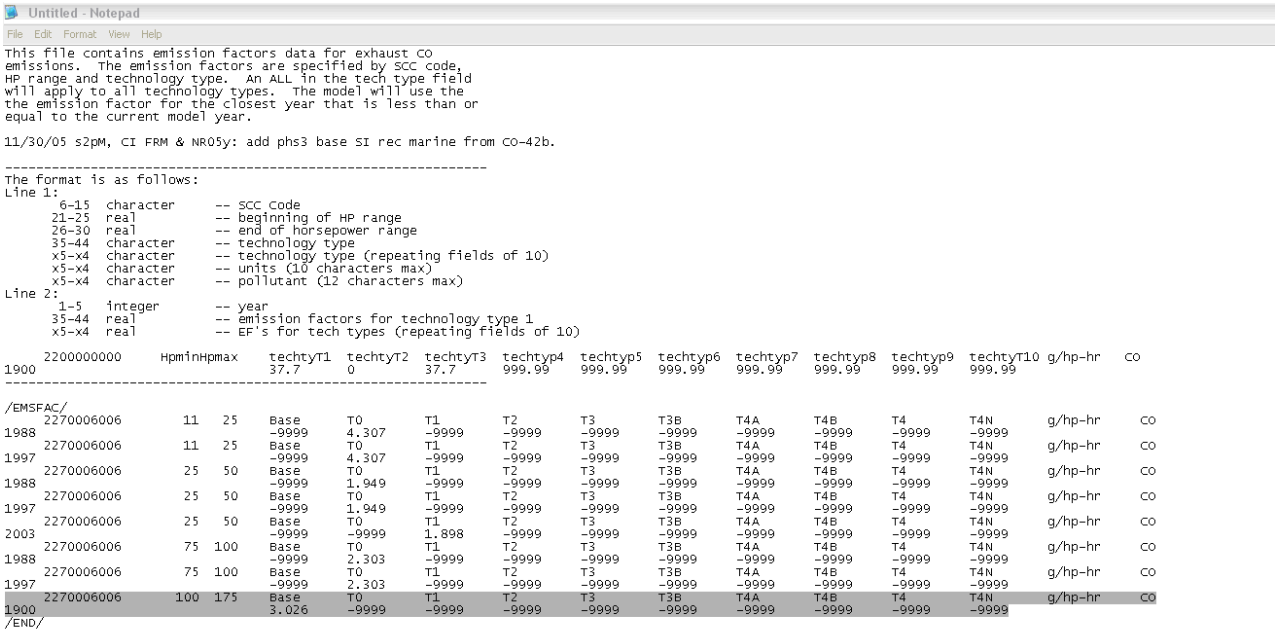

```
Untitled - Notepad
File  Edit  Format  View  Help
This file contains emission factors data for exhaust CO
emissions.  The emission factors are specified by SCC code,
HP range and technology type.  An ALL in the tech type field
will apply to all technology types.  The model will use the
the emission factor for the closest year that is less than or
equal to the current model year.

11/30/05 s2pM, CI FRM & NR05y: add phs3 base SI rec marine from CO-42b.

-------------------------------------------------------------
The format is as follows:
Line 1:
       6-15  character     -- SCC Code
      21-25  real          -- beginning of HP range
      26-30  real          -- end of horsepower range
      35-44  character     -- technology type
      x5-x4  character     -- technology type (repeating fields of 10)
      x5-x4  character     -- units (10 characters max)
      x5-x4  character     -- pollutant (12 characters max)
Line 2:
       1-5   integer       -- year
      35-44  real          -- emission factors for technology type 1
      x5-x4  real          -- EF's for tech types (repeating fields of 10)

     2200000000     HpminHpmax    techtyT1  techtyT2  techtyT3  techtyp4  techtyp5  techtyp6  techtyp7  techtyp8  techtyp9  techtyT10 g/hp-hr   CO
1900                              37.7      0         37.7      999.99    999.99    999.99    999.99    999.99    999.99    999.99
-------------------------------------------------------------

/EMSFAC/
     2270006006        11   25    Base      T0        T1        T2        T3        T3B       T4A       T4B       T4        T4N       g/hp-hr     CO
1988                              -9999     4.307     -9999     -9999     -9999     -9999     -9999     -9999     -9999     -9999
     2270006006        11   25    Base      T0        T1        T2        T3        T3B       T4A       T4B       T4        T4N       g/hp-hr     CO
1997                              -9999     4.307     -9999     -9999     -9999     -9999     -9999     -9999     -9999     -9999
     2270006006        25   50    Base      T0        T1        T2        T3        T3B       T4A       T4B       T4        T4N       g/hp-hr     CO
1988                              -9999     1.949     -9999     -9999     -9999     -9999     -9999     -9999     -9999     -9999
     2270006006        25   50    Base      T0        T1        T2        T3        T3B       T4A       T4B       T4        T4N       g/hp-hr     CO
1997                              -9999     1.949     -9999     -9999     -9999     -9999     -9999     -9999     -9999     -9999
     2270006006        25   50    Base      T0        T1        T2        T3        T3B       T4A       T4B       T4        T4N       g/hp-hr     CO
2003                              -9999     -9999     1.898     -9999     -9999     -9999     -9999     -9999     -9999     -9999
     2270006006        75  100    Base      T0        T1        T2        T3        T3B       T4A       T4B       T4        T4N       g/hp-hr     CO
1988                              -9999     2.303     -9999     -9999     -9999     -9999     -9999     -9999     -9999     -9999
     2270006006        75  100    Base      T0        T1        T2        T3        T3B       T4A       T4B       T4        T4N       g/hp-hr     CO
1997                              -9999     2.303     -9999     -9999     -9999     -9999     -9999     -9999     -9999     -9999
     2270006006       100  175    Base      T0        T1        T2        T3        T3B       T4A       T4B       T4        T4N       g/hp-hr     CO
1900                              3.026     -9999     -9999     -9999     -9999     -9999     -9999     -9999     -9999     -9999
/END/
```

Figure 7-2. Format of copied lines from SERDP test result files to customize NONROAD for military emissions factors derived from this study.

8. PROJECT PUBLICATIONS, CONCLUSIONS, AND RECOMMENDATIONS

8.1 Project Publications

The following articles partially or entirely supported by this project have been published by or submitted to peer-reviewed journals. To the extent possible, detailed data bases are included as supplemental files on the journal websites. Detailed data bases in electronic form are also available for specific applications. Copies of published and submitted articles are included in the Appendix.

- Barber, P.W.; Moosmüller, H.; Keislar, R.E.; Kuhns, H.D.; Mazzoleni, C.; and Watson, J.G. (2004). On-road measurement of automotive particle emissions by ultraviolet lidar and transmissometer: Theory. *Meas. Sci. Technol.*, **15**:2295-2302.
- Chakrabarty, R.K.; Moosmüller, H.; Arnott, W.P.; Garro, M.A.; and Walker, J. (2006). Structural and fractal properties of particles emitted from spark ignition engines. *Environ. Sci. Technol.*, **40**(21):6647-6654.
- Chen, L.-W.A.; Moosmüller, H.; Arnott, W.P.; and Watson, J.G. (2006). Novel approaches to measure diesel emissions. *J. Mine Ventilation Soc. South*, **59**(April/June):40-45.
- Cocker, D.R.; Shah, S.D.; Johnson, K.; Miller, J.W.; and Norbeck, J.M. (2004). Development and application of a mobile laboratory for measuring emissions from diesel engines 1. Regulated gaseous emissions. *Environ. Sci. Technol.*, **38**(7):2182-2189.
- Cocker, D.R.; Shah, S.D.; Johnson, K.C.; Zhu, X.N.; Miller, J.W.; and Norbeck, J.M. (2004). Development and application of a mobile laboratory for measuring emissions from diesel engines. 2. Sampling for toxics and particulate matter. *Environ. Sci. Technol.*, **38**(24):6809-6816.
- Durbin, T.D.; Cocker, D.R.; Sawant, A.A.; Johnson, K.; Miller, J.W.; Holden, B.B.; Helgeson, N.L.; and Jack, J.A. (2007). Regulated emissions from biodiesel fuels from on/off-road applications. *Atmos. Environ.*, **41**(27):5647-5658.
- Durbin, T.D.; Johnson, K.; Cocker, D.R.; Miller, J.W.; Maldonado, H.; Shah, A.; Ensfield, C.; Weaver, C.; Akard, M.; Harvey, N.; Symon, J.; Lanni, T.; Bachalo, W.D.; Payne, G.; Smallwood, G.; and Linke, M. (2007). Evaluation and comparison of portable emissions measurement systems and federal reference methods for emissions from a back-up generator and a diesel truck operated on a chassis dynamometer. *Environ. Sci. Technol.*, **41**(17):6199-6204.
- Huai, T.; Shah, S.D.; Miller, J.W.; Younglove, T.; Chernich, D.J.; and Ayala, A. (2006). Analysis of heavy-duty diesel truck activity and emissions data. *Atmos. Environ.*, **40**(13):2333-2344.
- Kelly, K.E.; Wagner, D.A.; Lighty, J.S.; Sarofim, A.F.; Bretecher, B.; Holden, B.B.; Helgeson, N.; Sahay, K.; and Nardi, Z. (2004). Evaluation of catalyzed and

electrically heated filters for removal of particulate emissions from diesel-A- and JP-8-fueled engines. *J. Air Waste Manage. Assoc.*, **54**(1):83-92.

- Kuhns, H.D.; Mazzoleni, C.; Moosmüller, H.; Nikolic, D.; Keislar, R.E.; Barber, P.W.; Li, Z.; Etyemezian, V.; and Watson, J.G. (2004). Remote sensing of PM, NO, CO, and HC emission factors for on-road gasoline and diesel engine vehicles in Las Vegas, NV. *Sci. Total Environ.*, **322**:123-137.
- Mazzoleni, C.; Kuhns, H.D.; Moosmüller, H.; Keislar, R.E.; Barber, P.W.; Robinson, N.F.; and Watson, J.G. (2004). On-road vehicle particulate matter and gaseous emission distributions in Las Vegas, Nevada, compared with other areas. *J. Air Waste Manage. Assoc.*, **54**(6):711-726.
- Mazzoleni, C.; Moosmüller, H.; Kuhns, H.D.; Keislar, R.E.; Barber, P.W.; Nikolic, D.; Nussbaum, N.J.; and Watson, J.G. (2004). Correlation between automotive CO, HC, NO, and PM emission factors from on-road remote sensing: Implications for inspection and maintenance programs. *Transport. Res.*, **D9**:477-496.
- Moosmüller, H.; Kuhns, H.D.; Mazzoleni, C.; Chang, M.-C.O.; Parthasarathy, G.; Nussbaum, N.J.; Nathagoundenpalayam, S.K.; Barber, P.W.; Nikolic, D.; and Watson, J.G. (2007). Sensitivity of cross-plume lidar detection of vehicle exhaust to particle size, shape, and composition. *Aerosol Sci. Technol.*, in preparation.
- Nussbaum, N.J.; Zhu, D.; Kuhns, H.D.; Mazzoleni, C.; Chang, M.-C.O.; Moosmüller, H.; Chow, J.C.; and Watson, J.G. (2008). The In-Plume Emissions Test-Stand: A novel instrument platform for the real-time characterization of combustion emissions. *J. Air Waste Manage. Assoc.*, submitted.
- Sawant, A.A.; Shah, S.D.; Zhu, X.N.; Miller, J.W.; and Cocker, D.R. (2007). Real-world emissions of carbonyl compounds from in-use heavy-duty diesel trucks and diesel Back-Up Generators (BUGS). *Atmos. Environ.*, **41**(21):4535-4547.
- Shah, S.D.; Cocker, D.R.; Johnson, K.C.; Lee, J.M.; Soriano, B.L.; and Miller, J.W. (2006). Emissions of regulated pollutants from in-use diesel back-up generators. *Atmos. Environ.*, **40**(22):4199-4209.
- Shah, S.D.; Cocker, D.R.; Johnson, K.C.; Lee, J.M.; Soriano, B.L.; and Miller, J.W. (2007). Reduction of particulate matter emissions from diesel backup generators equipped with four different exhaust aftertreatment devices. *Environ. Sci. Technol.*, **41**(14):5070-5076.
- Zhu, D.Z.; Nussbaum, N.J.; Kuhns, H.D.; Chang, M.-C.O.; Sodeman, D.A.; Uppapalli, S.; Moosmuller, H.; Chow, J.C.; and Watson, J.G. (2008). Emission factors for U.S. military generators (10 kW to 100 kW) measured with an In-Plume Emissions Measurement Test Stand. *Atmos. Environ.*, submitted.

Additional articles are under preparation for submission by the end of 2008 on: 1) results from the IPETS mobile source tests; 2) results from the VERSS mobile source tests; 3) description and results of the on-board PM monitoring tests; and 4) PM source profiles.

8.2 Summary and Conclusions

A comprehensive literature review found that several different test methods were found to be applied to diesel emission tests including: 1) laboratory engine or chassis dynamometer tests; 2) in-plume measurements from mobile laboratories and roadside monitors, 3) on-board exhaust measurements by portable emission monitoring systems, and 4) cross-plume measurements by remote sensors. Real-world tests have been made with in-plume and crossplume systems, and these emission rates often differ substantially from those of certification tests due to the greater range of engine age and maintenance, a wide variety of operating conditions, and fuels that often differ from those specified for certification. Portable emissions monitoring systems have not yet achieved the reliability and accuracy needed for useful emission factors. Tests using thermal denuders showed that $PM_{2.5}$ and UP emission factors vary with temperature, with more condensable material found at ambient temperatures than at the higher temperatures found in exhaust pipes. $PM_{2.5}$ source profiles are important for speciated emission inventories and source apportionment, but few of these area available for: 1) typical ambient temperatures that allow for condensation and initial chemical transformation, 2) non-road engines, applications and fuels; and 3) in a form that allows for easy access and use. EPA's SPECIATE software allow for archival of profiles acquired in this study for use by a broader applications community. The NONROAD emission model lacks real-world representations for many nonroad diesel emission factors. Measurements from tests such as those carried out in this report can be added to the NONROAD model. Although more than 1600 publications related to diesel emissions and fuels were identified, with 650 of them since the project commencement in 2003, knowledge about non-road emissions is minimal. Most tests have used certification methods that do not adequately reflect real-world emissions.

Engine and fuel use data are well defined on an annual basis for the Army, but not for the other services. The US Marine Corps also has good overall records, but does not have the spatially and temporal detail of the Army data base that would allow emissions to be easily estimated for individual military bases. Fuel use data is available for the Air Force and Navy, but the relatively small amount used for non-road diesel engines cannot be separated from the total fuel use, which is dominated by aircraft and ships. M1 tanks used 16% of all fuel for CY2001-2003. These tanks use turbines rather than CI engines. For the CI engines, the HMMWV (GM6.2L engine) used 18% of the total, the HEMTT (Detroit Diesel 8V92TA engine) used 11% of the total, 5-ton trucks (Cummins NHC250 and 6CTA8 engines) used 12% of the total, the LAV/APCs (Detroit Diesel 6V53T engine) used 7% of the total, and the FMTV (Caterpillar 3116-ATAAC engine) used 4% of the total. Together these engines and units accounted for more than 75% of the Army and Marine Corps fuel use. There were some, but not major, differences in year-to-year fuel consumption amounts. Operating cycles for military engines are not well understood. New engines with electronic control modules (ECMs) acquire some of the operating information needed to determine these, but these ECMs are not on most of the older military equipment. Using ECM data as these new engines penetrate the military fleet offers a higher potential to better characterize their operating characteristics.

Commercially-available Portable Emission Monitoring Systems (PEMS) for gas exhaust measurements were evaluated and found insufficient to meet the project goals. The commercial gas PEMS show promise for NO_x and CO_2 emissions, but their current detection limits are too imprecise for quantifying VOC, CO, and PM emissions from diesel engines. PEMS have the

advantage of being less costly to procure than other methods and being located on engines without causing interference with the routine operations.

A large part of the project was dedicated to developing and evaluating the UCR Mobile Emissions Laboratory (MEL) and the DRI In-Plume Emissions Test Stand (IPETS), the DRI Vehicle Emissions Remote Sensing System (VERSS) and the DRI on-board PM monitor. The MEL is the most well established technology, replicating the sampling, dilution system, and measurement devices that are usually confined to an emission testing laboratory. It offers the advantage of mobility, but its large size make it difficult to position in a location to record realworld source emissions. For real-world mobile source emissions, the MEL is only applicable to sampling the exhaust of the tractor that is towing it. The MEL, however, is the only instrument that can provide a bridge between certification tests expressed in g/bhp-hr and the g/kgfuel fuelbased emission factors that are more useful for air quality planning inventories. The IPETS is intermediate between the MEL and the PEMS, offering a movable platform that can be used in field situations, but is still to large and requires too much power to be mounted on the engine. IPETS is oriented toward real-world emissions, allowing exhaust samples to dilute and cool to ambient conditions prior to measurement. Simultaneous CO_2 measurements allow emissions concentrations in the plume to be related to the fuel consumption, resulting in a fuel-based emission factor. The current IPETS design has multiple measurements for CO2 and PM mass concentrations. Particle number measurements in different size fractions allow the important UP fraction to be determined. The Fourier Transform Infrared (FTIR) spectrometer is capable of quantify non-criteria pollutants such as NH_3 along with the normal certification pollutants. As with the MEL, the IPETS challenge is being able to extract a portion of the plume for analysis. While this is relatively straightforward for stationary sources such as generators where a probe can be located in the plume, it is more difficult for mobile sources. The VERSS remote sensing system is applicable to mobile sources following a set path. However, many non-road sources don't follow such paths.

VERSS is a cutting edge technology that takes advantage of recent advances in lasers, radiation detection, and high speed data acquisition. VERSS feasibility was proven in this project, but it was not deemed practical for taking many measurements. A major limitation is the lack of commercial replacement parts, as several components were produced specifically for the system. Although many advances were made in the technology as part of the project, time and budget limitations did not permit the development and implementation of the system as envisioned at the project onset.

Comparison tests among the different methods on the same emissions showed promising results, typically within ±30% for fuel-based emissions factors, but sometimes as high as a factor of two or more. PM was the most difficult observable to measure, owing to its many different measurement methods and the fact that its semi-volatile components are susceptible to temperature differences as the plume ages and cools.

Practical real-world emissions tests were carried out in four phases: 1) MEL tests of stationary diesel generators at UCR; 2) MEL chassis dynamometer tests mobile sources at UCR; 3) IPETS tests of stationary diesel generators at Camp Pendleton; and 4) IPETS, VERSS, and onboard PM tests of mobile sources at 29-Palms Marine Base. These tests demonstrated the feasibility of making measurements under field conditions, but not necessarily the practicality. On-base testing was difficult to arrange, owing to high demand from 2004-2007 for training and equipment. High staff turnover at the bases required multiple applications to be submitted for

testing. Tests were costly and cumbersome for the VERSS, which seems more suited to on-road than to non-road applications. The IPETS functioned well for stationary diesel generators, but it missed many of the elevated exhaust plumes from the large military mobile sources. The portable PM prototype, however, functioned well, and with further miniaturization, packaging, and combination with PEMS having lower detection limits could be adapted into a viable system for testing many engines without major interference to base operations. The MEL was too large and cumbersome for use on the bases, so engines were brought from cooperating bases for testing.

Large differences were found in emissions between different engines and operating modes. In general, real-world emissions were lower than those reported for certification of the same or similar engines. Cold starts for generators had the highest emissions, much higher than those found during the prescribed certification test cycles. Ultrafine particles emission factors for non-road diesels were estimated for the first time and were found to be (1.05 $\pm$ 1.09) $x10^{15}$ #/kgfuel for ten MTVR 7-ton truck, (2.35 $\pm$ 1.12) $x10^{16}$ #/kgfuel for two LVS, and (6.3 $\pm$ 1.9) $x10^{15}$ #/kgfuel for a single HDV. More than 95% of the measured particles were in the ultrafine particle mode.

The project resulted in a substantial increase in the number of $PM_{2.5}$ source profiles with organic speciation, and 25 of these valid individual profiles and composite profiles are being submitted to EPA's SPECIATE source profile software. On average, organic carbon (OC) accounted for 26 – 66% of $PM_{2.5}$, with 30 – 52% of OC found in the IMPROVE OC1 fraction. Elevated n-alkane abundances (4.6 ± 4.1%) were found for the MTVR, with lower abundances of ~0.4% in the LVS and AAV emissions. Branched n-alkane abundances were less than 0.04% for the diesel generators, and ranged from 0.5 ± 0.59% (MTVR) to 0.1 ± 0.008% (AAV) for the mobile source emissions. Polycyclic aromatic hydrocarbon (PAH) abundances were in the range of 0.03 to 0.08%. Trace element abundances were low, but they were ~3 – 10 times higher in mobile source $PM_{2.5}$ than in $PM_{2.5}$ from the diesel generators. Elevated potassium (K; 0.13 ± 0.28%), Ca (0.17 ± 0.11%), and Fe (0.32 ± 0.4%) abundances were found for the MTVR. Elevated Ca (0.5 ± 0.2%) was also reported for LVS. $PM_{2.5}$ $SO_4^=$ was comparable to the generators, in the range of 0.3 – 1.1%.

Though emission factors derived from the study were limited, they still make a substantial addition to the available information on emissions from non-road diesel engines, especially those used for military applications. Electronic data files were created that can be pasted into EPA's NONROAD emissions model that can be used to better estimate base emissions than would be available using the default emission factors.

8.3 Recommendations and Knowledge Gaps

Although this project made progress in developing and evaluating non-road measurement technologies, the number of tests is still small relative to the number needed to represent real-world emission distributions. Although the MEL, IPETS, and VERSS were shown to be feasible for military engine emissions quantification, they interfere too much with normal military operations to be practical. Smaller, portable units that acquire continuous measurements and can be mounted on mobile diesel sources are needed to acquire these larger data bases. Although these were not available for this project, technology is advancing rapidly and such instruments should be pursued in future non-road measurement studies.

9. REFERENCES

Abdul-Khalek, I.S.; Kittelson, D.B.; and Brear, F.(2000). Nanoparticle growth during dilution and cooling of diesel exhaust: Experimental investigation and theoretical assessment (SAE200-01-0515). In *SAE 2000 World Congress*. SAE, Detroit, MI, pp. 1-9.

Agarwal, A.K. (2007). Biofuels (alcohols and biodiesel) applications as fuels for internal combustion engines. *Progress in Energy and Combustion Science*, **33**(3):233-271.

Agarwal, D.; and Agarwal, A.K. (2007). Performance and emissions characteristics of Jatropha oil (preheated and blends) in a direct injection compression ignition engine. *Applied Thermal Engineering*, **27**(13):2314-2323.

Amann, C.A.; and Siegla, D.C. (1982). Diesel particulates- What they are and why. *Aerosol Sci. Technol.*, **1**:73-101.

Arnold, F.; Pirjola, L.; Aufmhoff, H.; Schuck, T.; Lähde, T.; and Hämeri, K. (2006). First gaseous sulfuric acid measurements in automobile exhaust: Implications for volatile nanoparticle formation. *Atmos. Environ.*, **40**(37):7097-7105.

Arnott, W.P.; Moosmüller, H.; Rogers, C.F.; Jin, T.; and Bruch, R. (1999). Photoacoustic spectrometer for measuring light absorption by aerosol: Instrument description. *Atmos. Environ.*, **33**(17):2845-2852.

Arnott, W.P.; Moosmüller, H.; Sheridan, P.J.; Ogren, J.A.; Raspet, R.; Slaton, W.V.; Hand, J.L.; Kreidenweis, S.M.; and Collett, J.L., Jr. (2003). Photoacoustic and filter-based ambient aerosol light absorption measurements: Instrument comparison and the role of relative humidity. *J. Geophys. Res.*, **108**(D1):AAC 15-1-AAC 15-11.

Arnott, W.P.; Zielinska, B.; Rogers, C.F.; Sagebiel, J.C.; Park, K.; Chow, J.C.; Moosmüller, H.; Watson, J.G.; Kelly, K.; Wagner, D.; Sarofim, A.; Lighty, J.; and Palmer, G. (2005). Evaluation of 1047 nm photoacoustic instruments and photoelectric aerosol sensors in source-sampling of black carbon aerosol and particle bound PAH's from gasoline and diesel powered vehicles. *Environ. Sci. Technol.*, **39**(14):5398-5406.

Arrigone, G.M.; and Hilton, M. (2005). Theory and practice in using Fourier transform infrared spectroscopy to detect hydrocarbons in emissions from gas turbine engines. *Fuel*, **84**(9):1052-1058.

Bachmann, J.D. (2007). Will the circle be unbroken: A history of the US national ambient air quality standards. *J. Air Waste Manage. Assoc.*, **57**(6):652-697.

Bagley, S.T.; Gratz, L.D.; Johnson, J.H.; and McDonald, J.F. (1998). Effects of an oxidation catalytic converter and a biodiesel fuel on the chemical, mutagenic, and particle size characteristics of emissions from a diesel engine. *Enivron. Sci. Technol.*, **32**(9):1183-1191.

Barber, P.W.; Moosmüller, H.; Keislar, R.E.; Kuhns, H.D.; Mazzoleni, C.; and Watson, J.G. (2004). On-road measurement of automotive particle emissions by ultraviolet lidar and transmissometer: Theory. *Meas. Sci. Technol.*, **15**:2295-2302.

Bari, S.; Yu, C.W.; and Lim, T.H. (2002). Performance deterioration and durability issues while running a diesel engine with crude palm oil. *Proceedings of the Institution of Mechanical Engineers Part D-Journal of Automobile Engineering*, **216**(D9):785-792.

Baum, M.M.; Kiyomiya, E.S.; Kumar, S.; Lappas, A.M.; Kapinus, V.A.; and Lord, H.C., III (2001). Multicomponent remote sensing of vehicle exhaust by dispersive absorption spectroscopy - 2. Direct on-road ammonia measurements. *Environ. Sci. Technol.*, **35**(18):3735-3741.

Baum, M.M.; Kiyomiya, E.S.; Kumar, S.; Lappas, A.M.; and Lord, H.C., III (2000). Multicomponent remote sensing of vehicle exhaust by dispersive absorption spectroscopy 1. Effect of fuel type and catalyst performance. *Environ. Sci. Technol.*, **34**(13):2851-2858.

Beckerman, B.; Jerrett, M.; Brook, J.R.; Verma, D.K.; Arain, M.A.; and Finkelstein, M.M. (2008). Correlation of nitrogen dioxide with other traffic pollutants near a major expressway. *Atmos. Environ.*, **42**(2):275-290.

Behymer, T.D.; and Hites, R.A. (1984). Similarity of some organic compounds in spark-ignition and diesel engine particulate extracts. *Enivron. Sci. Technol.*, **18**:203.

Bilcan, A.; Le Corre, O.; and Delebarre, A. (2003). Thermal efficiency and environmental performances of a biogas-diesel stationary engine. *Environmental Technology*, **24**(9):1165-1173.

Biluck, J. (2007). The use of biodiesel in a school transportation system: The case of Medford Township, New Jersey. *Inhal. Toxicol.*, **19**(12):1041-1043.

Bishop, G.A.; McLaren, S.E.; Stedman, D.H.; Pierson, W.R.; Zweidinger, R.B.; and Ray, W. (1996). Method comparisons of vehicle emissions measurements in the Fort McHenry and Tuscarora mountain tunnels. *Atmos. Environ.*, **30**(12):2307-2316.

Bishop, G.A.; Starkey, J.R.; Ihlenfeldt, A.; Williams, W.J.; and Stedman, D.H. (1989). IR long-path photometry: A remote sensing tool for automobile emissions. *Anal. Chem.*, **61**(10):671A-677A.

Bishop, G.A.; and Stedman, D.H. (1990). On-road carbon monoxide emission measurement comparisons for the 1988-1989 Colorado oxy-fuels program. *Enivron. Sci. Technol.*, **24**(6):843-847.

Bishop, G.A.; and Stedman, D.H. (1996). Measuring the emissions of passing cars. *Accounts of Chemical Res.*, **29**:489-495.

Bishop, G.A.; Stedman, D.H.; Hutton, R.B.; Bohren, L.; and Lacey, N. (2000). Drive-by motor vehicle emissions: Immediate feedback in reducing air pollution. *Environ. Sci. Technol.*, **34**(6):1110-1116.

Bishop, G.A.; Zhang, Y.; McLaren, S.E.; Guenther, P.L.; Beaton, S.P.; Peterson, J.E.; Stedman, D.H.; Pierson, W.R.; Knapp, K.T.; Zweidinger, R.B.; Duncan, J.W.; McArver, A.Q.; Groblicki, P.J.; and Day, F.J. (1994). Enhancements of remote sensing for vehicle emissions in tunnels. *J. Air Waste Manage. Assoc.*, **44**(2):169-175.

Biswas, P.; and Wu, C.Y. (2005). 2005 Critical Review: Nanoparticles and the environment. *J. Air Waste Manage. Assoc.*, **55**(6):708-746.

Boughedaoui, M.; Kerbachi, R.; and Joumard, R. (2008). On-board emission measurement of high-loaded light-duty vehicles in Algeria. *J. Air Waste Manage. Assoc.*, **58**:45-54.

Bradley, K.S.; Brooks, K.B.; Hubbard, L.K.; Popp, P.J.; and Stedman, D.H. (2000). Motor vehicle fleet emissions by OP-FTIR. *Environ. Sci. Technol.*, **34**(5):897-899.

Brandenberger, S.; Mohr, M.; Grob, K.; and Neukomb, H.P. (2005). Contribution of unburned lubricating oil and diesel fuel to particulate emission from passenger cars. *Atmos. Environ.*, **39**(37):6985-6994.

Brown, J.E.; Clayton, M.J.; Harris, D.B.; and King, F.G., Jr. (2000). Comparison of particle size distribution of heavy duty diesel exhaust using a dilution tailpipe sampler and an in-plume sampler during on-road operations. *J. Air Waste Manage. Assoc.*, **50**(8):1407-1416.

Buchholz, B.A.; Mueller, C.J.; Martin, G.C.; Cheng, A.S.; Dibble, R.W.; and Frantz, B.R. (2004). Tracing fuel component carbon in the emissions from diesel engines. *Nuclear Instruments & Methods in Physics Research Section B-Beam Interactions with Materials and Atoms*, **223-24**:837-841.

Bukowiechi, N.; Dommen, J.; Prevot, A.S.H.; Richter, R.; Weingartner, E.; and Baltensperger, U. (2002). A mobile pollutant measurement laboratory-measuring gas phase and aerosol ambient concentrations with high spatial and temporal resolution. *Atmos. Environ.*, **36**(36-37):5569-5579.

Bukowiecki, N.; Dommen, J.; Prevot, A.S.H.; Richter, R.; Weingartner, E.; and Baltensperger, U. (2003). Fine and ultrafine particles in the Zurich (Switzerland) area measured with a mobile laboratory. *Atmos. Chem. Phys. Discuss.*, **3**:2739-2782.

Bünger, J.; Krahl, J.; Baum, K.; Schröder, O.; Müller, M.; Westphal, G.; Ruhnau, P.; Schulz, T.G.; and Hallier, E. (2000). Cytotoxic and mutagenic effects, particle size and concentration analysis of diesel engine emissions using biodiesel and petrol diesel as fuel. *Arch Toxicol*, **74**(8):490-498.

Bunger, J.; Krahl, J.; Franke, H.U.; Munack, A.; and Hallier, E. (1998). Mutagenic and cytotoxic effects of exhaust particulate matter of biodiesel compared to fossil diesel fuel. *Mutation Research-Genetic Toxicology and Environmental Mutagenesis*, **415**(1-2):13-23.

Bunn, W.B.; Hesterberg, T.W.; Valberg, P.A.; Slavin, T.J.; Hart, G.; and Lapin, C.A. (2004). A reevaluation of the literature regarding the health assessment of diesel engine exhaust. *Inhal. Toxicol.*, **16**(14):889-900.

Burgard, D.A.; Bishop, G.A.; and Stedman, D.H. (2006). Remote sensing of ammonia and sulfur dioxide from on-road light duty vehicles. *Environ. Sci. Technol.*, **40**(22):7018-7022.

Burtscher, H. (2005). Physical characterization of particulate emissions from diesel engines: A review. *J. Aerosol Sci.*, **36**(7):896-932.

California Air Resources Board (1998). Proposed identification of diesel exhaust as a toxic air contaminant. Appendix III. Part A: Exposure assessment. Prepared by California Air Resources Board, Sacramento, CA.

California Air Resources Board (2007). EMFAC2007. Prepared by California Air Resources Board, Sacramento, CA. http://www.arb.ca.gov/msei/onroad/latest_version.htm.

Canagaratna, M.R.; Jayne, J.T.; Ghertner, D.A.; Herndon, S.; Shi, Q.; Jimenez, J.L.; Silva, P.J.; Williams, P.; Lanni, T.; Drewnick, F.; Demerjian, K.L.; Kolb, C.E.; and Worsnop, D.R. (2004). Chase studies of particulate emissions from in-use New York City vehicles. *Aerosol Sci. Technol.*, **38**(6):555-573.

Canakci, M. (2007). Combustion characteristics of a turbocharged DI compression ignition engine fueled with petroleum diesel fuels and biodiesel. *Bioresource Technology*, **98**:1167-1175.

Canakci, M.; and Van Gerpen, J.H. (2003). Comparison of engine performance and emissions for petroleum diesel fuel, yellow grease biodiesel, and soybean oil biodiesel. *Transactions of the ASAE*, **46**(4):937-944.

Cantu, A.; Pophal, G.; Hall, S.; and Laush, C.T. (1998). A unique application of an extractive FTIR ambient air monitoring system for the simultaneous detection of multiple-ppb-level VOCs. *Appl. Phys. B*, **67**:493-496.

Caravaggio, G.A.; Charland, J.P.; MacDonald, P.; and Graham, L. (2007). n-Alkane profiles of engine lubricating oil and particulate matter by molecular sieve extraction. *Environ. Sci. Technol.*, **41**(10):3697-3701.

Carraretto, C.; Macor, A.; Mirandola, A.; Stoppato, A.; and Tonon, S. (2004). Biodiesel as alternative fuel: Experimental analysis and energetic evaluations. *Energy*, **29**(12-15):2195-2211.

Cauda, E.; Hernandez, S.; Fino, D.; Saracco, G.; and Specchia, V. (2006). PM0.1 emissions during diesel trap regeneration. *Environ. Sci. Technol.*, **40**(17):5532-5537.

Cernansky, N.P. (1983). Diesel exhaust odor and irritants: A review. *J. Air Poll. Control Assoc.*, **33**(2):97-104.

Cetinkaya, M.; and Karaosmanoglu, F. (2005). A new application area for used cooking oil originated biodiesel: Generators. *Energy & Fuels*, **19**(2):645-652.

Chan, C.Y.; Xu, X.D.; Li, Y.S.; Wong, K.H.; Ding, G.A.; Chan, L.Y.; and Cheng, X.H. (2005). Characteristics of vertical profiles and sources of PM2.5, PM10 and carbonaceous species in Beijing. *Atmos. Environ.*, **39**:5113-5124.

Chan, T.; and Lippmann, M. (1977). Particle collection efficiencies of sampling cyclones: An empirical theory. *Enivron. Sci. Technol.*, **11**(4):377-386.

Chandraju, S.; and Prathima, B.K. (2004). Ethyl ester of Honge oil and palm oil blends with diesel as an ecofriendly fuel in heavy duty vehicles: An investigation. *Asian Journal of Chemistry*, **16**(1):147-155.

Chang, M.-C.O.; Chow, J.C.; Watson, J.G.; Glowacki, C.; Sheya, S.A.; and Prabhu, A. (2005). Characterization of fine particulate emissions from casting processes. *Aerosol Sci. Technol.*, **39**(10):947-959.

Chang, M.-C.O.; Yi, S.M.; Hopke, P.K.; England, G.C.; Chow, J.C.; and Watson, J.G. (2004). Measurement of ultrafine particle size distributions from coal-, oil-, and gas-fired stationary combustion sources. *J. Air Waste Manage. Assoc.*, **54**(12):1494-1505.

Chauhan, R.D.; Sharma, M.P.; Saini, R.P.; and Singal, S.K. (2007). Biodiesel from Jatropha as transport fuel - A case study of UP State, India. *Journal of Scientific & Industrial Research*, **66**(5):394-398.

Chen, C.H.; Huang, C.; Jing, Q.G.; Wang, H.K.; Pan, H.S.; Li, L.; Zhao, J.; Dai, Y.; Huang, H.Y.; Schipper, L.; and Streets, D.G. (2007). On-road emission characteristics of heavy-duty diesel vehicles in Shanghai. *Atmos. Environ.*, **41**(26):5334-5344.

Chen, Y.C.; and Wu, C.H. (2002). Emissions of submicron particles from a direct injection diesel engine by using biodiesel. *Journal of Environmental Science and Health-Part A*, **37**(5):829-843.

Chen, Y.Z.; Shah, N.; Braun, A.; Huggins, F.E.; and Huffman, G.P. (2005). Electron microscopy investigation of carbonaceous particulate matter generated by combustion of fossil fuels. *Energy & Fuels*, **19**(4):1644-1651.

Cheng, Y.S.; Zhou, Y.; Chow, J.C.; Watson, J.G.; and Frazier, C. (2001). Chemical composition of aerosols from kerosene heaters burning jet fuel. *Aerosol Sci. Technol.*, **35**(6):949-957.

Choi, S.H.; and Oh, Y. (2006). The emission effects by the use of biodiesel fuel. *International Journal of Modern Physics B*, **20**(25-27):4481-4486.

Chow, J.C. (1995). Critical review: Measurement methods to determine compliance with ambient air quality standards for suspended particles. *J. Air Waste Manage. Assoc.*, **45**(5):320-382.

Chow, J.C. (2001a). 2001 Critical review discussion - Diesel engines: Environmental impact and control. *J. Air Waste Manage. Assoc.*, **51**(9):1258-1270.

Chow, J.C. (2001b). Diesel engines: Environmental impact and control - A critical review introduction. *J. Air Waste Manage. Assoc.*, **51**(6):1258-1270.

Chow, J.C. (2002). 2002 Critical review introduction - Visibility: Science and regulation. *J. Air Waste Manage. Assoc.*, **52**(6):626-627.

Chow, J.C.; Bachmann, J.D.; Wierman, S.S.G.; Mathai, C.V.; Malm, W.C.; White, W.H.; Mueller, P.K.; Kumar, N.K.; and Watson, J.G. (2002). 2002 Critical review discussion - Visibility: Science and regulation. *J. Air Waste Manage. Assoc.*, **52**(9):973-999.

Chow, J.C.; and Watson, J.G. (1999). Ion chromatography in elemental analysis of airborne particles. In *Elemental Analysis of Airborne Particles, Vol. 1*, S. Landsberger and M. Creatchman, Eds. Gordon and Breach Science, Amsterdam, pp. 97-137.

Chow, J.C.; and Watson, J.G. (2008). New directions: Beyond compliance air quality measurements. *Atmos. Environ.*, **42**(21):5166-5168.

Chow, J.C.; Watson, J.G.; Chen, L.W.A.; Chang, M.C.O.; Robinson, N.F.; Trimble, D.; and Kohl, S. (2007a). The IMPROVE-A temperature protocol for thermal/optical carbon analysis: Maintaining consistency with a long-term database. *J. Air Waste Manage. Assoc.*, **57**(9):1014-1023.

Chow, J.C.; Watson, J.G.; and Chen, L.-W.A. (2004a). Contemporary inorganic and organic speciated particulate matter source profiles for geological material, motor vehicles, vegetative burning, industrial boilers, and residential cooking - Draft report. Prepared for Pechan and Associates, Inc., Springfield, VA, by Desert Research Institute, Reno, NV.

Chow, J.C.; Watson, J.G.; Chen, L.-W.A.; Arnott, W.P.; Moosmüller, H.; and Fung, K.K. (2004b). Equivalence of elemental carbon by Thermal/Optical Reflectance and Transmittance with different temperature protocols. *Environ. Sci. Technol.*, **38**(16):4414-4422.

Chow, J.C.; Watson, J.G.; Chen, L.-W.A.; Chang, M.-C.O.; Robinson, N.F.; Trimble, D.L.; and Kohl, S.D. (2007b). The IMPROVE_A temperature protocol for thermal/optical carbon analysis: Maintaining consistency with a long-term data base. *J. Air Waste Manage. Assoc.*, **57**:1014-1023.

Chow, J.C.; Watson, J.G.; Chen, L.-W.A.; Paredes-Miranda, G.; Chang, M.-C.O.; Trimble, D.; Fung, K.K.; Zhang, H.; and Yu, J.Z. (2005a). Refining temperature measures in thermal/optical carbon analysis. *Atmos. Chem. Phys.*, **5**(4):2961-2972.

Chow, J.C.; Watson, J.G.; Crow, D.; Lowenthal, D.H.; and Merrifield, T.M. (2001). Comparison of IMPROVE and NIOSH carbon measurements. *Aerosol Sci. Technol.*, **34**(1):23-34.

Chow, J.C.; Watson, J.G.; Feldman, H.J.; Nolan, J.; Wallerstein, B.R.; and Bachmann, J.D. (2007c). 2007 Critical review discussion - Will the circle be unbroken: A history of the U.S. National Ambient Air Quality Standards. *J. Air Waste Manage. Assoc.*, **57**(10):1151-1163.

Chow, J.C.; Watson, J.G.; Lowenthal, D.H.; Chen, L.-W.A.; Tropp, R.J.; Park, K.; and Magliano, K.L. (2006a). PM2.5 and PM10 mass measurements in California's San Joaquin Valley. *Aerosol Sci. Technol.*, **40**(10):796-810.

Chow, J.C.; Watson, J.G.; Lowenthal, D.H.; Chen, L.-W.A.; Zielinska, B.; Mazzoleni, L.R.; and Magliano, K.L. (2007d). Evaluation of organic markers for chemical mass balance source apportionment at the Fresno supersite. *Atmos. Chem. Phys.*, **7**(7):1741-2754. http://www.atmos-chem-phys.net/7/1741/2007/acp-7-1741-2007.pdf.

Chow, J.C.; Watson, J.G.; Mauderly, J.L.; Costa, D.L.; Wyzga, R.E.; Vedal, S.; Hidy, G.M.; Altshuler, S.L.; Marrack, D.; Heuss, J.M.; Wolff, G.T.; Pope, C.A., III; and Dockery, D.W. (2006b). 2006 critical review discussion - Health effects of fine particulate air pollution: Lines that connect. *J. Air Waste Manage. Assoc.*, **56**(10):1368-1380.

Chow, J.C.; Watson, J.G.; Pritchett, L.C.; Pierson, W.R.; Frazier, C.A.; and Purcell, R.G. (1993). The DRI Thermal/Optical Reflectance carbon analysis system: Description, evaluation and applications in U.S. air quality studies. *Atmos. Environ.*, **27A**(8):1185-1201.

Chow, J.C.; Watson, J.G.; Savage, N.; Solomon, J.; Cheng, Y.S.; McMurry, P.H.; Corey, L.M.; Bruce, G.M.; Pleus, R.C.; Biswas, P.; and Wu, C.Y. (2005b). 2005 Critical review discussion: Nanoparticles and the environment. *J. Air Waste Manage. Assoc.*, **55**(10):1411-1417.

Chow, J.C.; Yu, J.Z.; Watson, J.G.; Ho, S.S.H.; Bohannan, T.L.; Hays, M.D.; and Fung, K.K. (2007e). The application of thermal methods for determining chemical composition of carbonaceous aerosols: A Review. *Journal of Environmental Science and Health-Part A*, **42**(11):1521-1541.

Chung, A.; Chang, D.P.Y.; Kleeman, M.J.; Perry, K.D.; Cahill, T.A.; Dutcher, D.; McDougall, E.M.; and Stroud, K. (2001). Comparison of real-time instruments used to monitor airborne particulate matter. *J. Air Waste Manage. Assoc.*, **51**(1):109-120.

Chung, A.; Lall, A.A.; and Paulson, S.E. (2008). Particulate emissions by a small non-road diesel engine: Biodiesel and diesel characterization and mass measurements using the extended idealized aggregates theory. *Atmos. Environ.*, **42**(9):2129-2140.

Clean Air Scientific Advisory Committee (2000). Review of EPA's health assessment document for diesel exhaust (EPA 600/8-90/057E). Report No. EPA-SAB-CASAC-01-003. Prepared by U.S. Environmental Protection Agency, Science Advisory Board, Washington, DC. http://www.epa.gov/sab/casc0103.pdf.

Cocker, D.R.; Shah, S.D.; Johnson, K.; Miller, J.W.; and Norbeck, J.M. (2004a). Development and application of a mobile laboratory for measuring emissions from diesel engines 1. Regulated gaseous emissions. *Environ. Sci. Technol.*, **38**(7):2182-2189.

Cocker, D.R.; Shah, S.D.; Johnson, K.C.; Zhu, X.N.; Miller, J.W.; and Norbeck, J.M. (2004b). Development and application of a mobile laboratory for measuring emissions from diesel engines. 2. Sampling for toxics and particulate matter. *Environ. Sci. Technol.*, **38**(24):6809-6816.

Coffman, D.J.; and Hegg, D.A. (1995). A preliminary study of the effect of ammonia on particle nucleation in the marine boundary layer. *J. Geophys. Res.*, **100**(D4):7147-7160.

Collins, J.F.; Shepherd, P.; Durbin, T.D.; Lents, J.; Norbeck, J.; and Barth, M. (2007). Measurements of in-use emissions from modern vehicles using an on-board measurement system. *Environ. Sci. Technol.*, **41**(18):6554-6561.

Cook, R.; Touma, J.S.; Fernandez, A.; Brzezinski, D.; Bailey, C.; Scarbro, C.; Thurman, J.; Strum, M.; Ensley, D.; and Baldauf, R. (2007). Impact of underestimating the effects of cold temperature on motor vehicle start emissions of air toxics in the United States. *J. Air Waste Manage. Assoc.*, **57**:1469-1479.

Corporan, E.; Reich, R.; Monroig, O.; Dewitt, M.J.; Larson, V.; Aulich, T.; Mann, M.; and Seames, W. (2005). Impacts of biodiesel on pollutant emissions of a JP-8-fueled turbine engine. *J. Air Waste Manage. Assoc.*, **55**(7):940-949.

Correa, S.M.; and Arbilla, G. (2006). Aromatic hydrocarbons emissions in diesel and biodiesel exhaust. *Atmos. Environ.*, **40**(35):6821-6826.

Correa, S.M.; and Arbilla, G. (2008). Carbonyl emissions in diesel and biodiesel exhaust. *Atmos. Environ.*, **42**(4):769-775.

Countess, R.J.; Barnard, W.R.; Claiborn, C.S.; Gillette, D.A.; Latimer, D.A.; Pace, T.G.; and Watson, J.G. (2001). Methodology for estimating fugitive windblown and mechanically resuspended road dust emissions applicable for regional scale air quality modeling. Report No. 30203-9. Prepared by Western Regional Air Partnership, Denver, CO. http://wrapair.org.

Demirbas, A. (2002a). Biodiesel from vegetable oils via transesterification in supercritical methanol. *Energy Conversion and Management*, **43**(17):2349-2356.

Demirbas, A. (2002b). Diesel fuel from vegetable oil via transesterification and soap pyrolysis. *Energy Sources*, **24**(9):835-841.

Demirbas, A. (2007). Progress and recent trends in biofuels. *Progress in Energy and Combustion Science*, **33**(1):1-18.

Desantes, J.M.; Bermudez, V.; Pastor, J.V.; and Fuentes, E. (2004). Methodology for measuring exhaust aerosol size distributions from heavy duty diesel engines by means of a scanning mobility particle sizer. *Measurement Science & Technology*, **15**(10):2083-2098.

Dewulf, J.; van Langenhove, H.; and van de Velde, B. (2005). Exergy-based efficiency and renewability assessment of biofuel production. *Environ. Sci. Technol.*, **39**(10):3878-3882.

Dorado, M.P.; Arnal, J.M.; Gomez, J.; Gil, A.; and Lopez, F.J. (2002). The effect of a waste vegetable oil blend with diesel fuel on engine performance. *Transactions of the ASAE*, **45**(3):519-523.

Dorado, M.P.; Ballesteros, E.; Arnal, J.M.; Gomez, J.; and Gimenez, F.J.L. (2003). Testing waste olive oil methyl ester as a fuel in a diesel engine. *Energy & Fuels*, **17**(6):1560-1565.

Duc, P.M.; and Wattanavichien, K. (2007). Study on biogas premixed charge diesel dual fuelled engine. *Energy Conversion and Management*, **48**(8):2286-2308.

Duffield, J.A. (2007). Biodiesel: Production and economic issues. *Inhal. Toxicol.*, **19**(12):1029-1031.

Duran, A.; Carmona, M.; and Monteagudo, J.M. (2004). Modelling soot and SOF emissions from a diesel engine. *Chemosphere*, **56**(3):209-225.

Duran, A.; Carmona, M.; Monteagudo, J.M.; and Hernandez, J.J. (2003). An easy correlation to determine soluble and insoluble fractions in diesel particulate matter. *Fuel*, **82**(18):2173-2178.

Duran, A.; de Lucas, A.; Carmona, M.; Ramos, M.J.; and Armas, O. (2002). Accuracy of the European Standard Method to measure the amount of DPM emitted to the atmosphere. *Fuel*, **81**(16):2053-2060.

Duran, A.; Monteagudo, J.M.; Armas, O.; and Hernandez, J.J. (2006). Scrubbing effect on diesel particulate matter from transesterified waste oils blends. *Fuel*, **85**(7-8):923-928.

Durbin, T.D.; Cocker, D.R.; Sawant, A.A.; Johnson, K.; Miller, J.W.; Holden, B.B.; Helgeson, N.L.; and Jack, J.A. (2007a). Regulated emissions from biodiesel fuels from on/off-road applications. *Atmos. Environ.*, **41**(27):5647-5658.

Durbin, T.D.; Collins, J.R.; Norbeck, J.M.; and Smith, M.R. (2000). Effects of biodiesel, biodiesel blends, and a synthetic diesel on emissions from light heavy-duty diesel vehicles. *Environ. Sci. Technol.*, **34**(3):349-355.

Durbin, T.D.; Johnson, K.; Cocker, D.R.; Miller, J.W.; Maldonado, H.; Shah, A.; Ensfield, C.; Weaver, C.; Akard, M.; Harvey, N.; Symon, J.; Lanni, T.; Bachalo, W.D.; Payne, G.; Smallwood, G.; and Linke, M. (2007b). Evaluation and comparison of portable emissions measurement systems and federal reference methods for emissions from a back-up generator and a diesel truck operated on a chassis dynamometer. *Environ. Sci. Technol.*, **41**(17):6199-6204.

Durbin, T.D.; Johnson, K.; Miller, J.W.; Maldonado, H.; and Chernich, D. (2008). Emissions from heavy-duty vehicles under actual on-road driving conditions. *Atmos. Environ.*, **42**(20):4812-4821.

Durbin, T.D.; and Norbeck, J.M. (2002). Effects of biodiesel blends and ARCO EC-diesel on emissions from light heavy-duty diesel vehicles. *Environ. Sci. Technol.*, **36**(8):1686-1691.

Dwivedi, D.; Agarwal, A.K.; and Sharma, M. (2006). Particulate emission characterization of a biodiesel vs diesel-fuelled compression ignition transport engine: A comparative study. *Atmos. Environ.*, **40**(29):5586-5595.

Eichlseder, H.; and Wimmer, A. (2003). Potential of IC-engines as minimum emission propulsion system. *Atmos. Environ.*, **37**(37):5227-5236.

Ekstrom, M.; Sjodin, A.; and Andreasson, K. (2004). Evaluation of the COPERT III emission model with on-road optical remote sensing measurements. *Atmos. Environ.*, **38**(38):6631-6641.

England, G.C.; Watson, J.G.; Chow, J.C.; Zielinska, B.; Chang, M.-C.O.; Loos, K.R.; and Hidy, G.M. (2007a). Dilution-based emissions sampling from stationary sources: Part 1. Compact sampler, methodology and performance. *J. Air Waste Manage. Assoc.*, **57**(1):65-78.

England, G.C.; Watson, J.G.; Chow, J.C.; Zielinska, B.; Chang, M.-C.O.; Loos, K.R.; and Hidy, G.M. (2007b). Dilution-based emissions sampling from stationary sources: Part 2. Gas-fired combustors compared with other fuel-fired systems. *J. Air Waste Manage. Assoc.*, **57**(1):79-93.

Etyemezian, V.; Tesfaye, M.; Yimer, A.; Chow, J.C.; Mesfin, D.; Nega, T.; Nikolich, G.; Watson, J.G.; and Wondmagegn, M. (2005). Results from a pilot-scale air quality study in Addis Ababa, Ethiopia. *Atmos. Environ.*, **39**(40):7849-7860.

Fernandes, M.B.; and Brooks, P. (2003). Characterization of carbonaceous combustion residues: II. Nonpolar organic compounds. *Chemosphere*, **53**(5):447-458.

Fernando, S.; and Hanna, M. (2004). Development of a novel biofuel blend using ethanol-biodiesel-diesel microemulsions: EB-diesel. *Energy & Fuels*, **18**(6):1695-1703.

Fino, D. (2007). Diesel emission control: Catalytic filters for particulate removal. *Science and Technology of Advanced Materials*, **8**(1-2):93-100.

Fontaras, G.; Tzamkiozis, T.; Hatziemmanouil, E.; and Samaras, Z. (2007). Experimental study on the potential application of cottonseed oil-diesel blends as fuels for automotive diesel engines. *Process Safety and Environmental Protection*, **85**(B5):396-403.

Forson, F.K.; Oduro, E.K.; and Hammond-Donkoh, E. (2004). Performance of jatropha oil blends in a diesel engine. *Renewable Energy*, **29**(7):1135-1145.

Frank, B.P.; Tang, S.; Lanni, T.; Grygas, J.; Rideout, G.; Meyer, N.; and Beregszaszy, C. (2007). The effect of fuel type and aftertreatment method on ultrafine particle emissions from a heavy-duty diesel engine. *Aerosol Sci. Technol.*, **41**(11):1029-1039.

Fraser, M.P.; and Lakshmanan, K. (2003). Variation in composition of fine particulate emissions from heavy-duty diesel vehicles. *J. Geophys. Res.*, **107**(D21):8346.

Frey, H.C.; Unal, A.; Rouphail, N.M.; and Colyar, J.D. (2003). On-road measurement of vehicle tailpipe emissions using a portable instrument. *J. Air Waste Manage. Assoc.*, **53**(8):992-1002.

Frey, H.C.; Zhang, K.S.; and Rouphail, N.M. (2008). Fuel use and emissions comparisons for alternative routes, time of day, road grade, and vehicles based on in-use measurements. *Environ. Sci. Technol.*, **42**(7):2483-2489.

Fujita, E.M.; Campbell, D.E.; Arnott, W.P.; Chow, J.C.; and Zielinska, B. (2007a). Evaluations of the chemical mass balance method for determining contributions of gasoline and diesel exhaust to ambient carbonaceous aerosols. *J. Air Waste Manage. Assoc.*, **57**(6):721-740.

Fujita, E.M.; Watson, J.G.; Chow, J.C.; Robinson, N.F.; Richards, L.W.; and Kumar, N. (1998). Northern Front Range Air Quality Study. Volume C: Source apportionment and simulation methods and evaluation. Prepared for Colorado State University, Cooperative Institute for Research in the Atmosphere, Ft. Collins, CO, by Desert Research Institute, Reno, NV. http://charon.cira.colostate.edu/DRIFinal/ZipFiles/.

Fujita, E.M.; Zielinska, B.; Campbell, D.E.; Arnott, W.P.; Sagebiel, J.C.; Mazzoleni, L.R.; Chow, J.C.; Gabele, P.A.; Crews, W.; Snow, R.; Clark, N.N.; Wayne, W.S.; and Lawson, D.R. (2007b). Variations in speciated emissions from spark-ignition and compression-ignition motor vehicles in California's south coast air basin. *J. Air Waste Manage. Assoc.*, **57**(6):705-720.

Gardetto, E.; Bagian, T.; and Lindner, J. (2005). High-mileage study of on-board diagnostic emissions. *J. Air Waste Manage. Assoc.*, **55**(10):1480-1486.

Gautam, M.; Thompson, G.J.; Carder, D.K.; Clark, N.N.; Shade, B.C.; Riddle, W.C.; and Lyons, D.W. (2001). Measurement of in-use, on-board emissions from heavy-duty diesel vehicles: mobile emissions measurement system (paper no. SAE 2001-01-3643). Presentation. Society of Automotive Engineers, Warrendale, PA.

Gerhart, C.; and Rettenmoser, T. (2006). Particle number concentration measurements with a "wide-range" aerosol spectrometer system in combination with a PAH sensor for simple source apportionment. *Gefahrstoffe Reinhaltung der Luft*, **66**(11-12):477-481.

Gertler, A.W.; Kuhns, H.; bu-Allaban, M.; Damm, C.; Gillies, J.A.; Etyemezian, V.; Clayton, R.; and Proffitt, D. (2006). A case study of the impact of winter road sand/salt and street sweeping on road dust re-entrainment. *Atmos. Environ.*, **40**(31):5976-5985.

Giannelos, P.N.; Zannikos, F.; Stournas, S.; Lois, E.; and Anastopoulos, G. (2002). Tobacco seed oil as an alternative diesel fuel: physical and chemical properties. *Industrial Crops and Products*, **16**(1):1-9.

Giechaskiel, B.; Ntziachristos, L.; Samaras, Z.; Scheer, V.; Casati, R.; and Vogt, R. (2005). Formation potential of vehicle exhaust nucleation mode particles on-road and in the laboratory. *Atmos. Environ.*, **39**:3191-3198.

Gillies, J.A.; Etyemezian, V.; Kuhns, H.; Nikolic, D.; and Gillette, D.A. (2005). Effect of vehicle characteristics on unpaved road dust emissions. *Atmos. Environ.*, **39**(13):2341-2347.

Gillies, J.A.; and Gertler, A.W. (2000). Comparison and evaluation of chemically speciated mobile source $PM_{2.5}$ profiles. *J. Air Waste Manage. Assoc.*, **50**(8):1459-1480.

Gillies, J.A.; Kuhns, H.; Engelbrecht, J.P.; Uppapalli, S.; Etyemezian, V.; and Nikolich, G. (2007). Particulate emissions from US Department of Defense artillery backblast testing. *J. Air Waste Manage. Assoc.*, **57**(5):551-560.

Gomez-Rico, M.F.; Martin-Gullon, I.; Fullana, A.; Conesa, J.A.; and Font, R. (2003). Pyrolysis and combustion kinetics and emissions of waste lube oils. *Journal of Analytical and Applied Pyrolysis*, **68-9**:527-546.

Goode, J.G.; Yokelson, R.J.; Susott, R.A.; and Ward, D.E. (1999). Trace gas emissions from laboratory biomass fires measured by Fourier transform infrared spectroscopy: Fires in grass and surface fuels. *J. Geophys. Res.*, **104**:21237-21245.

Gouriou, F.; Morin, J.P.; and Weill, M.E. (2004). On-road measurements of particle number concentrations and size distributions in urban and tunnel environments. *Atmos. Environ.*, **38**(18):2831-2840.

Graboski, M.S.; and McCormick, R.L. (1998). Combustion of fat and vegetable oil derived fuels in diesel engines. *Prog. Energy Combust. Sci.*, **24**:125-164.

Green, L.C.; and Armstrong, S.R. (2003). Particulate matter in ambient air and mortality: toxicologic perspectives. *Regulatory Toxicology and Pharmacology*, **38**(3):326-335.

Gu, B.H.; Wang, J.; Zhou, X.T.; Wu, X.; Liu, F.; and Li, Y. (1998). Comparison of multivariate calibration methods for quantitative analysis of multicomponent mixture of air toxic organic compounds by FTIR. *J. Environ. Sci. Health-Part A-Toxics/Haz. Subst & Env. Eng.*, **33**(7):1419-1436.

Guenther, P.L.; Stedman, D.H.; Bishop, G.A.; Beaton, S.P.; Bean, J.H.; and Quine, R.W. (1995). A hydrocarbon detector for the remote sensing of vehicle exhaust emissions. *Rev. Sci. Instrum.*, **66**:3024-3029.

Haefliger, O.P.; Bucheli, T.D.; and Zenobi, R. (2000). Laser mass spectrometric analysis of organic atmospheric aerosols 1. Characterization of emission sources. *Environ. Sci. Technol.*, **34**(11):2178-2183.

Hamelinck, C.N.; and Faaij, A.P.C. (2006). Production of advanced biofuels. *International Sugar Journal*, **108**(1287):168-175.

Hansen, A.C.; Zhang, Q.; and Lyne, P.W.L. (2005). Ethanol-diesel fuel blends - a review. *Bioresource Technology*, **96**(3):277-285.

Harley, R.A.; McKeen, S.A.; Pearson, J.; Rodgers, M.O.; and Lonneman, W.A. (2001). Analysis of motor vehicle emissions during the Nashville/Middle Tennessee Ozone Study. *J. Geophys. Res.*, **106**(D4):3559-3567.

Hays, M.D.; and Lavrich, R.J. (2007). Developments in direct thermal extraction gas chromatography-mass spectrometry of fine aerosols. *Trac-Trends in Analytical Chemistry*, **26**(2):88-102.

He, C.; Morawska, L.; and Taplin, L. (2007). Particle emission characteristics of office printers. *Environ. Sci. Technol.*, **41**(17):6039-6045.

He, C.R.; Morawska, L.; and Gilbert, D. (2005). Particle deposition rates in residential houses. *Atmos. Environ.*, **39**(21):3891-3899.

He, C.R.; Morawska, L.D.; Hitchins, J.; and Gilbert, D. (2004). Contribution from indoor sources to particle number and mass concentrations in residential houses. *Atmos. Environ.*, **38**(21):3405-3415.

Heal, M.R.; Beverland, I.J.; Mccabe, M.; Hepburn, W.; and Agius, R.M. (2000). Intercomparison of five PM10 monitoring devices and the implications for exposure measurement in epidemiological research. *J. Environ. Monit.*, **2**:455-461.

Held, A.; Niessner, R.; Bosveld, F.; Wrzesinsky, T.; and Klemm, O. (2007). Evaluation and application of an electrical low pressure impactor in disjunct eddy covariance aerosol flux measurements. *Aerosol Sci. Technol.*, **41**(5):510-519.

Herndon, S.C.; Jayne, J.T.; Zahniser, M.S.; Worsnop, D.R.; Knighton, B.; Alwine, E.; Lamb, B.K.; Zavala, M.; Nelson, D.D.; McManus, J.B.; Shorter, J.H.; Canagaratna, M.R.; Onasch, T.B.; and Kolb, C.E. (2005a). Characterization of urban pollutant emission fluxes and ambient concentration distributions using a mobile laboratory with rapid response instrumentation. *Faraday Discussions*, **130**:327-339.

Herndon, S.C.; Onasch, T.B.; Frank, B.P.; Marr, L.C.; Jayne, J.T.; Canagaratna, M.R.; Grygas, J.; Lanni, T.; Anderson, B.E.; Worsnop, D.; and Miake-Lye, R.C. (2005b). Particulate emissions from in-use commercial aircraft. *Aerosol Sci. Technol.*, **39**(8):799-809.

Herndon, S.C.; Shorter, J.H.; Zahniser, M.S.; Nelson, D.D.; Jayne, J.; Brown, R.C.; Miake-Lye, R.C.; Waitz, I.; Silva, P.; Lanni, T.; Demerjian, K.L.; and Kolb, C.E. (2004). NO and NO2 emission ratios measured from in-use commercial aircraft during taxi and takeoff. *Environ. Sci. Technol.*, **38**(22):6078-6084.

Herndon, S.C.; Shorter, J.H.; Zahniser, M.S.; Wormhoudt, J.; Nelson, D.D.; Demerjian, K.L.; and Kolb, C.E. (2005c). Real-time measurements of SO2, H2CO, and CH4 emissions from in-use curbside passenger buses in New York City using a chase vehicle. *Environ. Sci. Technol.*, **39**(20):7984-7990.

Hildemann, L.M.; Markowski, G.R.; Jones, M.C.; and Cass, G.R. (1991). Submicrometer aerosol mass distributions of emissions from boilers, fireplaces, automobiles, diesel trucks, and meat-cooking operations. *Aerosol Sci. Technol.*, **14**(1):138-152.

Hill, J.; Nelson, E.; Tilman, D.; Polasky, S.; and Tiffany, D. (2006). Environmental, economic, and energetic costs and benefits of biodiesel and ethanol biofuels. *Proceed. Nat. Acad. Sci.*, **103**(30):11206-11210.

Ho, S.S.H.; and Yu, J.Z. (2004). In-injection port thermal desorption and subsequent gas chromatography-mass spectrometric analysis of polycyclic aromatic hydrocarbons and *n*-alkanes in atmospheric aerosol samples. *J. Chromatogr. A*, **1059**(1-2):121-129.

Ho, S.S.H.; Yu, J.Z.; Chow, J.C.; Zielinska, B.; Watson, J.G.; Sit, E.H.L.; and Schauer, J.J. (2008). Evaluation of an in-injection port thermal desorption-gas chromatography/mass spectrometry method for analysis of non-polar organic compounds in ambient aerosol samples. *Journal of Chromatography A*, **1200**(2):217-227.

Holden, B.B.; Jack, J.A.; Miller, J.W.; and Durbin, T.D. (2006). Effect of biodiesel on diesel engine ntrogen oxide and other regulated emissions. Report No. TR-2275-ENV. Prepared by Naval Facilities Engineering Service Center, Port Hueneme, CA.

Holmen, B.A.; and Qu, Y.G. (2004). Uncertainty in particle number modal analysis during transient operation of compressed natural gas, diesel, and trap-equipped diesel transit buses. *Environ. Sci. Technol.*, **38**(8):2413-2423.

Hribernik, A.; and Kegl, B. (2007). Influence of biodiesel fuel on the combustion and emission formation in a direct injection (DI) diesel engine. *Energy & Fuels*, **21**(3):1760-1767.

Huai, T.; Shah, S.D.; Miller, J.W.; Younglove, T.; Chernich, D.J.; and Ayala, A. (2006). Analysis of heavy-duty diesel truck activity and emissions data. *Atmos. Environ.*, **40**(13):2333-2344.

Huang, W.; Smith, T.J.; Ngo, L.; Wang, T.; Chen, H.Q.; Wu, F.G.; Herrick, R.F.; Christiani, D.C.; and Ding, H. (2007). Characterizing and biological monitoring of polycyclic aromatic hydrocarbons in exposures to diesel exhaust. *Environ. Sci. Technol.*, **41**(8):2711-2716.

Isakov, V.; Touma, J.S.; and Khlystov, A. (2007). A method of assessing air toxics concentrations in urban areas using mobile platform measurements. *J. Air Waste Manage. Assoc.*, **57**(11):1286-1295.

Jack, M.D.; Bahan, T.P.; Gray, M.N.; Hanson, J.L.; Heidt, T.L.; Huerta, F.A.; Nelson, D.R.; Paneral, A.J.; Peterson, C.M.; Polchin, G.C.; Rubin, L.H.; Tacelli, C.B.; Trautfield, W.C.; Wageneck, R.O.; Walter, G.A., et al.(1996). Remote sensing (RES) An adjunct to I/M HEV identification and clean car pre-screening. In *Proceedings of the Sixth CRC On-Road Vehicle Emissions Workshop*, p. P-1-P-14.

Jack, M.D.; Bahan, T.P.; Gray, M.N.; Hanson, J.L.; Heidt, T.L.; Nelson, D.R.; Peterson, C.M.; Polchin, G.C.; Rubin, L.H.; Trautfield, W.C.; Wageneck, R.O.; Walter, G.A.; Wills, J.D.; Alves, J.F.; Brown, J., et al.(1997). Advances in on-road vehicular emissions monitoring instruments (validation of nitric oxide and speed/acceleration using instrumented vehicles) and their utilization in real-world programs for high emitter and clean car identification. In *World Car Conference '97*, Riverside, CA.

Jackson, C.; Sze, C.; Schenk, C.; Olson, B.; and Laroo, C. (2005). Comparison of exhaust emissions from application of the ramped modal cycle and steady-state nonroad test. SAE 2005-01-1615. In *General Emissions 2005*. SAE International, Detroit, MI.

Jakober, C.A.; Riddle, S.G.; Robert, M.A.; Destaillats, H.; Charles, M.J.; Green, P.G.; and Kleeman, M.J. (2007). Quinone emissions from gasoline and diesel motor vehicles. *Environ. Sci. Technol.*, **41**(13):4548-4554.

Jamriska, M.; Morawska, L.; Thomas, S.; and He, C. (2004). Diesel bus emissions measured in a tunnel study. *Environ. Sci. Technol.*, **38**(24):6701-6709.

Ji, P.S.; and Harrison, R.M. (1999). Investigation of ultrafine particle formation during diesel exhaust dilution. *Environ. Sci. Technol.*, **33**:3730-3736.

Jiang, M.; Marr, L.C.; Dunlea, E.J.; Herndon, S.C.; Jayne, J.T.; Kolb, C.E.; Knighton, W.B.; Rogers, T.M.; Zavala, M.; Molina, L.T.; and Molina, M.J. (2005). Vehicle fleet emissions of black carbon, polycyclic aromatic hydrocarbons, and other pollutants measured by a mobile laboratory in Mexico City. *Atmos. Chem. Phys.*, **5**:3377-3387.

Jimenez, J.L. (1999). Understanding and quantifying motor vehicle emissions with vehcile specific power and TDLAS Remote Sensing. Ph.D. Dissertation, Massachusetts Institute of Technology, Cambridge, MA.

Jiménez, J.L.; Koplow, M.D.; Nelson, D.D.; Zahniser, M.S.; and Schmidt, S.E. (1999). Characterization of on-road vehicle NO emissions by a TDLAS remote sensor. *J. Air Waste Manage. Assoc.*, **49**(4):463-470.

Jiménez, J.L.; McManus, J.B.; Shorter, J.H.; Nelson, D.D.; Zahniser, M.S.; Koplow, M.; McRae, G.J.; and Kolb, C.E. (2000a). Cross road and mobile tunable infrared laser measurements of nitrous oxide emissions from motor vehicles. *Chemosphere - Global Change Science*, **2**(3-4):397-412.

Jiménez, J.L.; McRae, G.J.; Nelson, D.D.; Zahniser, M.S.; and Kolb, C.E. (2000b). Remote sensing of NO and NO_2 emissions from heavy-duty diesel trucks using tunable diode lasers. *Environ. Sci. Technol.*, **34**(12):2380-2387.

Johnson, B.J.; Huang, S.C.; Pitchford, M.L.; Ayoub, H.C.; and Naylor, M.H. (1998). Preliminary on-road measurement of the effect of oxygenated fuel on CO emissions near Las Vegas, Nevada. *J. Air Waste Manage. Assoc.*, **48**(1):59-64.

Johnson, J.P.; Kittelson, D.B.; and Watts, W.F. (2005). Source apportionment of diesel and spark ignition exhaust aerosol using on-road data from the Minneapolis metropolitan area. *Atmos. Environ.*, **39**(11):2111-2121.

Johnston, M.; and Holloway, T. (2007). A global comparison of national biodiesel production potentials. *Environ. Sci. Technol.*, **41**(23):7967-7973.

Joumard, R.; Andre, M.; Vidon, R.; and Tassel, P. (2003). Characterizing real unit emissions for light duty goods vehicles. *Atmos. Environ.*, **37**(37):5217-5225.

Jung, H.J.; Kittelson, D.B.; and Zachariah, M.R. (2006). Characteristics of SME biodiesel-fueled diesel particle emissions and the kinetics of oxidation. *Environ. Sci. Technol.*, **40**(16):4949-4955.

Kalam, M.A.; and Masjuki, H.H. (2002). Biodiesel from palmoil - an analysis of its properties and potential. *Biomass & Bioenergy*, **23**(6):471-479.

Kalam, M.A.; and Masjuki, H.H. (2004). Emissions and deposit characteristics of a small diesel engine when operated on preheated crude palm oil. *Biomass & Bioenergy*, **27**(3):289-297.

Kameda, T.; Nakao, T.; Stavarache, C.; Maeda, Y.; Hien, T.T.; Takenaka, N.; Okitsu, K.; and Bandow, H. (2007). Determination of polycyclic aromatic hydrocarbons and nitrated polycyclic aromatic compounds in diesel-engine exhaust particles from combustion process of biodiesel fuel. *Bunseki Kagaku*, **56**(4):241-248.

Kaul, S.; Saxena, R.C.; Kumar, A.; Negi, M.S.; Bhatnagar, A.K.; Goyal, H.B.; and Gupta, A.K. (2007). Corrosion behavior of biodiesel from seed oils of Indian origin on diesel engine parts. *Fuel Processing Technology*, **88**(3):303-307.

Kayes, D.; and Hochgreb, S. (1999a). Mechanisms of particulate matter formation in spark-ignition engines 1. Effect of engine operating conditions. *Environ. Sci. Technol.*, **33**(22):3957-3967.

Kayes, D.; and Hochgreb, S. (1999b). Mechanisms of particulate matter formation in spark-ignition engines 2. Effect of fuel, oil, and catalyst parameters. *Environ. Sci. Technol.*, **33**(22):3968-3977.

Kayes, D.; and Hochgreb, S. (1999c). Mechanisms of particulate matter formation in spark-ignition engines 3. Model of PM formation. *Environ. Sci. Technol.*, **33**(22):3978-3992.

Kean, A.J.; Sawyer, R.F.; and Harley, R.A. (2000). A fuel-based assessment of off-road diesel engine emissions. *J. Air Waste Manage. Assoc.*, **50**(11):1929-1939.

Kegl, B. (2007). Effects of biodiesel on emissions of a bus diesel engine. *Bioresource Technology*.

Kelly, K.E.; Wagner, D.A.; Lighty, J.S.; Sarofim, A.F.; Rogers, C.F.; Sagebiel, J.C.; Zielinska, B.; Arnott, W.P.; and Palmer, G. (2003). Characterization of exhaust particles from military vehicles fueled with diesel, gasoline, and JP-8. *J. Air Waste Manage. Assoc.*, **53**(3):273-282.

Kemme, M.R.; Brown, W.T.; Frame, E.A.; and Alvarez, R.A. (2004). Diesel powered equipment properties and activity database for DoD off-road sources. Report No. ERDC/CERL TR-04-DRAFT. Prepared by U.S. Army Corps of Engineers, Construction Engineering Research Laboratory, Champaign, IL.

Keskin, A.; Guru, M.; and Altiparmak, D. (2007). Biodiesel production from tall oil with synthesized Mn and Ni based additives: Effects of the additives on fuel consumption and emissions. *Fuel*, **86**(7-8):1139-1143.

Keskinen, J.; Pietarinen, K.; and Lehtimäki, M. (2003). Electrical low pressure impactor. *J. Aerosol Sci.*, **23**:353-360.

Khalek, I.A. (2000). Characterization of particle size distribution of a heavy-duty diesel engine during FTP transient cycle using ELPI. *SAE Technical Paper Series*, **2000-01-2001**.

Khalili, N.R.; Scheff, P.A.; and Holsen, T.M. (1995). PAH source fingerprints for coke ovens, diesel and gasoline engines, highway tunnels, and wood combustion emissions. *Atmos. Environ.*, **29**(4):533-542.

Khan, N.; Warith, M.A.; and Luk, G. (2007). A comparison of acute toxicity of biodiesel, biodiesel blends, and diesel on aquatic organisms. *J. Air Waste Manage. Assoc.*, **57**(3):286-296.

Khillare, P.S.; Balachandran, S.; and Hoque, R.R. (2005). Profile of PAHs in the diesel vehicle exhaust in Delhi. *Environ. Mon. Assess.*, **105**(1-3):411-417.

Kingham, S.; Durand, M.; Aberkane, T.; Harrison, J.; Wilson, J.G.; and Epton, M. (2006). Winter comparison of TEOM, MiniVol and DustTrak PM10 monitors in a woodsmoke environment. *Atmos. Environ.*, **40**(2):338-347.

Kinsey, J.S.; Mitchell, W.A.; Squier, W.C.; Linna, K.; King, F.G.; Logan, R.; Dong, Y.J.; Thompson, G.J.; and Clark, N.N. (2006). Evaluation of methods for the determination of diesel-generated fine particulate matter: Physical characterization results. *J. Aerosol Sci.*, **37**(1):63-87.

Kirchstetter, T.W.; Harley, R.A.; Kreisberg, N.M.; Stolzenburg, M.R.; and Hering, S.V. (1999). On-road measurement of fine particle and nitrogen oxide emissions from light- and heavy-duty motor vehicles. *Atmos. Environ.*, **33**(18):2955-2968.

Kirchstetter, T.W.; Harley, R.A.; Kreisberg, N.M.; Stolzenburg, M.R.; and Hering, S.V. (2002). Corrigendum to "On-road measurement of fine particle and nitrogen oxide emissions from light- and heavy-duty motor vehicles" (Atmos.Environ. 33 (18) (1999) 2955-2968). *Atmos. Environ.*, **36**(39-40):6059.

Kittelson, D.B. (1998). Engines and nanoparticles: A review. *J. Aerosol Sci.*, **29**(5/6):575-588.

Kittelson, D.B. (1999). Review of diesel particulate matter sampling methods. Prepared by Univ. of Minnesota, Dept. of Mechanical Engineering Center for Diesel Research, Minneapolis, MN. http://www.me.umn.edu/centers/cdr/Proj/EPA.html.

Kittelson, D.B.; Watts, W.F.; and Johnson, J.P. (2004a). Nanoparticle emissions on Minnesota highways. *Atmos. Environ.*, **38**(1):9-19.

Kittelson, D.B.; Watts, W.F.; and Johnson, J.P. (2006a). On-road and laboratory evaluation of combustion aerosols - Part 1: Summary of diesel engine results. *J. Aerosol Sci.*, **37**(8):913-930.

Kittelson, D.B.; Watts, W.F.; Johnson, J.P.; Remerowki, M.L.; Ische, E.E.; Oberdörster, G.; Gelein, R.A.; Elder, A.; Hopke, P.K.; Kim, E.; Zhao, W.; Zhou, L.; and Jeong, C.H. (2004b). On-road exposure to highway aerosols. 1. Aerosol and gas measurements. *Inhal. Toxicol.*, **16**(Suppl. 1):31-39.

Kittelson, D.B.; Watts, W.F.; Johnson, J.P.; Rowntree, C.; Payne, M.; Goodier, S.; Warrens, C.; Preston, H.; Zink, U.; Ortiz, M.; Goersmann, C.; Twigg, M.V.; Walker, A.P.; and Caldow, R. (2006b). On-road evaluation of two diesel exhaust aftertreatment devices. *J. Aerosol Sci.*, **37**(9):1140-1151.

Kittelson, D.B.; Watts, W.F.; Johnson, J.P.; Schauer, J.J.; and Lawson, D.R. (2006c). On-road and laboratory evaluation of combustion aerosols - Part 2: Summary of spark ignition engine results. *J. Aerosol Sci.*, **37**(8):931-949.

Kleeman, M.J.; Riddle, S.G.; Robert, M.A.; and Jakober, C.A. (2008). Lubricating oil and fuel contributions to particulate matter emissions from light-duty gasoline and heavy-duty diesel vehicles. *Environ. Sci. Technol.*, **42**(1):235-242.

Knapp, K.T. (1994). On-road vehicle emissions: U.S. studies. *Sci. Total Environ.*, **146/147**:209-215.

Ko, Y.W.; and Cho, C.H. (2006). Characterization of large fleets of vehicle exhaust emissions in middle Taiwan by remote sensing. *Sci. Total Environ.*, **354**(1):75-82.

Kowalewicz, A. (2005). Eco-diesel engine fuelled with rapeseed oil methyl ester and ethanol. Part 1: Efficiency and emission. *Proceedings of the Institution of Mechanical Engineers Part D-Journal of Automobile Engineering*, **219**(D5):715-723.

Kowalewicz, A. (2007). Performance, emissions and combustion parameters of eco-diesel fuelled with RME and ethanol. *Combustion Science and Technology*, **179**(11):2415-2435.

Krahl, J.; Bunger, J.; Schroder, O.; Munack, A.; and Knothe, G. (2002). Exhaust emissions and health effects of particulate matter from agricultural tractors operating on rapeseed oil methyl ester. *Journal of the American Oil Chemists Society*, **79**(7):717-724.

Krishnamurthy, M.; Carder, D.K.; Thompson, G.; and Gautam, M. (2007). Cost of lower NOx emissions: Increased CO2 emissions from heavy-duty diesel engines. *Atmos. Environ.*, **41**(3):666-675.

Krishnamurthy, N.; and Gautam, M. (2006). Development of a heavy-duty engine test cycle representative of on-highway not-to-exceed operation. *Proceedings of the Institution of Mechanical Engineers. Part D, Journal of automobile engineering*, **220**(6):837-848.

Kuhns, H.D.; Barber, P.W.; Keislar, R.E.; Mazzoleni, C.; Moosmüller, H.; Nikolic, D.; Robinson, N.F.; and Watson, J.G. (2002). Remote sensing of gaseous and particle emissions from onroad vehicles in Clark County, Nevada. Prepared for Clark County Department of Comprehensive Planning, Las Vegas, NV, by Desert Research Institute, Las Vegas, NV.

Kuhns, H.D.; Mazzoleni, C.; Moosmüller, H.; Nikolic, D.; Keislar, R.E.; Barber, P.W.; Li, Z.; Etyemezian, V.; and Watson, J.G. (2004). Remote sensing of PM, NO, CO, and HC emission factors for on-road gasoline and diesel engine vehicles in Las Vegas, NV. *Sci. Total Environ.*, **322**:123-137.

Kumar, N. (2007). Production of biodiesel from high FFA rice bran oil and its utilization in a small capacity diesel engine. *Journal of Scientific & Industrial Research*, **66**(5):399-402.

Labban, R.; Veranth, J.M.; Watson, J.G.; and Chow, J.C. (2006). Feasibility of soil dust source apportionment by the pyrolysis-gas chromatography/mass spectrometry method. *J. Air Waste Manage. Assoc.*, **56**(9):1230-1242.

Labeckas, G.; and Slavinskas, S. (2006). The effect of rapeseed oil methyl ester on direct injection Diesel engine performance and exhaust emissions. *Energy Conversion and Management*, **47**(13-14):1954-1967.

Lamoree, D.P.; and Turner, J.R. (1999). PM emissions emanating from limited-access highways. *J. Air Waste Manage. Assoc.*, **49**(PM):PM85-PM94.

Landis, A.E.; Miller, S.A.; and Theis, T.L. (2007). Life cycle of the corn-soybean agroecosystem for biobased production. *Environ. Sci. Technol.*, **41**(4):1457-1464.

Lapuerta, M.; Hernandez, J.J.; Ballesteros, R.; and Duran, A. (2003). Composition and size of diesel particulate emissions from a commercial European engine tested with present and future fuels. *Proceedings of the Institution of Mechanical Engineers Part D-Journal of Automobile Engineering*, **217**(D10):907-919.

Lapuerta, M.; Rodriguez-Fernandez, J.; and Agudelo, J.R. (2007). Diesel particulate emissions from used cooking oil biodiesel. *Bioresource Technology*.

Lara, A.S.; and Feng, L.J. (2006). Selected ion chromatograms and tandem mass spectrometry for detection of trace polycyclic aromatic hydrocarbons in diesel exhaust. *J. Air Waste Manage. Assoc.*, **56**(6):859-868.

Lebedevas, S.; Vaicekauskas, A.; Lebedeva, G.; Makareviciene, V.; and Janulis, P. (2007). Change in operational characteristics of diesel engines running on RME biodiesel fuel. *Energy & Fuels*, **21**(5):3010-3016.

Lebedevas, S.; Vaicekauskas, A.; Lebedeva, G.; Makareviciene, V.; Janulis, P.; and Kazancev, K. (2006). Use of waste fats of animal and vegetable origin for the production of biodiesel fuel: Quality, motor properties, and emissions of harmful components. *Energy & Fuels*, **20**(5):2274-2280.

Lee, R.; Pedley, J.; and Hobbs, C.(1998). Fuel quality impact on heavy duty diesel emissions - A literature review. Society of Automotive Engineers, Warrendale, PA.

Lee, S.W.; Herage, T.; and Young, B. (2004). Emission reduction potential from the combustion of soy methyl ester fuel blended with petroleum distillate fuel. *Fuel*, **83**:1607-1613.

Lehmann, U.; Niemela, V.; and Mohr, M. (2004). New method for time-resolved diesel engine exhaust particle mass measurement. *Environ. Sci. Technol.*, **38**(21):5704-5711.

Lemmetty, M.; Marjamäki, M.; and Keskinen, J. (2005). The ELPI response and data reduction - II: Properties of kernels and data inversion. *Aerosol Sci. Technol.*, **39**(7):583-595.

Lenaers, G. (1996). On-board real life emission measurements on a 3 way catalyst gasoline car in motor way-, rural- and city traffic and on two Euro-1 diesel city buses. *Sci. Total Environ.*, **190**:139-147.

Lenaers, G.; and DeVlieger, I. (1997). On-board emission measurements on petrol-driven cars and diesel city buses. *Int. J. Vehicle Des.*, **18**(3-4):368-378.

Lenaers, G.; Pelkmans, L.; and Debal, P. (2003). The realisation of an on-board emission measuring system serving as a R&D tool for ultra low emitting vehicles. *Int. J. Vehicle Des.*, **31**(3):253-268.

Levy, J.I.; Bennett, D.H.; Melly, S.J.; and Spengler, J.D. (2003). Influence of traffic patterns on particulate matter and polycyclic aromatic hydrocarbon concentrations in Roxbury, Massachusetts. *J. Expo. Anal. Environ. Epidemiol.*, **13**(5):364-371.

Li, N.; Hao, M.Q.; Phalen, R.F.; Hinds, W.C.; and Nel, A.E. (2003a). Particulate air pollutants and asthma: A paradigm for the role of oxidative stress in PM-induced adverse health effects. *Clinical Immunology*, **109**(3):250-265.

Li, S.N.; Chang, C.T.; Shih, H.Y.; Tang, A.; Li, A.; and Chen, Y.Y. (2003b). Using an extractive Fourier transform infrared spectrometer for improving cleanroom air quality in a semiconductor manufacturing plant. *AIHA Journal*, **64**(3):408-414.

Lima, D.G.; Soares, V.C.D.; Ribeiro, E.B.; Carvalho, D.A.; Cardoso, E.C.V.; Rassi, F.C.; Mundim, K.C.; Rubim, J.C.; and Suarez, P.A.Z. (2004). Diesel-like fuel obtained by pyrolysis of vegetable oils. *Journal of Analytical and Applied Pyrolysis*, **71**(2):987-996.

Lin, C.S.; Liou, N.W.; Chang, P.E.; Yang, J.C.; and Sun, E. (2007a). Fugitive coke oven gas emission profile by continuous line averaged open-path Fourier transform infrared monitoring. *J. Air Waste Manage. Assoc.*, **57**(4):472-479.

Lin, C.Y.; and Lin, H.A. (2006). Diesel engine performance and emission characteristics of biodiesel produced by the peroxidation process. *Fuel*, **85**:298-305.

Lin, C.Y.; and Lin, H.A. (2007). Engine performance and emission characteristics of a three-phase emulsion of biodiesel produced by peroxidation. *Fuel Processing Technology*, **88**(1):35-41.

Lin, L.; Lee, M.L.; and Eatough, D.J. (2007b). Gas chromatographic analysis of organic marker compounds in fine particulate matter using solid-phase microextraction. *J. Air Waste Manage. Assoc.*, **57**(1):53-58.

Lin, Y.C.; Lee, C.F.; and Fang, T. (2008a). Characterization of particle size distribution from diesel engines fueled with palm-biodiesel blends and paraffinic fuel blends. *Atmos. Environ.*, **42**(6):1133-1143.

Lin, Y.C.; Lee, W.J.; Chao, H.R.; Wang, S.L.; Tsou, T.C.; Chang-Chien, G.P.; and Tsai, P.J. (2008b). Approach for energy saving and pollution reducing by fueling diesel engines with emulsified biosolution/biodiesel/diesel blends. *Environ. Sci. Technol.*, **42**(10):3849-3855.

Lin, Y.C.; Lee, W.J.; Chen, C.C.; and Chen, C.B. (2006a). Saving energy and reducing emissions of both polycyclic aromatic hydrocarbons and particulate matter by adding bio-solution to emulsified diesel. *Environ. Sci. Technol.*, **40**(17):5553-5559.

Lin, Y.C.; Lee, W.J.; Wu, T.C.; and Wang, C.T. (2006b). Comparision of PAH and regulated harmful matter emissions from biodiesel blends and paraffinic fuel blends on engine accumulated mileage test. *Fuel*, **85**:2516-2523.

Lindgren, M.; and Hansson, P.A. (2004). Effects of transient conditions on exhaust emissions from two non-road diesel engines. *Biosystems Engineering*, **87**(1):57-66.

Lipsky, E.M.; and Robinson, A.L. (2006). Effects of dilution on fine particle mass and partitioning of semivolatile organics in diesel exhaust and wood smoke. *Environ. Sci. Technol.*, **40**(1):155-162.

Liu, Z.F.; Lu, M.M.; Birch, M.E.; Keener, T.C.; Khang, S.J.; and Liang, F.Y. (2005). Variations of the particulate carbon distribution from a nonroad diesel generator. *Environ. Sci. Technol.*, **39**(20):7840-7844.

Liu, Z.G.; Vasys, V.N.; and Kittelson, D.B. (2007). Nuclei-mode particulate emissions and their response to fuel sulfur content and primary dilution during transient operations of old and modern diesel engines. *Environ. Sci. Technol.*, **41**(18):6479-6483.

Lloyd, A.C.; and Cackette, T.A. (2001). Critical review - Diesel engines: Environmental impact and control. *J. Air Waste Manage. Assoc.*, **51**(6):809-847.

Lough, G.C.; Christensen, C.G.; Schauer, J.J.; Tortorelli, J.; Mani, E.; Lawson, D.R.; Clark, N.N.; and Gabele, P.A. (2007). Development of molecular marker source profiles for emissions from on-road gasoline and diesel vehicle fleets. *J. Air Waste Manage. Assoc.*, **57**(10):1190-1199.

Lowenthal, D.H.; Zielinska, B.; Chow, J.C.; Watson, J.G.; Gautam, M.; Ferguson, D.H.; Neuroth, G.R.; and Stevens, K.D. (1994). Characterization of heavy-duty diesel vehicle emissions. *Atmos. Environ.*, **28**(4):731-743.

Lyyranen, J.; Jokiniemi, J.; Kauppinen, E.I.; Backman, U.; and Vesala, H. (2004). Comparison of different dilution methods for measuring diesel particle emissions. *Aerosol Sci. Technol.*, **38**(1):12-23.

Ma, F.R.; and Hanna, M.A. (1999). Biodiesel production: a review. *Bioresource Technology*, **70**(1):1-15.

Machiele, P.A. (1989). Heavy duty vehicle emission conversion factors II (1962-2000). Report No. EPA-AA-SDSB-89-01. Prepared by U.S. Environmental Protection Agency, Research Triangle Park, NC.

Maciejczyk, P.B.; Offenberg, J.H.; Clemente, J.; Blaustein, M.; Thurston, G.D.; and Chen, L.C. (2004). Ambient pollutant concentrations measured by a mobile laboratory in South Bronx, NY. *Atmos. Environ.*, **38**(31):5283-5294.

Mamakos, A.; Ntziachristos, L.; and Samaras, Z. (2006). Evaluation of the Dekati mass monitor for the measurement of exhaust particle mass emissions. *Environ. Sci. Technol.*, **40**(15):4739-4745.

Maricq, M.; Podsiadlik, D.; and Chase, R. (1999). Gasoline vehicle particle size distributions: Comparison of steady state, FTP, and US06 measurements. *Environ. Sci. Technol.*, **33**:2007-2015.

Maricq, M.M. (2007). Chemical characterization of particulate emissions from diesel engines: A review. *J. Aerosol Sci.*, **38**(11):1079-1118.

Maricq, M.M.; Chase, R.E.; Xu, N.; and Podsiadlik, D.H. (2003). A constant-volume rapid exhaust dilution system for motor vehicle particulate matter number and mass measurements. *J. Air Waste Manage. Assoc.*, **53**(10):1196-1203.

Maricq, M.M.; Xu, N.; and Chase, R.E. (2006). Measuring particulate mass emissions with the electrical low pressure impactor. *Aerosol Sci. Technol.*, **40**(1):68-79.

Marjamäki, M.; Keskinen, J.; Chen, D.R.; and Pui, D.Y.H. (2000). Performance evaluation of the electrical low-pressure impactor (ELPI). *J. Aerosol Sci.*, **31**(2):249-261.

Marjamäki, M.; Lemmetty, M.; and Keskinen, J. (2005). ELPI response and data reduction - I: Response functions. *Aerosol Sci. Technol.*, **39**(7):575-582.

Markle, S.P.; and Brown, A.J. (1996). Naval ship engine exhaust emission characterization. *Naval Engineers Journal*, **108**(5):37-47.

Mauderly, J.L. (2001). Diesel emissions: Is more health research still needed? *Toxicol. Sci.*, **62**(1):6-9. PM:11399787.

Mauderly, J.L.; and Chow, J.C. (2008). Health effects of organic aerosols. *Inhal. Toxicol.*, **20**(3):257-288. http://dx.doi.org/10.1080/08958370701866008.

Mazurek, M.A.; Simoneit, B.R.T.; Cass, G.R.; and Gray, H.A. (1987). Quantitative high-resolution gas chromatography and high-resolution gas chromatography\mass spectrometry analyses of carbonaceous fine aerosol particles. *Int. J. Environ. Anal. Chem.*, **29**:119-139.

Mazzoleni, C.; Kuhns, H.D.; Moosmüller, H.; Keislar, R.E.; Barber, P.W.; Robinson, N.F.; and Watson, J.G. (2004a). On-road vehicle particulate matter and gaseous emission distributions in Las Vegas, Nevada, compared with other areas. *J. Air Waste Manage. Assoc.*, **54**(6):711-726.

Mazzoleni, C.; Kuhns, H.D.; Moosmüller, H.; Witt, J.; Nussbaum, N.J.; Chang, M.C.O.; Parthasarathy, G.; Nathagoundenpalayam, S.K.K.; Nikolich, G.; and Watson, J.G. (2007a). A

case study of real-world tailpipe emissions for school buses using a 20% biodiesel blend. *Sci. Total Environ.*, **385**:146-159.

Mazzoleni, C.; Kuhns, H.D.; Moosmüller, H.; Witt, J.; Nussbaum, N.J.; Chang, M.-C.O.; Parthasarathy, G.; Kumar, S.; Nathagoundenpalayam, K.; Nikolich, G.; and Watson, J.G. (2007b). A case study of real-world tailpipe emissions for school buses using a 20% biodiesel blend. *Sci. Total Environ.*, **385**:146-159.

Mazzoleni, C.; Moosmüller, H.; Kuhns, H.D.; Keislar, R.E.; Barber, P.W.; Nikolic, D.; Nussbaum, N.J.; and Watson, J.G. (2004b). Correlation between automotive CO, HC, NO, and PM emission factors from on-road remote sensing: Implications for inspection and maintenance programs. *Transport. Res.*, **D9**:477-496.

McCormick, R.L. (2007). The impact of biodiesel on pollutant emissions and public health MCCORMICK2007. *Inhal. Toxicol.*, **19**(12):1033-1039.

McCormick, R.L.; Graboski, M.S.; Alleman, T.L.; Herring, A.M.; and Tyson, K.S. (2001). Impact of biodiesel source material and chemical structure on emissions of criteria pollutants from a heavy-duty engine. *Environ. Sci. Technol.*, **35**(9):1742-1747.

McDonald, J.D.; Barr, E.B.; and White, R.K. (2004a). Design, characterization, and evaluation of a small-scale diesel exhaust exposure system. *Aerosol Sci. Technol.*, **38**(1):62-78.

McDonald, J.D.; Barr, E.B.; White, R.K.; Chow, J.C.; Schauer, J.J.; Zielinska, B.; and Grosjean, E. (2004b). Generation and characterization of four dilutions of diesel engine exhaust for a subchronic inhalation study. *Environ. Sci. Technol.*, **38**(9):2513-2522.

McDonald, J.D.; Eide, I.; Seagrave, J.; Zielinska, B.; Whitney, K.; Lawson, D.R.; and Mauderly, J.L. (2004c). Relationship between composition and toxicity of motor vehicle emission samples. *Environ. Health Perspect.*, **112**(15):1527-1538.

McDonald, J.D.; Harrod, K.S.; Seagrave, J.C.; Seilkop, S.K.; and Mauderly, J.L. (2004d). Effects of low sulfur fuel and a catalyzed particle trap on the composition and toxicity of diesel emissions. *Environ. Health Perspect.*, **112**(13):1307-1312.

Megahed, O.A.; Abdallah, R.I.; and Nabil, D. (2004). Rapeseed oil esters as diesel engine fuel. *Energy Sources*, **26**(2):119-126.

Miguel, A.H.; Kirchstetter, T.W.; Harley, R.A.; and Hering, S.V. (1998). On-road emissions of particulate polycyclic aromatic hydrocarbons and black carbon soot from gasoline and diesel vehicles. *Enivron. Sci. Technol.*, **32**(4):450-455.

Miller, T.L.; Davis, W.T.; Reed, G.D.; Doraiswamy, P.; and Fu, J.S. (2003). Characteristics and emissions of heavy-duty vehicles in Tennessee under the MOBILE6 model. *Transportation Research Record*, (1842):99-108.

Mishra, V.K.; and Padmanabhamutry, B. (2003). Performance evaluation of CALINE3, CAL3QHC and PART5 in predicting lead concentration in the atmosphere over Delhi. *Atmos. Environ.*, **37**(22):3077-3089.

Mohr, M.; Lehmann, U.; and Rutter, J. (2005). Comparison of mass-based and non-mass-based particle measurement systems for ultra-low emissions from automotive sources. *Environ. Sci. Technol.*, **39**(7):2229-2238.

Moosmüller, H.; Arnott, W.P.; and Rogers, C.F. (1997). Methods for real-time, *in situ* measurement of aerosol light absorption. *J. Air Waste Manage. Assoc.*, **47**(2):157-166.

Moosmüller, H.; Arnott, W.P.; Rogers, C.F.; Bowen, J.L.; Gillies, J.A.; Pierson, W.R.; Collins, J.F.; Durbin, T.D.; and Norbeck, J.M. (2001a). Time resolved characterization of diesel particulate emissions 1. Instruments for particle mass measurements. *Environ. Sci. Technol.*, **35**(4):781-787.

Moosmüller, H.; Arnott, W.P.; Rogers, C.F.; Bowen, J.L.; Gillies, J.A.; Pierson, W.R.; Collins, J.F.; Durbin, T.D.; and Norbeck, J.M. (2001b). Time resolved characterization of diesel particulate emissions 2. Instruments for elemental and organic carbon measurements. *Environ. Sci. Technol.*, **35**(10):1935-1942.

Moosmüller, H.; Arnott, W.P.; Rogers, C.F.; Chow, J.C.; Frazier, C.A.; Sherman, L.E.; and Dietrich, D.L. (1998). Photoacoustic and filter measurements related to aerosol light absorption during the Northern Front Range Air Quality Study (Colorado 1996/1997). *J. Geophys. Res.*, **103**(D21):28149-28157.

Moosmüller,H. and Keislar,R.E. (2003). Vehicle particulate sensor system. United States Patent No. 6,542,831 B1.

Moosmüller, H.; Mazzoleni, C.; Barber, P.W.; Kuhns, H.D.; Keislar, R.E.; and Watson, J.G. (2003). On-road measurement of automotive particle emissions by ultraviolet lidar and transmissometer: Instrument. *Environ. Sci. Technol.*, **37**(21):4971-4978.

Morawska, L.; Ristovski, Z.D.; Johnson, G.R.; Jayaratne, E.R.; and Mengersen, K. (2007). Novel method for on-road emission factor measurements using a plume capture trailer. *Environ. Sci. Technol.*, **41**(2):574-579.

Morris, J.A.; Bishop, G.A.; and Stedman, D.H. (1998). On-road remote sensing of heavy-duty diesel truck emissions in the Austin-San Marcos area. Prepared for Espey, Huston & Associates, Inc., by University of Denver, Denver, CO.

Morris, J.A.; Bishop, G.A.; Stedman, D.H.; Maly, P.; Scherer, S.; Countess, R.J.; Cohen, L.H.; Countess, S.J.; and Romon, R.(1999). Remote sensing and comparison of emissions from heavy-duty diesel trucks. In *9th CRC On-Road Vehicle Emissions Workshop*. Coordinating Research Council, Inc., Atlanta, GA, p. 4.27-4.39.

Munoz, M.; Moreno, F.; and Morea, J. (2004). Emissions of an automobile diesel engine fueled with sunflower methylester. *Transactions of the ASAE*, **47**(1):5-11.

Murillo, S.; Miguez, J.L.; Porteiro, J.; Granada, E.; and Moran, J.C. (2007). Performance and exhaust emissions in the use of biodiesel in outboard diesel engines. *Fuel*, **86**(12-13):1765-1771.

Nakamura, H.; Kihara, N.; Adachi, M.; Nakamura, S.; and Ishida, K. (2003). Development of hydrocarbon analyzer using heated-NDIR method and its application to on-board mass emission measurement system. *JSAE Review*, **24**(2):127-133.

Nelson, D.D.; Zahniser, M.S.; McManus, J.B.; Kolb, C.E.; and Jimenez, J.L. (1998). A tunable diode laser system for the remote sensing of on-road vehicle emissions. *Appl. Phys.*, **B67**:433-441.

Ning, Z.; Cheung, C.S.; and Liu, S.X. (2004). Experimental investigation of the effect of exhaust gas cooling on diesel particulate. *J. Aerosol Sci.*, **35**:333-345.

NRC (National Research Council) (1982). *Diesel Cars, Benefits, Risks and Public Policy*. The National Academies Press, Washington, DC.

Nwafor, O.M.I. (2003). The effect of elevated fuel inlet temperature on performance of diesel engine running on neat vegetable oil at constant speed conditions. *Renewable Energy*, **28**(2):171-181.

Nwafor, O.M.I. (2004a). Emission characteristics of diesel engine operating on rapeseed methyl ester. *Renewable Energy*, **29**(1):119-129.

Nwafor, O.M.I. (2004b). Emission characteristics of diesel engine running on vegetable oil with elevated fuel inlet temperature. *Biomass & Bioenergy*, **27**(5):507-511.

O'Shaughnessy, P.T.; and Slagley, J.M. (2002). Photometer response determination based on aerosol physical characteristics. *AIHA Journal*, **63**(5):578-585.

Oguz, O.; Ogut, H.; and Eryilmaz, T. (2007). Investigation of biodiesel production, quality and performance in Turkey. *Energy Sources Part A-Recovery Utilization and Environmental Effects*, **29**(16):1529-1535.

Pagels, J.; Gudmundsson, A.; Gustavsson, E.; Asking, L.; and Bohgard, M. (2005). Evaluation of aerodynamic particle sizer and electrical low-pressure impactor for unimodal and bimodal mass-weighted size distributions. *Aerosol Sci. Technol.*, **39**(9):871-887.

Pandiaraj, K.; Fox, B.; Morrow, D.J.; Persaud, S.; and Martin, J.P. (2002). Centralised control of diesel gen-sets for peak shaving and system support. *IEEE Proceedings-Generation Transmission and Distribution*, **149**(2):126-132.

Pang, X.B.; Shi, X.Y.; Mu, Y.J.; He, H.; Shuai, S.J.; Chen, H.; and Li, R.L. (2006). Characteristics of carbonyl compounds emission from a diesel-engine using biodiesel-ethanol-diesel as fuel. *Atmos. Environ.*, **40**(36):7057-7065.

Pattas, K.; Kyriakis, N.; Samaras, Z.; Pistikopoulos, P.; and Ntziachristos, L. (1998). Effect of DPF on particulate size distribution using an electrical low pressure impactor. *SAE Technical Paper Series*, **980544**.

Peiro, L.T.; Mende, Z.; and Durany, X.G.I. (2008). Exergy analysis of integrated waste management in the recovery and recycling of used cooking oils. *Environ. Sci. Technol.*, **42**(13):4977-4981.

Peng, C.Y.; Lan, C.H.; and Dai, Y.T. (2006). Speciation and quantification of vapor phases in soy biodiesel and waste cooking oil biodiesel. *Chemosphere*, **65**(11):2054-2062.

Peng, C.Y.; Yang, H.H.; Lan, C.H.; and Chien, S.M. (2008). Effects of the biodiesel blend fuel on aldehyde emissions from diesel engine exhaust. *Atmos. Environ.*, **42**(5):906-915.

Pereira, R.G.; Oliveira, C.D.; Oliveira, J.L.; Oliveira, P.C.P.; Fellows, C.E.; and Piamba, O.E. (2007). Exhaust emissions and electric energy generation in a stationary engine using blends of diesel and soybean biodiesel. *Renewable Energy*, **32**(14):2453-2460.

Peters, T.M.; Chein, H.M.; Lundgren, D.A.; and Keady, P.B. (1993). Comparison and combination of aerosol size distributions measured with a low pressure impactor, differential mobility particle sizer, electrical aerosol analyzer, and aerodynamic particle sizer. *Aerosol Sci. Technol.*, **19**(3):396-405.

Peters, T.M.; Ott, D.; and O'Shaughnessy, P.T. (2006). Comparison of the Grimm 1.108 and 1.109 portable aerosol spectrometer to the TSI 3321 aerodynamic particle sizer for dry particles. *Ann. Occup. Hyg.*, **50**(8):843-850.

Phuleria, H.C.; Sheesley, R.J.; Schauer, J.J.; Fine, P.M.; and Sioutas, C. (2007). Roadside measurements of size-segregated particulate organic compounds near gasoline and diesel-dominated freeways in Los Angeles, CA. *Atmos. Environ.*, **41**(22):4653-4671.

Pirjola, L.; Paasonen, P.; Pfeiffer, D.; Hussein, T.; Hameri, K.; Koskentalo, T.; Virtanen, A.; Ronkko, T.; Keskinen, J.; Pakkanen, T.A.; and Hillamo, R.E. (2006). Dispersion of particles and trace gases nearby a city highway: Mobile laboratory measurements in Finland. *Atmos. Environ.*, **40**(5):867-879.

Pirjola, L.; Parviainen, H.; Hussein, T.; Valli, A.; Hameri, K.; Aaalto, P.; Virtanen, A.; Keskinen, J.; Pakkanen, T.A.; Makela, T.; and Hillamo, R.E. (2004). "Sniffer" - a novel tool for chasing vehicles and measuring traffic pollutants. *Atmos. Environ.*, **38**(22):3625-3635.

Pokharel, S.S.; Bishop, G.A.; and Stedman, D.H. (2002). An on-road motor vehicle emissions inventory for Denver: An efficient alternative to modeling. *Atmos. Environ.*, **36**(33):5177-5184.

Pollack, A.K.; Dunker, A.M.; Fieber, J.K.; Heiken, J.G.; Cohen, J.P.; Shepard, S.B.; Schleyer, C.H.; and Yarwood, G. (1998). Revision of light-duty vehicle emission inventories using real-world measurements - Auto/oil program, Phase II. *J. Air Waste Manage. Assoc.*, **48**(4):291-305.

Poola, R.B.; and Sekar, R. (2003). Reduction of NOx and particulate emissions by using oxygen-enriched combustion air in a locomotive diesel engine. *Journal of Engineering for Gas Turbines and Power-Transactions of the Asme*, **125**(2):524-533.

Pope, C.A., III; and Dockery, D.W. (2006). Critical Review: Health effects of fine particulate air pollution: Lines that connect. *J. Air Waste Manage. Assoc.*, **56**(6):709-742.

Popp, P.J.; Bishop, G.A.; and Stedman, D.H. (1999). Development of a high-speed ultraviolet spectrometer for remote sensing of mobile source nitric oxide emissions. *J. Air Waste Manage. Assoc.*, **49**(12):1463-1468.

Pradeep, V.; and Sharma, R.P. (2007). Use of HOT EGR for NOx control in a compression ignition engine fuelled with bio-diesel from Jatropha oil. *Renewable Energy*, **32**(7):1136-1154.

Pramanik, K. (2003). Properties and use of jatropha curcas oil and diesel fuel blends in compression ignition engine. *Renewable Energy*, **28**(2):239-248.

Prucz, J.C.; Clark, N.N.; Gautam, M.; and Lyons, D.W. (2001). Exhaust emissions from engines of the Detroit Diesel Corporation in transit buses: A decade of trends. *Environ. Sci. Technol.*, **35**(9):1755-1764.

Prueksakorn, K.; and Gheewala, S.H. (2008). Full chain energy analysis of biodiesel from Jatropha curcas L. in Thailand. *Environ. Sci. Technol.*, **42**(9):3388-3393.

Puhan, S.; and Nagarajan, G. (2007). Mahua oil (madhuca indica oil) derivatives as a renewable fuel for diesel engine systems in India: A performance and emissions comparative study. *International Journal of Green Energy*, **4**(1):89-104.

Puhan, S.; Vedaraman, N.; Ram, B.V.B.; Sankarnarayanan, G.; and Jeychandran, K. (2005). Mahua oil (Madhuca Indica seed oil) methyl ester as biodiesel-preparation and emission characterstics. *Biomass & Bioenergy*, **28**(1):87-93.

Raadnui, S.; and Meenak, A. (2003). Effects of refined palm oil (RPO) fuel on wear of diesel engine components. *Wear*, **254**(12):1281-1288.

Raheman, H.; and Phadatare, A.G. (2004). Diesel engine emissions and performance from blends of karanja methyl ester and diesel. *Biomass & Bioenergy*, **27**(4):393-397.

Rakopoulos, C.D.; Antonopoulos, K.A.; and Rakopoulos, D.C. (2007). Experimental heat release analysis and emissions of a HSDI diesel engine fueled with ethanol-diesel fuel blends. *Energy*, **32**(10):1791-1808.

Rakopoulos, C.D.; Hountalas, D.T.; Rakopoulos, D.C.; and Levendis, Y.A. (2004). Comparative environmental evaluation of JP-8 and diesel fuels burned in direct injection (DI) or indirect injection (IDI) diesel engines and in a laboratory furnace. *Energy & Fuels*, **18**(5):1302-1308.

Ramadhas, A.S.; Jayaraj, S.; and Muraleedharan, C. (2004). Use of vegetable oils as IC engine fuels - A review. *Renewable Energy*, **29**(5):727-742.

Ramamurthy, R.; Clark, N.N.; Lyons, D.W.; and Atkinson, C.M.(1998). Models for predicting transient heavy duty vechicle emissions. In *SAE Technical Paper 982652*, Warrendale, PA.

Raspet, R.; Slaton, W.V.; Arnott, W.P.; and Moosmüller, H. (2003). Evaporation-condensation effects on resonant photoacoustics of volatile aerosols. *J. Atmos. Oceanic Technol.*, **20**(5):685-695.

Reddy, C.M.; Demello, J.A.; Carmichael, C.A.; Peacock, E.E.; Xu, L.; and Arey, J.S. (2008). Determination of biodiesel blending percentages using natural abundance radiocarbon analysis: Testing the accuracy of retail biodiesel blends. *Environ. Sci. Technol.*, **42**(7):2476-2482.

Rejesus, R.M.; Hornbaker, R.H.; and Hansen, A. (2004). The costs of using E-diesel to reduce emissions from agricultural machinery. *Journal of Sustainable Agriculture*, **24**(2):63-75.

Ren, Y.; Huang, Z.H.; Miao, H.Y.; Jiang, D.M.; Zeng, K.; Liu, B.; and Wang, X.B. (2007). Combustion and emission characteristics of a direct-injection diesel engine fueled with diesel-diethyl adipate blends. *Energy & Fuels*, **21**(3):1474-1482.

Reyes, F.; Grutter, M.; Jazcilevich, A.; and Gonzalez-Oropeza, R. (2006). Tecnical note: Analysis of non-regulated vehicular emissions by extractive FTIR spectrometry: tests on a hybrid car in Mexico City. *Atmos. Chem. Phys.*, **6**:5339-5346.

Reyes, J.F.; and Sepulveda, J. (2006). PM-10 emissions and power of a diesel engine fueled with crude and refined biodiesel from salmon oil. *Fuel*, **85**:1714-1719.

Ribeiro, N.M.; Pinto, A.C.; Quintella, C.M.; da Rocha, G.O.; Teixeira, L.S.G.; Guarieiro, L.L.N.; Rangel, M.D.; Veloso, M.C.C.; Rezende, M.J.C.; da Cruz, R.S.; de Oliveira, A.M.; Torres, E.A.; and de Andrade, J.B. (2007). The role of additives for diesel and diesel blended (Ethanol or biodiesel) fuels: A review. *Energy & Fuels*, **21**(4):2433-2445.

Riddle, S.G.; Robert, M.A.; Jakober, C.A.; Hannigan, M.P.; and Kleeman, M.J. (2007). Size distribution of trace organic species emitted from heavy-duty diesel vehicles. *Environ. Sci. Technol.*, **41**(6):1962-1969.

Riddle, S.G.; Robert, M.A.; Jakober, C.A.; Hannigan, M.P.; and Kleeman, M.J. (2008). Size distribution of trace organic species emitted from heavy-duty diesel vehicles (vol 41, pg 1962, 2007). *Environ. Sci. Technol.*, **42**(3):974-976.

Riedl, M.; and az-Sanchez, D. (2005). Biology of diesel exhaust effects on respiratory function. *Journal of Allergy and Clinical Immunology*, **115**(2):221-228.

Ristimaki, J.; Vaaraslahti, K.; Lappi, M.; and Keskinen, J. (2007). Hydrocarbon condensation in heavy-duty diesel exhaust. *Environ. Sci. Technol.*, **41**(18):6397-6402.

Ristovski, Z.D.; Jayaratne, E.R.; Lim, M.; Ayoko, G.A.; and Morawska, L. (2006). Influence of diesel fuel sulfur on nanoparticle emissions from city buses. *Environ. Sci. Technol.*, **40**(4):1314-1320.

Rogers, C.F.; Sagebiel, J.C.; Zielinska, B.; Arnott, W.P.; Fujita, E.M.; McDonald, J.D.; Griffin, J.B.; Kelly, K.; Overacker, D.; Wagner, D.; Lighty, J.S.; Sarofim, A.; and Palmer, G. (2003). Characterization of submicron exhaust particles from engines operating without load on diesel and JP-8 fuels. *Aerosol Sci. Technol.*, **37**:355-368.

Rogge, W.F.; Hildemann, L.M.; Mazurek, M.A.; Cass, G.R.; and Simoneit, B.R.T. (1993). Sources of fine organic aerosol - 2. Noncatalyst and catalyst-equipped automobiles and heavy-duty diesel trucks. *Enivron. Sci. Technol.*, **27**(4):636-651.

Ronkko, T.; Virtanen, A.; Vaaraslahti, K.; Keskinen, J.; Pirjola, L.; and Lappi, M. (2006). Effect of dilution conditions and driving parameters on nucleation mode particles in diesel exhaust: Laboratory and on-road study. *Atmos. Environ.*, **40**(16):2893-2901.

Ropkins, K.; Quinn, R.; Beebe, J.; Li, H.; Daham, B.; Tate, J.; Bell, M.; and Andrews, G. (2007). Real-world comparison of probe vehicle emissions and fuel consumption using diesel and 5% biodiesel (B5) blend. *Sci. Total Environ.*, **376**(1-3):267-284.

Ross, M.; Goodwin, R.; Watkins, R.; Wenzel, T.; and Wang, M.Q. (1998). Real-world emissions from conventional passenger cars. *J. Air Waste Manage. Assoc.*, **48**(6):502-515.

Russell, A.G. (2008). EPA Supersites Program-related emissions-based particulate matter modeling: Initial applications and advances. *J. Air Waste Manage. Assoc.*, **58**(2):289-302.

Ryu, K.; and Oh, Y. (2004). Combustion characteristics of an agricultural diesel engine using biodiesel fuel. *Ksme International Journal*, **18**(4):709-717.

Saathoff, H.; Naumann, K.H.; Schnaiter, M.; Schöck, W.; Möhler, O.; Schurath, U.; Weingartner, E.; Gysel, M.; and Baltensperger, U. (2003). Coating of soot and (NH4)2SO4 particles by ozonolysis products of α-pinene. *J. Aerosol Sci.*, **34**(10):1297-1321.

Sahoo, P.K.; Das, L.M.; Babu, M.K.G.; and Naik, S.N. (2007). Biodiesel development from high acid value polanga seed oil and performance evaluation in a CI engine. *Fuel*, **86**(3):448-454.

Saitoh, K.; Kawabata, S.; Shirai, T.; Sato, T.; and Odaka, M. (2003). Comparison of surface organic compound mass spectrum patterns by LD-TOFMS for megalopolis atmospheric particles and diesel exhaust Particles (DEP). *Water,Air and Soil Pollution: Focus*, **3**:167-174.

Saiyasitpanich, P.; Lu, M.; Keener, T.C.; Liang, F.; and Khang, S.J. (2005). The effect of diesel fuel sulfur content on particulate matter emissions for a nonroad diesel generator. *J. Air Waste Manage. Assoc.*, **55**(7):993-998.

Sakurai, H.; Park, K.; McMurry, P.H.; Zarling, D.D.; Kittelson, D.B.; and Ziemann, P.J. (2003a). Size-dependent mixing characteristics of volatile and nonvolatile components in diesel exhaust aerosols. *Environ. Sci. Technol.*, **37**(24):5487-5495.

Sakurai, H.; Tobias, H.J.; Park, K.; Zarling, D.; Docherty, K.S.; Kittelson, D.B.; McMurry, P.H.; and Ziemann, P.J. (2003b). On-line measurements of diesel nanoparticle composition and volatility. *Atmos. Environ.*, **37**(9-10):1199-1210.

Salcedo, D.; Onasch, T.B.; Dzepina, K.; Canagaratna, M.R.; Zhang, Q.; Huffman, J.A.; DeCarlo, P.F.; Jayne, J.T.; Mortimer, P.; Worsnop, D.R.; Kolb, C.E.; Johnson, K.S.; Zuberi, B.; Marr, L.C.; Volkamer, R.; Molina, L.T.; Molina, M.J.; Cardenas, B.; Bernabe, R.M.; Marquez, C.; Gaffney, J.S.; Marley, N.A.; Laskin, A.; Shutthanandan, V.; Xie, Y.; Brune, W.; Lesher, R.; Shirley, T.; and Jimenez, J.L. (2006). Characterization of ambient aerosols in Mexico City during the MCMA-2003 campaign with Aerosol Mass Spectrometry: results from the CENICA Supersite. *Atmos. Chem. Phys.*, **6**:925-946.

Samaras, Z.; and Zierock, K.H. (1995). Off-road vehicles: A comparison of emissions with those from road transport. *Sci. Total Environ.*, **169**:249-255.

Sastre, J.A.L.; Alonso, J.S.J.; Garcia, C.R.A.; Romero-Avila, E.J.L.; and Alonso, C.R. (2003). A study of the decrease in fossil CO2 emissions of energy generation by using vegetable oils as combustible. *Building and Environment*, **38**(1):129-133.

Sattler, M.L. (2002). Technologies for reducing NOx emissions from off-road diesel vehicles: An overview. *Environ. Manag.*, **52**:20-29.

Savvidis, D.; Grammatikis, V.; Pecqueur, M.; Triandafyllis, J.; Vosniakos, F.; Zoumakis, N.; and Kelesis, A. (2006). Four-stroke diesel engines operated on plant oil methylester mixtures - Performance and environmental effects. *Fresenius Environmental Bulletin*, **15**(8):898-904.

Sawant, A.A.; Nigam, A.; Miller, J.W.; Johnson, K.C.; and Cocker, D.R. (2007a). Regulated and non-regulated emissions from in-use diesel-electric switching locomotives. *Environ. Sci. Technol.*, **41**(17):6074-6083.

Sawant, A.A.; Shah, S.D.; Zhu, X.N.; Miller, J.W.; and Cocker, D.R. (2007b). Real-world emissions of carbonyl compounds from in-use heavy-duty diesel trucks and diesel Back-Up Generators (BUGS). *Atmos. Environ.*, **41**(21):4535-4547.

Sawyer, R.F.; Harley, R.A.; Cadle, S.H.; Norbeck, J.M.; Slott, R.S.; and Bravo, H.A. (1998). Mobile sources critical review. Prepared for Coordinating Research Council, Atlanta, GA.

Sawyer, R.F.; Harley, R.A.; Cadle, S.H.; Norbeck, J.M.; Slott, R.S.; and Bravo, H.A. (2000). Mobile sources critical review: 1998 NARSTO assessment. *Atmos. Environ.*, **34**(12-14):2161-2181.

Schaefer-Sindlinger, A.; Lappas, I.; Vogt, C.D.; Ito, T.; Kurachi, H.; Makino, M.; and Takahashi, A. (2007). Efficient material design for diesel particulate filters. *Topics in Catalysis*, **42-43**(1-4):307-317.

Schauer, J.J.; Kleeman, M.J.; Cass, G.R.; and Simoneit, B.R.T. (1999). Measurement of emissions from air pollution sources - 2. C_1 through C_{30} organic compounds from medium duty diesel trucks. *Environ. Sci. Technol.*, **33**(10):1578-1587.

Schexnayder, C.J.; and David, S.A. (2002). Past and future of construction equipment - Part IV. *Journal of Construction Engineering and Management-Asce*, **128**(4):279-286.

Schneider, J.; Hock, N.; Weimer, S.; Borrmann, S.; Kirchner, U.; Vogt, R.; and Scheer, V. (2005). Nucleation particles in diesel exhaust: Composition inferred from in situ mass spectrometric analysis. *Environ. Sci. Technol.*, **39**(16):6153-6161.

Schoepflin, T.N.; and Dailey, D.J. (2003). Dynamic camera calibration of roadside traffic management cameras for vehicle speed estimation. *Ieee Transactions on Intelligent Transportation Systems*, **4**(2):90-98.

Schuetzle, D.; Lee, F.S.C.; Prater, T.J.; and Tejada, S.B. (1981). The identification of polynuclear aromatic hydrocarbon (PAH) derivatives in mutagenic fractions of diesel particulate extracts. *Int. J. Environ. Anal. Chem.*, **9**:93-144.

Schuetzle, D.; and Perez, J.M. (1983). Factors influencing the emissions of nitrated-polynuclear aromatic hydrocarbons (nitro-PAH) from diesel engines. *J. Air Poll. Control Assoc.*, **33**(8):751-755.

Semenov, V.G. (2003). Optimization of the composition of binary alternative diesel fuel. *Chemistry and Technology of Fuels and Oils*, **39**(4):192-196.

Sendzikiene, E.; Makareviciene, V.; and Janulis, P. (2006). Influence of fuel oxygen content on diesel engine exhaust emissions. *Renewable Energy*, **31**:2505-2512.

Shah, S.D.; Cocker, D.R.; Johnson, K.C.; Lee, J.M.; Soriano, B.L.; and Miller, J.W. (2006a). Emissions of regulated pollutants from in-use diesel back-up generators. *Atmos. Environ.*, **40**(22):4199-4209.

Shah, S.D.; Cocker, D.R.; Johnson, K.C.; Lee, J.M.; Soriano, B.L.; and Miller, J.W. (2007). Reduction of particulate matter emissions from diesel backup generators equipped with four different exhaust aftertreatment devices. *Environ. Sci. Technol.*, **41**(14):5070-5076.

Shah, S.D.; Cocker, D.R.; Miller, J.W.; and Norbeck, J.M. (2004). Emission rates of particulate matter and elemental and organic carbon from in-use diesel engines. *Environ. Sci. Technol.*, **38**(9):2544-2550.

Shah, S.D.; Johnson, K.C.; Miller, J.W.; and Cocker, D.R. (2006b). Emission rates of regulated pollutants from on-road heavy-duty diesel vehicles. *Atmos. Environ.*, **40**(1):147-153.

Shah, S.D.; Ogunyoku, T.A.; Miller, J.W.; and Cocker, D.R. (2005). On-road emission rates of PAH and n-alkane compounds from heavy-duty diesel vehicles. *Environ. Sci. Technol.*, **39**(14):5276-5284.

Shen, S.; Jaques, P.A.; Zhu, Y.F.; Geller, M.D.; and Sioutas, C. (2002). Evaluation of the SMPS-APS system as a continuous monitor for measuring PM2.5, PM10 and coarse (PM2.5-10) concentrations. *Atmos. Environ.*, **36**(24):3939-3950.

Shi, J.P.; and Harrison, R.M. (1999). Investigation of ultrafine particle formation during diesel exhaust dilution. *Environ. Sci. Technol.*, **33**(21):3730-3736.

Shi, J.P.; Harrison, R.M.; and Brear, F. (1999a). Particle size distribution from a modern heavy duty diesel engine. *Sci. Total Environ.*, **235**(1-3):305-317.

Shi, J.P.; Khan, A.A.; and Harrison, R.M. (1999b). Measurements of ultrafine particle concentration and size distribution in the urban atmosphere. *Sci. Total Environ.*, **235**(1-3):51-64.

Shi, X.Y.; Pang, X.B.; Mu, Y.J.; He, H.; Shuai, S.J.; Wang, J.X.; Chen, H.; and Li, R.L. (2006). Emission reduction potential of using ethanol-biodiesel-diesel fuel blend on a heavy-duty diesel engine. *Atmos. Environ.*, **40**(14):2567-2574.

Shorter, J.H.; Herndon, S.; Zahniser, M.S.; Nelson, D.D.; Wormhoudt, J.; Demerjian, K.L.; and Kolb, C.E. (2005). Real-time measurements of nitrogen oxide emissions from in-use New York City transit buses using a chase vehicle. *Environ. Sci. Technol.*, **39**(20):7991-8000.

Siegl, W.O.; Hammerle, R.H.; Herrmann, H.M.; Wenclawiak, B.W.; and Luers-Jongen, B. (1999). Organic emissions profile for a light-duty diesel vehicle. *Atmos. Environ.*, **33**(5):797-806.

Silva, E.J.; Zaniquelli, M.E.D.; and Loh, W. (2007). Light-scattering investigation on microemulsion formation in mixtures of diesel oil (or hydrocarbons) plus ethanol plus additives. *Energy & Fuels*, **21**(1):222-226.

Simoneit, B.R.T. (1999). A review of biomarker compounds as source indicators and tracers for air pollution. *Environ. Sci. Pollut. Res.*, **6**(3):159-169.

Singer, B.C.; Harley, R.A.; Littlejohn, D.; Ho, J.; and Vo, T. (1998). Scaling of infrared remote sensor hydrocarbon measurements for motor vehicle emission inventory calculations. *Environ. Sci. Technol.*, **32**(21):3241-3248.

Singh, R.N.; Singh, S.P.; and Pathak, B.S. (2007). Investigations on operation of CI engine using producer gas and rice bran oil in mixed fuel mode. *Renewable Energy*, **32**(9):1565-1580.

Sivaprakasam, S.; and Saravanan, C.G. (2007). Optimization of the transesterification process for biodiesel production and use of biodiesel in a compression ignition engine. *Energy & Fuels*, **21**(5):2998-3003.

Somers, J.H.; and Kittredge, G.D. (1971). Review of federally sponsored research on diesel exhaust odors. *J. Air Poll. Control Assoc.*, **21**(12):764-769.

Sonntag, D.B.; Gao, H.O.; and Holmen, B.A. (2008). Variability of particle number emissions from diesel and hybrid diesel-electric buses in real driving conditions. *Environ. Sci. Technol.*, **42**(15):5637-5643.

Spencer, M.T.; Shields, L.G.; Sodeman, D.A.; Toner, S.M.; and Prather, K.A. (2006). Comparison of oil and fuel particle chemical signatures with particle emissions from heavy and light duty vehicles. *Atmos. Environ.*, **40**(27):5224-5235.

St.Denis, M.; and Lindner, J. (2005). Review of light-duty diesel and heavy-duty diesel gasoline inspection programs. *J. Air Waste Manage. Assoc.*, **55**(12):1876-1884.

Stauffer, E.; and Byron, D. (2007). Alternative fuels in fire debris analysis: Biodiesel basics. *J. Forensic Sci.*, **52**(2):371-379.

Stephens, R.D.; and Cadle, S.H. (1991). Remote sensing measurements of carbon monoxide emissions from on-road vehicles. *J. Air Waste Manage. Assoc.*, **41**(1):39-46.

Strommen, M.R.; and Kamens, R.M. (1997). Development and application of a dual-impedance radial diffusion model to simulate the partitioning of semivolatile organic compounds in combustion aerosols. *Enivron. Sci. Technol.*, **31**(10):2983-2990.

Swanson, K.J.; Madden, M.C.; and Ghio, A.J. (2007). Biodiesel exhaust: The need for health effects research. *Environ. Health Perspect.*, **115**(4):496-499.

Tan, R.R.; Culaba, A.B.; and Purvis, M.R.I. (2004). Carbon balance implications of coconut biodiesel utilization in the Philippine automotive transport sector. *Biomass & Bioenergy*, **26**(6):579-585.

Tang, S.; Frank, B.P.; Lanni, T.; Rideout, G.; Meyer, N.; and Beregszaszy, C. (2007). Unregulated emissions from a heavy-duty diesel engine with various fuels and emission control systems. *Environ. Sci. Technol.*, **41**(14):5037-5043.

Tang, U.W.; and Wang, Z. (2006). Determining gaseous emission factors and driver's particle exposures during traffic congestion by vehicle-following measurement techniques. *J. Air Waste Manage. Assoc.*, **56**(11):1532-1539.

Tat, A.E.; Van Gerpen, J.H.; and Wang, P.S. (2007a). Fuel property effects on injection timing, ignition timing, and oxides of nitrogen emissions from biodiesel-fueled engines. *Transactions of the Asabe*, **50**(4):1123-1128.

Tat, M.E.; Wang, P.S.; Van Gerpen, J.H.; and Clemente, T.E. (2007b). Exhaust emissions from an engine fueled with biodiesel from high-oleic soybeans. *Journal of the American Oil Chemists Society*, **84**(9):865-869.

Teikari, M.; Linnainmaa, M.; Laitinen, J.; Kalliokoski, P.; Vincent, J.; Tiita, P.; and Raunemaa, T. (2003). Laboratory and field testing of particle size-selective sampling methods for mineral dusts. *AIHA Journal*, **64**(3):312-318.

Tobias, H.J.; Beving, D.E.; Ziemann, P.J.; Sakurai, H.; Zuk, M.; McMurry, P.H.; Zarling, D.; Waytulonis, R.; and Kittelson, D.B. (2001). Chemical analysis of diesel engine nanoparticles using a nano-DMA/Thermal Desorption Particle Beam Mass Spectrometer. *Environ. Sci. Technol.*, **35**(11):2233-2243.

Tong, H.Y.; and Karasek, F.W. (1984). Quantitation of polycyclic aromatic hydrocarbons in diesel exhaust particulate matter by high-performance liquid chromatography fractionation and high resolution gas chromatography. *Anal. Chem.*, **56**:2129-2134.

Tong, H.Y.; Sweetman, J.A.; Karasek, F.W.; Jellum, E.; and Thorsrud, A.K. (1984). Quantitative analysis of polycyclic aromatic compounds in diesel exhaust particulate extracts by combined chromatographic techniques. *J. Chromatogr.*, **312**:183-202.

Tritthart, P.; ruhri, F.; and Cartellieri, W. (1992). The contribution of the lube oil to particulate emissions from heavy duty diesel vehicles. *Mechanical Engineering*, **80**:535-552.

Tsolakis, A.; and Megaritis, A. (2004). Exhaust gas assisted reforming of rapeseed methyl ester for reduced exhaust emissions of CI engines. *Biomass & Bioenergy*, **27**(5):493-505.

Tsolakis, A.; Megaritis, A.; and Wyszynski, M.L. (2003). Application of exhaust gas fuel reforming in compression ignition engines fueled by diesel and biodiesel fuel mixtures. *Energy & Fuels*, **17**(6):1464-1473.

Tsukamoto, Y.; Goto, Y.; and Odaka, M. (2000). Continuous measurement of diesel particulate emissions by an electrical-low-pressure impactor. *SAE Technical Paper Series*, **2000-01-1138**.

Turrio-Baldassarri, L.; Battistelli, C.L.; Conti, L.; Crebelli, R.; De Berardis, B.; Iamiceli, A.L.; Gambino, M.; and Iannaccone, S. (2004). Emission comparison of urban bus engine fueled with diesel oil and 'biodiesel' blend. *Sci. Total Environ.*, **327**(1-3):147-162.

U.S.EPA (1995). Draft user's guide to PART5: A program for calculating particle emissions from motor vehicles. Report No. EPA-AA-AQAB-94-2. Prepared by US EPA, Office of Mobile Sources, Ann Arbor, MI.

U.S.EPA (1997). National ambient air quality standards for ozone: Final rule. *Federal Register*, **62**(138):2-37. http://www.epa.gov/ttn/oarpg/t1/fr_notices/o3naaqs.pdf.

U.S.EPA (1999a). 40 CFR Part 51 - Regional haze regulations: Final rule. *Federal Register*, **64**(126):35714-35774. http://frwebgate.access.gpo.gov/cgi-bin/getpage.cgi?position=all&page=35714&dbname=1999_register.

U.S.EPA (1999b). SPECIATE: EPA's repository of total organic compound and particulate matter speciated profiles for a variety of sources for use in source apportionment studies. Prepared by U.S. Environmental Protection Agency, Office of Air Quality Planning and Standards, Research Triangle Park, NC. **http://www.epa.gov/ttn/chief/software/speciate/**.

U.S.EPA (2000). Health assessment document for diesel exhaust - SAB review draft. Report No. EPA/600/8-90/057E. Prepared by U.S. Environmental Protection Agency, Office of Research and Development, National Center for Environmental Assessment, Washington, DC. http://www.epa.gov/ncea/pdfs/diesel/frmatterfinal.pdf.

U.S.EPA (2001). 40 CFR Parts 69, 80, and 86: Control of air pollution from new motor vehicles: Heavy-duty engine and vehicle standards and highway diesel fuel sulfur control requirements - final rule. *Federal Register*, **66**(12):5001-5193.

U.S.EPA (2002). A comprehensive analysis of biodiesel impacts on exhaust emissions. Report No. EPA420-P-02-001. Prepared by U.S. Environmental Protection Agency, Ann Arbor, MI.

U.S.EPA (2003a). Control of emissions of air pollution from nonroad diesel engines and fuel; proposed rule - 40 CFR Parts 69, 80, 89, et. al. *Federal Register*, **68**(100):28328-28603.

U.S.EPA (2003b). National air quality and emissions trends report: 2003 special studies edition. Report No. EPA 454/R-03-005. Prepared by U.S. Environmental Protection Agency, Research Triangle Park, NC. http://www.epa.gov/air/airtrends/aqtrnd03/toc.html.

U.S.EPA (2005). NONROAD model (nonroad engines, equipment, and vehicles). Prepared by U.S. Environmental Protection Agency, Research Triangle Park, NC. http://www.epa.gov/omswww/nonrdmdl.htm.

U.S.EPA (2006). National ambient air quality standard for particulate matter: Final Rule. *Federal Register*, **71**(200):61144-61233. http://frwebgate.access.gpo.gov/cgi-bin/getpage.cgi?dbname=2006_register&position=all&page=61144.

U.S.EPA (2007a). National ambient air quality standards for ozone: Proposed rule. *Federal Register*, **72**(132):37818-37918. http://www.epa.gov/ttn/naaqs/standards/ozone/data/frnotice_07-11-07.pdf.

U.S.EPA (2007b). SPECIATE Version 4.0. Prepared by U.S. Environmental Protection Agency, Research Triangle Park, NC. http://www.epa.gov/ttn/chief/software/speciate/index.html.

U.S.EPA (2008a). AMTIC PAMS information. Prepared by U.S. Environmental Protection Agency, Research Triangle Park, NC. http://www.epa.gov/ttn/amtic/pamsmain.html.

U.S.EPA (2008b). MOBILE6. Prepared by U.S. Environmental Protection Agency, Research Triangle Park, NC. http://www.epa.gov/oms/m6.htm.

U.S.Mine Safety and Health Administration (2001). Diesel particulate matter exposure of underground metal and nonmetal miners; Final rule (30 CFR Part 57). *Federal Register*, **66**(13):5706-5910.

Ulusoy, Y.; Tekin, Y.; Cetinkaya, M.; and Karaosmanoglu, F. (2004). The engine tests of biodiesel from used frying oil. *Energy Sources*, **26**(10):927-932.

Uma, R.; Kandpal, T.C.; and Kishore, V. (2004). Emission characteristics of an electricity generation system in diesel alone and dual fuel modes. *Biomass & Bioenergy*, **27**(2):195-203.

Unal, A.; Frey, H.C.; and Rouphail, N.M. (2004). Quantification of highway vehicle emissions hot spots based upon on-board measurements. *J. Air Waste Manage. Assoc.*, **54**(2):130-140.

Usta, N. (2005). Use of tobacco seed oil methyl ester in a turbocharged indirect injection diesel engine. *Biomass & Bioenergy*, **28**(1):77-86.

Vaaraslahti, K.; Keskinen, J.; Giechaskjel, B.; Solla, A.; Murtonen, T.; and Vesala, H. (2005). Effect of lubricant on the formation of heavy-duty diesel exhaust nanoparticles. *Environ. Sci. Technol.*, **39**(21):8497-8504.

Vaaraslahti, K.; Ristimaki, J.; Virtanen, A.; Keskinen, J.; Giechaskiel, B.; and Solla, A. (2006). Effect of oxidation catalysts on diesel soot particles. *Environ. Sci. Technol.*, **40**(15):4776-4781.

van Gulijk, C.; Marijnissen, J.; Makkee, M.; and Moulijn, J.A. (2003a). The choice of instrument (ELPI and/or SMPS) for diesel soot particulate measurements. *SAE Technical Paper Series*, **2003-01-0784**.

van Gulijk, C.; Marijnissen, J.C.M.; Makkee, M.; and Moulijn, J.A. (2000). Evaluation of the ELPI for diesel soot measurements. *J. Aerosol Sci.*, **31**(Suppl. 1):S394-S395.

van Gulijk, C.; Marijnissen, J.C.M.; Makkee, M.; and Moulijn, J.A. (2003b). Oil-soaked sintered impactors for the ELPI in diesel particulate measurements. *J. Aerosol Sci.*, **34**(5):635-640.

van Gulijk, C.; Marijnissen, J.C.M.; Makkee, M.; Moulijn, J.A.; and Schmidt-Ott, A. (2004). Measuring diesel soot with a scanning mobility particle sizer and an electrical low-pressure impactor: Performance assessment with a model for fractal-like agglomerates. *J. Aerosol Sci.*, **35**(5):633-655.

van Gulijk, C.; Schouten, J.M.; Marijnissen, J.C.M.; Makkee, M.; and Moulijn, J.A. (2001). Restriction for the ELPI in diesel particulate measurements. *J. Aerosol Sci.*, **32**(9):1117-1130.

Velasco, E.; Lamb, B.; Westberg, H.; Allwine, E.; Sosa, G.; rriaga-Colina, J.L.; Jobson, B.T.; Alexander, M.L.; Prazeller, P.; Knighton, W.B.; Rogers, T.M.; Grutter, M.; Herndon, S.C.; Kolb, C.E.; Zavala, M.; de Foy, B.; Volkamer, R.; Molina, L.T.; and Molina, M.J. (2007). Distribution, magnitudes, reactivities, ratios and diurnal patterns of volatile organic compounds in the Valley of Mexico during the MCMA 2002 & 2003 field campaigns. *Atmos. Chem. Phys.*, **7**:329-353.

Virtanen, A.; Marjamäki, M.; Ristimaki, J.; and Keskinen, J. (2001). Fine particle losses in electrical low-pressure impactor. *J. Aerosol Sci.*, **32**(3):389-401.

Virtanen, A.; Ristimaki, J.; and Keskinen, J. (2004). Method for measuring effective density and fractal dimension of aerosol agglomerates. *Aerosol Sci. Technol.*, **38**(5):437-446.

Vivek; and Gupta, A.K. (2004). Biodiesel production from Karanja oil. *Journal of Scientific & Industrial Research*, **63**(1):39-47.

Vlieger, I.D. (1997). On-board emission and fuel consumption measurement campaign on petrol-driven passenger cars. *Atmos. Environ.*, **31**(22):3753-3761.

Vogt, R.; Kirchner, V.; Scheer, K.P.; Hinz, K.P.; Trimborn, A.; and Spengler, B. (2003a). Identification of diesel exhaust particles at an Autobahn, urban & rural location using single-particle mass spectrometry. *J. Aerosol Sci.*, **34**(3):319-337.

Vogt, R.; Scheer, V.; Casati, R.; and Benter, T. (2003b). On-road measurement of particle emission in the exhaust plume of a diesel passenger car. *Environ. Sci. Technol.*, **37**(18):4070-4076.

Vouitsis, E.; Ntziachristos, L.; and Samaras, Z. (2003). Particulate matter mass measurements for low emitting diesel powered vehicles: what's next? *Progress in Energy and Combustion Science*, **29**(6):635-672.

Walsh, P.A.(1996). Remote sensing data - An assessment of fleet variability. In *Proceedings of the Sixth CRC On-Road Vehicle Emissions Workshop*, San Diego, CA.

Walsh, P.A.; Sagebiel, J.C.; Lawson, D.R.; Knapp, K.T.; and Bishop, G.A. (1996). Comparison of auto emission measurement techniques. *Sci. Total Environ.*, **189**/**190**:175-180.

Wan, J.X.; and az-Sanchez, D. (2007). Antioxidant enzyme induction: A new protective approach against the adverse effects of diesel exhaust particles. *Inhal. Toxicol.*, **19**:177-182.

Wang, J.; Maiorov, M.; Jeffries, J.B.; Garbuzov, D.Z.; Connolly, J.C.; and Hanson, R.K. (2000a). A potential remote sensor of CO in vehicle exhausts using 2.3μm diode lasers. *Measurement Science & Technology*, **11**:1576-1584.

Wang, W.G.; Lyons, D.W.; Clark, N.N.; Gautam, M.; and Norton, P.M. (2000b). Emissions from nine heavy trucks fueled by diesel and biodiesel blend without engine modification. *Environ. Sci. Technol.*, **34**(6):933-939.

Watson, J.G. (2002). Visibility: Science and regulation. *J. Air Waste Manage. Assoc.*, **52**(6):628-713.

Watson, J.G.; Barber, P.W.; Chang, M.-C.O.; Chow, J.C.; Etyemezian, V.; Green, M.C.; Keislar, R.E.; Kuhns, H.D.; Mazzoleni, C.; Moosmüller, H.; Nicolic, D.; and Whitaker, C.E. (2007). Southern Nevada Air Quality Study - Final Report. Report No. FTA-NV-26-7003-2006.01. Prepared for Federal Transit Administration, Washington DC, by Desert Research Institute, Reno, NV.

Watson, J.G.; Chen, L.-W.A.; Chow, J.C.; Lowenthal, D.H.; and Doraiswamy, P. (2008). Source apportionment: Findings from the U.S. Supersite Program. *J. Air Waste Manage. Assoc.*, **58**(2):265-288.

Watson, J.G.; and Chow, J.C. (2007). Receptor models for source apportionment of suspended particles. In *Introduction to Environmental Forensics, 2nd Edition*, 2 ed., B. Murphy and R. Morrison, Eds. Academic Press, New York, NY, pp. 279-316.

Watson, J.G.; Chow, J.C.; and Frazier, C.A. (1999). X-ray fluorescence analysis of ambient air samples. In *Elemental Analysis of Airborne Particles, Vol. 1*, S. Landsberger and M. Creatchman, Eds. Gordon and Breach Science, Amsterdam, pp. 67-96.

Watson, J.G.; Chow, J.C.; and Fujita, E.M. (2001). Review of volatile organic compound source apportionment by chemical mass balance. *Atmos. Environ.*, **35**(9):1567-1584. ftp://ftp.cgenv.com/pub/downloads/Watson.pdf.

Watson, J.G.; Chow, J.C.; Lowenthal, D.H.; Pritchett, L.C.; Frazier, C.A.; Neuroth, G.R.; and Robbins, R. (1994). Differences in the carbon composition of source profiles for diesel- and gasoline-powered vehicles. *Atmos. Environ.*, **28**(15):2493-2505.

Watson, J.G.; Chow, J.C.; and Pace, T.G. (2000). Fugitive dust emissions. In *Air Pollution Engineering Manual, Second Edition*, 2nd ed., W.T. Davis, Ed. John Wiley & Sons, Inc., New York, pp. 117-135.

Watson, J.G.; Fujita, E.M.; Chow, J.C.; Zielinska, B.; Richards, L.W.; Neff, W.D.; and Dietrich, D. (1998). Northern Front Range Air Quality Study. Final report. Prepared for Colorado State University, Fort Collins, CO, by Desert Research Institute, Reno, NV. http://charon.cira.colostate.edu/DRIFinal/ZipFiles/.

Watson, J.G.; Zhu, T.; Chow, J.C.; Engelbrecht, J.P.; Fujita, E.M.; and Wilson, W.E. (2002). Receptor modeling application framework for particle source apportionment. *Chemosphere*, **49**(9):1093-1136.

Weijers, E.P.; Khlystov, A.Y.; Kos, G.P.A.; and Erisman, J.W. (2004). Variability of particulate matter concentrations along roads and motorways determined by a moving measurement unit. *Atmos. Environ.*, **38**(19):2993-3002.

Westerdahl, D.; Fruin, S.; Sax, T.; Fine, P.M.; and Sioutas, C. (2005). Mobile platform measurements of ultrafine particles and associated pollutant concentrations on freeways and residential streets in Los Angeles. *Atmos. Environ.*, **39**(20):3597-3610.

Westerholm, R.; and Li, H. (1994). A multivariate statistical analysis of fuel-related polycyclic aromatic hydrocarbons emissions from heavy-duty diesel vehicles. *Enivron. Sci. Technol.*, **28**(5):965-972.

Westerholm, R.N.; Almén, J.; Li, H.; Rannug, J.U.; Egebägg, K.E.; and Grägg, K. (1991). Chemical and biological characterization of particulate-, semivolatile-, and gas-phase-associated compounds in diluted heavy-duty diesel exhausts: A comparison of three different semivolatile-phase samplers. *Enivron. Sci. Technol.*, **25**:332-338.

Wichmann, H.E. (2007). Diesel exhaust particles. *Inhal. Toxicol.*, **19**:241-244.

Witze, P.O.; Chase, R.E.; Maricq, M.M.; Podsiadlik, D.H.; and Xu, N. (2004). Time-resolved measurement of exhaust PM for FTP-75: Comparison of LII, ELPI and TEOM techniques. *SAE Technical Paper Series*, **2004-01-0964**.

Wong, C.P.; Chan, T.L.; and Leung, C.W. (2003). Characterisation of diesel exhaust particle number and size distributions using mini-dilution tunnel and ejector-diluter measurement techniques. *Atmos. Environ.*, **37**(31):4435-4446.

Wright, R.S.; Howe, G.B.; and Jayanty, R.K.M. (1998). Evaluation of a portable Fourier transform infrared gas analyzer for measurements of air toxics in pollution prevention research. *J. Air Waste Manage. Assoc.*, **48**(11):1077-1084.

Wynne, J.H.; Beal, E.J.; Lloyd, C.T.; Hardy, D.R.; Mushrush, G.W.; and Hughes, J.M. (2004). Soybean-derived fuel liquids as additives for middle distillate transportation fuels. *Energy Sources*, **26**(1):19-24.

Xu, X.H.; Brook, J.R.; and Guo, Y.S. (2007). A statistical assessment of saturation and mobile sampling strategies to estimate long-term average concentrations across urban areas. *J. Air Waste Manage. Assoc.*, **57**(11):1396-1406.

Yang, H.H.; Chien, S.M.; Lo, M.Y.; Lan, J.C.W.; Lu, W.C.; and Ku, Y.Y. (2007a). Effects of biodiesel on emissions of regulated air pollutants and polycyclic aromatic hydrocarbons under engine durability testing. *Atmos. Environ.*, **41**:7232-7240.

Yang, H.H.; Lo, M.Y.; Lan, J.C.W.; Wang, J.S.; and Hsieh, D.P.H. (2007b). Characteristics of trans,trans-2,4-decadienal and polycyclic aromatic hydrocarbons in exhaust of diesel engine fueled with biodiesel. *Atmos. Environ.*, **41**(16):3373-3380.

Yanowitz, J. (2003). Particulate matter emissions during transient locomotive operation: Preliminary study. *J. Air Waste Manage. Assoc.*, **53**(10):1241-1247.

Yao, M.; Williamson, D.G.; and McFadden, J. (2005). Use of subsampled traffic data to estimate roadway emissions, including conversion to MOBILE6 vehicle classifications. *J. Air Waste Manage. Assoc.*, **55**(8):1245-1253.

Yao, X.H.; Lau, N.T.; Chan, C.K.; and Fang, M. (2007a). Size distributions and condensation growth of submicron particles in on-road vehicle plumes in Hong Kong. *Atmos. Environ.*, **41**(16):3328-3338.

Yao, X.H.; Lau, N.T.; Fang, M.; and Chan, C.K. (2006). Use of stationary and mobile measurements to study power plant emissions. *J. Air Waste Manage. Assoc.*, **56**(2):144-151.

Yao, Z.L.; Wang, Q.D.; He, K.B.; Huo, H.; Ma, Y.L.; and Zhang, Q. (2007b). Characteristics of real-world vehicular emissions in Chinese cities. *J. Air Waste Manage. Assoc.*, **57**(11):1379-1386.

Yi, H.H.; Hao, J.M.; Duan, L.; Li, X.H.; and Guo, X.M. (2006). Characteristics of inhalable particulate matter concentration and size distribution from power plants in China. *J. Air Waste Manage. Assoc.*, **56**(9):1243-1251.

Ying, W.; and Zhou, L.B. (2007). Performance and emissions of a compression-ignition engine fueled with dimethyl ether and rapeseed oil blends. *Energy & Fuels*, **21**(3):1454-1458.

Yli-Tuomi, T.; Aarnio, P.; Pirjola, L.; Makela, T.; Hillamo, R.; and Jantunen, M. (2005). Emissions of fine particles, NOx, and CO from on-road vehicles in Finland. *Atmos. Environ.*, **39**(35):6696-6706.

Yu, F.Q. (2006). From molecular clusters to nanoparticles: second-generation ion-mediated nucleation model. *Atmos. Chem. Phys.*, **6**:5193-5211.

Yuan, C.S.; Lin, H.Y.; Lee, W.J.; Lin, Y.C.; Wu, T.S.; and Chen, K.F. (2007). A new alternative fuel for reduction of polycyclic aromatic hydrocarbon and particulate matter emissions from diesel engines. *J. Air Waste Manage. Assoc.*, **57**(4):465-471.

Zabetta, E.C.; Hupa, M.; and Niemi, S. (2006). Bio-derived fuels may ease the regeneration of diesel particulate traps. *Fuel*, **85**(17-18):2666-2670.

Zahniser, M.S.; Nelson, D.D.; McManus, J.B.; Shorter, J.H.; Kolb, C.E.; McRae, G.J.; and Koplow, M.D.(1996). Infrared laser remote sensing to monitor on-road NOX emissions from motor vehicles. In *Proceedings of the Sixth CRC On-Road Vehicle Emissions Workshop*, pp. 9-61-9-72.

Zavala, M.; Herndon, S.C.; Slott, R.S.; Dunlea, E.J.; Marr, L.C.; Shorter, J.H.; Zahniser, M.; Knighton, W.B.; Rogers, T.M.; Kolb, C.E.; Molina, L.T.; and Molina, M.J. (2006). Characterization of on-road vehicle emissions in the Mexico City Metropolitan Area using a mobile laboratory in chase and fleet average measurement modes during the MCMA-2003 field campaign. *Atmos. Chem. Phys.*, **6**:5129-5142.

Zervas, E.; and Dorlhene, P. (2006). Comparison of exhaust particle number measured by EEPS, CPC, and ELPI. *Aerosol Sci. Technol.*, **40**(11):977-984.

Zervas, E.; Dorlhene, P.; Forti, L.; Perrin, C.; Momique, J.C.; Monier, R.; Ing, H.; and Lopez, B. (2005). Interlaboratory test of exhaust PM using ELPI. *Aerosol Sci. Technol.*, **39**(4):333-346.

Zhang, B.; Fu, W.B.; and Gong, J.S. (2006). Study of fuel consumption when introducing DME or ethanol into diesel engine. *Fuel*, **85**(5-6):778-782.

Zhang, K.; and Frey, C. (2008). Evaluation of response time of a portable system for in-use vehicle tailpipe emissions measurement. *Environ. Sci. Technol.*, **42**(1):221-227.

Zhang, K.M.; Wexler, A.S.; Niemeier, D.A.; Zhu, Y.F.; Hinds, W.C.; and Sioutas, C. (2005). Evolution of particle number distribution near roadways. Part III: Traffic analysis and on-road size resolved particulate emission factors. *Atmos. Environ.*, **39**(22):4155-4166.

Zhang, Y.; Bishop, G.A.; and Stedman, D.H. (1994). Automobile emissions are statistically γ-distributed. *Enivron. Sci. Technol.*, **28**(7):1370-1374.

Zhang, Y.; Stedman, D.H.; Bishop, G.A.; Beaton, S.P.; Guenther, P.L.; and McVey, I.F. (1996). Enhancement of remote sensing for mobile source nitric oxide. *J. Air Waste Manage. Assoc.*, **46**(1):25-29.

Zhang, Y.; Stedman, D.H.; Bishop, G.A.; Guenther, P.L.; and Beaton, S.P. (1995). Worldwide on-road vehicle exhaust emissions study by remote sensing. *Environ. Sci. Technol.*, **29**:2286-2294.

Zheng, M.; Cass, G.R.; Schauer, J.J.; and Edgerton, E.S. (2002). Source apportionment of $PM_{2.5}$ in the southeastern United States using solvent-extractable organic compounds as tracers. *Environ. Sci. Technol.*, **36**(11):2361-2371.

Zheng, M.; Reader, G.T.; and Hawley, J.G. (2004). Diesel engine exhaust gas recirculation - a review on advanced and novel concepts. *Energy Conversion and Management*, **45**(6):883-900.

Zielinska, B.; Campbell, D.; Lawson, D.R.; Ireson, R.G.; Weaver, C.S.; Hesterberg, T.W.; Larson, T.; Davey, M.; and Liu, L.J.S. (2008). Detailed characterization and profiles of crankcase and diesel particulate matter exhaust emissions using speciated organics. *Environ. Sci. Technol.*, **42**(15):5661-5666.

Zou, L.; and Atkinson, S. (2003). Characterizing vehicle emissions from the burning of biodiesel made from vegetable oil. *Environ. Technol.*, **24**(10):1253-1260.